Alain Glumineau
Jesús de León Morales

Sensorless AC Electric Motor Control

Robust Advanced Design Techniques and Applications

AIC

Springer

Advances in Industrial Control

Series editors

Michael J. Grimble, Glasgow, UK
Michael A. Johnson, Kidlington, UK

Alain Glumineau · Jesús de León Morales

Sensorless AC Electric Motor Control

Robust Advanced Design Techniques and Applications

Springer

Alain Glumineau
IRCCyN/Ecole Centrale de Nantes
The University of Nantes Angers Le Mans
Nantes
France

Jesús de León Morales
Facultad de Ingeniería Mecánica y Eléctrica
Universidad Autónoma de Nuevo León
Nuevo León
Mexico

To my family

Alain Glumineau

To Adeline, Marine and Rafael

Jesús de León Morales

Series Editors' Foreword

The series *Advances in Industrial Control* aims to report and encourage technology transfer in control engineering. The rapid development of control technology has an impact on all areas of the control discipline. New theory, new controllers, actuators, sensors, new industrial processes, computer methods, new applications, new philosophies…, new challenges. Much of this development work resides in industrial reports, feasibility study papers, and the reports of advanced collaborative projects. The series offers an opportunity for researchers to present an extended exposition of such new work in all aspects of industrial control for wider and rapid dissemination.

One of the interesting aspects of editing a control monograph series like *Advances in Industrial Control* is the insight gained as to how control systems theory and control engineering is developing and the interaction between theory and practice. An example is that of nonlinear systems theory, where there are slow but increasing signs of applications using these techniques. We can cite the following monographs from the series to support this thesis:

- *Nonlinear Process Control* by Peter L. Lee (Ed.) (ISBN 978-3-540-19856-7, 1993);
- *Nonlinear* H_2/H_∞ *Constrained Feedback Control* by Murad Abu-Khalaf, Jie Huang and Frank L. Lewis (ISBN 978-1-84628-349-9, 2006);
- *Induction Motor Control Design* by Riccardo Marino, Patrizio Tomei and Cristiano M. Verrelli (ISBN 978-1-84996-283-4, 2010); and
- *Nonlinear Control of Vehicles and Robots* by Béla Lantos and Lőrinc Márton (ISBN 978-1-84996-121-9, 2011).

Nonlinear systems theory is a well-established field of study yet the usual engineering response to system nonlinearity is linearization, multiple models, controller scheduling, and occasional recourse to adaptive and robust control to overcome the uncertainties, and mismatch that the initial linearization approach has introduced. It is therefore interesting to observe some practitioners using existing nonlinear systems theory directly with real-world systems and processes. The most promising application areas are those where there is a well-established historical

archive of nonlinear models, suitable for the procedures of nonlinear systems theory. One such field is the control of electrical machines.

The models of electrical machine systems are quite well-defined and have been known for many years. They have a fairly small number of state variables, are nonlinear, and multivariable. Despite small state dimensions, these systems have unmeasurable state variables or states that the engineer wishes to avoid measuring because the appropriate sensors are either costly or difficult and expensive to implement in the physical machine. Add to this model parameters that are uncertain (only approximately known) and/or time-varying, along with the presence of system noise and it is easily seen that the nonlinear control of electrical machines is challenging.

With these difficult characteristics, electrical machines are often used as a benchmark system by academic researchers to test out new control approaches but they also constitute a real-world application field in their own right. Industrially and commercially electrical machines are the essential technological workhorses in the power industries, the utility industries, transport, and many other fields. Such importance makes this *Advances in Industrial Control* monograph *Sensorless AC Electric Motor Control: Robust Advanced Design Techniques and Applications* by Alain Glumineau and Jesús De León Morales a valuable contribution to the series. The authors focus on two issues:

 i. AC electrical machine control (permanent magnet synchronous motors, and induction motors); and
 ii. the application of nonlinear system techniques.

After revising the models of permanent magnet synchronous motors, and induction motors in Chap. 1, the reader is led through carefully structured chapters that deal with system observability, observer construction, and on to four chapters on control studies that use the observer–controller tandem. The ultimate objective of this work is the sensorless control of AC machines, where the nonlinear observers are used as "soft" sensors for the system controllers. An experimental facility is described in Chap. 1 and this provides experimental validation results for the later control chapters. This is a very instructive addition to the literature of AC motor control and to the *Advances in Industrial Control* monograph series.

Industrial Control Centre, Glasgow, Scotland, UK   Michael J. Grimble
                                                                    Michael A. Johnson

Preface

Thanks to the technology developments and the recent advances in control theory, it is possible to implement new controllers to a large number of Alternative Current (AC) machines. These controllers are more robust with respect to uncertainties, and more efficient under a wide range of operation conditions in very useful applications. One the most attractive applications of the electrical machines is for transport: vehicle traction that is currently in important development.

The control of AC machines is a challenging problem which has attracted attention thanks to its several applications. For instance, the control problem of the induction motor has recently attracted attention due to its complexity: the induction motor is a nonlinear multi-variable system. Classically, the measurable outputs are the stator currents and voltages. The rotor speed measurement is not always available because of the high costs of sensors, their weakness, or noise sensitivity (the performance at low speed can be poor). Furthermore, the rotor speed is a function of the stator currents and rotor fluxes. The rotor fluxes measurement is not an easy task: it is necessary to introduce sensors in the motor which is expensive and physically complicated to install. When the rotor speed cannot directly be computed from these variables, its control becomes more difficult. On the other hand, the load torque and some parameters like the rotor resistance are usually unknown or inaccurately known and, moreover, time varying. Then, the mathematical models of the AC machines contain parametric uncertainties. Regarding the permanent magnetic synchronous motors, the position and rotor speed knowledge require sensors. However, the introduction of more sensors in the machine implies more complexity and the possibility to introduce failures in the machine. This fact weakens the motor robustness and increases the system cost. The rotor resistance is a time varying parameter depending on the motor temperature. Generally, other parameters (inductance and inertia for instance) are not well known with a sufficient precision. All these elements introduce uncertainties in the model used to design the control, so the control of the machines becomes more complex and its action less efficient.

Clearly, to achieve high-performance objectives, the design of robust controllers requires suitable models describing the dynamical behavior of the machines.

For AC machines, the models are nonlinear and multi-variable (multi-state variables, multi-outputs to track, and multi-control inputs). Moreover, in practice, all the state variables are not measurable, which implies that the implementation of the controller is to be limited. To overcome this difficulty, observation theory provides a solution to reconstruct the unmeasurable state by using observer. Moreover, when the AC machine operates at low speed, some important difficulties appear owing to the loss of the observability property. This property is very important for the estimation of the system state and thus is a preliminary step in the observer design.

Sensorless control of electrical machines implies the new and interesting challenging problem of eliminating the mechanical sensors. The solution to this problem has focused the attention recently in the control community. For this reason, the robust sensorless control of electrical machines is considered as an open problem. To solve this problem, first, it is necessary to study the observability property of these machines. It is well known that the observability of nonlinear systems can depend on the input. In the sensorless case of electrical machines and from the measurement of the inputs (stator voltages) and measured outputs (stator currents), this property could be lost. This situation complicates the reconstruction of the system state. Several concepts and results are introduced in this book as tools to verify if a system is observable or under which conditions it is observable. For that purpose, a precise analysis is necessary for AC machines.

If the system is observable then the design of an observer can begin: it is known that for nonlinear systems there is no general observable form for which an observer can be constructed. Nevertheless, there exist conditions for which a nonlinear system can be exactly transformed into another one so that it is possible to design an observer. The classes of nonlinear system for which an observer can be designed, include: (1) "Luenberger type" (i.e., linear plus a nonlinear output injection), (2) "triangular form" type, or (3) "extended Kalman like" type, like state affine observers or adaptive state affine observers. Furthermore, in terms of convergence, these observers can be divided into two classes: one based on asymptotic methods and the other with finite-time convergence. Recently, the observer design for AC machines is one of the most studied topics in electrical machines research.

The control of the induction motor and synchronous motors have important developments thanks to the advances in power electronics, signal processing, and the progress in computer technology allowing the implementation of sophisticated control strategies. Among the classical control techniques to drive electrical machines, we can find the field-oriented control, or those based on state space representation such as feedback linearization, which have been used in many applications. However, these controllers have shown some limitations in practice.

Recently, the sensorless control problem of AC electrical machines has been intensively addressed and significant contributions have been published to give a solution to this problem. Several observer–controller schemes have been proposed, where conditions are obtained to guarantee the closed-loop stability of the system.

This book presents the basic fundamentals of electrical machines with an emphasis on the permanent magnet synchronous motor and on the induction motor, as well as their mathematical models in different frames and state space

representation. After the observability of these AC machines is analyzed, an important contribution is the machines nonlinear observer design. Furthermore, robust control designs based on the backstepping technique and on the sliding mode control are presented. The combination of the observer and controller designs is analyzed and implemented on industrial benchmarks and their results are discussed.

It is clear that the objective of the book is to provide a framework that subsumes significant developments on observer and controller designs for AC electric machines. More precisely, the purpose of the book is to present robust AC machine control designs based on backstepping techniques and sliding mode controls that are combined with nonlinear observers based on either asymptotic or finite-time convergence designs. These observer–controller schemes are evaluated on significant industrial benchmarks with digital simulations and experimental results, showing their performance.

The book is intended to be a reference for practicing engineers, students, and academics, interested in knowing the most recent significant developments on observer design and robust nonlinear sensor or sensorless control techniques applied to AC electrical machines.

Acknowledgments

Nantes, France   Alain Glumineau
Monterrey, Mexico   Jesús de León Morales
November 2014

Contents

Acronyms and Nomenclature

EMF	Electro-Motive Force
IM	Induction Motor
IPMSM	Interior Permanent Magnet Synchronous Motor
PMSM	Permanent Magnet Synchronous Motor
SPMSM	Surface Permanent Magnet Synchronous Motor
$v_s = [v_{sa}, v_{sb}, v_{sc}]^T$	Three-phase stator voltages
$v_r = [v_{ra}, v_{rb}, v_{rc}]^T$	Three-phase rotor voltages
$i_s = [i_{sa}, i_{sb}, i_{sc}]^T$	Three-phase stator currents
$i_r = [i_{ra}, i_{rb}, i_{rc}]^T$	Three-phase rotor currents
$\phi_s = [\phi_{sa}, \phi_{sb}, \phi_{sc}]^T$	Stator fluxes
$\phi_r = [\phi_{ra}, \phi_{rb}, \phi_{rc}]^T$	Rotor fluxes
$v_{s\alpha,\beta} = [v_{s\alpha}, v_{s\beta}]^T$	Two-phase stator voltages in the fixed frame (α, β)
$i_{s\alpha,\beta} = [i_{s\alpha}, i_{s\beta}]^T$	Two-phase stator currents in the fixed frame (α, β)
$v_{r\alpha,\beta} = [v_{r\alpha}, v_{r\beta}]^T$	Two-phase rotor voltages in the fixed frame (α, β)
$i_{r\alpha,\beta} = [i_{r\alpha}, i_{r\beta}]^T$	Two-phase rotor currents in the fixed frame (α, β)
$\phi_{s\alpha,\beta} = [\phi_{s\alpha}, \phi_{s\beta}]^T$	Two-phase stator fluxe in the fixed frame (α, β)
$\phi_{r\alpha,\beta} = [\phi_{r\alpha}, \phi_{r\beta}]^T$	Two-phase rotor fluxes in the fixed frame (α, β)
$v_{sd,q} = [v_{sd}, v_{sq}]^T$	Two-phase stator voltages in the rotating frame (d, q)
$i_{sd,q} = [i_{sd}, i_{sq}]^T$	Two-phase stator currents in the rotating frame (d, q)
$v_{rd,q} = [v_{rd}, v_{rq}]^T$	Two-phase rotor voltages in the rotating frame (d, q)
$i_{rd,q} = [i_{rd}, i_{rq}]^T$	Two-phase rotor currents in the rotating frame (d, q)
$\phi_{sd,q} = [\phi_{sd}, \phi_{sq}]^T$	Two-phase stator fluxes in the rotating frame (d, q)
$\phi_{rd,q} = [\phi_{rd}, \phi_{rq}]^T$	Two-phase rotor fluxes in the rotating frame (d, q)
Φ_r	Rotor magnetic field
Λ	Inductances matrix
L_{as}, L_{ar}	Self stator and rotor inductances

M_{as}	Two-phase stator mutual inductance
M_{ar}	Two-phase rotor mutual inductance
R_s, R_r	Stator and rotor resistances
$L_s = L_{as} - M_{as}$	Stator cyclic inductance
$L_r = L_{ar} - M_{ar}$	Rotor cyclic inductance
$M_{sr} = \frac{3}{2}M$	Stator and rotor mutual cyclic inductance
$\mathbf{Rs}, \mathbf{Rr}$	Diagonal stator and rotor resistances matrices
$\mathbf{Ls}, \mathbf{Lr}$	Stator and rotor inductances matrices
$\mathbf{Lsr}$	Stator-rotor mutual inductances matrix
J	Motor and Load inertia
f_v	Viscous damping coefficient
f_s	Coulomb friction torque
T_l	Load torque
T_e	Electromagnetic torque
p	Pole pair number
Ω	Rotor mechanical speed
ω	PMSM stator electrical angular frequency
$p\Omega$	Electrical angular frequency associated to the speed $p\Omega$
ω_r	IM rotor electrical angular frequency (or slip pulsation)
$\omega_s = \omega_r + p\Omega$	IM stator electrical angular frequency
$g = \frac{\omega_r}{\omega_s}$	Rotor slip
θ_m	Rotor angular position
θ_e	Electrical position
$\theta_s = \rho$	(d,q) frame angular position
θ_r	Relative angular position of the rotor w.r.t. the (d,q) frame
σ	Blondel leakage coefficient

Chapter 1
Dynamical Models of AC Machines

Abstract This chapter presents a detailed review of the basic concepts describing the mechanical and electrical behavior of alternative current (AC) machines, which will be used extensively in the following chapters. AC machines, specifically the permanent magnet synchronous motor (PMSM) and the induction motor (IM), will be studied. A particular emphasis on the modeling devoted to the control of such machines is considered. The dynamical properties and the mathematical descriptions are introduced. New applications of electric motors are appearing, for instance, electric vehicles owing to their renewable nature and their reduced environmental impact. These applications require controllers that achieve high performance. All the control algorithms presented in this book are validated on specific benchmarks checking the important features of the motor control under several operating conditions. For instance, specific reference trajectories at low speed with nominal load torque are defined and will be used to compare the performance of the controller and observer algorithms. Moreover, most of these algorithms have been tested on an experimental setup and the results are reported to illustrate their performances under parametric uncertainties and unknown disturbances such as an abrupt load torque.

1.1 Applications of AC Machines

The applications of AC machines play an important part in many types of domestic and industrial areas.

One of the most important applications of AC machines is the traction system for electric vehicles. The purpose of this subsection is to give an overview of the state of the art for Hybrid Electric Vehicles (HEV) and Electric Vehicles (EV), with emphasis on AC machines for traction system.

1.2 Electric Vehicles: Traction System

The recent developments of the internal combustion engine (ICE) have changed the industry and the lifestyle of society in the last years. The most important companies produce many automobiles in the world, satisfying the necessity of transport, comfort,

and security of passengers. However, serious problems have appeared. For instance, the air quality in the cities in the world has deteriorated, and the temperature of the earth is increasing affecting wildlife and agriculture. The increase in oil consumption is causing petroleum sources to be rapidly exhausted.

The governments of several countries are adopting laws to reduce gas emissions and to develop safer, cleaner, and more efficient vehicles. New solutions have been proposed to reduce emission of gases, one of them being the introduction of the electric drive train technology.

Furthermore, electric transportation has received renewed interest, mainly the electric vehicles, because they have many advantages over the conventional internal combustion engine (ICE) vehicle, such as (i) no gas emissions, (ii) high efficiency, (iii) no consumption of petroleum, and (iv) easy operation with minimal noise.

On the other hand, an attractive solution that satisfies the standards of operation and the reduction of gas emission is the hybrid electric vehicle. HEV combines the advantages of internal combustion engines and electric vehicles, by introducing significant improvements in energy efficiency (new energy sources), vehicle performance, and gas emissions reduction.
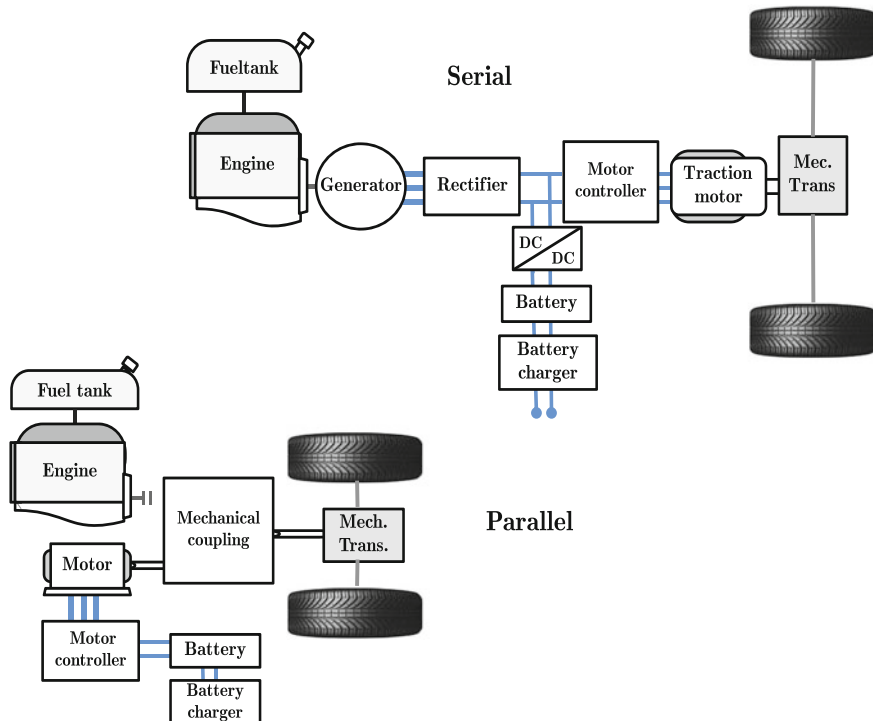
HEV combines two or more sources of energy to power the vehicle. For example, the internal combustion engine (ICE) is combined with an electric motor supplied by batteries, solar energy, or fuel cells. An interesting way to optimize fuel consumption and reduce emissions in an HEV, compared with ICE alone powered vehicles, is the use of regenerative braking combined with a small ICE. Then, in accordance with the above, HEV is one of the attractive alternatives to electric traction.

Application of electric machines, used to provide the traction of hybrid and electric vehicles, has attracted the interest of many automakers. The electric motor is the heart of the traction system of the EV that can provide a bidirectional torque quickly over a wide speed range, satisfying a driving profile. To satisfy these operating conditions, AC machines, such as the AC induction motor and the Interior Permanent Magnet Synchronous motors (PMSM and IM), are the better choice.

The bidirectional power conversion units represent the major equipment for electric traction in electric vehicles. These bidirectional power conversion units consist of the following elements: Electric machines for traction and generation, power electronics (converters), and battery.

Furthermore, to reduce fuel consumption, the performance improvement of EV under different driving conditions and the use of low-cost systems are possible thanks to the advances in several technological domains such as in the power electronic converters, electric machines, energy storage, power management, or applying the recent developments in linear and nonlinear control theory and optimization.

It is worth mentioning that vehicle makers have proposed various configurations of HEVs and EVs, taking into account several criteria such as improving performance, fuel consumption, lower weight, reasonable cost, volume, and so on. The most important schemes are parallel and series configurations (see Fig. 1.1). In this figure is shown the distribution of the main elements constituting the traction system for structures in series and parallel of an HEV.

Fig. 1.1 Serial and parallel configuration for HEV

The electric motor for traction is one of the most important components of an electric vehicle. The choice of electric traction system depends on a number of factors such as:

(i) *Vehicle constraints*. The most important are the volume and the weight, which depend on the vehicle type and payload.

(ii) *Energy source*. The chemical batteries, fuel cells, ultracapacitors, and flywheels. It is worth mentioning that these energy sources present some drawbacks:

    (1) Heavy weight.
    (2) Lower flexibility.
    (3) Performance degradation.

(iii) *Driver's expectation* defined by a driving profile, which takes into account the (a) acceleration, (b) maximum speed, (c) climbing capability, (d) braking, and (e) operation range determined from the configuration of the drivetrain, which is made up of three subsystems

    (1) *Electric motor traction system*: the power electronic subsystem, electric motor, mechanical transmission, driven wheels.

(2) *Energy sources system*: the energy source, energy management unit, energy refueling unit.
(3) *Auxiliary system*: the power steering unit, climate control unit, and auxiliary supply unit.

The performance of the electric vehicle is usually evaluated in terms of

(i) *Acceleration time*, i.e., the time to accelerate the vehicle from a low speed $V_1 = 0 \, \text{km/h}$ to a high speed $V_2 = 100 \, \text{km/h}$.
(ii) *Maximum speed* depends on the speed-power characteristics of the traction motor.

Traction electric motor characteristics

A review of the state of the art related to electric-traction systems shows that the squirrel cage induction motor and the permanent magnets synchronous motor are the more used machines for electric traction systems.

The requirements often encountered in electric traction systems are the following:

(1) High power and high power density;
(2) High torque at low speed for starting and climbing;
(3) Wide speed range, especially for constant-torque and constant-power operating conditions;
(4) Fast torque response;
(5) High efficiency over wide speed and torque ranges;
(6) High robustness for various vehicle operating conditions.

It is clear that if the above requirements are satisfied, an improved traction system is obtained. However, it is necessary to have suitable control systems to reduce the energy consumption, to improve the performance, and have a comfortable and safe driving.

As we will see in the following chapters, to achieve the control objectives taking into account the above requirements, the control design demands to analyze the electric machines. Thus, the main characteristics of AC machines are now introduced, and their advantages and limitations are discussed.

DC motors

At first, DC motors played an important role in electric traction thanks to their torque-speed characteristics which are suitable for traction applications. Moreover, their speed controls and electronics are simple. However, DC motors are bulky and heavy; they usually have low efficiency and low reliability. Furthermore, due to the mechanical commutator and brushes, the DC motor needs frequent maintenance.

The developments in power electronics, digital signal processors, and the progress in control theory have made it possible to replace DC motors in traction applications with induction and synchronous motors. It is worth mentioning that commutatorless

motors are more attractive owing to their high reliability and low requirements of maintenance during operation.

AC Machines

The main characteristics of an electric motor for vehicle traction are as follows:

(1) Ability to produce high torque at low speed, including zero speed.
(2) Operation at a constant power speed range.
(3) Operation of the motor and its drive circuits over the whole speed range with high efficiency, high reliability, and low maintenance.
(4) Four-quadrant operation with regenerative breaking, returning the overhauling energy into storage device.

Induction Motor

The popularity of induction motors is due to their robustness and operation reliability. They are small in volume and weight, do not require much maintenance, and are of reasonable cost compared to the DC motor. However, induction motors are difficult to control because of their complexity and nonlinear behavior. They require powerful and robust algorithms to achieve the control objectives under a wide range of operations. These algorithms need information about the speed, rotor flux, and load torque, which usually are not easy to measure; for example, the speed is polluted by noise. Moreover, the installation of sensors to measure the rotor flux inside the induction motor is difficult and expensive.

From a practical point of view, the maintenance and fragility of sensors, especially the mechanical speed and load torque sensors, the variations of rotor and stator resistances owing to temperature change are some serious problems. This limits the implementation of efficient control strategies.

Comparing the advantages and limitations of AC machines, it follows that the squirrel cage induction motor is one of the most used motors in industrial applications owing to its high reliability, ruggedness, low maintenance, low cost, and the ability to operate in diverse environments. However, conventional control strategies for induction motors such as variable-voltage variable frequency cannot provide the desired performance on a wide range of operations. Thanks to the advances in power electronics and micro-controllers as well as to the advances in control theory, the improvements for induction motor control are now possible. On the other hand, one of the most well-known control strategies applied in the industry is the *Field-Oriented Controller* (FOC), which has been implemented to overcome the most important difficulties of AC motors. However, using the FOC to control induction motors for traction applications does not prevent some drawbacks as low efficiency at light loads and limited constant-power operation range. Thus, to improve the induction motor efficiency, new control techniques have been proposed and developed and constitute an important progress in EV applications, especially traction systems using induction motors. One of the most difficult problems is the control without mechanical sensors (or if the sensor breaks down) that induces the loss of motor control.

Permanent Magnet Synchronous Motors

Another AC machine used in industrial applications is the permanent magnet synchronous motor. The synchronous motor can be found in a variety of application domains such as traction, energy generation (wind-powered systems), and robotics. Regarding electric traction, the PMSM is more suitable than induction motor, owing to the synchronous machine having interesting advantages, among which are:

(1) The overall weight and volume are significantly reduced for a given output power;
(2) Better efficiency;
(3) Heat is efficiently dissipated, the Joule losses are smaller due to absence of rotor currents.

However, the PMSM have a short constant-power region owing to their rather limited field weakening capability, resulting from the presence of the permanent magnet field.

It is clear that with the recent technological advances it is now possible and attractive to implement robust and powerful nonlinear controllers to reduce energy consumption and to improve performance under a wide range of power-speed operating domains.

1.3 The Concordia/Clark and Park Transformations

In the following section, the mathematical models of AC electric machines describing their electromechanical behaviors are derived. The three-phase mathematical models of the induction and permanent magnet synchronous motors are developed. The classical models using the Concordia/Clarke and Park transformations are derived to define the two-phase equivalent models of AC machines. Using these transformations, many concepts, interpretations, and simplified models can be obtained to analyze the AC machine behavior.

An approach to study AC machines is to transform the variables (voltages, currents, and flux linkages) stated in a fixed reference frame to a rotating frame defined by the Concordia/Clarke and Park transformations. These transformations are used in the analysis of AC machines to reduce the complexity of the differential equation describing the behavior of the AC machines by eliminating time-varying terms in the inductances.

The transformation from a three-phase (stationary (a, b, c) frame) to a two-phase (rotatory direct-quadrature frame or (d, q) frame) transformation is referred as the *Park transformation*. However, this transformation can be decomposed in two transformations. A first transformation from a fixed three-phase system to a fixed two-phase system (Clarke's/Concordia's transformations). Next, by a transformation from a fixed two-phase frame to a rotating two-phase frame associated to a rotating variable (mechanical position and flux, for instance).

Before applying these transformations to AC machines, some assumptions are introduced (see [54]):

Modeling assumptions

- Uniform gap thickness and no notch effect;
- Sinusoidal distribution of the induction in the air gap;
- Linear magnetic characteristic (no saturation);
- Temperature effect, skin effect, hysteresis phenomenon, and Foucault's currents are neglected.

Using the overall Park transformation, the electric equations of a three-phase model (stationary (a, b, c) frame) of the motor are transformed into the two-phase model (rotatory $(d, q, 0)$ frame). The $(d, q, 0)$ transformation can reduce three AC variables (voltages, currents, …) to two DC variables.

A general representation of the Park transformation is given as

$$
\begin{bmatrix} x_d \\ x_q \\ x_0 \end{bmatrix} = \mathsf{P}(\xi) \begin{bmatrix} x_a \\ x_b \\ x_c \end{bmatrix}
\tag{1.1}
$$

where

$$
\mathsf{P}(\xi) = \eta \begin{bmatrix} \cos(\xi) & \cos(\xi - \frac{2\pi}{3}) & \cos(\xi + \frac{2\pi}{3}) \\ \sin(\xi) & \sin(\xi - \frac{2\pi}{3}) & \sin(\xi + \frac{2\pi}{3}) \\ \lambda & \lambda & \lambda \end{bmatrix}
\tag{1.2}
$$

with ξ as the angle between the axis α of the stationary reference frame and the real axis-d of the rotating reference frame, and with η as the ratio between the amplitude of the three-phase system variables x_a, x_b, x_c (voltages, currents, ...) with respect to the amplitude of the corresponding two-phase system variables x_d, x_q, x_0 and λ being a constant.

Then, two different Park transformations can be defined:

(1) Park transformation preserving amplitude and
(2) Park transformation preserving power.

1.3.1 The Park Transformation Preserving Amplitude

The $\mathsf{P}(\xi)$ transformation preserving amplitude transforms a three-phase system stated in a stationary (a, b, c) frame into a rotatory $(d, q, 0)$ frame by choosing

$$
\eta = \frac{2}{3}, \qquad \lambda = \frac{1}{2}
\tag{1.3}
$$

in (1.2), i.e.

$$\begin{bmatrix} x_d \\ x_q \\ x_0 \end{bmatrix} = \mathsf{P}(\xi) \begin{bmatrix} x_a \\ x_b \\ x_c \end{bmatrix} \tag{1.4}$$

where

$$\mathsf{P}(\xi) = \frac{2}{3} \begin{bmatrix} \cos(\xi) & \cos(\xi - \frac{2\pi}{3}) & \cos(\xi + \frac{2\pi}{3}) \\ \sin(\xi) & \sin(\xi - \frac{2\pi}{3}) & \sin(\xi + \frac{2\pi}{3}) \\ \frac{1}{2} & \frac{1}{2} & \frac{1}{2} \end{bmatrix}. \tag{1.5}$$

The inverse transformation of (1.2) is given by

$$\mathsf{P}^{-1}(\xi) = \begin{bmatrix} \cos(\xi) & \sin(\xi) & 1 \\ \cos(\xi - \frac{2\pi}{3}) & \sin(\xi - \frac{2\pi}{3}) & 1 \\ \cos(\xi + \frac{2\pi}{3}) & \sin(\xi + \frac{2\pi}{3}) & 1 \end{bmatrix}. \tag{1.6}$$

1.3.2 The Clarke Transformation

By choosing $\xi = 0$, in the Park transformation (1.5), the resulting matrix $\mathsf{C}_{32} = \mathsf{P}(0)$ is given as

$$\mathsf{C}_{32} = \frac{2}{3} \begin{bmatrix} 1 & -\frac{1}{2} & -\frac{1}{2} \\ 0 & \frac{\sqrt{3}}{2} & \frac{-\sqrt{3}}{2} \\ \frac{1}{2} & \frac{1}{2} & \frac{1}{2} \end{bmatrix}, \quad \text{and} \quad (\mathsf{C}_{32})^{-1} = \begin{bmatrix} 1 & 0 & 1 \\ -\frac{1}{2} & \frac{\sqrt{3}}{2} & 1 \\ -\frac{1}{2} & \frac{-\sqrt{3}}{2} & 1 \end{bmatrix}. \tag{1.7}$$

The matrix C_{32} is known as the *Clarke transformation*. The Clarke transformation converts the balanced three-phase quantities into balanced two-phase orthogonal quantities by keeping the amplitude of the variables. For an electric system, for example, this implies that power is not kept.
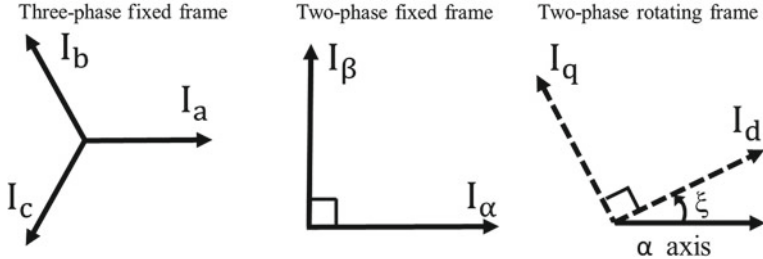
Furthermore, the Park transformation (1.5) can be expressed in terms of the Clarke transformation C_{32} and a Rotation matrix $\mathsf{R}(\xi)$, as

$$\mathsf{R}(\xi) = \begin{bmatrix} \cos\xi & -\sin\xi & 0 \\ \sin\xi & \cos\xi & 0 \\ 0 & 0 & 1 \end{bmatrix} \tag{1.8}$$

as follows

$$\mathsf{P}(\xi) = \mathsf{R}(\xi)\mathsf{C}_{32}. \tag{1.9}$$

For a symmetrical three-phase machine in a stationary (a, b, c) frame, the three-phase variables can be represented in a two-phase stationary reference (α, β) frame.

Fig. 1.2 The Clark/Concordia-Park transformations

Defining the plane (α, β) with direct and quadrature axes as shown in Fig. 1.2, if the source is a symmetric balanced three-phase, then the currents satisfy $\sum i = 0$. Equation (1.1) verifies easily that the current in the homopolar axis $i_0 = (1/\sqrt{3})(i_a + i_b + i_c)$ is null.

Hereinafter, the 0-axis is not considered. Then, the three-phase to two-phase transformation $(abc \Rightarrow \alpha\beta)$ is now given by

$$\begin{bmatrix} x_\alpha \\ x_\beta \end{bmatrix} = C_{32}^T \begin{bmatrix} x_a \\ x_b \\ x_c \end{bmatrix} \tag{1.10}$$

where

$$C_{32}^T = \frac{2}{3} \begin{bmatrix} 1 & -\frac{1}{2} & -\frac{1}{2} \\ 0 & \frac{\sqrt{3}}{2} & \frac{-\sqrt{3}}{2} \end{bmatrix}. \tag{1.11}$$

Notice that the inverse transformation is given as

$$\begin{bmatrix} x_a \\ x_b \\ x_c \end{bmatrix} = C_{32} \begin{bmatrix} x_\alpha \\ x_\beta \end{bmatrix} \tag{1.12}$$

where $C_{32} = \begin{bmatrix} 1 & 0 \\ -\frac{1}{2} & \frac{\sqrt{3}}{2} \\ -\frac{1}{2} & \frac{-\sqrt{3}}{2} \end{bmatrix}.$

1.3.3 The Park Transformation Preserving Power

In order to pass from the three-phase system $((a, b, c)$ frame) to the two-phase system $((d, q)$ frame) preserving the instantaneous power, the following condition must hold:

$$[V_{dq}]^T [I_{dq}] = [V_{abc}]^T [I_{abc}]$$

or

$$v_d i_d + v_q i_q = v_a i_a + v_b i_b + v_c i_c.$$

Then, the modified Park transformation preserving power of the system is obtained by choosing

$$\eta = \sqrt{\frac{2}{3}}, \qquad \lambda = \frac{1}{\sqrt{2}} \tag{1.13}$$

in (1.2), i.e., the transformation from a three-phase stationary (a, b, c) frame to a three-phase rotatory $(d, q, 0)$ frame is given as

$$\mathsf{Po}(\xi) = \sqrt{\frac{2}{3}} \begin{bmatrix} \cos(\xi) & \cos(\xi - \frac{2\pi}{3}) & \cos(\xi + \frac{2\pi}{3}) \\ \sin(\xi) & \sin(\xi - \frac{2\pi}{3}) & \sin(\xi + \frac{2\pi}{3}) \\ \frac{1}{\sqrt{2}} & \frac{1}{\sqrt{2}} & \frac{1}{\sqrt{2}} \end{bmatrix}, \tag{1.14}$$

and its inverse is given as

$$(\mathsf{Po})^{-1}(\xi) = \sqrt{\frac{2}{3}} \begin{bmatrix} \cos(\xi) & \sin(\xi) & 1 \\ \cos(\xi - \frac{2\pi}{3}) & \sin(\xi - \frac{2\pi}{3}) & 1 \\ \cos(\xi + \frac{2\pi}{3}) & \sin(\xi + \frac{2\pi}{3}) & 1 \end{bmatrix}. \tag{1.15}$$

1.3.4 The Concordia Transformation

Choosing the angle $\xi = 0$ in (1.14), the resulting Park transformation matrix preserving power (1.14) is of the form

$$\mathsf{Co} = \sqrt{\frac{2}{3}} \begin{bmatrix} 1 & -\frac{1}{2} & -\frac{1}{2} \\ 0 & \frac{\sqrt{3}}{2} & -\frac{\sqrt{3}}{2} \\ \frac{1}{\sqrt{2}} & \frac{1}{\sqrt{2}} & \frac{1}{\sqrt{2}} \end{bmatrix}, \qquad (\mathsf{Co})^{-1} = \sqrt{\frac{2}{3}} \begin{bmatrix} 1 & 0 & \frac{1}{\sqrt{2}} \\ -\frac{1}{2} & \frac{\sqrt{3}}{2} & \frac{1}{\sqrt{2}} \\ -\frac{1}{2} & -\frac{\sqrt{3}}{2} & \frac{1}{\sqrt{2}} \end{bmatrix}. \tag{1.16}$$

The matrix Co is known as the *Concordia transformation matrix*.

Furthermore, the Park transformation preserving the power (1.14) can be expressed in terms of the Concordia transformation Co and a Rotation matrix $\mathsf{R}(\xi)$ as

$$\mathsf{R}(\xi) = \begin{bmatrix} \cos \xi & -\sin \xi & 0 \\ \sin \xi & \cos \xi & 0 \\ 0 & 0 & 1 \end{bmatrix} \tag{1.17}$$

as follows

$$\mathsf{Po}(\xi) = \mathsf{R}(\xi)\mathsf{Co}. \tag{1.18}$$

1.3.5 Transformation Matrices

The following transformation transforms variables from the stationary reference (α, β) frame into the rotating reference (d, q) frame $(\alpha\beta \rightarrow dq)$

$$\begin{bmatrix} x_d \\ x_q \end{bmatrix} = \mathsf{P}_{\alpha\beta \rightarrow dq}(\xi) \begin{bmatrix} x_\alpha \\ x_\beta \end{bmatrix} \tag{1.19}$$

where

$$\mathsf{P}_{\alpha\beta \rightarrow dq}(\xi) = \begin{bmatrix} \cos\xi & \sin\xi \\ -\sin\xi & \cos\xi \end{bmatrix} \tag{1.20}$$

with $\mathsf{P}_{\alpha\beta \rightarrow dq}(\xi)$ is the Park transformation.

The angle ξ can be chosen as follows:

  (i) $\xi = \xi_s$, for the stator variables and
 (ii) $\xi = \xi_s - \xi_r$, for the rotor variables.

The Park Matrix can be easily obtained as

$$x_{\alpha\beta} = \mathsf{P}_{\alpha\beta \rightarrow dq}^{-1}(\xi) x_{dq}$$

where

$$\mathsf{P}_{\alpha\beta \rightarrow dq}^{-1}(\xi) = \begin{bmatrix} \cos\xi & -\sin\xi \\ \sin\xi & \cos\xi \end{bmatrix}.$$

1.3.6 Transformation from a Stationary Reference $(\alpha, \beta, 0)$ Frame to a Rotating Reference $(d, q, 0)$ Frame

The previous transformation can be completed as follows. Depending on the frame alignment at $t=0$, the $(d, q, 0)$ components are deduced from the $(\alpha, \beta, 0)$ components as follows: if the rotating frame is aligned with the a-axis, the change in variable transforming the $(\alpha, \beta, 0)$ variables into the $(d, q, 0)$ frame is:

$$\begin{bmatrix} x_d \\ x_q \\ x_0 \end{bmatrix} = \mathsf{R}(\xi_s) \begin{bmatrix} x_\alpha \\ x_\beta \\ x_0 \end{bmatrix} \tag{1.21}$$

where the rotation matrix $\mathsf{R}(\xi)$ is given as

$$\mathsf{R}(\xi) = \begin{bmatrix} \cos\xi & -\sin\xi & 0 \\ \sin\xi & \cos\xi & 0 \\ 0 & 0 & 1 \end{bmatrix}$$

with the d-axis angle ξ located with respect to the fixed (α, β) frame.

1.4 Permanent Magnet Synchronous Motor

1.4.1 Description

The permanent-magnet synchronous motor (PMSM) has been widely used in the industry for variable speed applications due to its high performance reliability and power density. Owing to the progress in the permanent magnet materials, micro and power electronics, fast digital signal processors, and modern control technologies, permanent magnet synchronous machines have become more widespread in industrial applications, such as in automobiles, robotics, aeronautics, and aerospace domains.

In the sequel, we introduce the most important characteristics of the PMSM.

1.4.2 Classification of Permanent Magnet Synchronous Motors (PMSM)

The physical characteristics of the PMSM are associated with its rotor and stator structures.

The **Stator** is composed of a three-phase wound such that the Electromotive Forces (EMF) are generated by the rotation of the rotor field. Furthermore, the EMF can be sinusoidal or trapezoidal. This wound is represented by the three axes (a, b, c) phase shifted, one from the other, by 120 electrical degrees.

The **Rotor** incorporates permanent magnets to produce a magnetic field. Regarding winding, the permanent magnets have the advantage to eliminate the brushes, the rotor losses, and the need for a controlled DC source to provide the excitation current. However, the amplitude of the rotor flux is constant.

On the other hand, there exist several ways to place the magnets in the rotor (see Fig. 1.3).
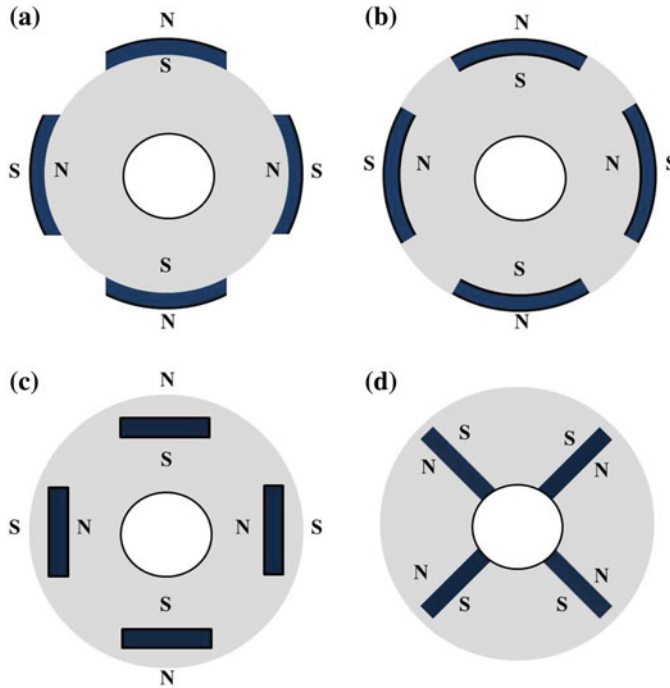
Following the magnet position, the PMSM can be classified into four major types:

- *Surface mounted magnets type*
  The magnets are placed on the surface of the rotor using high strength glue. They present a homogeneous gap, the motor is a non-salient pole. The inductances do not depend on the rotor position (Fig. 1.3a). The inductance of the axe-d is equal to those of the axe-q. This configuration of the rotor is simple to obtain. This type of rotor is the most usual. On the other hand, the magnets are exposed to a demagnetizing field. Moreover, they are subject to the centrifuge forces which can cause the detachment of the rotor.
- *Inset magnets type*
  The inset magnets are placed on the surface of the rotor. However, the space between the magnets is filled with iron (see Fig. 1.3b). Alternation between the iron and the magnets causes a salient effect. The inductance in the d-axe is slightly different from the inductance in the q-axe.

Fig. 1.3 PMSM rotor permanent magnets layout: **a** surface permanent magnets, **b** inset permanent magnets, **c** interior permanent magnets, **d** flux concentrating

- *Interior magnets type*
  The magnets are integrated in the rotor's body (Fig. 1.3c): the motor is a salient pole type. In this case, the rotor magnetism is anisotropic, the inductances depend on the rotor position. The magnets are placed in the rotor, providing more mechanical durability and robustness at high speeds. On the other hand, this motor is more expensive to manufacture and more complex to control.
- *Flux concentrating type*
  As shown in Fig. 1.3d, the magnets are deeply placed in the rotor's body. The magnets and their axes are radial. The flux on a polar arc of the rotor is a result of two separated magnets. The advantage of this configuration is the possibility to concentrate the flux generated by the permanent magnets in the rotor and to obtain a stronger induction in the gap. This type of machine has a salience effect.

However, surface permanent magnet synchronous motors and interior permanent magnet synchronous motors are the most used in the industry. Furthermore, the permanent magnet synchronous motors can be classified according to the electromotive force profiles (see [9, 91]):

- Sinusoidal,
- Trapezoidal.

Particularly, the synchronous machines with sinusoidal EMF are classified into two subcategories in terms of magnets position

1. **Non-salient Poles**: the magnets are located in the rotor surface (Fig. 1.3a): Surface Permanent Magnet Synchronous Motor (SPMSM)
2. **Salient Poles**: the magnets are buried into the rotor (Fig. 1.3c, d): Interior Permanent Magnet Synchronous Motor (IPMSM).

1.4.3 Modeling Assumptions

The study of an electric motor behavior is a hard task and requires, first of all, good knowledge of its model to properly predict its dynamic behavior under different operating conditions.

Modeling a permanent magnet synchronous motor is similar to a classical synchronous machine, except that the flux from the magnets is constant. Then, the model is derived from the classical synchronous machine [17]. In the following study, the machine has a stator and a rotor with symmetric distribution with p pairs of poles ($p = 2$ on Fig. 1.3).

To simplify the modeling of the machine, the following assumptions are introduced (see [9]):

Assumptions

- The damping effect of the rotor is neglected.
- The magnetic circuit of the machine is not saturated.
- The distribution of the *magnetomotive forces* (MMF) is sinusoidal.
- The coupling capacitors between the windings are neglected.
- The hysteresis phenomena and the Foucault's currents are neglected.
- The gap irregularities owing to the stator slots are neglected.

Under these assumptions and using basic concepts, the electrical and mechanical equations describing the dynamical behavior of the PMSM are obtained. The model will be essential to design and implement the controllers and the observers introduced in the following chapters.

1.4.3.1 Electric Equations

The three-phase stator voltage equations can be expressed as

$$\left[V_{sabc}\right] = R_s \left[I_{sabc}\right] + \frac{d\left[\Psi_{sabc}\right]}{dt} \tag{1.22}$$

where $\left[V_{sabc}\right] = \left[v_{sa}, v_{sb}, v_{sc}\right]^T$ are the voltages of each stator phase phase; R_s is the stator resistance; $\left[I_{sabc}\right] = [i_{sa}, i_{sb}, i_{sc}]^T$ are the phase stator currents and

$\left[\Psi_{sabc}\right] = [\Psi_{sa}, \Psi_{sb}, \Psi_{sc}]^T$ are the stator fluxes, which are given as

$$\left[\Psi_{sabc}\right] = \left[\mathsf{L}_{ss}\right]\left[I_{sabc}\right] + \left[\Psi_{rabc}\right] \tag{1.23}$$

where $\left[\Psi_{rabc}\right] = [\Psi_{ra}, \Psi_{rb}, \Psi_{rc}]^T$ is given by

$$\begin{bmatrix} \Psi_{ra} \\ \Psi_{rb} \\ \Psi_{rc} \end{bmatrix} = \Psi_r \begin{bmatrix} \cos(p\theta_m) \\ \cos(p\theta_m - 2\pi/3) \\ \cos(p\theta_m + 2\pi/3) \end{bmatrix} \tag{1.24}$$

with Ψ_r as the amplitude of the flux generated by the permanent magnets, θ_m as the rotor position angle, and p as the pole pair number. For the pole salient machines, the inductance matrix $\left[\mathsf{L}_{ss}\right]$ can be expressed as

$$\left[\mathsf{L}_{ss}\right] = \left[\mathsf{L}_{so}\right] + \left[\mathsf{L}_{sv}\right],$$

where

$$\left[\mathsf{L}_{ss}\right] = \begin{bmatrix} L_{aa} & M_{ab} & M_{ac} \\ M_{ba} & L_{bb} & M_{bc} \\ M_{ca} & M_{cb} & L_{cc} \end{bmatrix}, \tag{1.25}$$

with

$$\left[\mathsf{L}_{so}\right] = \begin{bmatrix} L_{so} & M_{so} & M_{so} \\ M_{so} & L_{so} & M_{so} \\ M_{so} & M_{so} & L_{so} \end{bmatrix}, \tag{1.26}$$

and

$$\left[\mathsf{L}_{sv}\right] = L_{sv} \begin{bmatrix} \cos(2p\theta_m) & \cos(2p\theta_m) - \frac{2\pi}{3} & \cos(2p\theta_m + \frac{2\pi}{3}) \\ \cos(2p\theta_m - \frac{2\pi}{3}) & \cos(2p\theta_m + \frac{2\pi}{3}) & \cos(2p\theta_m) \\ \cos(2p\theta_m + \frac{2\pi}{3}) & \cos(2p\theta_m) & \cos(2p\theta_m - \frac{2\pi}{3}) \end{bmatrix} \tag{1.27}$$

L_{so}, L_{sv} and M_{so} are positive parameters depending on the machine.

Replacing (1.23) in (1.22), it follows that

$$\left[V_{sabc}\right] = R_s \left[I_{sabc}\right] + \frac{d}{dt}\left\{\left[\mathsf{L}_{ss}\right]\left[I_{sabc}\right] + \left[\Psi_{rabc}\right]\right\}. \tag{1.28}$$

Notice the stator phase voltage equation of the three-phase PMSM represented in the three-phase stationary frame (*abc*-axis: three-phase stationary frame) is time varying and nonlinear.

Now, an equivalent two-phase representation in a fixed frame is introduced.

Using the Concordia transformation (1.16)

$$\begin{bmatrix} x_{s\alpha} \\ x_{s\beta} \end{bmatrix} = \mathsf{Co}^T \begin{bmatrix} x_{sa} \\ x_{sb} \\ x_{sc} \end{bmatrix} \tag{1.29}$$

where

$$\mathsf{Co} = \sqrt{\frac{2}{3}} \begin{bmatrix} 1 & 0 \\ -\frac{1}{2} & \frac{\sqrt{3}}{2} \\ -\frac{1}{2} & -\frac{\sqrt{3}}{2} \end{bmatrix}, \tag{1.30}$$

multiplying by Co the left side of Eq. (1.28) and using the identity $\mathsf{Co}^T \mathsf{Co} = I_{2\times 2}$ with x a variable (voltage, current or flux), it follows that

$$[V_{s\alpha\beta}] = R_s [I_{s\alpha\beta}] + \frac{d [\Lambda_{ss}]}{dt} [I_{s\alpha\beta}]$$

$$+ [\Lambda_{ss}] \frac{d [I_{s\alpha\beta}]}{dt} + \frac{d [\Psi_{r\alpha\beta}]}{dt} \tag{1.31}$$

with $[\Lambda_{ss}] = \{\mathsf{Co}^T [\mathsf{L}_{ss}] \mathsf{Co}\}$.

Taking $M_{so} = -\frac{1}{2} L_{so}$ and using the following trigonometric equivalences:

$$\cos(p\theta_m - 2\pi/3) = \cos(p\theta_m)\cos(2\pi/3) + \sin(p\theta_m)\sin(2\pi/3)$$

and

$$\cos(p\theta_m + 2\pi/3) = \cos(p\theta_m)\cos(2\pi/3) - \sin(p\theta_m)\sin(2\pi/3)$$

where $\cos(2\pi/3) = -\frac{1}{2}$ and $\sin(2\pi/3) = \sqrt{3}/2$, it follows that

$$[\Lambda_{ss}] = \frac{3}{2} L_{sv} \begin{bmatrix} \cos(2p\theta_m) & \sin(2p\theta_m) \\ \sin(2p\theta_m) & \cos(2p\theta_m) \end{bmatrix} + \frac{3}{2} L_{so} \begin{bmatrix} 1 & 0 \\ 0 & 1 \end{bmatrix} \tag{1.32}$$

$$= \begin{bmatrix} L_\alpha & L_{\alpha\beta} \\ L_{\alpha\beta} & L_\beta \end{bmatrix} \tag{1.33}$$

whose the time derivative is given by

$$\frac{d [\Lambda_{ss}]}{dt} = L_{sv} p\Omega \begin{bmatrix} -\sin(2p\theta_m) & \cos(2p\theta_m) \\ \cos(2p\theta_m) & \sin(2p\theta_m) \end{bmatrix}. \tag{1.34}$$

Furthermore, using the Concordia transformation, the fluxes $\Psi_{r\alpha}$ and $\Psi_{r\beta}$ can be expressed as

$$\begin{bmatrix} \Psi_{r\alpha} \\ \Psi_{r\beta} \end{bmatrix} = \mathbf{Co}^T \begin{bmatrix} \Psi_{ra} \\ \Psi_{rb} \\ \Psi_{rc} \end{bmatrix} \tag{1.35}$$

$$= \sqrt{\frac{2}{3}} \begin{bmatrix} 1 & -\frac{1}{2} & -\frac{1}{2} \\ 0 & \frac{\sqrt{3}}{2} & -\frac{\sqrt{3}}{2} \end{bmatrix} \Psi_r \begin{bmatrix} \cos(p\theta_m) \\ \cos(p\theta_m - 2\pi/3) \\ \cos(p\theta_m + 2\pi/3) \end{bmatrix}. \tag{1.36}$$

It follows that

$$\begin{bmatrix} \Psi_{r\alpha} \\ \Psi_{r\beta} \end{bmatrix} = \sqrt{\frac{3}{2}} \, \Psi_r \begin{bmatrix} \cos(p\theta_m) \\ \sin(p\theta_m) \end{bmatrix} \tag{1.37}$$

where $\mathcal{J} = \begin{bmatrix} 0 & 1 \\ -1 & 0 \end{bmatrix}$ is a skew-symmetric matrix, satisfying the following property:

$$\mathcal{J}^T \mathcal{J} = I$$

The time derivative of (1.37) is of the form

$$\begin{bmatrix} \dfrac{d\Psi_{r\alpha}}{dt} \\ \dfrac{d\Psi_{r\beta}}{dt} \end{bmatrix} = \begin{bmatrix} -p\Omega\Psi_{r\beta} \\ p\Omega\Psi_{r\alpha} \end{bmatrix} \tag{1.38}$$

or expressed in compact form

$$\frac{d[\Psi_{r\alpha\beta}]}{dt} = -p\Omega\mathcal{J}[\Psi_{r\alpha\beta}]. \tag{1.39}$$

The electromagnetic model of the PMSM is

$$\frac{d[I_{s\alpha\beta}]}{dt} = [\Lambda_{ss}]^{-1} \left\{ -\left[R_s + \frac{d[\Lambda_{ss}]}{dt} \right][I_{s\alpha\beta}] \right.$$

$$\left. + p\Omega\mathcal{J}[\Psi_{r\alpha\beta}] + [V_{s\alpha\beta}] \right\} \tag{1.40}$$

$$\frac{d[\Psi_{r\alpha\beta}]}{dt} = -p\Omega\mathcal{J}[\Psi_{r\alpha\beta}].$$

IPMSM model

Now, from (1.40) the IPMSM model can be obtained. Defining the constant inductances L_{sv} and L_{so}, in terms of the new parameters L_d and L_q, we obtain

$$L_{sv} = \frac{L_d - L_q}{3} \tag{1.41}$$

$$L_{so} = \frac{L_d + L_q}{3}. \tag{1.42}$$

The matrix Λ_{ss} can be expressed, in terms of L_d and L_q, as follows:

$$\left[\Lambda_{ss}\right] = \frac{L_d - L_q}{2} \begin{bmatrix} \cos(2p\theta_m) & \sin(2p\theta_m) \\ \sin(2p\theta_m) & \cos(2p\theta_m) \end{bmatrix} + \frac{L_d + L_q}{2} \begin{bmatrix} 1 & 0 \\ 0 & 1 \end{bmatrix}. \tag{1.43}$$

whose time derivative is given as

$$\frac{d\left[\Lambda_{ss}\right]}{dt} = 3p\Omega\{L_d - L_q\} \begin{bmatrix} -\sin(2p\theta_m) & \cos(2p\theta_m) \\ \cos(2p\theta_m) & \sin(2p\theta_m) \end{bmatrix}. \tag{1.44}$$

Then substituting (1.43) and (1.44) into (1.40) will be used to define the state space IPMSM model in the following subsections.

SPMSM model

From (1.40) for the case of non-salient poles, $L_d = L_q = L_s$, a simplified model is obtained. The SPMSM model is given as

$$L_s \frac{d\left[I_{s\alpha\beta}\right]}{dt} = -R_s\left[I_{s\alpha\beta}\right] + p\Omega\mathcal{J}[\Psi_{r\alpha\beta}] + \left[V_{s\alpha\beta}\right] \tag{1.45}$$

$$\frac{d[\Psi_{r\alpha\beta}]}{dt} = -p\Omega\mathcal{J}[\Psi_{r\alpha\beta}].$$

1.4.3.2 Transformation from a Fixed (a, b, c) Frame to a Rotating (d, q) Frame

To derive an equivalent two-phase representation in order to facilitate the analysis and control design, the Park transformation is usually employed to obtain the expression of the model in the (d, q) frame. This transformation renders simpler the dynamical equations of the PMSM.

As introduced previously in this chapter, this method is divided into two steps:

1. *Three-phase-Two-phase Transformation*: from an (a, b, c) three-phase stationary frame to an (α, β) two-phase stationary frame. This transformation is called the Concordia (obtained form Park transformation preserving energy) or Clarke transformation (obtained from Park transformation preserving amplitudes).

2. *Fixed frame-Rotating frame Transformation*: from an (α, β) two-phase stationary frame to a two-phase synchronous rotating (d, q) frame, this transformation is called the Park transformation.

By applying the first transformation, i.e., the Concordia transformation Co, then the second step is the application of the Park transformation P to Eq. (1.29), in order to obtain the two-phase synchronous rotating representation of the PMSM. The resulting voltage equations are given as

$$\begin{bmatrix} x_{sd} \\ x_{sq} \end{bmatrix} = \mathsf{P}(\theta_e)^T \begin{bmatrix} x_{s\alpha} \\ x_{s\beta} \end{bmatrix} \tag{1.46}$$

where $\mathsf{P}(\theta_e) = \begin{bmatrix} \cos\theta_e & -\sin\theta_e \\ \sin\theta_e & \cos\theta_e \end{bmatrix}$, with $\theta_e = p\theta_m$ is the rotor electrical position, i.e., the electrical angle defined from the position of the rotor with respect to stator. Then,

$$\begin{bmatrix} x_{sd} \\ x_{sq} \end{bmatrix} = \mathsf{P}(\theta_e)^T \begin{bmatrix} x_{s\alpha} \\ x_{s\beta} \end{bmatrix}$$

$$= \mathsf{P}(\theta_e)^T \mathsf{Co}^T \begin{bmatrix} x_{sa} \\ x_{sb} \\ x_{sc} \end{bmatrix}. \tag{1.47}$$

Combining Eq. (1.47) with (1.28), it follows that

$$\mathsf{Co}\mathsf{P}(\theta_e)\mathsf{P}(\theta_e)^T\mathsf{Co}^T\left[V_{sabc}\right] = R_s\mathsf{Co}\mathsf{P}(\theta_e)\mathsf{P}(\theta_e)^T\mathsf{Co}^T\left[I_{sabc}\right] + \frac{d}{dt}\left\{\left[\Psi_{rabc}\right]\right\}$$

$$+ \frac{d}{dt}\left\{\left[\mathsf{L}_{ss}\right]\mathsf{Co}\mathsf{P}(\theta_e)\mathsf{P}(\theta_e)^T\mathsf{Co}^T\left[I_{sabc}\right]\right\} \tag{1.48}$$

or

$$\mathsf{Co}\mathsf{P}(\theta_e)\left[V_{sdq}\right] = R_s\mathsf{Co}\mathsf{P}(\theta_e)\left[I_{sdq}\right]$$

$$+ \frac{d}{dt}\left\{\left[\mathsf{L}_{ss}\right]\mathsf{Co}\mathsf{P}(\theta_e)\left[I_{sdq}\right]\right\} - p\Omega\mathsf{Co}\mathcal{J}\mathsf{Co}^T\left[\Psi_{rabc}\right].$$

Now, multiplying both sides of the above equation by $\mathsf{P}(\theta_e)^T\mathsf{Co}^T$, and using the following expressions:

$$\mathsf{P}(\theta_e)\mathcal{J}\mathsf{P}(\theta_e)^T = \mathcal{J}, \tag{1.49}$$

$$\mathsf{P}(\theta_e)[Diag]\mathsf{P}(\theta_e)^T = [Diag] \tag{1.50}$$

$$\mathsf{P}(\theta_e)\frac{d\mathsf{P}(\theta_e)^T}{dt} = \mathcal{J} \tag{1.51}$$

where $[Diag]$ is a diagonal matrix, after straightforward computations, we obtain the model of the PMSM in the (d, q) frame

$$\left[V_{sdq}\right] = R_s \left[I_{sdq}\right] + \mathsf{P}(\theta_e)^T \frac{d}{dt}\{[\Lambda_{ss}]\,\mathsf{P}(\theta_e)\}\left[I_{sdq}\right]$$

$$+ \mathsf{P}(\theta_e)^T [\Lambda_{ss}]\,\mathsf{P}(\theta_e)\frac{d}{dt}\left\{[I_{sdq}]\right\} - p\Omega\,\mathcal{J}\left[\Psi_{rdq}\right]. \qquad (1.52)$$

IPMSM case

Defining

$$[L_{dq}] = \mathsf{P}(\theta_e)^T \mathsf{Co}^T \left[\mathsf{L}_{ss}\right] \mathsf{CoP}(\theta_e)$$

$$= \begin{bmatrix} L_d & 0 \\ 0 & L_q \end{bmatrix}$$

$$= \begin{bmatrix} \dfrac{3(L_{so} + L_{sv})}{2} & 0 \\ 0 & \dfrac{3(L_{so} - L_{sv})}{2} \end{bmatrix} \qquad (1.53)$$

and assuming that the amplitude of the flux produced by the permanent magnets is constant, after some computations, the voltage equation of the IPMSM is given as

$$[V_{sdq}] = \{[R_s] - p\Omega[L_{dq}]\mathcal{J}\}[I_{sdq}] + [L_{dq}]\frac{d[I_{sdq}]}{dt} - p\Omega\,\mathcal{J}[\Psi_{rdq}]. \qquad (1.54)$$

Moreover, for a specific value of θ_e, the q-component of the rotor flux equal to zero (i.e., $\Psi_{rq} = 0$) and the d-component of the rotor flux equal to Ψ_r, ($\Psi_{rd} = \Psi_r$), it follows that

$$\begin{bmatrix} v_{sd} \\ v_{sq} \end{bmatrix} = \begin{bmatrix} R_s & -p\Omega L_q \\ p\Omega L_d & R_s \end{bmatrix}\begin{bmatrix} i_{sd} \\ i_{sq} \end{bmatrix} + \begin{bmatrix} L_d & 0 \\ 0 & L_q \end{bmatrix}\begin{bmatrix} \dfrac{di_{sd}}{dt} \\ \dfrac{di_{sq}}{dt} \end{bmatrix} - \begin{bmatrix} 0 \\ p\Omega\Psi_r \end{bmatrix}. \qquad (1.55)$$

> *The Electromagnetic model of the IPMSM in the rotor*
> *flux oriented (d,q) frame is*
> $$\frac{di_{sd}}{dt} = -\frac{R_s}{L_d}i_{sd} - p\Omega\frac{L_q}{L_d}i_{sq} + \frac{v_{sd}}{L_d} \qquad (1.56)$$
> $$\frac{di_{sq}}{dt} = -\frac{R_s}{L_q}i_{sq} + p\Omega\frac{L_d}{L_q}i_{sd} + \frac{v_{sq}}{L_q} - p\Omega\frac{\Psi_r}{L_q}.$$

1.4.3.3 Mechanical Equations

The rotor electrical position θ_e is determined by the equation

$$\frac{d\theta_e}{dt} = \omega. \qquad (1.57)$$

and the rotor speed Ω is given by

$$J\frac{d\Omega}{dt} + f_v\Omega = T_e - T_l \qquad (1.58)$$

where $\omega = p\Omega$, ω is the angular electrical speed, p is the pole pair number, Ω is the rotor angular speed, T_e is the electromagnetic torque, T_l is the load torque, J is the inertia moment, i.e., the inertia of the synchronous machine plus the load inertia, f_v is the viscous friction coefficient.

1.4.3.4 Electromagnetic Torque

IPMSM case

The electromagnetic torque T_e is generated by the interaction between the rotor magnets poles and the poles induced by the magnetomotive forces in the air gap. Then, the electromagnetic torque T_e is given as [17]

$$T_e = p(L_d - L_q)i_{sd}i_{sq} + p(\Psi_{rd}i_{sq} - \Psi_{rq}i_{sd}). \qquad (1.59)$$

Then replacing (1.59) in (1.58), it follows that

$$J\frac{d\Omega}{dt} + f_v\Omega = p(L_d - L_q)i_{sd}i_{sq} + p(\Psi_{rd}i_{sq} - \Psi_{rq}i_{sd}) - T_l. \qquad (1.60)$$

Furthermore, choosing the orientation of the (d, q) frame such that the q-component of the rotor flux is equal to zero ($\Psi_{rq} = 0$) and the d-component of the rotor flux is equal to Ψ_r ($\Psi_{rd} = \Psi_r$), then (1.60) can be expressed as follows

$$J\frac{d\Omega}{dt} + f_v\Omega = p(L_d - L_q)i_{sd}i_{sq} + p\Psi_r i_{sq} - T_l. \qquad (1.61)$$

The model of the IPMSM, in the rotor flux oriented (d, q) frame is

$$\frac{di_{sd}}{dt} = -\frac{R_s}{L_d}i_{sd} - p\Omega\frac{L_q}{L_d}i_{sq} + \frac{v_{sd}}{L_d}$$

$$\frac{di_{sq}}{dt} = -\frac{R_s}{L_q}i_{sq} + p\Omega\frac{L_d}{L_q}i_{sd} + \frac{v_{sq}}{L_q} - p\Omega\frac{\Psi_r}{L_q} \qquad (1.62)$$

$$\frac{d\Omega}{dt} = -\frac{f_v}{J}\Omega + \frac{1}{J}p(L_d - L_q)i_{sd}i_{sq} + p\Psi_r i_{sq} - \frac{1}{J}T_l.$$

SPMSM case

For the SPMSM, the stator inductances in the d-axis and q-axis are the same ($L_d = L_q = L_s$). The reluctance torque $p(L_d - L_q)i_{sd}i_{sq}$ is then equal to zero. The electromagnetic torque is only given as

$$T_e = p\Psi_r i_{sq}. \tag{1.63}$$

Equation (1.63) shows that the torque is proportional to the current in the q-axe. This confirms the analogy between this machine and the DC machine.

Replacing (1.63) in (1.61) with $L_d = L_q = L_s$, it follows that the rotor speed dynamics is given as

$$J\frac{d\Omega}{dt} = -f_v\Omega + p\Psi_r i_{sq} - T_l. \tag{1.64}$$

By combining the electric Eq. (1.56) with the mechanical Eq. (1.64), it follows that:

> *The complete model of the SPMSM, in the rotor*
>
> *flux oriented (d,q) frame, is*
>
> $$\frac{di_{sd}}{dt} = -\frac{R_s}{L_s}i_{sd} + p\Omega i_{sq} + \frac{v_{sd}}{L_s}$$
>
> $$\frac{di_{sq}}{dt} = -\frac{R_s}{L_s}i_{sq} - p\Omega i_{sd} + \frac{v_{sq}}{L_s} - p\Omega\frac{\Psi_r}{L_s} \qquad (1.65)$$
>
> $$\frac{d\Omega}{dt} = -\frac{f_v}{J}\Omega + \frac{p\Psi_r}{J}i_{sq} - \frac{1}{J}T_l.$$

1.4.4 Nonlinear Model in State-Space Representation

Generally, the behavior of a physical process and its interaction with the outside world can be mathematically modeled, and the resulting mathematical description is called the *system*. It interacts with the outside world in three different ways.

Inputs variables: (1) Input controls are variables that can be designed to influence the system dynamics, (2) perturbations are generally unmeasured external signals that have an effect on the system behavior but they are not controlled.

Output variables: Variables that are measured and/or for which the control objectives are defined. They are a subset of all the variables describing the system.

The state of the system represents all the variables of the system dynamics. It is represented by a vector, denoted by $x(t)$.

The evolution at time t of the system state is described by an ordinary differential equation

$$\dot{x}(t) = \mathbb{F}(x(t), u(t)) \tag{1.66}$$

with $\mathbb{F}$ is a smooth vector field. Furthermore, the relation between the state and the output is described by means of the function h as follows:

$$y(t) = h(x(t))$$

where the components of h are $\mathcal{C}^\infty$ functions (the class of functions continuously differentiable). Then a dynamical system is defined in a state-space representation, as follows:

$$\Sigma : \begin{cases} \dot{x}(t) = \mathbb{F}(x(t), u(t)) \\ y(t) = h(x(t)). \end{cases} \tag{1.67}$$

However, for most of the systems, the input acts in an affine manner and so the following representation is used:

$$\Sigma : \begin{cases} \dot{x} = f(x) + g(x)u \\ y = h(x). \end{cases} \tag{1.68}$$

This representation will be used for control design, while the representation (1.67) will be used for the dynamics observation analysis of all the AC machines studied in this book.

Usually, to obtain a model in a state-space representation of electric machines, it is necessary to define a vector state x, the input u, and the output y. Here, the vector state is represented by the electrical variables (currents) and the mechanical variables (speed and/or position). The input is mainly composed of the stator voltages. A special input: the disturbance forces the dynamics of the system but it is not controllable: the load torque T_l. The outputs are the stator currents and the mechanical speed. For the mechanical sensorless purpose only the currents are measured.

Now, the mathematical models of the PMSM (SPMSM or IPMSM) machines are introduced in a state-space representation, and will be used to the control and observer designs.

1.4.4.1 Model in the (d, q) Frame

For the torque or angular speed control, the nonlinear state-space model of the IPMSM (1.56) in the (d, q) frame, is given as

$$\begin{bmatrix} \dfrac{di_{sd}}{dt} \\[2ex] \dfrac{di_{sq}}{dt} \\[2ex] \dfrac{d\Omega}{dt} \end{bmatrix} = \begin{bmatrix} -\dfrac{R_s}{L_d}i_{sd} + \dfrac{pL_q}{L_d}i_{sq}\Omega \\[2ex] -\dfrac{R_s}{L_q}i_{sq} - \dfrac{pL_d}{L_q}i_{sd}\Omega - \dfrac{p\Psi_r}{L_q}\Omega \\[2ex] \dfrac{p\Psi_r}{J}i_{sq} - \dfrac{p(L_q - L_d)}{J}i_{sd}i_{sq} - \dfrac{f_v}{J}\Omega \end{bmatrix} + \begin{bmatrix} \dfrac{1}{L_d} & 0 & 0 \\[2ex] 0 & \dfrac{1}{L_q} & 0 \\[2ex] 0 & 0 & -\dfrac{1}{J} \end{bmatrix} \begin{bmatrix} v_{sd} \\[2ex] v_{sq} \\[2ex] T_l \end{bmatrix}$$

$$\tag{1.69}$$

where the state is $[i_{sd}, i_{sq}, \Omega]$, the input is $[v_{sd}, v_{sq}, T_l]$, where T_l is assumed to be an unknown input. The measurable output is the stator currents $[i_{sd}, i_{sq}]$.

For the rotor position control, it is necessary to take into account the rotor position θ_m as a new state variable.

The complete model of the IPMSM, in the rotor rotating frame, is

$$
\begin{bmatrix} \dfrac{di_{sd}}{dt} \\[2mm] \dfrac{di_{sq}}{dt} \\[2mm] \dfrac{d\Omega}{dt} \\[2mm] \dfrac{d\theta_m}{dt} \end{bmatrix} = \begin{bmatrix} -\dfrac{R_s}{L_d}i_{sd} + \dfrac{pL_q}{L_d}i_{sq}\Omega \\[2mm] -\dfrac{R_s}{L_q}i_{sq} - \dfrac{pL_d}{L_q}i_{sd}\Omega - \dfrac{p\Psi_r}{L_q}\Omega \\[2mm] \dfrac{p\Psi_r}{J}i_{sq} - \dfrac{p\left(L_q - L_d\right)}{J}i_{sd}i_{sq} - \dfrac{f_v}{J}\Omega \\[2mm] \Omega \end{bmatrix} + \begin{bmatrix} \dfrac{1}{L_d} & 0 & 0 \\[2mm] 0 & \dfrac{1}{L_q} & 0 \\[2mm] 0 & 0 & -\dfrac{1}{J} \\[2mm] 0 & 0 & 0 \end{bmatrix}\begin{bmatrix} v_{sd} \\[2mm] v_{sq} \\[2mm] T_l \end{bmatrix},
$$

$$(1.70)$$

where the state is now defined as $[i_{sd}, i_{sq}, \Omega, \theta_m]$, the input is $[v_{sd}, v_{sq}, T_l]$, and the measurable output is $[i_{sd}, i_{sq}, \Omega, \theta_m]$ or only $[i_{sd}, i_{sq}]$ for the sensorless case (i.e., without mechanical sensor).

Remark 1.1 The load torque T_l can also be considered as a component of the vector state or as an unknown parameter to be estimated. It depends on the observation strategy.

If the permanent magnet synchronous machine is without salient poles (SPMSM case), i.e., the inductances in d-axis and q-axis are equal ($L_d = L_q = L_s$), then model (1.70) becomes

$$
\begin{bmatrix} \dfrac{di_{sd}}{dt} \\[2mm] \dfrac{di_{sq}}{dt} \\[2mm] \dfrac{d\Omega}{dt} \\[2mm] \dfrac{d\theta_m}{dt} \end{bmatrix} = \begin{bmatrix} -\dfrac{R_s}{L_s}i_{sd} + pi_{sq}\Omega \\[2mm] -\dfrac{R_s}{L_s}i_{sq} - pi_{sd}\Omega - \dfrac{p\Psi_r}{L_s}\Omega \\[2mm] \dfrac{p\Psi_r}{J}i_{sq} - \dfrac{f_v}{J}\Omega \\[2mm] \Omega \end{bmatrix} + \begin{bmatrix} \dfrac{1}{L_s} & 0 & 0 \\[2mm] 0 & \dfrac{1}{L_s} & 0 \\[2mm] 0 & 0 & -\dfrac{1}{J} \\[2mm] 0 & 0 & 0 \end{bmatrix}\begin{bmatrix} v_{sd} \\[2mm] v_{sq} \\[2mm] T_l \end{bmatrix} \quad (1.71)
$$

where the vector state is $[i_{sd}, i_{sq}, \Omega, \theta_m]$, the input is $[v_{s\alpha}, v_{s\beta}, T_l]$, and the measurable output is $[i_{sd}, i_{sq}, \Omega]$. Notice that in this model, the load torque is considered as an input for the PMSM. For the sensorless case, the measurable output is only the stator currents $[i_{sd}, i_{sq}]$ (see Remark 1.1).

1.4.4.2 The Two-Phase Equivalent Model in the (α, β) Frame

The two-phase frame equivalent model of a three-phase motor, in the stator stationary (α, β) frame, is obtained from model (1.54) (see [14]), by using the transformation

$$\begin{bmatrix} x_{s\alpha} \\ x_{s\beta} \end{bmatrix} = \mathsf{P}(\theta_e) \begin{bmatrix} x_{sd} \\ x_{sq} \end{bmatrix}. \tag{1.72}$$

By multiplying the left side of the electric equation of the IPMSM by $\mathsf{P}(\theta_e)$, it follows that

$$[V_{sdq}] = \{[R_s] - p\Omega[L_{dq}]\mathcal{J}\}[I_{sdq}] + [L_{dq}]\frac{d[I_{sdq}]}{dt} - p\Omega\mathcal{J}[\Psi_{rdq}]. \tag{1.73}$$

By using (1.72) and the identity $\mathsf{P}(\theta_e)^T\mathsf{P}(\theta_e) = I_{2\times2}$ and after some simplifications, it can be rewritten as

$$\begin{aligned}
[V_{s\alpha\beta}] = {} & \mathsf{P}(\theta_e)\{[R_s] - p\Omega[L_{dq}]\mathcal{J}\}\mathsf{P}(\theta_e)^T[I_{s\alpha\beta}] \\
& + \mathsf{P}(\theta_e)[L_{dq}]\frac{d}{dt}\{\mathsf{P}(\theta_e)^T[I_{s\alpha\beta}]\} \\
& - p\Omega\mathsf{P}(\theta_e)\mathcal{J}\mathsf{P}(\theta_e)^T[\Psi_{r\alpha\beta}].
\end{aligned} \tag{1.74}$$

The following expressions hold:

$$\mathsf{P}(\theta_e)\mathcal{J}\mathsf{P}(\theta_e)^T = \mathcal{J}, \tag{1.75}$$

$$\mathsf{P}(\theta_e)[Diag]\mathsf{P}(\theta_e)^T = [Diag] \tag{1.76}$$

$$\mathsf{P}(\theta_e)\frac{d\mathsf{P}(\theta_e)^T}{dt} = \mathcal{J}. \tag{1.77}$$

It turns out that

$$[V_{s\alpha\beta}] = [R_s][I_{s\alpha\beta}] + [L_{dq}]\frac{d[I_{s\alpha\beta}]}{dt} - p\Omega\mathcal{J}[\Psi_{r\alpha\beta}] \tag{1.78}$$

or equivalently

$$\begin{bmatrix} v_{s\alpha} \\ v_{s\beta} \end{bmatrix} = \begin{bmatrix} R_s & 0 \\ 0 & R_s \end{bmatrix} \begin{bmatrix} i_{s\alpha} \\ i_{s\beta} \end{bmatrix} + \begin{bmatrix} L_d & 0 \\ 0 & L_q \end{bmatrix} \begin{bmatrix} \frac{di_{s\alpha}}{dt} \\ \frac{di_{s\beta}}{dt} \end{bmatrix} + \begin{bmatrix} -p\Omega\Psi_{r\alpha} \\ p\Omega\Psi_{r\beta} \end{bmatrix}. \tag{1.79}$$

The complete model of the IPMSM, in the stationary (α, β) frame, is given as

$$
\begin{bmatrix}
\dfrac{di_{s\alpha}}{dt} \\[2mm]
\dfrac{di_{s\beta}}{dt} \\[2mm]
\dfrac{d\Psi_{r\alpha}}{dt} \\[2mm]
\dfrac{d\Psi_{r\beta}}{dt} \\[2mm]
\dfrac{d\Omega}{dt} \\[2mm]
\dfrac{d\theta_m}{dt}
\end{bmatrix}
=
\begin{bmatrix}
\dfrac{-R_s}{L_d}i_{s\alpha} - \dfrac{\Psi_{r\alpha}}{L_d} \\[2mm]
\dfrac{-R_s}{L_q}i_{s\beta} + \dfrac{\Psi_{r\beta}}{L_q} \\[2mm]
-p\Omega\Psi_{r\beta} \\[2mm]
p\Omega\Psi_{r\alpha} \\[2mm]
\dfrac{p\Psi_r}{J}(i_{s\beta}\cos\theta_e - i_{s\alpha}\sin(\theta_e)) - \dfrac{f_v}{J}\Omega \\[2mm]
\Omega
\end{bmatrix}
+
\begin{bmatrix}
\dfrac{1}{L_d} & 0 & 0 \\[2mm]
0 & \dfrac{1}{L_q} & 0 \\[2mm]
0 & 0 & 0 \\[2mm]
0 & 0 & 0 \\[2mm]
0 & 0 & \dfrac{-1}{J} \\[2mm]
0 & 0 & 0
\end{bmatrix}
\begin{bmatrix}
v_{s\alpha} \\[2mm]
v_{s\beta} \\[2mm]
T_l
\end{bmatrix}
$$

$$(1.80)$$

where the vector state is $[i_{s\alpha}, i_{s\beta}, \Psi_{r\alpha}, \Psi_{r\beta}, \Omega, \theta_m]$, the input is $[v_{s\alpha}, v_{s\beta}, T_l]$, and the measurable output is $[i_{s\alpha}, i_{s\beta}, \Omega]$. For the sensorless case, the measurable output is composed by the stator currents $[i_{s\alpha}, i_{s\beta}]$.

Furthermore, define e_α and e_β as the electromotive forces that are expressed as

$$
\begin{cases}
e_{r\alpha} = -\sqrt{\frac{3}{2}}\Psi_r\omega\sin(\theta_e), \\[3mm]
e_{r\beta} = \sqrt{\frac{3}{2}}\Psi_r\omega\cos(\theta_e).
\end{cases}
\tag{1.81}
$$

Notice that the rotor electrical position is given as

$$
tg(\theta_e) = -\frac{e_{r\alpha}}{e_{r\beta}}.
\tag{1.82}
$$

The model of the IPMSM, in the stationary (α, β) frame, is

$$
\begin{bmatrix}
\dfrac{di_{s\alpha}}{dt} \\[2mm]
\dfrac{di_{s\beta}}{dt} \\[2mm]
\dfrac{de_{r\alpha}}{dt} \\[2mm]
\dfrac{de_{r\beta}}{dt} \\[2mm]
\dfrac{d\Omega}{dt} \\[2mm]
\dfrac{d\theta_m}{dt}
\end{bmatrix}
=
\begin{bmatrix}
\dfrac{-R_s}{L_d}i_{s\alpha} - \dfrac{e_{r\alpha}}{L_d} \\[2mm]
\dfrac{-R_s}{L_q}i_{s\beta} + \dfrac{e_{r\beta}}{L_q} \\[2mm]
-p\Omega e_{r\beta} \\[2mm]
p\Omega e_{r\alpha} \\[2mm]
\dfrac{p\Psi_r}{J}(i_{s\beta}\cos\theta_e - i_{s\alpha}\sin(\theta_e)) - \dfrac{f_v}{J}\Omega \\[2mm]
\Omega
\end{bmatrix}
+
\begin{bmatrix}
\dfrac{1}{L_d} & 0 & 0 \\[2mm]
0 & \dfrac{1}{L_q} & 0 \\[2mm]
0 & 0 & 0 \\[2mm]
0 & 0 & 0 \\[2mm]
0 & 0 & \dfrac{-1}{J} \\[2mm]
0 & 0 & 0
\end{bmatrix}
\begin{bmatrix}
v_{s\alpha} \\[2mm]
v_{s\beta} \\[2mm]
T_l
\end{bmatrix}.
$$

$$(1.83)$$

The model of the SPMSM, in the stationary (α, β) frame, is

$$
\begin{bmatrix}
\dfrac{di_{s\alpha}}{dt} \\[2mm]
\dfrac{di_{s\beta}}{dt} \\[2mm]
\dfrac{de_{r\alpha}}{dt} \\[2mm]
\dfrac{de_{r\beta}}{dt} \\[2mm]
\dfrac{d\Omega}{dt} \\[2mm]
\dfrac{d\theta_m}{dt}
\end{bmatrix}
=
\begin{bmatrix}
\dfrac{-R_s}{L_s}i_{s\alpha} - \dfrac{e_{r\alpha}}{L_s} \\[2mm]
\dfrac{-R_s}{L_s}i_{s\beta} + \dfrac{e_{r\beta}}{L_s} \\[2mm]
-p\Omega e_{r\beta} \\[2mm]
p\Omega e_{r\alpha} \\[2mm]
\dfrac{p\Psi_r}{J}(i_{s\beta}\cos\theta_e - i_{s\alpha}\sin(\theta_e)) - \dfrac{f_v}{J}\Omega \\[2mm]
\Omega
\end{bmatrix}
+
\begin{bmatrix}
\dfrac{1}{L_s} & 0 & 0 \\[2mm]
0 & \dfrac{1}{L_s} & 0 \\[2mm]
0 & 0 & 0 \\[2mm]
0 & 0 & 0 \\[2mm]
0 & 0 & \dfrac{-1}{J} \\[2mm]
0 & 0 & 0
\end{bmatrix}
\begin{bmatrix}
v_{s\alpha} \\[2mm]
v_{s\beta} \\[2mm]
T_l
\end{bmatrix}
$$

$$\tag{1.84}$$

with the vector state is $[i_{s\alpha}, i_{s\beta}, e_{r\alpha}, e_{r\beta}, \Omega, \theta_m]$, the input is $[v_{s\alpha}, v_{s\beta}, T_l]$, and the measurable output is $[i_{s\alpha}, i_{s\beta}, \Omega]$. In the sensorless case, the measurable output is $[i_{s\alpha}, i_{s\beta}]$.

1.5 Induction Motor

1.5.1 Motor Description and Modeling Assumptions

An induction machine can be decomposed into two main parts: stator and rotor. The stator is the static part of the machine with coils, most often three-phase, housed in slots and connected to the power source. The rotor is the rotating part of the machine that can be of two main types:

- *The coiled rotor*, which is of cylindrical form, carrying on coil windings in the interior of a magnetic circuit consisting of disks stacked on the machine shaft. The coil windings are usually identical to those of the stator. An electrical connection of the coil winding is available thanks to three rings and brushes.
- *Squirrel cage rotor*, which is the most common induction motor, is composed of a set of conductive bars placed around the periphery of the rotor forming a cylinder and connected to conducting end rings at each end. No electrical connection is necessary. The rotor coils are then in short-circuit and the rotor voltages are zero.

1.5.2 Dynamic Model of the Induction Motor

Electric and Mechanical Equations of the Induction Motor

The three-phase induction motor model is obtained from the application of the electromagnetic and mechanical principles.

The three-phase stator voltage equations, represented in a stationary (a, b, c) frame, can be expressed as

$$\left[V_{sabc} \right] = R_s \left[I_{sabc} \right] + \frac{d \left[\Phi_{sabc} \right]}{dt} \tag{1.85}$$

and

$$\left[V_{rabc} \right] = R_r \left[I_{rabc} \right] + \frac{d \left[\Phi_{rabc} \right]}{dt} \tag{1.86}$$

where $\left[V_{sabc} \right] = [v_{sa}, v_{sb}, v_{sc}]^T$ $\left(\left[V_{rabc} \right] = [v_{ra}, v_{rb}, v_{rc}]^T \right)$ are the voltages of each stator (rotor) phase; R_s is the stator resistance; $\left[I_{sabc} \right] = [i_{sa}, i_{sb}, i_{sc}]^T$ $\left(\left[I_{rabc} \right] = [i_{ra}, i_{rb}, i_{rc}]^T \right)$ are the phase stator (rotor) currents; and $\left[\Phi_{sabc} \right] = [\phi_{sa}, \phi_{sb}, \phi_{sc}]^T$ $\left(\left[\Phi_{rabc} \right] = [\phi_{ra}, \phi_{rb}, \phi_{rc}]^T \right)$ are the stator (rotor) fluxes.

Let Λ be the inductance matrix of the induction motor, which is defined as

$$\Lambda = \begin{bmatrix} \mathsf{L}_{os} & \mathsf{M}_{osr} \\ \mathsf{M}_{osr}^T & \mathsf{L}_{or} \end{bmatrix} \tag{1.87}$$

where

$$\mathsf{L}_{os} = \begin{bmatrix} l_{as} & M_{as} & M_{as} \\ M_{as} & l_{as} & M_{as} \\ M_{as} & M_{as} & l_{as} \end{bmatrix}, \quad \mathsf{L}_{or} = \begin{bmatrix} l_{ar} & M_{ar} & M_{ar} \\ M_{ar} & l_{ar} & M_{ar} \\ M_{ar} & M_{ar} & l_{ar} \end{bmatrix},$$

$$\mathsf{M}_{osr} = M \begin{bmatrix} \cos(p\theta_m) & \cos(p\theta_m + \frac{2\pi}{3}) & \cos(p\theta_m - \frac{2\pi}{3}) \\ \cos(p\theta_m - \frac{2\pi}{3}) & \cos(p\theta_m) & \cos(p\theta_m + \frac{2\pi}{3}) \\ \cos(p\theta_m + \frac{2\pi}{3}) & \cos(p\theta_m - \frac{2\pi}{3}) & \cos(p\theta_m) \end{bmatrix},$$

where θ_e is the electrical position with $\theta_e = p\theta_m$, l_{ar} are the self-inductances, M_{ar} is the mutual inductance between two rotor phases, and M_{as} is the mutual inductance between two stator phases.

The magnetic fluxes are given as

$$\left[\Phi_{sabc} \right] = \left[\mathsf{L}_{os} \right] \left[I_{sabc} \right] + \left[\mathsf{M}_{osr} \right] \left[I_{rabc} \right] \tag{1.88}$$

and

$$\left[\Phi_{rabc}\right] = \left[\mathsf{L}_{or}\right]\left[I_{rabc}\right] + \left[\mathsf{M}_{osr}\right]\left[I_{sabc}\right]. \tag{1.89}$$

Applying the Park transformation (1.47) to the electric equations (1.85) and (1.86), where θ_s is the (d, q) frame angular position and θ_r is the rotor relative angular position w.r.t. the (d, q) frame. Then, the equations of the squirrel cage induction motor in the (d, q) frame are given by

$$\left[V_{sdq}\right] = R_s\left[I_{sdq}\right] + \frac{d\left[\Phi_{sdq}\right]}{dt} - \frac{d\theta_s}{dt}\mathcal{J}\left[\Phi_{sdq}\right] \tag{1.90}$$

and

$$\left[V_{rdq}\right] = 0 = R_r\left[I_{rdq}\right] + \frac{d\left[\Phi_{rdq}\right]}{dt} - \frac{d\theta_r}{dt}\mathcal{J}\left[\Phi_{rdq}\right]. \tag{1.91}$$

Writting the magnetic fluxes (1.88) and (1.89), in the rotating (d, q) frame, yields:

$$\left[\Phi_{sdq}\right] = L_s\left[I_{sdq}\right] + M_{sr}\left[I_{rdq}\right] \tag{1.92}$$

and

$$\left[\Phi_{rdq}\right] = L_r\left[I_{rdq}\right] + M_{sr}\left[I_{sdq}\right] \tag{1.93}$$

where L_s, L_r are respectively the stator and rotor cyclic inductances and M_{sr} the mutual cyclic inductance.

From (1.90) and (1.91), the dynamics of the fluxes, expressed in the rotatory (d, q) frame, are given by

$$\frac{d\left[\Phi_{sdq}\right]}{dt} = -R_s\left[I_{sdq}\right] + \omega_s\mathcal{J}\left[\Phi_{sdq}\right] + \left[V_{sdq}\right] \tag{1.94}$$

and

$$\frac{d\left[\Phi_{rdq}\right]}{dt} = -R_r\left[I_{rdq}\right] + (\omega_s - p\Omega)\mathcal{J}\left[\Phi_{rdq}\right]. \tag{1.95}$$

Replacing (1.92) and (1.93) in (1.94) and (1.95) respectively, it follows that

$$\begin{bmatrix} L_s\dfrac{d[I_{sdq}]}{dt} + M_{sr}\dfrac{d[I_{rdq}]}{dt} \\ M_{sr}\dfrac{d[I_{sdq}]}{dt} + L_r\dfrac{d[I_{rdq}]}{dt} \end{bmatrix} = \begin{bmatrix} -R_s\left[I_{sdq}\right] + \omega_s\mathcal{J}\left[\Phi_{sdq}\right] + \left[V_{sdq}\right] \\ -R_r\left[I_{rdq}\right] + (\omega_s - p\Omega)\mathcal{J}\left[\Phi_{rdq}\right] \end{bmatrix} \tag{1.96}$$

Written (1.96) in terms of I_{rdq} and Φ_{rdq}, it follows that

$$
\frac{d[I_{sdq}]}{dt} = \left\{ -\frac{R_s}{L_s\sigma} I_{2x2} - \frac{R_r M_{sr}^2}{\sigma L_s L_r^2} I_{2x2} + \omega_s \mathcal{J} \right\} [I_{sdq}]
$$
$$
+ \left\{ \frac{R_r M_{sr}}{\sigma L_s L_r^2} I_{2x2} + \frac{M_{sr}}{\sigma L_s L_r} p\Omega \mathcal{J} \right\} [\Phi_{rdq}] + \frac{1}{L_s\sigma} [V_{sdq}] \quad (1.97)
$$

$$
\frac{d[\Phi_{rdq}]}{dt} = \left\{ \frac{R_r M_{sr}}{L_r} \right\} [I_{sdq}] + \left\{ -\frac{R_r}{L_r} I_{2x2} + (\omega_s - p\Omega)\mathcal{J} \right\} [\Phi_{rdq}] \ (1.98)
$$

where ω_s is the stator pulsation given by

$$
\omega_s = p\Omega + \frac{a M_{sr} i_{sq}}{\phi_{rd}}, \tag{1.99}
$$

σ is the Blondel leakage coefficient:

$$
\sigma = 1 - (M_{sr}^2/L_s L_r), \tag{1.100}
$$

and I_{2x2} is the identity matrix of dimension 2.

On the other hand,

$$
\frac{d\theta_s}{dt} = \omega_s \tag{1.101}
$$

$$
\frac{d\theta_m}{dt} = \Omega \tag{1.102}
$$

$$
\frac{d\theta_r}{dt} = \omega_r = \omega_s - p. \tag{1.103}
$$

Moreover, the electromagnetic torque T_e expressed in the (d, q) frame, is given by

$$
T_e = \frac{p M_{sr}}{L_r} (\phi_{rd} i_{sq} - \phi_{rq} i_{sd}). \tag{1.104}
$$

Equation (1.104) shows that the torque is a nonlinear function of fluxes and currents.

To obtain a complete model of the induction motor, it is necessary to add the mechanical equation

$$
\frac{d\Omega}{dt} = \frac{T_e}{J} - \frac{T_l}{J} - \frac{f_v}{J}\Omega
$$
$$
= \frac{1}{J} \left\{ \frac{p M_{sr}}{L_r} (\phi_{rd} i_{sq} - \phi_{rq} i_{sd}) \right\} - \frac{T_l}{J} - \frac{f_v}{J}\Omega. \tag{1.105}
$$

Then, the Induction Motor Model, in the rotating (d, q) frame, is given by

$$\frac{d[I_{sdq}]}{dt} = \left\{ -\frac{R_s}{L_s\sigma}I_{2\times2} - \frac{R_r M_{sr}^2}{\sigma L_s L_r^2}I_{2\times2} + \omega_s\mathcal{J} \right\} [I_{sdq}]$$
$$+ \left\{ \frac{R_r M_{sr}}{\sigma L_s L_r^2}I_{2\times2} + \frac{M_{sr}}{\sigma L_s L_r}p\Omega\mathcal{J} \right\} [\Phi_{rdq}] + \frac{1}{L_s\sigma}[V_{sdq}]$$
$$\frac{d[\Phi_{rdq}]}{dt} = \left\{ \frac{R_r M_{sr}}{L_r} \right\} [I_{sdq}] + \left\{ -\frac{R_r}{L_r}I_{2\times2} + (\omega_s - p\Omega)\mathcal{J} \right\} [\Phi_{rdq}] \quad (1.106)$$
$$\frac{d\Omega}{dt} = \frac{1}{J} \left\{ \frac{p M_{sr}}{L_r}(\phi_{rd}i_{sq} - \phi_{rq}i_{sd}) \right\} - \frac{T_l}{J} - \frac{f_v}{J}\Omega.$$

1.5.3 IM Model in the State-Space Representation

The state-space model of the induction motor requires to define the state x, the input u and the output y. Usually, the flux of the induction motor is not available through measurements, then the stator currents are selected as the measured output of the model. However, in the case of a control with a speed sensor, the speed is an additional measurable output.

Moreover, the load torque is considered as a bounded non-controlled input (usually unknown). The load torque could be also considered as a state variable which can be estimated by means of an observer.

The input of the model is composed by the stator voltages. The state vector consists of the currents, the magnetic variables (fluxes), and the mechanical variables (angular speed and the position when necessary). For the magnetic variables, we have considered the rotor fluxes instead of the stator fluxes. In the following, for modeling purpose, the rotating frame reference could be chosen according to the rotor field orientation.

1.5.3.1 IM Model in the Rotatory (d, q) Frame

Consider the induction motor model (1.106) written in the rotatory (d, q) frame:

$$\frac{di_{sd}}{dt} = -\gamma i_{sd} + \omega_s i_{sq} + ba\phi_{rd} + bp\Omega\phi_{rq} + m_1 v_{sd}$$
$$\frac{di_{sq}}{dt} = -\omega_s i_{sd} - \gamma i_{sq} - bp\Omega\phi_{rd} + ba\phi_{rq} + m_1 v_{sq}$$
$$\frac{d\phi_{rd}}{dt} = aM_{sr}i_{sd} - a\phi_{rd} + (\omega_s - p\Omega)\phi_{rq} \quad (1.107)$$
$$\frac{d\phi_{rq}}{dt} = aM_{sr}i_{sq} - (\omega_s - p\Omega)\phi_{rd} - a\phi_{rq}$$

$$\frac{d\Omega}{dt} = m(\phi_{rd}i_{sq} - \phi_{rq}i_{sd}) - c\Omega - \frac{1}{J}T_l$$

where a, b, c, γ, σ, m and m_1 are parameters defined as

$$a = R_r/L_r, \quad b = M_{sr}/\sigma L_s L_r, \quad c = f_v/J, \quad \gamma = (L_r^2 R_s + M_{sr}^2 R_r)/(\sigma L_s L_r^2),$$
$$\sigma = 1 - (M_{sr}^2/L_s L_r), \quad m = pM_{sr}/JL_r, \quad m_1 = 1/\sigma L_s.$$

Defining the state vector x_{dq}, the input u and the output y as

$$x_{dq} = \begin{bmatrix} i_{sd} \\ i_{sq} \\ \phi_{rd} \\ \phi_{rq} \\ \Omega \end{bmatrix}, \quad u = \begin{bmatrix} v_{sd} \\ v_{sq} \\ T_l \end{bmatrix}, \quad y = h(x_{dq}) = \begin{bmatrix} i_{sd} \\ i_{sq} \end{bmatrix},$$

where $x_{dq} \in \Re^5$, $u \in \Re^3$ and $y \in \Re^2$. Then the state-space dynamics of the IM (1.107), in the (d, q) frame, is given as

$$\begin{bmatrix} \frac{di_{sd}}{dt} \\ \frac{di_{sq}}{dt} \\ \frac{d\phi_{rd}}{dt} \\ \frac{d\phi_{rq}}{dt} \\ \frac{d\Omega}{dt} \end{bmatrix} = \begin{bmatrix} -\gamma i_{sd} + \omega_s i_{sq} + ba\phi_{rd} + bp\Omega\phi_{rq} \\ -\omega_s i_{sd} - \gamma i_{sq} - bp\Omega\phi_{rd} + ba\phi_{rq} \\ aM_{sr}i_{sd} - a\phi_{rd} + (\omega_s - p\Omega)\phi_{rq} \\ aM_{sr}i_{sq} - (\omega_s - p\Omega)\phi_{rd} - a\phi_{rq} \\ m(\phi_{rd}i_{sq} - \phi_{rq}i_{sd}) - c\Omega \end{bmatrix} + \begin{bmatrix} m_1 & 0 & 0 \\ 0 & m_1 & 0 \\ 0 & 0 & 0 \\ 0 & 0 & 0 \\ 0 & 0 & -\frac{1}{J} \end{bmatrix} \begin{bmatrix} v_{sd} \\ v_{sq} \\ T_l \end{bmatrix}$$

$$y = h(x_{dq}) = \begin{bmatrix} i_{sd} \\ i_{sq} \end{bmatrix}, \tag{1.108}$$

which is a nonlinear system of the form

$$\dot{x} = f(x) + g(x)u$$
$$y = h(x). \tag{1.109}$$

Notice that if the angular speed Ω is measurable, then the electric equations can be represented as

$$
\begin{bmatrix}
\dfrac{di_{sd}}{dt} \\[2mm]
\dfrac{di_{sq}}{dt} \\[2mm]
\dfrac{d\phi_{rd}}{dt} \\[2mm]
\dfrac{d\phi_{rq}}{dt}
\end{bmatrix}
=
\begin{bmatrix}
-\gamma & \omega_s & ba & bp\Omega \\
-\omega_s & -\gamma & -bp\Omega & ba \\
aM_{sr} & 0 & -a & (\omega_s - p\Omega) \\
0 & aM_{sr} & -(\omega_s - p\Omega) & -a
\end{bmatrix}
\begin{bmatrix}
i_{sd} \\
i_{sq} \\
\phi_{rd} \\
\phi_{rq}
\end{bmatrix}
+
\begin{bmatrix}
m_1 v_{sd} \\
m_1 v_{sq} \\
0 \\
0
\end{bmatrix}
$$

$$
y = h(x_{dq}) =
\begin{bmatrix}
i_{sd} \\
i_{sq} \\
\Omega
\end{bmatrix}
\tag{1.110}
$$

which can be expressed in a compact form as

$$
\begin{cases}
\dot{x} = A(\Omega(t))x + \phi(u(t)) \\
y = h(x).
\end{cases}
\tag{1.111}
$$

When the mechanical speed $\Omega(t)$ is available through measurements, then system (1.111) can be considered as a linear time variant system plus an injection term depending on the input, i.e.,

$$
\begin{cases}
\dot{x} = A(t)x + \phi(u(t)) \\
y = h(x).
\end{cases}
\tag{1.112}
$$

Furthermore, in the mechanical equation of (1.108), the load torque T_l is considered as perturbation. For robustness purpose, it could be necessary to estimate the load torque. Then, in order to overcome this difficulty a solution is to extend the state vector x by introducing the load torque T_l as a new state variable.

A way to model the load torque dynamics is to assume that T_l changes slowly or is piecewise constant. A good approximation of these dynamics is given as

$$
\frac{dT_l}{dt} = 0.
\tag{1.113}
$$

The extended nonlinear model of the induction motor (1.108), in the rotatory (d, q) frame, is then given as

$$
\begin{bmatrix}
\dfrac{di_{sd}}{dt} \\
\dfrac{di_{sq}}{dt} \\
\dfrac{d\phi_{rd}}{dt} \\
\dfrac{d\phi_{rq}}{dt} \\
\dfrac{d\Omega}{dt} \\
\dfrac{dT_l}{dt}
\end{bmatrix}
=
\begin{bmatrix}
-\gamma i_{sd} + \omega_s i_{sq} + ba\phi_{rd} + bp\Omega\phi_{rq} \\
-\omega_s i_{sd} - \gamma i_{sq} - bp\Omega\phi_{rd} + ba\phi_{rq} \\
aM_{sr}i_{sd} - a\phi_{rd} + (\omega_s - p\Omega)\phi_{rq} \\
aM_{sr}i_{sq} - (\omega_s - p\Omega)\phi_{rd} - a\phi_{rq} \\
m(\phi_{rd}i_{sq} - \phi_{rq}i_{sd}) - c\Omega - \dfrac{1}{J}T_l \\
0
\end{bmatrix}
+
\begin{bmatrix}
m_1 & 0 \\
0 & m_1 \\
0 & 0 \\
0 & 0 \\
0 & 0 \\
0 & 0
\end{bmatrix}
\begin{bmatrix}
v_{sd} \\
v_{sq}
\end{bmatrix}
\quad (1.114)
$$

with a state vector $x_{dq} = \begin{bmatrix} i_{sd} & i_{sq} & \phi_{rd} & \phi_{rq} & \Omega & T_l \end{bmatrix}^T$.

If the angular speed Ω is available through measurement, system (1.114) can be rewritten in a special form:

Cascade model of the IM, in the rotating (d, q) frame

$$
\begin{bmatrix}
\dfrac{di_{sd}}{dt} \\
\dfrac{di_{sq}}{dt} \\
\dfrac{d\phi_{rd}}{dt} \\
\dfrac{d\phi_{rq}}{dt}
\end{bmatrix}
=
\begin{bmatrix}
-\gamma & \omega_s & ba & bp\Omega \\
-\omega_s & -\gamma & -bp\Omega & ba \\
aM_{sr} & 0 & -a & (\omega_s - p\Omega) \\
0 & aM_{sr} & -(\omega_s - p\Omega) & -a
\end{bmatrix}
\begin{bmatrix}
i_{sd} \\
i_{sq} \\
\phi_{rd} \\
\phi_{rq}
\end{bmatrix}
+
\begin{bmatrix}
m_1 v_{sd} \\
m_1 v_{sq} \\
0 \\
0
\end{bmatrix}
$$

$$
y_1 = \begin{bmatrix} i_{sd} \\ i_{sq} \end{bmatrix}
$$

$$
\begin{bmatrix}
\dfrac{d\Omega}{dt} \\
\dfrac{dT_l}{dt}
\end{bmatrix}
=
\begin{bmatrix}
-c & -\dfrac{1}{J} \\
0 & 0
\end{bmatrix}
\begin{bmatrix}
\Omega \\
T_l
\end{bmatrix}
+
\begin{bmatrix}
m(\phi_{rd}i_{sq} - \phi_{rq}i_{sd}) \\
0
\end{bmatrix}
$$

$$
y_2 = \begin{bmatrix} \Omega \end{bmatrix}. \quad\quad (1.115)
$$

If the rotor position and the angular speed are not available by measurement, other alternative representation has to be used to estimate the fluxes, load torque, and rotor resistance of the IM from the only measurement of the stator currents. Furthermore, assuming that the load torque and the stator resistance are slowly varying with respect to the electromagnetic time constant, the dynamics of these two variables can be approximated by

$$\frac{dT_l}{dt} = 0, \quad \frac{dR_s}{dt} = 0. \tag{1.116}$$

Remark 1.2 The load torque T_l is an unknown variable. Only its bound is assumed available. The stator resistance R_s changes with the temperature. The resistance value bound is also available. Thus the load torque and stator resistance values are assumed to be approximated by piecewise constant functions.

Define $\gamma = \gamma_1 + m_1 R_s$, where $\gamma_1 = M_{sr}^2 R_r / \sigma L_s L_r^2$. Thus, without the mechanical sensors, the extended IM model (1.115) may be seen as the interconnection between the subsystems:

$$
\begin{bmatrix} \dfrac{di_{sd}}{dt} \\ \dfrac{d\Omega}{dt} \\ \dfrac{dR_s}{dt} \end{bmatrix} = \begin{bmatrix} 0 & bp\phi_{rq} & -m_1 i_{sd} \\ -m\phi_{rq} & -c & 0 \\ 0 & 0 & 0 \end{bmatrix} \begin{bmatrix} i_{sd} \\ \Omega \\ R_s \end{bmatrix}
$$
$$
+ \begin{bmatrix} -\gamma_1 i_{sd} + ab\phi_{rd} + m_1 u_{sd} + \omega_s i_{sq} \\ m\phi_{rd} i_{sq} \\ 0 \end{bmatrix} + \begin{bmatrix} 0 \\ -\dfrac{1}{J} \\ 0 \end{bmatrix} T_l \tag{1.117}
$$
$$
y_1 = i_{sd}
$$

and

$$
\begin{bmatrix} \dfrac{di_{sq}}{dt} \\ \dfrac{d\phi_{rd}}{dt} \\ \dfrac{d\phi_{rq}}{dt} \end{bmatrix} = \begin{bmatrix} -\gamma_1 & -bp\Omega & ab \\ 0 & -a & -p\Omega \\ 0 & p\Omega & -a \end{bmatrix} \begin{bmatrix} i_{sq} \\ \phi_{rd} \\ \phi_{rq} \end{bmatrix}
$$
$$
+ \begin{bmatrix} -m_1 R_s i_{sq} - \omega_s i_{sd} + m_1 u_{sq} \\ \omega_s \phi_{rq} + a M_{sr} i_{sd} \\ -\omega_s \phi_{rd} + a M_{sr} i_{sq} \end{bmatrix} \tag{1.118}
$$
$$
y_2 = i_{sq}
$$

or, in a compact form:

$$
\Sigma_1 : \begin{cases} \dot{X}_1 = A_1(X_2, y)X_1 + g_1(u, y, X_2, X_1) + \Phi T_l \\ y_1 = C_1 X_1 \end{cases}
$$

$$
\Sigma_2 : \begin{cases} \dot{X}_2 = A_2(X_1)X_2 + g_2(u, y, X_1, X_2) \\ y_2 = C_2 X_2 \end{cases} \tag{1.119}
$$

with

$$A_1(\cdot) = \begin{bmatrix} 0 & bp\phi_{rq} & -m_1 i_{sd} \\ -m\phi_{rq} & -c & 0 \\ 0 & 0 & 0 \end{bmatrix}, \quad g_1(\cdot) = \begin{bmatrix} \omega_s i_{sq} - \gamma_1 i_{sd} + ab\phi_{rd} + m_1 u_{sd} \\ m\phi_{rd} i_{sq} \\ 0 \end{bmatrix}$$

$$A_2(\cdot) = \begin{bmatrix} -\gamma_1 & -bp\Omega & ab \\ 0 & -a & -p\Omega \\ 0 & p\Omega & -a \end{bmatrix}, \quad g_2(\cdot) = \begin{bmatrix} -m_1 R_s i_{sq} - \omega_s i_{sd} + m_1 u_{sq} \\ \omega_s \phi_{rq} + a M_{sr} i_{sd} \\ -\omega_s \phi_{rd} + a M_{sr} i_{sq} \end{bmatrix}$$

$$\Phi = \begin{bmatrix} 0 \\ -\dfrac{1}{J} \\ 0 \end{bmatrix}, \qquad C_1 = C_2 = [\, 1 \; 0 \; 0 \,],$$

and $X_1 = [i_{sd} \; \Omega \; R_s]^T$ and $X_2 = [i_{sq} \; \phi_{rd} \; \phi_{rq}]^T$ are the state vectors; $u = [u_{sd} \; u_{sq}]^T$ is the input, and $y = [i_{sd} \; i_{sq}]^T$ is the output of the IM model. Finally, T_l is considered as an unknown parameter which can be identified by means of an observer (see Remark 1.2).

1.5.3.2 IM Model in the Stator Fixed (α, β) Frame

The nonlinear model of the induction motor, written in the fixed (α, β) frame, can be easily obtained from model (1.108) in the (d, q) frame, by imposing the projection angle θ_s and its derivative equal to zero ($\theta_s = 0$ and $\dot{\theta}_s = \omega_s = 0$). Then the state vector x, the input u, and the output y, on (α, β) frame, are given as

$$x_{\alpha\beta} = \begin{bmatrix} i_{s\alpha} \\ i_{s\beta} \\ \phi_{r\alpha} \\ \phi_{r\beta} \\ \Omega \end{bmatrix}, \quad u = \begin{bmatrix} v_{s\alpha} \\ v_{s\beta} \\ T_l \end{bmatrix}, \quad y = \begin{bmatrix} i_{s\alpha} \\ i_{s\beta} \end{bmatrix}.$$

The model of the induction motor, in the (α, β) frame, is given as

$$\begin{bmatrix} \dfrac{di_{s\alpha}}{dt} \\ \dfrac{di_{s\beta}}{dt} \\ \dfrac{d\phi_{r\alpha}}{dt} \\ \dfrac{d\phi_{r\beta}}{dt} \\ \dfrac{d\Omega}{dt} \end{bmatrix} = \begin{bmatrix} -\gamma i_{s\alpha} + ba\phi_{r\alpha} + bp\Omega\phi_{r\beta} \\ -\gamma i_{s\beta} - bp\Omega\phi_{r\alpha} + ba\phi_{r\beta} \\ a M_{sr} i_{s\alpha} - a\phi_{r\alpha} - p\Omega\phi_{r\beta} \\ a M_{sr} i_{s\beta} + p\Omega\phi_{r\alpha} - a\phi_{r\beta} \\ m(\phi_{r\alpha} i_{s\beta} - \phi_{r\beta} i_{s\alpha}) - c\Omega \end{bmatrix} + \begin{bmatrix} m_1 & 0 & 0 \\ 0 & m_1 & 0 \\ 0 & 0 & 0 \\ 0 & 0 & 0 \\ 0 & 0 & -\dfrac{1}{J} \end{bmatrix} \begin{bmatrix} v_{s\alpha} \\ v_{s\beta} \\ T_l \end{bmatrix} \quad (1.120)$$

Furthermore, assuming that the load torque changes slowly, and considering the load torque as a component of the state vector, it follows that the extended model of the induction motor, in the (α, β) frame, is given as

$$
\begin{bmatrix}
\dfrac{di_{s\alpha}}{dt} \\[4pt]
\dfrac{di_{s\beta}}{dt} \\[4pt]
\dfrac{d\phi_{r\alpha}}{dt} \\[4pt]
\dfrac{d\phi_{r\beta}}{dt} \\[4pt]
\dfrac{d\Omega}{dt} \\[4pt]
\dfrac{dT_l}{dt}
\end{bmatrix}
=
\begin{bmatrix}
-\gamma i_{s\alpha} + ba\phi_{r\alpha} + bp\Omega\phi_{r\beta} \\[4pt]
-\gamma i_{s\beta} - bp\Omega\phi_{r\alpha} + ba\phi_{r\beta} \\[4pt]
aM_{sr}i_{s\alpha} - a\phi_{r\beta} - p\Omega\phi_{r\beta} \\[4pt]
aM_{sr}i_{s\beta} + p\Omega\phi_{r\alpha} - a\phi_{r\beta} \\[4pt]
m(\phi_{r\alpha}i_{s\beta} - \phi_{r\beta}i_{s\alpha}) - c\Omega - \dfrac{1}{J}T_l \\[4pt]
0
\end{bmatrix}
+
\begin{bmatrix}
m_1 & 0 \\
0 & m_1 \\
0 & 0 \\
0 & 0 \\
0 & 0 \\
0 & 0
\end{bmatrix}
\begin{bmatrix}
v_{s\alpha} \\
v_{s\beta}
\end{bmatrix}
\quad (1.121)
$$

where the components of the state vector are $x_{\alpha\beta} = \begin{bmatrix} i_{s\alpha} & i_{s\beta} & \phi_{r\alpha} & \phi_{r\beta} & \Omega & T_l \end{bmatrix}^T$. Assuming that the rotor speed Ω is available through measurements, the IM model can also be represented as two interconnected subsystems (electric-magnetic and mechanical parts) in the following form:

$$
\begin{bmatrix}
\dfrac{di_{s\alpha}}{dt} \\[4pt]
\dfrac{di_{s\beta}}{dt} \\[4pt]
\dfrac{d\phi_{r\alpha}}{dt} \\[4pt]
\dfrac{d\phi_{r\beta}}{dt}
\end{bmatrix}
=
\begin{bmatrix}
-\gamma & 0 & ba & bp\Omega \\
0 & -\gamma & -bp\Omega & ba \\
aM_{sr} & 0 & -a & -p\Omega \\
0 & aM_{sr} & p\Omega & -a
\end{bmatrix}
\begin{bmatrix}
i_{s\alpha} \\
i_{s\beta} \\
\phi_{r\alpha} \\
\phi_{r\beta}
\end{bmatrix}
+
\begin{bmatrix}
m_1 v_{s\alpha} \\
m_1 v_{s\beta} \\
0 \\
0
\end{bmatrix}
\quad (1.122)
$$

$$
\begin{bmatrix}
\dfrac{d\Omega}{dt} \\[4pt]
\dfrac{dT_l}{dt}
\end{bmatrix}
=
\begin{bmatrix}
-c & \dfrac{-1}{J} \\
0 & 0
\end{bmatrix}
\begin{bmatrix}
\Omega \\
T_l
\end{bmatrix}
+
\begin{bmatrix}
m(\phi_{r\alpha}i_{s\beta} - \phi_{r\beta}i_{s\alpha}) \\
0
\end{bmatrix}
\quad (1.123)
$$

$$
y =
\begin{bmatrix}
i_{s\alpha} \\
i_{s\beta} \\
\Omega
\end{bmatrix}.
\quad (1.124)
$$

1.5.3.3 IM Model in the Rotating (d, q) Frame Associated to the Rotor Flux

Model (1.108) in the (d, q) frame depends on the stator pulsation ω_s. This pulsation can be calculated by using a specific orientation of the (d, q) frame, i.e., the d-axe

coincides with the rotor flux vector. Therefore, the component of the flux in quadrature (q-axe) as well as its derivative vanish, i.e.,

$$\phi_{rq} \equiv \frac{d\phi_{rq}}{dt} \equiv 0. \tag{1.125}$$

Defining $d\rho/dt = \omega_s$, where ρ is the field angle, and using the fact that (1.125) holds; so from Eq. (1.108), it follows that

$$\frac{d\rho}{dt} = \omega_s = p\Omega + \frac{aM_{sr}}{\phi_{rd}}i_{sq}. \tag{1.126}$$

The electromagnetic torque (1.104) becomes

$$T_e = \frac{pM_{sr}}{L_r}\phi_{rd}i_{sq}. \tag{1.127}$$

The nonlinear model of the induction motor, expressed in the rotating (d, q) frame associated to the rotor field, is obtained directly from the general model (1.108). By replacing the stator pulsation ω_s and the differential equation of ϕ_{rq} by the time differential equation of ρ in (1.108) yields

$$
\begin{bmatrix} \dfrac{di_{sd}}{dt} \\ \dfrac{di_{sq}}{dt} \\ \dfrac{d\phi_{rd}}{dt} \\ \dfrac{d\rho}{dt} \\ \dfrac{d\Omega}{dt} \end{bmatrix} =
\begin{bmatrix} -\gamma i_{sd} + ab\phi_{rd} + p\Omega i_{sq} + a\dfrac{M_{sr}}{\phi_{rd}}i_{sq}^2 \\ -\gamma i_{sq} - bp\Omega\phi_{rd} - p\Omega i_{sd} - a\dfrac{M_{sr}}{\phi_{rd}}i_{sd}i_{sq} \\ -a\phi_{rd} + aM_{sr}i_{sd} \\ p\Omega + a\frac{M_{sr}}{\phi_{rd}}i_{sq} \\ m\phi_{rd}i_{sq} - c\Omega \end{bmatrix} +
\begin{bmatrix} m_1 & 0 & 0 \\ 0 & m_1 & 0 \\ 0 & 0 & 0 \\ 0 & 0 & 0 \\ 0 & 0 & -\dfrac{1}{J} \end{bmatrix}
\begin{bmatrix} v_{sd} \\ v_{sq} \\ T_l \end{bmatrix}.
$$

The measurable output is

$$y = \begin{bmatrix} i_{sd} \\ i_{sq} \end{bmatrix}. \tag{1.128}$$

From Eq. (1.126), the *slip pulsation* ω_r is defined as

$$\omega_r = \omega_s - p\Omega \tag{1.129}$$

where $\omega_r = \dfrac{aM_{sr}}{\phi_{rd}}i_{sq}.$

1.6 Operating Conditions and Benchmark

All the observer and control algorithms presented in this book are evaluated in the framework of specific trajectories and significant robustness tests noted "Benchmarks". These benchmarks have been defined, on the one hand, in cooperation with the Electrical Engineering and Automatic Control Laboratories under the support of the french National CNRS Work Group "Control of Electrical Systems," and on the other hand in cooperation with Electrical Industrial Companies.

1.6.1 Benchmarks for AC Machines
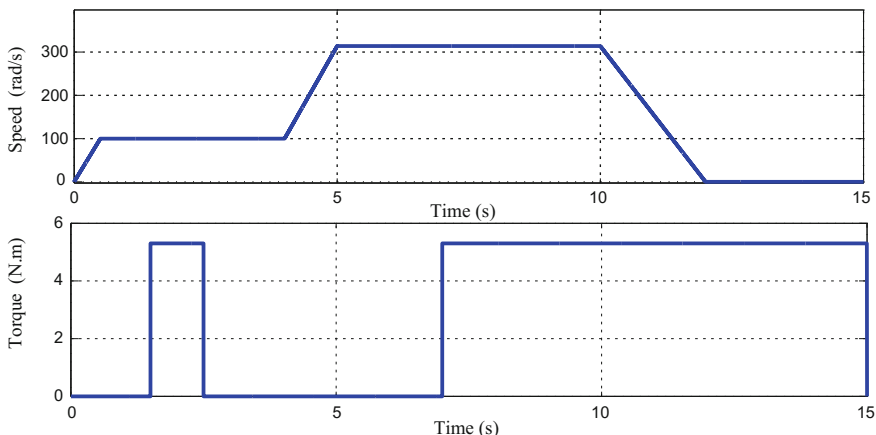
Permanent Magnet Synchronous Motor Benchmark

The motor is tested according to industrial test trajectories (see [34] for details). Following the nominal values of the torque, the speed and the flux of a PMSM motor, the reference trajectories are defined (see Fig. 1.4) such that, at initial time, the rotor speed and the load torque values are zero.

Then the reference speed is carried to 100 rad/s; and from 1.5 to 2.5 s, the load torque is applied. This first step is to test the performance and the robustness of the controller-observer without mechanical sensors at low speed.

From 4 to 5 s, the speed is carried out to its nominal value (300 rad/s) and remains constant until $t = 10$ s.

From $t = 10$ to 12 s, the rotor speed is reduced to zero and is maintained thereafter. The load torque is applied from 7 to 15 s.


Fig. 1.4 PMSM industrial benchmark trajectories; *top* reference speed ω_m; *bottom* load torque disturbance T_l

Robustness with respect to parameter variations and unknown load torque

The stator resistance as well as the stator inductance can vary from their nominal values. So their deviation effects are studied. Significant robustness tests are defined by stator, rotor resistance variations, stator, rotor inductance variations, and load torque variations:

- ±50 % of resistance variation,
- ±20 % of inductance variation,
- ±100 % of nominal load torque.

Induction Motor Benchmark

The experimental test takes place on a significant benchmark. The trajectories of this benchmark have been considered taking into account industrial operation conditions.

Following the nominal values of the torque, the rotor speed and the flux of an induction motor, the reference trajectories are defined (see Fig. 1.5) such that, at the initial time, the speed and the load torque references are chosen as zero until the flux reaches its nominal value. Then the reference speed is carried to 20 rad/s and from 1.5 to 2.5 s the load torque is applied. This first step tests the performance and the robustness of the controller+observer without mechanical sensors at low speed.

From $t = 3$ to 4 s, the speed is carried out to its nominal value (100 rad/s) and remains constant until $t = 6$ s. The load torque is applied from the time 5 s.

Unobservability test

This second step is defined to test the controller+observer behavior without mechanical sensors, during a great transient speed and the robustness performance at high speed. Then the motor is driven to reach a negative constant low speed value from 7 s until 9 s. This speed is chosen to obtain a stator pulsation equal to zero. This last step tests the robustness of the controller-observer scheme in case of an unobservability phenomena (introduced latter in Chap. 2) in the time interval from $t = 7$ to 9 s, as shown in [31].

Finally, the induction motor is driven in order to leave the unobservability conditions.
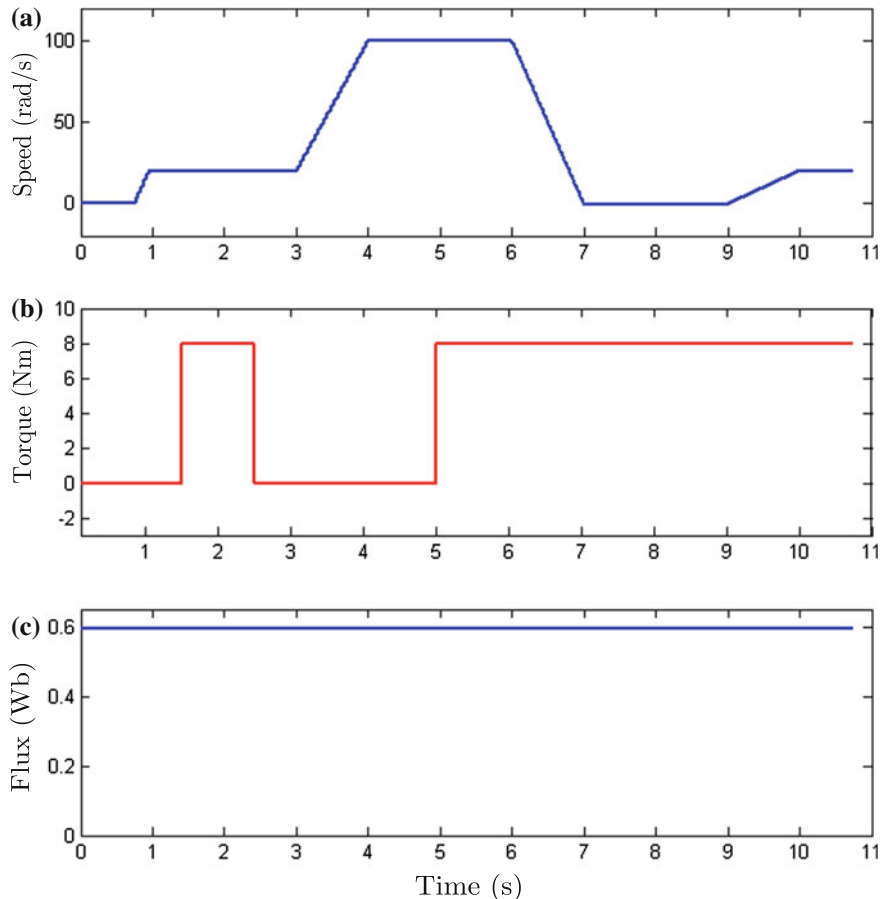
Robustness with respect to parameter variations and unknown load torque

Moreover, significant robustness tests are defined by stator, rotor resistance variations, stator, rotor inductance variations, and load torque variations:

- ±50 % of resistance variation,
- ±20 % of inductance variation,
- ±100 % of nominal load torque.

1.6.2 Experimental Setup

Most of the observer-controller schemes presented in this book have been experimentally tested on a setup allowing to drive synchronous motors (PMSM and
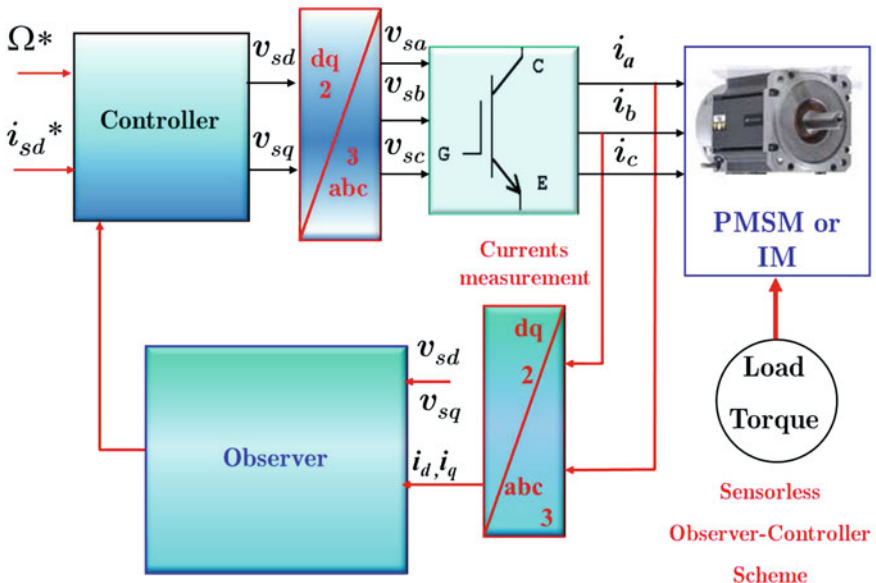
Fig. 1.5 IM benchmark trajectories. **a** Reference speed ω_m, **b** load torque disturbance T_l, **c** reference flux ϕ_{rd}^*

IPMSM) and induction motors. A load torque is applied thanks to a connected synchronous motor that is load controlled by means of a torque sensor and an industrial drive (see Figs. 1.6 and 1.7). More precisely, the experimental setup is equipped with:

Hardware characteristics

1. Three-phase inverter operated by a symmetrical Pulse Width Modulation (PWM) with a 5 kHz switching frequency,
2. A permanent magnet synchronous motor controlled by an industrial drive to provide the desired load torque.
3. A custom floating-point digital signal processor dSPACE (DS1103) board, and its interface. The dSPACE board performs data acquisition: two stator currents, DC-link voltage, load torque, and rotor speed, with a 512 ppr incremental encoder that

Fig. 1.6   Observer-controller scheme

**Fig. 1.7**   IRCCyN experimental setup

supplies the speed (of course, only for monitoring purpose in case of the sensorless tests). The DS1103 board also allows to compute the control algorithm and to generate the PWM signals sent to the power inverter system.

Software characteristics

The software associated with the data acquisition and the control system are:

(1) Matlab/Simulink,
(2) A user-developed interface between the Simulink Controller-Observer program and the dSPACE system board.

The algorithms are implemented in the dSPACE board and have a maximal time computational cost of $100\,\mu s$. The experimental sampling time T is taken to $200\,\mu s$.

Permanent Magnet Synchronous Motor characteristics

The parameters of the SPMSM used to test the controller and observer algorithms are reported in Table 1.1.

The parameters of the IPMSM used to evaluate the control and observer algorithms are reported in Table 1.2.

Induction Motor characteristics

All the control and observer algorithms designed in this book will be tested using a 1.5 kW Induction Motor, whose data are reported in Tables 1.3 and 1.4.

Table 1.1 Nominal SPMSM parameters

Current	9.67 A	Torque	9 Nm
Speed	3,000 rpm	Ψ_r	0.18 Wb
R_s	0.45 ohm	p	3
L_d	3.42 mH	L_q	3.42 mH
J	0.00679 kg $\cdot$ m^2	f_v	0.004 kg $\cdot$ m^2

Table 1.2 Nominal IPMSM parameters

Current	6 A	Torque	5.3 Nm
Speed	3,000 rpm	Ψ_r	0.341 Wb
R_s	3.25 ohm	p	3
L_d	18 mH	L_q	34 mH
J	0.00417 kg $\cdot$ m^2	f_v	0.0034 kg $\cdot$ m^2

Table 1.3 Nominal induction motor parameters values of the setup

Nominal rate power	1.5 kW
Nominal angular speed	1,430 rpm
Number of pole pairs	2
Nominal voltage	220 V
Nominal current	7.5 A

Table 1.4 Induction motor identified parameters

R_s	1.633Ω	M_{sr}	0.099H
R_r	0.93Ω	J	0.0111 Nm $\cdot$ s^2/rad
L_s	0.142H	f_v	0.0018 Nm $\cdot$ s/rad
L_r	0.076H		

1.7 Conclusions

In this chapter, an overview of typical applications for AC machines has been first given. In particular, it has been reminded that one of the most attractive applications of AC machines is the traction system of electric vehicles and hybrid electric vehicles. A general view on the state of the art for such vehicles and traction systems has been presented.

Then the models allowing to describe the dynamical behavior of the AC machines (PMSM and IM) have been introduced. These models have been expressed either in a fixed (α, β) frame or in a rotating (d, q) frame in order to describe the dynamical behavior of these machines.

Taking into account industrial considerations, specific benchmarks (test procedures) have been defined to apply significant tests and to evaluate the performance of the sensorless IM and PMSM controllers. These benchmarks will be used to test all the proposed controller and observer strategies developed in this book. Finally, the experimental setup as well as the associated characteristics of the PMSM, IPMSM, and induction motor have been described.

1.8 Bibliographical Notes

Many papers are devoted to the introduction of the dynamical models of AC machines. Only the references directly consulted for the writing of this chapter are now listed. The main point of AC machines modeling is to simplify the complexity of the model by using appropriate transformations, from three-phase model to two-phase model associated to fixed or rotating frames. More precisely, to apply these transformations to AC machine models, some assumptions are necessary: see [54]. For detailed introductions to these modeling approaches, the reader can refer to the books: [17, 33].

The modeling of the synchronous motor can be classified according to the electromotive force as introduced in [9, 91]. The permanent magnet synchronous motor model is identical to the classical synchronous machine model, except that the rotor flux is represented by the constant flux of the magnets. Then the model is obtained from the classical synchronous machine model: [17, 33]. The induction motor model is also introduced. Details on its model can be also found in [17, 33].

After introducing the different models of AC machines (synchronous and induction machines), in this chapter, significant reference trajectories are introduced in order to check the performance of the observer-controller algorithms described in the following chapters (see [22, 31, 34] for details).

Chapter 2
Observability Property of AC Machines

Abstract In many cases the implementation of control algorithms requires the knowledge of all the components of the state vector. However, because of the high cost of sensors, the reduction of the physical space inside or around the motor, the weight, or the increase of the system complexity, it is often necessary to limit the number of sensors. A similar situation arises when a sensor breaks down. A solution to avoid these difficulties is to eliminate the sensors by replacing them with soft sensors, which are well known as observers in control theory. The soft sensor can also be used to increase the reliability by redundancy with respect to hardware sensors. However, before designing an observer, it is necessary to verify if the system satisfies the observability property. Several techniques and tools have been developed to study whether a nonlinear system is observable or not. Generally, the observability property of a nonlinear system can depend on the inputs. An analysis of the inputs applied to the system is then required to verify if there exist some input that renders the system unobservable. It is clear that in this case the observer may not work correctly. Usually, these inputs are used to control the system, so they are necessary. It is possible to deal with this problem by introducing a class of inputs for which it is conceivable to construct an observer. These inputs are called persistent inputs: inputs with a sufficient quantity of information, so that the observability property is retained. Regarding AC machines, an intrinsic characteristic is that the observability property of the machines is, in most cases, lost at low speed. This phenomenon limits the implementation or degrades the performance of the control algorithms. Then, from the mathematical model of AC machines, a study of the observability property has to be made. If this property is satisfied from the only available measurements, i.e., currents and voltages, the next step is to check if a nonlinear observer can be designed to estimate the nonmeasurable variables, in order to be able to implement the control algorithms.

2.1 Observability Property of AC Machines

The purpose of this chapter is first to introduce definitions and concepts about the observability theory and observer normal forms for nonlinear systems, and then to apply these concepts to AC machines. More precisely, for the PMSM it will be shown

that if the angle position and/or rotor speed are not measurable, it is necessary to check under which conditions the machine is observable. Similarly, it will be shown that for IM, since the rotor flux is not easily measurable and if the rotor speed measurement is not available, then the observability of the machine is affected. This information can be used to know if it is possible to reconstruct the nonmeasurable components of the state.

A way to reconstruct the state of the system is the use of an *observer*. An observer is a mathematical algorithm (often called *soft sensor*) which is able to reconstruct the state of the system from the limited information obtained from the measured output and the input.

In this chapter, the observation problem of nonlinear systems is presented. Contrary to the linear systems, the observability of the nonlinear systems can depend on the applied input. Taking into account this difficulty, definitions and concepts to determine if a nonlinear system is observable will be introduced.

It is well known that if a linear system is observable, it is possible to design an observer to reconstruct the nonmeasurable state. However, for nonlinear system, even if the system is observable, it is not obvious how to design an observer. To overcome this difficulty some solutions have been proposed. For example, there is a class of nonlinear systems that, by means of a diffeomorphism, can be transformed into a linear system plus an input–output injection, for which it is possible to design an observer, called the nonlinear Luenberger observer.

On the other hand, there is another class of nonlinear systems, such that after a transformation of coordinates, can be represented into a nonlinear system for which the observability property is preserved for any input. For this class of systems several results have been proposed how to design an observer.

By contrast, there is a class of nonlinear systems where the observability depends on the input, i.e., there are inputs rendering the system unobservable. However, for such a class of systems the observability property can be preserved provided the input is persistent [3]. In this case, the observer design is possible for such a class of nonlinear systems, working in the presence of inputs that render the system unobservable.

Taking into account the above, note that there is no normal (canonical) observability form for general nonlinear systems, for which it is possible to construct an observer.

The purpose of this chapter is to analyze the observability property of the PMSM and the IM, and to establish the conditions to reconstruct the nonmeasurable state of these machines.

More precisely, first, an analysis of the observability property for nonlinear systems is presented. After that, since the observability of the system depends on the input, definitions on the different classes of inputs will be introduced. Finally, several structures have been introduced for which it is possible to design an observer.

2.2 Observability

First of all, what is observability? The answer to this question is: *Observability is the possibility to reconstruct the full trajectory of the system from the data obtained from the input and output measurements.*

2.2.1 Observability of Linear Systems

The observability theory of linear systems is well known. The main result is the observability of the linear systems only requires the output measurements and thus does not depend on the input applied to the system. The methodology to verify this property is based on the Kalman criteria of observability. This criteria is verified from the structural representation of the linear system.

The observability of a linear system can be established as follows:

A time invariant linear system is represented by

$$\begin{cases} \dot{x} = Ax + Bu \\ y = Cx \end{cases} \tag{2.1}$$

where $x(t) \in \mathfrak{R}^n$ represents the state, $u(t) \in \mathfrak{R}^m$ is the input and $y(t) \in \mathfrak{R}^p$ is the output; and A, B, and C are matrices of compatible dimensions. System (2.1) is observable, if and only if the observability matrix $\mathcal{O}_{A,C}$

$$\mathcal{O}_{A,C} = \begin{bmatrix} C \\ CA \\ \vdots \\ CA^{(n-1)} \end{bmatrix}$$

has full rank, i.e., $rank\mathcal{O}_{A,C} = n$, where n is the dimension of the system.

Notice that this condition is independent of the input applied to the system. Furthermore, this result can be extended to the Linear Time-Variant systems.

2.2.2 Observability of Nonlinear Systems

In this section, the observability property of a nonlinear system will be investigated.

Furthermore, since the observability of a nonlinear system can be lost, tools to verify under what conditions a nonlinear system are observable will be introduced.

The observability analysis of a nonlinear system can be divided into two main cases when:

(1) the observability property of the system is independent of the input,
(2) the observability property depends on the input.

For the class of systems where the observability property does not depend on the input, we can find some normal (canonical) forms for which it is possible to design an observer. This class of nonlinear systems, which can be transformed into such a canonical form is called the *u uniformly observable systems class*.

However, if the observability property can be lost when an input is applied to the system, the observer design becomes more difficult and it is necessary to take into account this class of inputs.

On the other hand, several methodologies have been proposed to estimate the state of nonlinear systems. A classical approximate methodology to design an observer is to apply linear techniques to estimate the system state. The first step is the approximate linearization of the nonlinear system around an equilibrium point. The resulting linearized system can be used to design an observer. Of course, this observer can only be efficient around the equilibrium point. Another way to construct an observer is based on the algorithm called the Extended Kalman Filter.

The Extended Kalman Filter is widely used, because its design is relatively simple and this observer gives good results for the nonlinear system observation. However, there is no theoretical justification concerning its effectiveness and no analytic proof of convergence. The observer works in a neighborhood of a particular point, which limits its dynamic performance. Another possibility to design an observer for a nonlinear system is to transform it into another system for which a class of observers is known. For this purpose, several methodologies have been proposed to transform a nonlinear system into particular classes of general nonlinear systems. For example, in [46] for the SISO case and in [75] for the MIMO case, a nonlinear system is transformed into a linear system (or a linear system plus an output injection) for which it is possible to design a linear observer called a *General Luenberger Observer*. When this transformation does not exist, it is possible to search to transform the nonlinear system to a linear time-variant system plus an input–output injection for which an exact Kalman Like Observer can be designed [83].

An Extension of the Kalman Filter (EKF) for the deterministic nonlinear systems is the high gain observer provided that the system can be transformed into a canonical representation, for which the observability property is satisfied for any input.

Before introducing the main results of the observability theory for the nonlinear systems, we introduce some definitions and concepts from the nonlinear control theory [65].

Let q be a point in E^n, a n-dimensional Euclidean space, and U a neighborhood of q.

Let $\varphi(q) = (x_1(q), \ldots, x_n(q)) : U \rightarrow V \subset \Re^n$ be a homeomorphism, that is bijective, with φ and φ^{-1} continuous. (U, φ) is called a coordinate neighborhood or coordinate chart and the real numbers $x_1(q), \ldots, x_n(q)$; which vary continuously are local coordinates of $q \in E^n$, $x_i(q)$ is called the ith coordinate function.

If both φ and φ^{-1} are smooth maps, φ is called a diffeomorphism. If both φ and φ^{-1} are defined in $\Re^n$ and are smooth maps, φ is called a global diffeomorphism.

Given two coordinates neighborhoods (U, φ) and (W, ψ), with $U \cap W \neq 0$ where $\varphi(q) = (x_1(q), \dots, x_n(q))$, and $\psi(q) = (z_1(q), \dots, z_n(q))$. The homeomorphism

$$\psi \circ \varphi^{-1} : \Re^n \to \Re^n$$

is a coordinate transformation in $U \cap W$, i.e.,

$$z(x) = \psi \circ \varphi^{-1}(x).$$

If x and z are represented by vectors with n components, namely

$$x = \begin{bmatrix} x_1 \\ \vdots \\ x_n \end{bmatrix}, \quad z = \begin{bmatrix} z_1 \\ \vdots \\ z_n \end{bmatrix} \tag{2.2}$$

the coordinate transformations are expressed by n real valued continuous functions defined in $\Re^n$, i.e.,

$$x = \begin{bmatrix} x_1(z_1, \dots, z_n) \\ \vdots \\ x_n(z_1, \dots, z_n) \end{bmatrix}, \quad z = \begin{bmatrix} z_1(x_1, \dots, x_n) \\ \vdots \\ z_n(x_1, \dots, x_n) \end{bmatrix}. \tag{2.3}$$

A well-known result from calculus which provides a sufficient condition for a map to be a diffeomorphism is given next.

Theorem 2.1 (Inverse Function) *Let U an open subset of $\Re^n$ and let $\varphi = (\varphi_1, \dots \varphi_n) : U \to \Re^n$ be a smooth map. If the Jacobian matrix*

$$\frac{\partial \varphi}{\partial x} = \begin{bmatrix} \dfrac{\partial \varphi_1}{\partial x_1} & \cdots & \dfrac{\partial \varphi_1}{\partial x_n} \\ \cdots & \cdots & \cdots \\ \dfrac{\partial \varphi_n}{\partial x_1} & \cdots & \dfrac{\partial \varphi_n}{\partial x_n} \end{bmatrix} \tag{2.4}$$

is nonsingular at some point $p \in U$, then there exists a neighborhood $V \subset U$ of q such that $\varphi : V \to \varphi(V)$ is a diffeomorphism.

Let $h : U \subset E^n \to \Re$ be a real-valued function defined on U. Depending on the coordinate neighborhoods (U, φ) chosen, the function h is expressed in local coordinates as

$$h_\varphi = h \circ \varphi^{-1} : \Re^n \to \Re.$$

The expression h_φ depends on the chosen local coordinates.

The differential of a smooth function $h : U \subset E^n \rightarrow \Re$ is defined in local coordinates as

$$dh = \frac{\partial h}{\partial x_1} dx_1 + \cdots + \frac{\partial h}{\partial x_n} dx_n \tag{2.5}$$

and may be seen as the product of a row vector with the differential column vector of the state

$$dh = \left[\frac{\partial h}{\partial x_1}, \ldots, \frac{\partial h}{\partial x_n} \right] dx . \tag{2.6}$$

Consider the following class of nonlinear systems of the form

$$\begin{cases} \dot{x}(t) = \mathbb{F}(x(t), u(t)) \\ y(t) = h(x(t)) \end{cases} \tag{2.7}$$

where $x(t) \in \Re^n$ represents the state, $u(t) \in \Re^m$ is the input and $y(t) \in \Re^p$ is the output; $\mathbb{F}$ is a smooth vector field and h is C^∞ function.

Definition 2.1 ([46]) The Lie derivative of the function h_i along the vector field $\mathbb{F}$ is defined as

$$L_{\mathbb{F}} h_i(x) = \frac{\partial h_i}{\partial x} \mathbb{F}.$$

Furthermore, $dL_{\mathbb{F}}^j h_i$, $i = 1, \ldots, p$; $j = 1, \ldots, m$; are the differentials of the Lie derivative of function h_i along the vector field $\mathbb{F}$, denoted as

$$dL_{\mathbb{F}}^j h_i = \frac{\partial L_{\mathbb{F}}^{j-1} h_i}{\partial x} \mathbb{F}.$$

2.2.2.1 Observability and Classes of Inputs

For a complete study of the observability property, we now introduce some definitions on the observability of nonlinear systems [42].

Definition 2.2 (*Indistinguishability*) For system (2.7), two points x and $\bar{x} \in \Re^n$ are indistinguishable if for every applied input

$$u(t), \qquad \forall T > 0$$

the outputs $h(x(t))$ and $h(\bar{x}(t))$ are identical on $[0, T]$, where x and $\bar{x}$ are the trajectories, issues of x and $\bar{x}$ at time $t = 0$.

Note $\mathbb{I}(x_o)$ the set of all points that are indistinguishable from x_0.

Definition 2.3 (*Observability*)

System (2.7) is observable at x_o, if $\mathbb{I}(x_o) = x_o$.
System (2.7) is observable, if $\mathbb{I}(x) = x$ for all $x \in \Re^n$.

Furthermore, for any pair of distinct points $(x, \overline{x})$, there exists an input which distinguishes them on the interval $[0, T]$, for $T > 0$.

Notice that observability is a global concept. A local concept, which is stronger than the observability, will be defined.

Definition 2.4 Let be $x_0 \in \Re^n$ and $V \subset \Re^n$ a neighborhood of x_0. $x_1 \in V$ is said V-indistinguishable of x_0, if x_1 is indistinguishable of x_0.

A weaker result is that which consists to distinguish a point from its neighborhood.

Definition 2.5 (*Weak Observability*) System (2.7) is said weakly observable if $\forall x_0 \in W$, there exists a neighborhood V of x_0 such that $W \subset V$, $\mathbb{I}_W(x_0) = x_0$.

Definition 2.6 The observation space of a system is defined as the smallest real vector space, denoted by $\mathcal{O}(h)$, of C^∞ functions containing the components of h and closed under Lie derivation along the field $\mathbb{F}(x, u)$ for any constant input u.

For linear systems, Definitions 2.3 and 2.5 are equivalent and result in the algebraic criterion known as the Kalman's observability criterion recalled before.

Definition 2.7 (*Observability rank condition* [45]) System (2.7) is said to satisfy the observability rank condition in x if

$$dim\{d\mathcal{O}(h)\} = n.$$

Furthermore, if the observability rank condition holds $\forall x \in \Re^n$, then system (2.7) is observable in the rank sense.

Theorem 2.2 *If system* (2.7) *is observable in the rank sense, then it is weakly observable.*

Additional conditions may be used to design an observer for nonlinear systems. For that, we introduce an important class of inputs for which the observability property is satisfied to design an observer independently of the input.

Definition 2.8 An input is universal on the interval $[0, T]$, for $T > 0$, if it distinguishes all pairs of distinct points on the interval $[0, T]$.

Definition 2.9 A system is uniformly observable if every input is universal.

Now, consider the class of multioutput nonlinear systems

$$\begin{cases} \dot{x} = f(x) & x \in \Re^n \\ y = h(x) & y \in \Re^p \end{cases} \tag{2.8}$$

where $h_1, \ldots, h_p$ are smooth functions, $dh_1, \ldots, dh_p$ are linearly independent in $\Re^n$, f is a smooth vector field.

Definition 2.10   A system is locally observable if every state x_o can be distinguished from its neighborhoods by using system trajectories remaining close to x_o.

Theorem 2.3   *System* (2.8) *is locally observable at x_o if*

$$rank\{dh_i, \ldots, dL_f^j h_i, i = 1, \ldots, p; j \geq 0\} = n \tag{2.9}$$

$\forall x \in U_0 \subset \Re^n$.

Observability indices may be defined for locally observable systems satisfying (2.9).

Definition 2.11   (*Observability Indices* [65]) A set of observability indices $\{k_1, \ldots, k_p\}$ is uniquely associated at x to system (2.8), satisfying (2.9) as follows

$$k_i = card\{\mathcal{S}_j \geq i, j \geq 0\}, i = 1, \ldots, p. \tag{2.10}$$

where

$$\mathcal{S}_0 = rank\{dh_i, i = 1, \ldots, p.\} \tag{2.11}$$

$$\cdots$$

$$\begin{aligned}
\mathcal{S}_k = {} & rank\{dh_i, \ldots, dL_f^k h_i, i = 1, \ldots, p.\} \\
& - rank\{dh_i, \ldots, dL_f^{k-1} h_i, i = 1, \ldots, p.\}
\end{aligned} \tag{2.12}$$

$$\cdots$$

$$\begin{aligned}
\mathcal{S}_{n-1} = {} & rank\{dh_i, \ldots, dL_f^{n-1} h_i, i = 1, \ldots, p.\} \\
& - rank\{dh_i, \ldots, dL_f^{n-2} h_i, i = 1, \ldots, p.\}
\end{aligned} \tag{2.13}$$

Then, the observability property can be verified as follows:

Definition 2.12   (*Locally Weakly Observability*) The system (2.8) is locally weakly observable at x^0 if there exists $U(x^0)$, and p integers $\{k_1, \ldots, k_p\}$ that form the smallest p-tuple with respect to the lexicographic ordering, such that

$$\text{(i)} \qquad k_1 \geq k_2 \geq \cdots \geq k_p \geq 0; \tag{2.14}$$

$$\text{(ii)} \qquad \sum_{i=1}^{p} k_i = n; \tag{2.15}$$

$$
\text{(iii)} \qquad rank \begin{bmatrix} dh_1 \\ dL_f h_1 \\ \vdots \\ dL_f^{k_1-1} h_1 \\ \vdots \\ dh_p \\ dL_f h_p \\ \vdots \\ dL_f^{k_p-1} h_p \end{bmatrix} = n \tag{2.16}
$$

for all $x \in U(x^0)$.

Nonlinear Transformations

Generally, the design of an observer for nonlinear systems is not an easy task. However, it turns out that by means of a change in coordinates (a diffeomorphism), the original nonlinear system can be transformed into another system for which it is easier to design an observer.

Now, some concepts concerning the transformation of a nonlinear system into a special class of system are introduced.

Given r smooth real-valued functions $\{\varphi_1, \ldots, \varphi_r\}$ in U, then

$$
rank\{d\varphi_1, \ldots, d\varphi_r\} = r
$$

in $q \in U$, is equivalent to

$$
rank \begin{bmatrix} \dfrac{\partial \varphi_1}{\partial x_1} & \cdots & \dfrac{\partial \varphi_1}{\partial x_r} \\ \cdots & \cdots & \cdots \\ \dfrac{\partial \varphi_r}{\partial x_1} & \cdots & \dfrac{\partial \varphi_r}{\partial x_r} \end{bmatrix} = r \tag{2.17}
$$

for $x = q$.

Theorem 2.4 (Inverse Function Theorem) *If $rank\{d\varphi_1, \ldots, d\varphi_n\} = n$ at some point $q \in U$ an open subset of $\Re^n$, then there exists a neighborhood $V \subset U$ of q such that $\varphi : V \to \varphi(V)$ is a diffeomorphism.*

Definition 2.13 Two systems Σ_1 and Σ_2 are locally diffeomorphic in $x_0 \in \Re^n$, if and only if there exists a diffeomorphism Ψ, defined on a neighborhood of x_0, transforming Σ_1 into Σ_2.

Theorem 2.5 *There exists a set of functions $\phi_1(x), \ldots, \phi_n(x)$ of observation space $\mathcal{O}(\phi)$ such that $\Psi = (\phi_1(x), \ldots, \phi_n(x))^T$ is a diffeomorphism on $\Re^n$, then system (2.7) is observable.*

Consider the following nonlinear system

$$\begin{cases} \dot{x} = f(x) + g(x)u, & x \in \Re^n, \qquad u \in \Re \\ y = h(x), & y \in \Re. \end{cases} \tag{2.18}$$

Necessary and sufficient conditions are obtained such that an observable nonlinear system of the form (2.18) can be transformed into a system of the form

$$\begin{cases} \dot{x} = Ax + \phi(y, u) \\ y = Cx \end{cases} \tag{2.19}$$

where the term $\phi(y, u)$ is an output–input injection, (see [46] for the SISO case, and [75] for the MIMO case). For this class of system, an extended Luenberger observer can be designed.

Furthermore, the system can be transformed into another nonlinear system for which it is possible to design an observer, for instance, transformed into the state affine system

$$\begin{cases} \dot{x} = A(u)x + \phi(y, u) \\ y = Cx \end{cases} \tag{2.20}$$

or in the general form

$$\begin{cases} \dot{x} = A(u, y)x + \phi(y, u) \\ y = Cx \end{cases} \tag{2.21}$$

where the matrices $A(u)$ and $A(u, y)$ have particular forms (see [3] for more details).

2.3 Permanent Magnet Synchronous Motor Observability Analysis (PMSM)

One of the most important difficulty to control the synchronous motor is when the speed and the position are not available from measurement. This can affect the observability properties of the machine. Significant improvements have been made in the area of the sensorless control of the permanent magnet synchronous motors. However, to implement such a controller, it is necessary to reconstruct the state of the motor. Then, before designing an observer it is necessary to investigate the observability property of the permanent magnet synchronous motor.

It will be shown by the following observability study that an interesting field of research is related to the high-performance sensorless position control of synchronous machines. It involves zero speed control at a determined rotor position. An additional problem is the observer structure is strongly dependent on

machine parameters. The position estimation is generally difficult due to scalar speed estimation. Theoretically, the position can be calculated by integrating the speed, but in practice the result will suffer drift problems and moreover the initial position is not always known. There are three main methods to estimate the position: tracking observer based, tracking state filter, and arctangent calculation based. The position estimation of the arctangent direct calculation has no time delay. However, it suffers from large position estimation error due to the noise. The effect of noise can be mitigated by using a state filter but the estimate has lagging fault.

The first methods used to solve the sensorless position estimation are the approaches using the back Electromotive Force (EMF) with fundamental excitation, and spatial salience image, the tracking methods using excitation in addition. The salience tracking methods are suitable for zero-speed operation, whereas the back EMF-based methods fail at low speed.

To know the variety of different methods for sensorless control, it is very important to understand the dynamics properties of the electric machines.

2.3.1 IPMSM Observability Analysis

To verify if the Internal Permanent Magnet Synchronous Motor (IPMSM) is observable, it is assumed that the magnetic flux is not saturated, the magnetic field is sinusoidal, and the influence of the magnetic hysteresis is negligible on the IPMSM.

Observation Objective: *by using only the measurement of the currents and voltages, to simultaneously reconstruct (online) the rotor speed, position, load torque, and stator resistance value of the IPMSM.*

Now, we show under which conditions the IPMSM is observable. The observability analysis is made in two steps:

- From the stator currents and its first time derivatives, the observability of the speed and the position will be studied in the (α, β) frame.
- Secondly, to analyze the observability of the system including the stator resistance and the load torque, higher time derivatives of the stator current measurements will be taken into account.
  For simplicity, this second step of the observability analysis is made by using the IPMSM equations in the (d, q) frame.

2.3.1.1 Observability Analysis of the Speed ω and the Position θ_e in the (α, β) Frame

In this section, the IPMSM observability properties will be analyzed in open loop, assuming that all the parameters are known.

Consider the IPMSM electric equations, in the stationary (α, β) frame, given as

$$
\begin{bmatrix} \dfrac{di_{s\alpha}}{dt} \\ \dfrac{di_{s\beta}}{dt} \end{bmatrix} = (\Lambda_{ss})^{-1} \left\{ -\begin{pmatrix} R_s - 2\omega L_{\alpha\beta} & 2\omega L_1 \cos(2\theta_e) \\ 2\omega L_1 \cos(2\theta_e) & R_s + 2\omega L_{\alpha\beta} \end{pmatrix} \begin{pmatrix} i_{s\alpha} \\ i_{s\beta} \end{pmatrix} \right.
$$
$$
\left. - p\Omega\Psi_r \begin{pmatrix} -\sin\theta_e \\ \cos\theta_e \end{pmatrix} + \begin{pmatrix} v_{s\alpha} \\ v_{s\beta} \end{pmatrix} \right\} \tag{2.22}
$$

where

$$
(\Lambda_{ss})^{-1} = \frac{1}{L_d L_q} \begin{pmatrix} L_\beta & -L_{\alpha\beta} \\ -L_{\alpha\beta} & L_\alpha \end{pmatrix}. \tag{2.23}
$$

The determinant $Det(\Lambda_{ss})$ is given as

$$
Det(\Lambda_{ss}) = L_\alpha L_\beta - \left(L_{\alpha\beta}\right)^2 = L_0^2 - L_1^2 = L_d L_q, \tag{2.24}
$$

where

$$
L_\alpha = L_0 + L_1 \cos(2\theta_e),\ L_\beta = L_0 - L_1 \cos(2\theta_e),\ L_{\alpha\beta} = L_1 \sin(2\theta_e). \tag{2.25}
$$

and

$$
L_0 = \frac{L_d + L_q}{2}, \quad L_1 = \frac{L_d - L_q}{2}. \tag{2.26}
$$

Moreover, the mechanical equations of the IPMSM are

$$
\begin{cases} J\dfrac{d\Omega}{dt} = -f\Omega + 2pL_1 i_{s\alpha} i_{s\beta} + p(\Psi_{r\alpha} i_{s\beta} - \Psi_{r\beta} i_{s\alpha}) - T_l \\ \dfrac{d\theta_m}{dt} = \Omega. \end{cases} \tag{2.27}
$$

Then, the complete model is given as

$$
\begin{cases} \begin{bmatrix} \dfrac{di_{s\alpha}}{dt} \\ \dfrac{di_{s\beta}}{dt} \end{bmatrix} = (\Lambda_{ss})^{-1} \left\{ -\begin{bmatrix} R_s - 2\omega L_{\alpha\beta} & 2\omega L_1 \cos(2\theta_e) \\ 2\omega L_1 \cos(2\theta_e) & R_s + 2\omega L_{\alpha\beta} \end{bmatrix} \begin{bmatrix} i_{s\alpha} \\ i_{s\beta} \end{bmatrix} \right. \\ \qquad\qquad \left. - p\Omega\Psi_r \begin{bmatrix} -\sin\theta_e \\ \cos\theta_e \end{bmatrix} \right\} + (\Lambda_{ss})^{-1} \begin{bmatrix} v_{s\alpha} \\ v_{s\beta} \end{bmatrix} \\ \dfrac{d\Omega}{dt} = -\dfrac{f}{J}\Omega + \dfrac{2pL_1}{J} i_{s\alpha} i_{s\beta} + \dfrac{p}{J}(\Psi_{r\alpha} i_{s\beta} - \Psi_{r\beta} i_{s\alpha}) - \dfrac{1}{J}T_l \\ \dfrac{d\theta_m}{dt} = \Omega \end{cases}
$$

which is of the general form

$$\begin{cases} \dfrac{dX_{\alpha\beta}}{dt} = \mathbb{F}(X_{\alpha\beta}, v_{\alpha\beta}) \\ y \quad = h(X_{\alpha\beta}) \end{cases} \tag{2.28}$$

where

$$X_{\alpha\beta} = \begin{bmatrix} i_{s\alpha} \\ i_{s\beta} \\ \Omega \\ \theta_m \end{bmatrix}, \quad v_{\alpha\beta} = \begin{bmatrix} v_{s\alpha} \\ v_{s\beta} \end{bmatrix}, \quad h(X_{\alpha\beta}) = \begin{bmatrix} h_1 \\ h_2 \end{bmatrix} = \begin{bmatrix} i_{s\alpha} \\ i_{s\beta} \end{bmatrix},$$

and $X_{\alpha\beta}$ is the state, $v_{\alpha\beta}$ is the input, and $h(X_{\alpha\beta})$ is the measurable output whose components are the stator currents $i_{s\alpha}$ and $i_{s\beta}$.

The observation space $\mathcal{O}_{\alpha\beta}(X_{\alpha\beta})$ containing the components of h_1, h_2; and closed under Lie derivation along the field $\mathbb{F}$, is given by (see [46])

$$\mathcal{O}_{\alpha\beta}(X_{\alpha\beta}) = \{h_1, h_2, L_{\mathbb{F}}h_1, L_{\mathbb{F}}h_2\}.$$

Then, the observability analysis of the IPMSM is made by verifying if the matrix

$$d\mathcal{O}_{\alpha\beta}(X_{\alpha\beta}) = \begin{bmatrix} dh_1 \\ dh_2 \\ dL_{\mathbb{F}}h_1 \\ dL_{\mathbb{F}}h_2 \end{bmatrix} \tag{2.29}$$

satisfies the condition of Theorem 2.3, i.e., the rank of $d\mathcal{O}_{\alpha\beta}(X_{\alpha\beta})$ is equal to $n = 4$.

It is equivalent to determine if matrix $d\mathcal{O}_{\alpha\beta}$ is nonsingular, which implies to evaluate the determinant of the matrix $d\mathcal{O}_{\alpha\beta}$ given by:

$$\begin{aligned} Det\,(d\mathcal{O}_{\alpha\beta}) = {} & \frac{2L_1\Psi_r(L_0+L_1)}{Det\,(\Lambda_{ss})^2}(v_{s\alpha}\sin\theta_e - v_{s\beta}\cos\theta_e) \\ & - \frac{2R_sL_1\Psi_r(L_0+L_1)}{Det\,(\Lambda_{ss})^2}(i_{s\alpha}\sin\theta_e - i_{s\beta}\cos\theta_e) \\ & + \frac{\Psi_r^2\omega(L_0+L_1)^2}{Det\,(\Lambda_{ss})^2} + \frac{4L_1^2L_0}{Det\,(\Lambda_{ss})^2}(i_{s\beta}v_{s\alpha} - i_{s\alpha}v_{s\beta}) \\ & + \frac{8L_1L_0\Psi_r\omega(L_0+L_1)(i_{s\alpha}\cos\theta_e + i_{s\beta}\sin\theta_e)}{Det\,(\Lambda_{ss})^2} \\ & + \frac{4L_1^3 i_{s\beta}}{Det\,(\Lambda_{ss})^2}(v_{s\alpha}\cos 2\theta_e + v_{s\beta}\sin 2\theta_e) \\ & + \frac{4L_1^3 i_{s\alpha}}{Det\,(\Lambda_{ss})^2}(v_{s\alpha}\sin 2\theta_e - v_{s\beta}\cos 2\theta_e) \end{aligned}$$

$$+ \left[\frac{8L_1^2 L_0^2 \omega - 4R_s L_1^3 \sin 2\theta_e + 8L_1^3 L_0 \omega \cos 2\theta_e}{Det\,(\Lambda_{ss})^2} \right] (i_{s\alpha}^2 + i_{s\beta}^2)$$

$$+ \frac{2L_1^2 \Psi_r \omega (L_0 + L_1)}{Det\,(\Lambda_{ss})^2} (i_{s\alpha} \cos \theta_e - i_{s\beta} \sin \theta_e).$$

Analyzing the expression of $Det\,(d\mathcal{O}_{\alpha\beta})$, it can be remarked that, for $\omega \neq 0$, $Det\,(d\mathcal{O}_{\alpha\beta})$ cannot be null. Thus, we can first conclude that the IPMSM is observable if $\omega \neq 0$.

For $\omega = 0$, a complementary study is now developed. Using the following transformation

$$v_{sq} = -v_{s\alpha} sin\theta_e + v_{s\beta} cos\theta_e$$
$$i_{sq} = -i_{s\alpha} sin\theta_e + i_{s\beta} cos\theta_e, \qquad (2.30)$$

it is possible to study the observability condition. $Det\,(d\mathcal{O}_{\alpha\beta})$ can be written at zero speed as

$$Det\,(P_{\alpha\beta}) = \frac{2L_1 \Psi_r (L_0 + L_1) L_q}{Det\,(\Lambda_{ss})^2} \frac{di_{sq}}{dt} + \left[\frac{4L_1^2}{Det\,(\Lambda_{ss})^2} (L_1 + L_0) \right] (v_{sd} i_{sq})$$

$$- \left[\frac{8L_1^2}{\Psi_r Det\,(\Lambda_{ss})^2} (L_1 + L_0) \right] (v_{sq} i_{sq}^2).$$

Proposition 2.1 *The state of the IPMSM is observable at zero speed* $(\Omega = p\omega = 0)$ *if*

$$L_1 [-\frac{4L_1^2}{\Psi_r} v_{sq} i_{sq}^2 + (2L_1 v_{sd} - \Psi_r R_s) i_{sq} + \Psi_r v_{sq}] \neq 0, \qquad (2.31)$$

or equivalently, if one of the following conditions are not satisfied:

(i) *if* $v_{sq} = 0$ *and* $v_{sd} \neq \dfrac{\Psi_r R_s}{2L_1}$, *then,* $i_{sq} = 0$ *and* $T_e = 0$.

(ii) *if* $v_{sq} = 0$ *and* $v_{sd} = \dfrac{\Psi_r R_s}{2L_1}$.

(iii) *if* $v_{sq} \neq 0$ *and* $v_{sd} = \dfrac{\Psi_r R_s}{2L_1}$, *then* $i_{sq} = \dfrac{\Phi_r}{2L_1}$ *and* $T_e = \dfrac{p\Psi_r^2}{L_1}$

(iv) *if* $v_{sq} \neq 0$ *and* $v_{sd} \neq \dfrac{\Psi_r R_s}{2L_1}$, *then*

$$i_{sq} = \frac{-(2L_1 v_{sd} - \Psi_r R_s) \pm [(2L_1 v_{sd} - \Psi_r R_s)^2 + (16L_1^2 v_{sq}^2)]^{1/2}}{-8L_1^2 v_{sq}/\Psi_r},$$

and $T_e \neq 0$.

Remark 2.1 The four cases can be checked by using the parameters values for a given machine. The condition (i) can only be verified at standstill (the currents and the voltages are zero). This particular case is easily detected by the electrical measurements. The physical meaning of the case (iv) is that a nonzero load torque exists at zero speed.

On the other hand, taking into account that the parameters of the motor given in Sect. 1.6.2, the cases (ii), (iii), and (iv) are unrealistic, i.e., these cases cannot occur in the IPMSM physical operation domain.

2.3.1.2 IPMSM Observability Analysis for the Stator Resistance R_s and the Load Torque T_l in the (d, q) Frame

Next, a sufficient condition for the observability of the IPMSM, including the stator resistance and the load torque, is given. For computational simplicity, we analyze this observability in the (d, q) frame by using higher time derivatives of the measured output.

Consider the extended model of (1.70), where the rotor resistance R_s and the load torque T_l are the components of the extended state vector, and described by

$$
\begin{cases}
\dfrac{di_{sd}}{dt} = -\dfrac{R_s}{L_d}i_{sd} - p\Omega\dfrac{L_q}{L_d}i_{sq} + \dfrac{v_q}{L_d} \\[2mm]
\dfrac{di_{sq}}{dt} = -\dfrac{R_s}{L_q}i_{sq} + p\Omega\dfrac{L_d}{L_q}i_{sd} + \dfrac{v_d}{L_q} - p\Omega\dfrac{\Psi_r}{L_q} \\[2mm]
\dfrac{d\Omega}{dt} = -\dfrac{f}{J}\Omega + \dfrac{1}{J}p(L_d - L_q)i_{sd}i_{sq} + p\Psi_r i_{sq} - \dfrac{1}{J}T_l \\[2mm]
\dfrac{dT_l}{dt} = 0 \\[2mm]
\dfrac{dR_s}{dt} = 0
\end{cases}
\tag{2.32}
$$

which is of the general form

$$
\begin{cases}
\dfrac{dX_{dq}}{dt} = \mathbb{F}(X_{dq}, v_{dq}) \\[2mm]
y \quad\;\; = h(X_{dq})
\end{cases}
\tag{2.33}
$$

where X_{dq} is an extended state vector and $y = h(X_{dq})$ is the measurable output, that are given by

$$
X_{dq} = \begin{bmatrix} i_{sd} \\ i_{sq} \\ \Omega \\ R_s \\ T_l \end{bmatrix}, \qquad
h(X_{dq}) = \begin{bmatrix} h_1 \\ h_2 \end{bmatrix} = \begin{bmatrix} i_{sd} \\ i_{sq} \end{bmatrix}.
$$

The observation space $\mathcal{O}_{dq}$ defined by the vector space of the functions constituted by the measurements of the stator currents i_{sd} and i_{sq} and closed under Lie derivatives along the field $\mathbb{F}$, is given by $\{h_1, h_2, L_{\mathbb{F}}h_1, L_{\mathbb{F}}h_2, L_{\mathbb{F}}^{(2)}h_2\}$.

Following the same procedure as before, the observability analysis is made by verifying the condition of Theorems 2.3 and 2.5, i.e., by analyzing the rank of the matrix

$$
d\mathcal{O}_{dq}(X_{dq}) = \begin{bmatrix} dh_1 \\ dh_2 \\ dL_{\mathbb{F}}h_1 \\ dL_{\mathbb{F}}h_2 \\ dL_{\mathbb{F}}^{(2)}h_2 \end{bmatrix}.
$$

This is equivalent to determine if the determinant

$$
Det(d\mathcal{O}_{dq}) = a i_{sq}^6 + b i_{sq}^4 + c i_{sq}^2,
$$

is different to zero where

$$
a = -\frac{p^2(L_d - L_q)^3}{JL_q^2\phi_f^2}, b = -\frac{p^2(L_d - L_q)}{JL_q\phi_f} \quad \text{and} \quad c = -\frac{p^2(L_d - L_q)}{JL_q\phi_f} + \frac{p^2\phi_f(L_d - L_q)}{JL_q^2L_d^2}.
$$

From $Det(d\mathcal{O}_{dq})$, it is clear that the rank condition is not satisfied when $i_{sq} = 0$. Then, we can establish the following result.

Proposition 2.2 *Consider the IPMSM model* (2.32) *and assume that the stator currents are measurable. Then, the rotor speed Ω, the stator resistance R_s and the load torque T_l are observable if and only if*

$$
i_{sq} \neq 0.
$$

Remark 2.2 In this case, the motor does not produce any torque, i.e., it does not play a role with respect to the load.

2.3.2 SPMSM Observability Analysis

Now, the observability property of the SPMSM will be studied.

Consider model (2.28) and remark that the inductances are such that:

$$
L_s := L_d = L_q = L_0, \quad \text{and} \quad L_1 = 0.
$$

It follows that the model of the SPMSM, in the (α, β) frame, is given by

$$
\begin{cases}
\dfrac{di_{s\alpha}}{dt} = -\dfrac{R_s}{L_s}i_{s\alpha} + p\Omega\Psi_r \sin(p\theta_m) + \dfrac{1}{L_s}v_{s\alpha} \\[2mm]
\dfrac{di_{s\beta}}{dt} = -\dfrac{R_s}{L_s}i_{s\beta} - p\Omega\Psi_r \cos(p\theta_m) + \dfrac{1}{L_s}v_{s\beta} \\[2mm]
\dfrac{d\Omega}{dt} = -\dfrac{f}{J}\Omega + \dfrac{p}{J}\sqrt{\dfrac{2}{3}}\Psi_r(i_{s\beta}\cos(p\theta - m) - i_{s\alpha}\sin(p\theta_m)) - \dfrac{1}{J}T_l \\[2mm]
\dfrac{d\theta_m}{dt} = \Omega
\end{cases}
\tag{2.34}
$$

which is of the general form

$$
\frac{dX_{\alpha\beta}}{dt} = \mathbb{F}(X_{\alpha\beta}, v_{\alpha\beta}) \tag{2.35}
$$

$$
y = h(X_{\alpha\beta}) \tag{2.36}
$$

where

$$
X_{\alpha\beta} = \begin{pmatrix} i_{s\alpha} \\ i_{s\beta} \\ \Omega \\ \theta_m \end{pmatrix}, \quad v_{\alpha\beta} = \begin{pmatrix} v_{s\alpha} \\ v_{s\beta} \end{pmatrix}, \quad h(X_{\alpha\beta}) = \begin{pmatrix} h_1 \\ h_2 \end{pmatrix} = \begin{pmatrix} i_{s\alpha} \\ i_{s\beta} \end{pmatrix},
$$

with $X_{\alpha\beta}$ is the state, $v_{\alpha\beta}$ is the stator voltages vector and is the system input; $h(X_{\alpha\beta})$ components are the measurable outputs: the stator currents $i_{s\alpha}$ and $i_{s\beta}$.

2.3.2.1 Observation Objective

Consider that in the (α, β) frame, the stator currents $i_{s\alpha}$ and $i_{s\beta}$ are the measurable outputs, the stator voltages $v_{s\alpha}$ and $v_{s\beta}$ are the control inputs of the motor.

The objective is to reconstruct the rotor speed Ω and the position θ_m assuming that they are not available by measurement and moreover under the fact that the stator-winding resistance R_s and the stator-winding inductance L_s are inaccurately known.

The property of observability of the SPMSM is determined by using first Definition 2.6, where the observation space $\mathcal{O}_1$ is constituted of measured outputs and their Lie derivatives along the vector field $\mathbb{F}$, i.e., $\mathcal{O}_1 = \{h_1, h_2, L_{\mathbb{F}}h_1, L_{\mathbb{F}}h_2\}$ and the measured output is

$$
h(x) = \begin{bmatrix} h_1 \\ h_2 \end{bmatrix} = \begin{bmatrix} x_1 \\ x_2 \end{bmatrix}.
$$

From Theorem 2.3, it follows that

$$
d\mathcal{O}_1(x) = \begin{bmatrix} dh_1 \\ dh_2 \\ dL_{\mathbb{F}}h_1 \\ dL_{\mathbb{F}}h_2 \end{bmatrix}. \tag{2.37}
$$

Then, by evaluating the determinant of matrix $d\mathcal{O}_1(x)$, we obtain

$$Det(d\mathcal{O}_1) = \frac{\Psi_r^2 \omega}{L_s^2}.$$

Proposition 2.3 *Consider that the magnet flux Ψ_r and the inductance L_0 are different from zero. The SPMSM is observable if and only if its electrical speed is not null, i.e., if $\omega \neq 0$.*

Remark 2.3 Notice that even by using higher order derivatives of the measured outputs to study the observability property, no additional information for the observability analysis is obtained.

2.4 Induction Motor Observability Analysis

The purpose of this section is to analyze the observability of the induction motor in order to reconstruct the nonmeasurable components of the state vector, i.e., the rotor flux, the rotor speed, and also unknown parameters: the load torque and the rotor resistance.

2.4.1 Mathematical Model in the (d, q) Rotor Flux Frame

Consider the mathematical model of the induction motor, in a state-space representation (1.108) and (1.128) written in the (d, q) frame depending on the stator pulsation ω_s, where

$$\phi_{rq} = \dot{\phi}_{rq} = 0. \tag{2.38}$$

From (1.108) and (2.38), the flux angle ρ is given by

$$\dot{\rho} = \omega_s = p\Omega + \frac{aM_{sr}}{\phi_{rd}}i_{sq}. \tag{2.39}$$

Furthermore, the Electromagnetic Torque equation is given by

$$T_e = \frac{pM_{sr}}{L_r}\phi_{rd}i_{sq}. \tag{2.40}$$

Replacing the stator pulsation ω_s and the differential equation of ϕ_{rq}, by those of the flux angle ρ obtained from (2.39) in the nonlinear model of the induction motor (1.108), it follows that

$$
\begin{bmatrix} \dot{i}_{sd} \\ \dot{i}_{sq} \\ \dot{\phi}_{rd} \\ \dot{\rho} \\ \dot{\Omega} \end{bmatrix} = \begin{bmatrix} -\gamma i_{sd} + ab\phi_{rd} + p\Omega i_{sq} + a\dfrac{M_{sr}}{\phi_{rd}}i_{sq}^2 \\ -\gamma i_{sq} - bp\Omega\phi_{rd} - p\Omega i_{sd} - a\dfrac{M_{sr}}{\phi_{rd}}i_{sd}i_{sq} \\ -a\phi_{rd} + aM_{sr}i_{sd} \\ p\Omega + a\dfrac{M_{sr}}{\phi_{rd}}i_{sq} \\ m\phi_{rd}i_{sq} - c\Omega - \dfrac{1}{J}T_l \end{bmatrix} + \begin{bmatrix} m_1 & 0 \\ 0 & m_1 \\ 0 & 0 \\ 0 & 0 \\ 0 & 0 \end{bmatrix} \begin{bmatrix} v_{sd} \\ v_{sq} \end{bmatrix}.
$$

$$(2.41)$$

Remark 2.4 From (2.39), the slip pulsation is given by $\omega_r = \omega_s - p\Omega$, where

$$
\omega_r = \frac{aM_{sr}}{\phi_{rd}}i_{sq}. \tag{2.42}
$$

2.4.2 Introduction to the Sensorless IM Observability

Several works have studied the observability of the induction motor (see [11, 32, 44]). In [32], sufficient conditions under which the induction motor loses the observability property have been presented. This study has been realized using model (1.121). In this subsection, we present a similar study using the model (1.115). To analyze the observability of the induction motor, the criteria of the observability rank will be applied (see [30]).

2.4.3 Induction Motor Observability with Speed Measurement

Consider the induction motor model (1.114). For the analysis of the observability of the induction motor, firstly assume that the rotor speed is measured.

The induction motor model is:

$$
\begin{bmatrix} \dfrac{di_{sd}}{dt} \\ \dfrac{di_{sq}}{dt} \\ \dfrac{d\phi_{rd}}{dt} \\ \dfrac{d\phi_{rq}}{dt} \\ \dfrac{d\Omega}{dt} \\ \dfrac{dT_l}{dt} \end{bmatrix} = \begin{bmatrix} -\gamma i_{sd} + \omega_s i_{sq} + ba\phi_{rd} + bp\Omega\phi_{rq} + m_1 v_{sd} \\ -\omega_s i_{sd} - \gamma i_{sq} - bp\Omega\phi_{rd} + ba\phi_{rq} + m_1 v_{sq} \\ aM_{sr}i_{sd} - a\phi_{rd} + (\omega_s - p\Omega)\phi_{rq} \\ aM_{sr}i_{sq} - (\omega_s - p\Omega)\phi_{rd} - a\phi_{rq} \\ m(\phi_{rd}i_{sq} - \phi_{rq}i_{sd}) - c\Omega - \dfrac{1}{J}T_l \\ 0 \end{bmatrix} \tag{2.43}
$$

where the state, the input and the measurable output are given by

$$x = \begin{bmatrix} x_1 \\ x_2 \\ x_3 \\ x_4 \\ x_5 \\ x_6 \end{bmatrix} = \begin{bmatrix} i_{sd} \\ i_{sq} \\ \phi_{rd} \\ \phi_{rq} \\ \Omega \\ T_l \end{bmatrix} \in \mathfrak{R}^6, \quad u = \begin{bmatrix} v_{sd} \\ v_{sq} \end{bmatrix} \in \mathfrak{R}^2,$$

$$h(x) = \begin{bmatrix} h_1 \\ h_2 \\ h_5 \end{bmatrix} = \begin{bmatrix} x_1 \\ x_2 \\ x_5 \end{bmatrix} = \begin{bmatrix} i_{sd} \\ i_{sq} \\ \Omega \end{bmatrix} \in \mathfrak{R}^3,$$

and the vector field is given by

$$\mathbb{F}(x,u) = \begin{bmatrix} -\gamma x_1 + \omega_s x_2 + ba x_3 + bp x_5 x_4 + m_1 v_{sd} \\ -\gamma x_2 - \omega_s x_1 + ba x_4 - bp x_5 x_3 + m_1 v_{sq} \\ -a x_3 + (\omega_s - p x_5) x_4 + a M_{sr} x_1 \\ -a x_4 - (\omega_s - p x_5) x_3 + a M_{sr} x_2 \\ m(x_3 x_2 - x_4 x_1) - c x_5 - \dfrac{1}{J} x_6 \\ 0 \end{bmatrix}.$$

Notice that the rotor speed is considered as an output as well as the stator currents.

Consider the observation space $\mathcal{O}_{IM,0}(x)$ of functions containing the components of h and closed under Lie derivation along the vector field $\mathbb{F}$, i.e., $\mathcal{O}_{IM0}(x) = \{h_1, h_2, h_5, L_{\mathbb{F}} h_1, L_{\mathbb{F}} h_2, L_{\mathbb{F}} h_5\}$.

To verify the observability rank condition, it is sufficient to check that the rank of matrix

$$d\mathcal{O}_{IM,0}(x) = \begin{bmatrix} dh_1 \\ dh_2 \\ dh_5 \\ dL_{\mathbb{F}} h_1 \\ dL_{\mathbb{F}} h_2 \\ dL_{\mathbb{F}} h_5 \end{bmatrix}$$

is equal to $n = 6$.

The matrix $d\mathcal{O}_{IM,0}(x)$ characterizing the observability of the system (2.43) in the rank sense, is given by

$$d\mathcal{O}_{IM0}(x) = \begin{bmatrix} 1 & 0 & 0 & 0 & 0 & 0 \\ 0 & 1 & 0 & 0 & 0 & 0 \\ 0 & 0 & 0 & 0 & 1 & 0 \\ -\gamma & \omega_s & ba & bp x_5 & bp x_4 & 0 \\ -\omega_s & -\gamma & -bp x_5 & ba & -bp x_3 & 0 \\ -m x_4 & m x_3 & m x_2 & m x_1 & -c & -\dfrac{1}{J} \end{bmatrix}.$$

Next, computing the determinant $d\mathcal{O}_{IM,0}(x)$, it follows that

$$Det(d\mathcal{O}_{IM,0}(x)) = -\frac{b^2}{J}(a^2 + (px_5)^2).$$

Notice that the determinant $Det(d\mathcal{O}_{IM,0}(x))$ is different from zero for any value of the rotor speed. Then, the matrix $d\mathcal{O}_{IM,0}(x)$ is full rank. As a consequence, using the rotor speed and the stator currents measurements, we can conclude that the IM is observable.

Remark 2.5 The determinant $Det(d\mathcal{O}_{IM0}(x))$ is independent of the stator pulsation ω_s. An identical result is obtained in [32] from the model (1.121).

2.4.4 Observability of the Induction Motor: Sensorless Case

In the sequel, the observability study will be determined assuming that the rotor speed Ω is not available from measurement.

In the (mechanical) sensorless case, only the stator currents are measured. From (1.115), the model of the IM, for the sensorless case, is

$$\begin{cases} \dot{x} = \mathbb{F}(x, u) \\ y = h(x) \end{cases} \tag{2.44}$$

where

$$x = \begin{bmatrix} x_1 \\ x_2 \\ x_3 \\ x_4 \\ x_5 \\ x_6 \end{bmatrix} = \begin{bmatrix} i_{sd} \\ i_{sq} \\ \phi_{rd} \\ \phi_{rq} \\ \Omega \\ T_l \end{bmatrix} \in \mathfrak{R}^6, \quad u = \begin{bmatrix} v_{sd} \\ v_{sq} \end{bmatrix} \in \mathfrak{R}^2,$$

$$h(x) = \begin{bmatrix} h_1 \\ h_2 \end{bmatrix} = \begin{bmatrix} x_1 \\ x_2 \end{bmatrix} = \begin{bmatrix} i_{sd} \\ i_{sq} \end{bmatrix} \in \mathfrak{R}^2$$

and the vector field $\mathbb{F}$ is given by

$$\mathbb{F}(x, u) = \begin{bmatrix} -\gamma x_1 + \omega_s x_2 + bax_3 + bpx_5x_4 + m_1 v_{sd} \\ -\gamma x_2 - \omega_s x_1 + bax_4 - bpx_5x_3 + m_1 v_{sq} \\ -ax_3 + (\omega_s - px_5)x_4 + aM_{sr}x_1 \\ -ax_4 - (\omega_s - px_5)x_3 + aM_{sr}x_2 \\ m(x_3x_2 - x_4x_1) - cx_5 - \frac{1}{J}x_6 \\ 0 \end{bmatrix}.$$

From Definition 2.6, the observation space $\mathcal{O}_{IM,1}(x)$ constituted by the components of the output and closed under Lie derivation is given by:

$$\{h_1, h_2, L_{\mathbb{F}}h_1, L_{\mathbb{F}}h_2, L_{\mathbb{F}}^2h_1, L_{\mathbb{F}}^2h_2\}.$$

Then, from Theorems 2.3 and 2.5, and to verify the observability rank condition, it can be checked that the matrix $d\mathcal{O}_{IM,1}(x)$

$$d\mathcal{O}_{IM,1}(x) = \begin{bmatrix} dh_1 \\ dh_2 \\ dL_{\mathbb{F}}h_1 \\ dL_{\mathbb{F}}h_2 \\ dL_{\mathbb{F}}^2h_1 \\ dL_{\mathbb{F}}^2h_2 \end{bmatrix}.$$

satisfies the observability rank condition if the determinant of

$$d\mathcal{O}_{IM,1}(x) = \begin{bmatrix} 1 & 0 & 0 & 0 & 0 & 0 \\ 0 & 1 & 0 & 0 & 0 & 0 \\ -\gamma & \omega_s & ba & bpx_5 & bpx_4 & 0 \\ -\omega_s & -\gamma & -bpx_5 & ba & -bpx_3 & 0 \\ a_1 & a_2 & a_3 & a_4 & a_5 & a_6 \\ b_1 & b_2 & b_3 & b_4 & b_5 & b_6 \end{bmatrix}$$

is different from zero, where

$a_1 = \gamma^2 - bM_{sr}a^2 - bpmx_4^2 - \omega_s^2$

$a_2 = bpmx_3x_4 + bpaM_{sr}x_5 + \dot{\omega}_s - 2\gamma\omega_s$

$a_3 = -ba^2 + bpmx_2x_4 + bp^2x_5^2 - \gamma ba - 2bpx_5\omega_s$

$a_4 = -2bapx_5 + bp(mx_2x_3 - mx_4x_1 - cx_5 - \dfrac{x_6}{J}) - \gamma bpx_5 - bpmx_4x_1 - 2ba\omega_s$

$a_5 = -bapx_4 - bpcx_4 + bp(-ax_4 + px_5x_3 + aM_{sr}x_2)$
$\qquad - \gamma bpx_4 + bp^2x_5x_3 - 2bpx_3\omega_s,$

$a_6 = -\dfrac{bp}{J}x_4$

and

$b_1 = bpmx_3x_4 - bpaM_{sr}x_5 - \dot{\omega}_s + 2\gamma\omega_s$

$b_2 = \gamma^2 + bM_{sr}a^2 - bpmx_3^2 - \omega_s^2$

$b_3 = 2bapx_5 - bp(mx_2x_3 - mx_4x_1 - cx_5 - \dfrac{x_6}{J}) + \gamma bpx_5 - bpmx_2x_3 - 2ba\omega_s$

$b_4 = -ba^2 + bpmx_1x_3 + bp^2x_5^2 - \gamma ba - 2bpx_5\omega_s$

$$b_5 = bapx_3 + bpcx_3 - bp(-ax_3 - px_5x_3 + aM_{sr}x_1)$$
$$\quad - \gamma bpx_3 + bp^2x_5x_3 - 2bpx_4\omega_s,$$
$$b_6 = \frac{bp}{J}x_3.$$

More precisely, the determinant of matrix $d\mathcal{O}_{IM,1}(x)$ is given by

$$Det\,(d\mathcal{O}_{IM,1}(x)) = -\frac{b^3p^2}{J}[-(px_5x_3 + ax_4)(x_3a_3 + x_4b_3)$$

$$+ (ax_3 - px_4x_5)(x_3a_4 + x_4b_4) + (\frac{a}{p^2} - px_5^2)(x_3a_5 + x_4b_5)].$$

From the complexity of a_3, a_4, a_5, b_3, b_4 and b_5, the determinant of the matrix $d\mathcal{O}_{IM,1}(x)$ is difficult to directly analyze.

Consequently, to study the observability of the induction motor without mechanical speed sensor, the following subcases will be analyzed.

(i) Case 1: $\dot{\Omega} = 0$, i.e., constant rotor speed.
(ii) Case 2: $\omega_s = 0$.
(iii) Case 3: $\dot{\phi}_{rd} = \dot{\phi}_{rq} = \omega_s = 0$.
(iv) Case 4: $\dot{\phi}_{rd} = \dot{\phi}_{rq} = \omega_s = 0$ and $\dot{\Omega} = 0$.

2.4.4.1 Case 1: $\dot{\Omega} = 0$, i.e., Constant Rotor Speed

Consider the case where the IM rotor speed is constant, then the resulting model (1.114) is simplified:

$$\begin{cases} \dot{x} = \mathbb{F}(x, u) \\ y = h(x) \end{cases} \tag{2.45}$$

$$x = \begin{bmatrix} x_1 \\ x_2 \\ x_3 \\ x_4 \\ x_5 \end{bmatrix} = \begin{bmatrix} i_{sd} \\ i_{sq} \\ \phi_{rd} \\ \phi_{rq} \\ \Omega \end{bmatrix} \in \Re^5, \quad u = \begin{bmatrix} v_{sd} \\ v_{sq} \end{bmatrix}, \quad h(x) = \begin{bmatrix} h_1 \\ h_2 \end{bmatrix} = \begin{bmatrix} x_1 \\ x_2 \end{bmatrix} = \begin{bmatrix} i_{sd} \\ i_{sq} \end{bmatrix}$$

and the vector field is given by

$$\mathbb{F}(x, u) = \begin{bmatrix} bax_3 + bpx_5x_4 - \gamma x_1 + \omega_s x_2 + m_1 v_{sd} \\ bax_4 - bpx_5x_3 - \gamma x_2 - \omega_s x_1 + m_1 v_{sq} \\ -ax_3 + (\omega_s - px_5)x_4 + aM_{sr}x_1 \\ -ax_4 - (\omega_s - px_5)x_3 + aM_{sr}x_2 \\ 0 \end{bmatrix}.$$

Consider the following two observation spaces $\mathcal{O}_{IMS,1,\dot{\Omega}}(x)$ and $\mathcal{O}_{IMS,2,\dot{\Omega}}(x)$ of functions containing the components of h and closed under Lie derivation given by $\mathcal{O}_{IMS,1,\dot{\Omega}}(x) = \{h_1, L_{\mathbb{F}}h_1, L_{\mathbb{F}}^2h_1, h_2, L_{\mathbb{F}}h_2\}$ and $\mathcal{O}_{IMS,2,\dot{\Omega}}(x) = \{h_1, L_fh_1, h_2, L_{\mathbb{F}}h_2, L_{\mathbb{F}}^2h_2\}$, respectively.

From Theorems 2.3 and 2.5, and to verify the observability rank condition, the matrices $d\mathcal{O}_{IMS,1,\dot{\Omega}=0}(x)$ and $d\mathcal{O}_{IMS,2,\dot{\Omega}=0}(x)$ are computed

$$d\mathcal{O}_{IMS,1,\dot{\Omega}=0}(x) = \begin{bmatrix} dh_1 \\ dL_{\mathbb{F}}h_1 \\ dL_{\mathbb{F}}^2h_1 \\ dh_2 \\ dL_{\mathbb{F}}h_2 \end{bmatrix}, \quad d\mathcal{O}_{IMS,2,\dot{\Omega}=0}(x) = \begin{bmatrix} dh_1 \\ dL_{\mathbb{F}}h_1 \\ dh_2 \\ dL_{\mathbb{F}}h_2 \\ dL_{\mathbb{F}}^2h_2 \end{bmatrix}.$$

The matrices $d\mathcal{O}_{IMS,1,\dot{\Omega}=0}(x)$ and $d\mathcal{O}_{IMS,2,\dot{\Omega}=0}(x)$ are expressed in terms of the induction motor dynamics and then,

$$d\mathcal{O}_{IMS,1,\dot{\Omega}=0}(x) = \begin{bmatrix} 1 & 0 & 0 & 0 & 0 \\ -\gamma & \omega_s & ba & bpx_5 & bpx_4 \\ \gamma^2 + ba^2 M_{sr} - \omega_s\, bM_{sr}apx_5 - 2\omega_s\gamma & b_7 & b_8 & b_9 \\ 0 & 1 & 0 & 0 & 0 \\ -\omega_s & -\gamma & -bpx_5 & ba & -bpx_3 \end{bmatrix}$$

$$d\mathcal{O}_{IMS,2,\dot{\Omega}=0}(x) = \begin{bmatrix} 1 & 0 & 0 & 0 & 0 \\ -\gamma & \omega_s & ba & bpx_5 & bpx_4 \\ 0 & 1 & 0 & 0 & 0 \\ -\omega_s & -\gamma & -bpx_5 & ba & -bpx_3 \\ -bM_{sr}apx_5 + 2\omega_s\gamma\ \gamma^2 + ba^2 M_{sr} - \omega_s^2 & b_{10} & b_{11} & b_{12} \end{bmatrix}$$

where

$$\begin{aligned}
b_7 &= -ba^2 + bp^2x_5^2 - \gamma ba - 2bp\omega_s x_5 \\
b_8 &= -2bapx_5 - bp\gamma x_5 + 2ba\omega_s \\
b_9 &= -bpax_4 + bp\dot{x}_4 + bp^2x_5x_3 - \gamma bpx_4 - bp\omega_s x_3 \\
b_{10} &= 2bapx_5 + bp\gamma x_5 - 2ba\omega_s \\
b_{11} &= -ba^2 + bp^2x_5^2 - \gamma ba - 2bp\omega_s x_5 \\
b_{12} &= bpax_3 - bp\dot{x}_3 + bp^2x_5x4 + \gamma bpx_3 - bp\omega_s x_4
\end{aligned}$$

must be of dimension equal to 5, respectively.

It can be directly verified that the determinants are

$$Det(d\mathcal{O}_{IMS,1,\dot{\Omega}=0}(x)) = -b^3 p^3(\dot{x}_4 + \omega_s x_3)(\frac{a^2}{p^2} + x_5^2),$$

$$Det(d\mathcal{O}_{IMS,2,\dot{\Omega}=0}(x)) = b^3 p^3 (\dot{x}_3 - \omega_s x_4)(\frac{a^2}{p^2} + x_5^2).$$

From the determinants $Det(d\mathcal{O}_{IMS,2,\dot{\Omega}=0}(x))$ and $Det(d\mathcal{O}_{IMS,2,\dot{\Omega}=0}(x))$ it can be remarked that $\dot{x}_4 = -\omega_s x_3$, $\dot{x}_3 = \omega_s x_4$ or $\dot{x}_4 = \dot{x}_3 = \omega_s = 0$, represent the observability singularities for the case 1. Then, for these particular dynamics, the observability rank condition is not satisfied.

2.4.4.2 Case 2: $\omega_s = 0$.

Consider that the synchronous speed $\omega_s = 0$, the load torque T_l and the rotor speed Ω are not available by measurement. The resulting model of the Induction Motor (1.114) used to analyze the observability properties is then defined in terms of the state, input and measurable output as follows:

$$x = \begin{bmatrix} x_1 \\ x_2 \\ x_3 \\ x_4 \\ x_5 \\ x_6 \end{bmatrix} = \begin{bmatrix} i_{sd} \\ i_{sq} \\ \phi_{rd} \\ \phi_{rq} \\ \Omega \\ T_l \end{bmatrix} \in \Re^6, \quad u = \begin{bmatrix} v_{sd} \\ v_{sq} \end{bmatrix}, \quad h(x) = \begin{bmatrix} h_1 \\ h_2 \end{bmatrix} = \begin{bmatrix} x_1 \\ x_2 \end{bmatrix} = \begin{bmatrix} i_{sd} \\ i_{sq} \end{bmatrix}$$

and

$$\mathbb{F}(x,u) = \begin{bmatrix} bax_3 + bpx_5x_4 - \gamma x_1 + m_1 v_{sd} \\ bax_4 - bpx_5x_3 - \gamma x_2 + m_1 v_{sq} \\ -ax_3 - px_5x_4 + aM_{sr}x_1 \\ -ax_4 + px_5x_3 + aM_{sr}x_2 \\ m(x_3x_2 - x_4x_1) - cx_5 - \frac{1}{J}x_6 \\ 0 \end{bmatrix}.$$

The observation space $\mathcal{O}_{IMS,3,\omega_s=0}(x)$ of functions containing the components of h and closed under Lie derivation, is given by

$$\mathcal{O}_{IMS,3,\omega_s=0}(x) = \{h_1, h_2, L_{\mathbb{F}}h_1, L_{\mathbb{F}}h_2, L_{\mathbb{F}}^2 h_1, L_{\mathbb{F}}^2 h_2\}.$$

From Definition 2.11, and to verify the observability rank condition, the rank of matrix

$$dO_{IMS,3,\omega_s=0}(x) = \begin{bmatrix} dh_1 \\ dh_2 \\ dL_{\mathbb{F}}h_1 \\ dL_{\mathbb{F}}h_2 \\ dL_{\mathbb{F}}^2 h_1 \\ dL_{\mathbb{F}}^2 h_2 \end{bmatrix},$$

has to be full rank (see Theorems 2.3 and 2.5). This is equivalent verifying if the determinant

$$Det\left(dO_{IMS,3,\omega_s=0}(x)\right) = Det \begin{bmatrix} 1 & 0 & 0 & 0 & 0 & 0 \\ 0 & 1 & 0 & 0 & 0 & 0 \\ -\gamma & 0 & ba & bpx_5 & bpx_4 & 0 \\ 0 & -\gamma & -bpx_5 & ba & -bpx_3 & 0 \\ a_7 & b_1 & a_8 & a_9 & a_{10} & \dfrac{-bpx_4}{J} \\ b_2 & a_{11} & a_{12} & a_{13} & a_{14} & \dfrac{bpx_3}{J} \end{bmatrix}$$

is different from zero, where

$$b_1 = bp(mx_3x_4 + M_{sr}ax_5)$$
$$b_2 = bp(mx_3x_4 - M_{sr}ax_5)$$
$$a_7 = -bpmx_4^2 + \gamma^2 + bM_{sr}a^2$$
$$a_8 = bpmx_4x_2 - \gamma ba - ba^2 + bp^2x_5^2$$
$$a_9 = bp\dot{x}_5 + bpmx_4x_1 - \gamma bpx_5 - 2bpax_5$$
$$a_{10} = -bpcx_4 - bp\gamma x_4 - 2bpax_4 + bp^2x_5x_3 + bpaM_{sr}x_2$$
$$a_{11} = -bpmx_3^2 + \gamma^2 + bM_{sr}a^2$$
$$a_{12} = -bp\dot{x}_5 + bpmx_3x_2 + \gamma bpx_5 + 2bapx_5$$
$$a_{13} = bpmx_3x_1 + \gamma ba + bp^2x_5^2 - ba^2$$
$$a_{14} = bpcx_3 + \gamma bpx_3 + 2bpax_3 - bpM_{sr}ax_1 + 2bp^2x_4x_5.$$

This is equivalent analyzing

$$Det\left(d\mathcal{O}_{IMS,3,\omega_s=0}(x)\right) = \frac{b^4 p^3 a}{J} \overbrace{(x_3^2 + x_4^2)}^{\phi_{rd}^2+\phi_{rq}^2}(\dot{x}_5 + \frac{a}{bp}x_5 + \frac{p}{ba}x_5^3)$$

$$+ \frac{b^3 p M_{sr} a^2}{m} \overbrace{m(x_3 x_2 - x_4 x_1)}^{T_e}. \qquad (2.46)$$

Remark 2.6 Notice that the analysis of the determinant $d\mathcal{O}_{IMS,3,\omega_s=0}(x)$ is not an easy task. However, we can see that the points $T_e = 0$ and $\phi_{rd}^2 + \phi_{rq}^2 = 0$, appears as an observability singularity of the system. These conditions are not of practical interest, because these conditions are satisfied only if the machine has a flux equal to zero and then the electromechanical torque is obviously zero. The motor does not play any role with respect to the load.

2.4.4.3 Case 3: $\dot{\phi}_{rd} = \dot{\phi}_{rq} = \omega_s = 0$

This case represents the operating condition when the fluxes are constant and the synchronous speed is equal to zero. Under these conditions, the induction motor (1.114) is described by the following state, input and measurable output as

$$x = \begin{bmatrix} x_1 \\ x_2 \\ x_3 \\ x_4 \\ x_5 \\ x_6 \end{bmatrix} = \begin{bmatrix} i_{sd} \\ i_{sq} \\ \phi_{rd} \\ \phi_{rq} \\ \Omega \\ T_l \end{bmatrix} \in \Re^6, \quad u = \begin{bmatrix} u_{sd} \\ u_{sq} \end{bmatrix}, \quad h(x) = \begin{bmatrix} h_1 \\ h_2 \end{bmatrix} = \begin{bmatrix} x_1 \\ x_2 \end{bmatrix} = \begin{bmatrix} i_{sd} \\ i_{sq} \end{bmatrix}$$

and

$$\mathbb{F}(x,u) = \begin{bmatrix} bax_3 + bpx_5x_4 - \gamma x_1 + m_1 v_{sd} \\ bax_4 - bpx_5x_3 - \gamma x_2 + m_1 v_{sq} \\ 0 \\ 0 \\ m(x_3 x_2 - x_4 x_1) - cx_5 - \frac{1}{J}x_6 \\ 0 \end{bmatrix}.$$

The observation space $\mathcal{O}_{IMS,4}(x)$ generated by h, and closed under Lie derivation along of field $\mathbb{F}$, is given by

$$\mathcal{O}_{IMS,4}(x) = \{h_1, h_2, L_{\mathbb{F}}h_1, L_{\mathbb{F}}h_2, L_{\mathbb{F}}^2 h_1, L_{\mathbb{F}}^2 h_2\}.$$

From Definition 2.11, and by verifying the observability rank condition, it follows that the matrix

$$dO_{IMS,4}(x) = \begin{bmatrix} dh_1 \\ dh_2 \\ dL_{\mathbb{F}}h_1 \\ dL_{\mathbb{F}}h_2 \\ dL_{\mathbb{F}}^2 h_1 \\ dL_{\mathbb{F}}^2 h_2 \end{bmatrix}$$

must be of full rank (see Theorems 2.3 and 2.5). It follows that matrix

$$dO_{IMS,4}(x) = \begin{bmatrix} 1 & 0 & 0 & 0 & 0 & 0 \\ 0 & 1 & 0 & 0 & 0 & 0 \\ -\gamma & 0 & ba & bpx_5 & bpx_4 & 0 \\ 0 & -\gamma & -bpx_5 & ba & -bpx_3 & 0 \\ a'_7 & bpmx_3x_4 & a'_8 & a'_9 & a'_{10} & \dfrac{-bpx_4}{J} \\ bpmx_3x_4 & a'_{11} & a'_{12} & a'_{13} & a'_{14} & \dfrac{bpx_3}{J} \end{bmatrix}$$

where

$$a'_7 = -bpmx_4^2 + \gamma^2$$
$$a'_8 = bpmx_4x_2 - \gamma ba$$
$$a'_9 = bp\dot{x}_5 + bpmx_4x_1 - \gamma bpx_5$$
$$a'_{10} = -bpcx_4 - bp\gamma x_4$$
$$a'_{11} = -bpmx_3^2 + \gamma^2$$
$$a'_{12} = -bp\dot{x}_5 + bpmx_3x_2 + \gamma bpx_5$$
$$a'_{13} = bpmx_3x_1 + \gamma ba$$
$$a'_{14} = bpcx_3 + \gamma bpx_3$$

has its determinant $Det(dO_{IMS,4}(x))$ given by

$$Det(dO_{IMS,4}(x)) = \frac{b^4 p^3 a}{J} \overbrace{(x_3^2 + x_4^2)}^{\phi_{rd}^2 + \phi_{rq}^2} \dot{x}_5.$$

must be different to zero. Notice that the determinant $Det(dO_{IMS,4}(x))$ is equal to zero for

$$\phi_{rd}^2 + \phi_{rq}^2 = 0$$

or

$$\dot{\Omega} = \dot{x}_5 = 0.$$

Remark 2.7

- Case $\phi_{rd}^2 + \phi_{rq}^2 = 0$ has no practical interest because the IM cannot operate without flux. The case $\dot{x}_5 = 0$ implies that the rotor speed is constant. Then we can conclude that the determinant is zero if the speed is constant. Thus the observability of the IM cannot be establish under constant speed, with zero stator pulsation ω_s, the components of the rotor flux ϕ_{rd} and ϕ_{rq} are constants.
- Case 3 is important as the field-oriented control (a classical control strategy) imposes the flux ϕ_{rd} to be constant (i.e., $\dot{\phi}_{rd} = 0$) and the flux ϕ_{rq} to be equal zero. Then the observability of the IM is no longer satisfied when the speed is constant (steady state) and the stator pulsation ω_s is zero.
- From *Case 1* and *Case 3*, we can conclude that it is not possible to verify the observability of the induction motor by using only the stator current measurement and their derivatives up to order 2.

To analyze the observability property of the induction motor from the measurements (the stator currents) and their derivatives up to order 2 in the case where the machine speed is constant ($\dot{\Omega} = 0$), the component of the flux are constant ($\dot{\phi}_{rd} = \dot{\phi}_{rq} = 0$) and the stator pulsation is zero ($\omega_s = 0$), is described in the following subsection.

2.4.4.4 Case 4: $\dot{\phi}_{rd} = \dot{\phi}_{rq} = \omega_s = 0$ and $\dot{\Omega} = 0$

For $\dot{\phi}_{rd} = \dot{\phi}_{rq} = \omega_s = 0$ and $\dot{\Omega} = 0$, the model of induction motor (1.115) is described by

$$
x = \begin{bmatrix} x_1 \\ x_2 \\ x_3 \\ x_4 \\ x_5 \end{bmatrix} = \begin{bmatrix} i_{sd} \\ i_{sq} \\ \phi_{rd} \\ \phi_{rq} \\ \Omega \end{bmatrix} \in \Re^5, \quad u = \begin{bmatrix} u_{sd} \\ u_{sq} \end{bmatrix}, \quad h(x) = \begin{bmatrix} h_1 \\ h_2 \end{bmatrix} = \begin{bmatrix} x_1 \\ x_2 \end{bmatrix} = \begin{bmatrix} i_{sd} \\ i_{sq} \end{bmatrix}
$$

and

$$
\mathbb{F}(x, u) = \begin{bmatrix} bax_3 + bpx_5x_4 - \gamma x_1 + m_1 v_{sd} \\ bax_4 - bpx_5x_3 - \gamma x_2 + m_1 v_{sq} \\ 0 \\ 0 \\ 0 \end{bmatrix}.
$$

The observation space $\mathcal{O}_{IMS,5}(x)$ generated by the components of h and closed under Lie derivation along the field $\mathbb{F}$ is given by

$$
\mathcal{O}_{IMS,5}(x) = \{h_1, h_2, L_{\mathbb{F}}h_1, L_{\mathbb{F}}h_2, L_{\mathbb{F}}^2 h_1, L_f^2 h_2, L_{\mathbb{F}}^3 h_1, L_{\mathbb{F}}^3 h_2, L_{\mathbb{F}}^4 h_1, L_{\mathbb{F}}^4 h_2\}.
$$

The observability rank condition can be verified if matrix
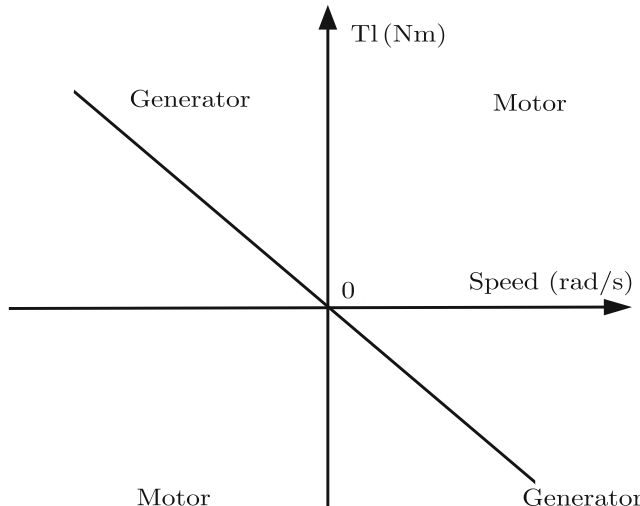
$$
d\mathcal{O}_{IMS,5}(x) =
\begin{bmatrix}
dh_1 \\
dh_2 \\
dL_{\mathbb{F}}h_1 \\
dL_{\mathbb{F}}h_2 \\
dL_{\mathbb{F}}^2 h_1 \\
dL_{\mathbb{F}}^2 h_2 \\
dL_{\mathbb{F}}^3 h_1 \\
dL_{\mathbb{F}}^3 h_2 \\
dL_{\mathbb{F}}^4 h_1 \\
dL_{\mathbb{F}}^4 h_2
\end{bmatrix}
=
\begin{bmatrix}
1 & 0 & 0 & 0 & 0 & 0 \\
0 & 1 & 0 & 0 & 0 & 0 \\
-\gamma & 0 & ba & bpx_5 & bpx_4 & 0 \\
0 & -\gamma & -bpx_5 & ba & -bpx_3 & 0 \\
\gamma^2 & 0 & -\gamma ba & -\gamma bpx_5 & -\gamma bpx_4 & 0 \\
0 & \gamma^2 & \gamma bpx_5 & -\gamma ba & \gamma bpx_3 & 0 \\
-\gamma^3 & 0 & \gamma^2 ba & \gamma^2 bpx_5 & \gamma^2 bpx_4 & 0 \\
0 & -\gamma^3 & -\gamma^2 bpx_5 & \gamma^2 ba & -\gamma^2 bpx_3 & 0 \\
\gamma^4 & 0 & -\gamma^3 ba & -\gamma^3 bpx_5 & -\gamma^3 bpx_4 & 0 \\
0 & \gamma^4 & \gamma^3 bpx_5 & -\gamma^3 ba & \gamma^3 bpx_3 & 0
\end{bmatrix}
$$

is of full rank (see Theorems 2.3 and 2.5).

Thus the observability of the IM can be established under the following operation conditions of the machine: the (d, q)-components of rotor flux ϕ_{rd} and ϕ_{rq} are *constant*, *zero stator pulsation*, and *constant speed* even using the derivatives of high order of the measurements.

2.4.5 Unobservability Line

From (2.40), the stator pulsation (2.39) can be expressed as follows:

Fig. 2.1 Unobservability line in the plane (T_l, Ω)

$$\omega_s = p\Omega + \frac{R_r T_e}{p\phi_{rd}^2}.$$ (2.47)

For $\omega_s = 0$ and ϕ_{rd} constant, we obtain that the electromagnetic torque is given by

$$T_e = -K\Omega$$ (2.48)

where $K = \dfrac{P^2\phi_{rd}^2}{R_r}$. If the machine speed is constant ($\dot{\Omega} = 0$), the dynamical equation (1.105) becomes

$$T_e = f_v\Omega + T_l.$$ (2.49)

From (2.48) and (2.49) a line can be drawn in the load torque-mechanical speed plane (T_l, Ω) (see Fig. 2.1):

$$T_l = -M\Omega$$ (2.50)

with $M = \dfrac{P^2\phi_{rd}^2}{R_r} + f_v$.

This unobservability line is located in the second and fourth quadrants of the plane (T_l, Ω), when the machine operates in generator mode (the load torque and the mechanical speed are of the opposite sign) as shown in Fig. 2.1. This line is used to check industrial drives in order to characterize their sensorless behavior at slow speed.

2.5 Normal Forms for Observer Design

As seen in the above sections, there are different structures used to represent a nonlinear system, in particular to represent the AC machines. Normal forms are obtained based on the information available from measurement and from the observation objectives. Furthermore, there are a large number of observers which have been developed for linear and nonlinear systems. Several efforts have been made to construct an observer for a general class of nonlinear system. Extensions of the linear case have been proposed which are adaptations of linear observers to nonlinear systems.

They have been derived using different techniques or methodologies:

Extended observers: general Luenberger observer, Kalman filter, state affine systems observer, linear plus an output injection, high gain observer, adaptive observers mainly. These observers have an estimation error that converges exponentially or asymptotically to zero.

Sliding mode observers: classical sliding mode, super-twisting, high-order sliding mode, adaptive sliding mode for instance. One the most important characteristics of these observers is their finite-time convergence to zero and their robustness under uncertainties.

However, when considering nonlinear systems, the construction of an observer is not easy (see [4, 30, 42]). We can distinguish two classes of systems: those of which are observable for any input and those that have singular inputs.

For those which are observable for any input, i.e., *uniformly observable*, the first results have been obtained in the case when the nonlinear system can be transformed, by means of a diffeomorphism, into a linear system plus an output–input injection.

Consider the class of nonlinear system described by a state-space representation of the form (2.18). System (2.18) can be transformed into one of the following state-space representations:

(1) *Linear system plus an output–input injection*

$$\begin{cases} \dot{\xi} = A\xi + \phi(u, y) \\ y = C\xi \end{cases} \tag{2.51}$$

which is observable for any input, if and only if the pair (C, A) is observable.

(2) *Triangular form*

The generalization of the above class of nonlinear systems is of the form

$$\begin{cases} \dot{\xi} = A\xi + \phi(u, \xi) \\ y = C\xi \end{cases} \tag{2.52}$$

where the term $\phi(u, \xi)$ is in the triangular form, i.e.,

$$\phi(u, \xi) = (\phi(u, \xi_1), \phi(u, \xi_1, \xi_2), \ldots, \phi(u, \xi_1, \ldots, \xi_n))^T,$$

which has been introduced in [28].

Notice that these classes of nonlinear systems are observable for any input, so the observer design is possible.

An interesting class of systems which will be studied in the book is:

(3) *State affine system plus an input–output injection*

This class of systems is represented as

$$\begin{cases} \dot{\xi} = A(u)\xi + \phi(u, y) \\ y = C\xi \end{cases} \tag{2.53}$$

where the components of the matrix A depends on the input u.

Notice that this system has inputs rendering the system unobservable. These inputs are called *bad inputs* [87]. Despite this fact, stronger notions like persistency is used to design observers, i.e., there exists an observer working for the class of persistent inputs.

(4) *State affine system plus a nonlinear term*

A general class of state affine systems is given by the class of systems of the form

$$\begin{cases} \dot{\xi} = A(u, y, s)\xi + \phi(u, \xi) \\ y = C\xi \end{cases} \tag{2.54}$$

for which it is possible to design an observer. Notice that the matrix $A(u, y, s)$ depends on the input u, the output y, and a known signal s [83].

Regarding these above classes of systems, several authors are interested to characterize them, where necessary and sufficient conditions are given to transform a general nonlinear system into state affine systems plus an output–input injection or plus a nonlinear term.

(5) *Interconnected state affine system plus nonlinear terms*

Finally, we can find systems that can be partitioned in a set of interconnected subsystem, represented in subsystems of the following form

$$\begin{cases} \dot{\xi}_1 = A_1(u)\xi_1 + \phi_1(u, \xi_2, \ldots, \xi_r) \\ \dot{\xi}_2 = A_2(u)\xi_2 + \phi_1(u, \xi_1, \ldots, \xi_r) \\ \cdots \\ \dot{\xi}_r = A_r(u)\xi_r + \phi_r(u, \xi_2, \ldots, \xi_{r-1}) \\ y_1 = C\xi_1 \\ y_2 = C\xi_2 \\ \cdots \\ y_r = C\xi_r. \end{cases} \tag{2.55}$$

In Chap. 3, two main classes of observers for nonlinear systems will be considered to reconstruct the components of the state vector which are not measurable.

(1) *Extended observers*: high gain observer, observer for state affine system, and nonlinear interconnected observers.
(2) *Sliding mode observers*: for nonlinear systems: Super-twisting and high order sliding mode observers.

2.6 Conclusions

One of the most important structural properties of dynamical systems has been studied in this chapter: the observability of nonlinear systems. As it has been seen in this chapter, the nonlinear observability property can depend on the input (explicitly or implicitly), and some definitions have been introduced to classify the inputs (universal and persistent inputs). Then, the observability of the AC machines has been analyzed, and the conditions under which the PMSM and the IM are observable have been determined along with their physical interpretation. This will be useful in the subsequent chapters to guarantee the convergence of the designed observers.

2.7 Bibliographical Notes

The observability study of nonlinear systems and next, the design of an observer is generally not a trivial task. Concerning the observability of nonlinear systems, the main definitions, used in this book, can be found in [42, 46, 65]. A classical observability criterion can be defined by using an observation space closed under Lie derivation as introduced in [46]. The key role of the input for the observability of the nonlinear systems is described in [3].

From these definitions, some authors have studied the observability of the AC machines. Nevertheless, the studies on the synchronous motor observability are rather uncommon, even if some results can be found in [20, 40, 92, 93]. Similarly, for the induction motor observability analysis, some results are available in [11, 32, 44]. In [32], sufficient conditions under which the induction motor loses the observability property have been presented.

Chapter 3
Observer Design for AC Motors

Abstract Assuming that for AC electrical machines, the only measurable variables are the currents and the voltages, the mathematical models of the synchronous and induction motors are used to study their respective observability property. If this property is satisfied and under some necessary conditions introduced later, observers are designed to estimate the non-measurable variables of the electric machines. First, some definitions and an introduction to the Nonlinear Observers design are developed. Next, a classification in terms of the convergence rate of two classes of observers is studied: (1) Observers with an asymptotic convergence. (2) Observers with a finite-time convergence. Furthermore, as for nonlinear systems there are no canonical forms, several observer structures are introduced to be next applied to AC machines. From the mathematical model of the PMSM, rewritten in the form of two interconnected subsystems, an adaptive interconnected observer can be designed to estimate the rotor speed, rotor position, and load torque. Some assumptions are considered in order to ensure its asymptotic convergence of the observer. Because the stator resistance depends on the temperature which introduces a variation with respect to its nominal value, then in order to determine its real value, an adaptive interconnected observer is designed to estimate the stator resistance and simultaneously the rotor speed, rotor position, and non-measured load torque. Sufficient conditions are obtained to ensure the asymptotic convergence. Then, a super-twisting observer for a class of nonlinear systems is considered. The advantages of this observer are robustness with respect to parametric uncertainties and finite-time convergence which allows to guarantee that the separation principle can be satisfied when a controller is next applied. Similarly, from the IMPSM mathematical model, an adaptive interconnected observer is designed to estimate the rotor position, rotor speed, load torque, and stator resistance. Finally, for the induction motor, an adaptive interconnected observer is designed to simultaneously estimate the rotor speed, the fluxes, and the load torque. To guarantee the robustness property, an extension of the above observer under parametric uncertainties is developed and, by using practical stability concepts, the practical stability of the estimation error is ensured.

3.1 Observers for Nonlinear Systems

The observation problem for nonlinear systems can be formulated as follows:

Given a dynamical system described by (1.67), *find the estimated state* $\hat{x}(t)$ *of* $x(t)$ *from the knowledge of the input* $u(t)$ *and the output* $y(t)$ *for* $t \in [0, T]$, *for* $T > 0$.

Notice that the estimated state is the solution of an auxiliary system:

$$\dot{\hat{x}}(t) = \mathbb{F}(\hat{x}(t), u(t)) + K(h(\hat{x}(t)), u(t)), y(t)), \tag{3.1}$$

where $K(h(\hat{x}(t), u(t)), y(t))$ is a correction term depending on: the estimated state, the measurable output and possibly on the input.

A general definition of an observer is given as

Definition 3.1 Consider an auxiliary system:

$$\begin{cases} \dot{\xi}(t) = F(\xi(t), u(t), y(t)) \\ \hat{x}(t) = H(\xi(t), u(t), y(t)), \end{cases} \tag{3.2}$$

then, system (3.2) is called an observer of system (1.67) with the estimation error $e(t)(=\hat{x}(t) - x(t)) \to 0$ as $t \to \infty$.

For instance, the estimated state of an observer can be used

  (i) *by a control algorithm*,
 (ii) *to monitor the evolution of the system*,
(iii) *to detect failures on the system*.

In all these cases, the study of the following properties is necessary:

(1) *Observability of the system.*
    Determine whether to reconstruct the state of the system is possible by analyzing the observability property of its mathematical model.
(2) *Convergence of the observer.*
    To analyze under what conditions the estimation error converges to zero, either in finite-time or asymptotically or exponentially.

Remark 3.1 Moreover, contrary to the linear case, if the observability property is satisfied for the nonlinear systems, it does not automatically imply the design of an observer.

(3) *Stability of the system in closed-loop.*
    There is no a priori separation principle for nonlinear systems. Thus, to study the stability condition of the closed-loop system is necessary when the controller uses the estimated state provided by the observer.

3.1.1 Definitions and Preliminary Results

In 1963, Luenberger outlined the observer theory to reconstruct the state of time invariant linear systems. The observers, their applications, and their links with the main concepts of the systems control theory make this topic an interesting domain of research. Later, Kalman introduced the state variable methods. The observer theory for linear time variant systems has been developed. The so-called Kalman filter is also an approximate solution to the observation problem of nonlinear systems. Although its properties are not theoretically proved, this filter works well in practice but under restrictive hypotheses. Thus, for nonlinear systems, the observer design is not an easy task.

There is no systematic and unique procedure to establish an observable normal form for the general nonlinear systems. An interesting normal form is the one for which an observer can be designed by an extension of the Luenberger form called the high-gain observer.

Now, in this chapter, some classes of nonlinear systems are introduced for which to construct an observer is possible. The systems are assumed to be observable (see definitions given in Chap. 2).

Consider the following nonlinear system:

$$\begin{cases} \dot{x} = f(x) + g(x)u \\ y = h(x) \end{cases} \tag{3.3}$$

where $x \in \Re^n$ is the state vector, $u \in \Re^m$ is the input, and $y \in \Re^p$ the output vector. Furthermore, $f(x)$ and $g(x)$ are smooth vector fields and the functions $\{h_1, \ldots, h_p\}$ are assumed to be sufficiently smooth on U, a neighborhood of x (see [46]).

3.1.2 A High Gain Observer

Consider that system (3.3) can be transformed, by means of a diffeomorphism, into the following system:

$$\begin{cases} \dot{\xi} = A\xi + \phi(u, y) \\ y = C\xi \end{cases} \tag{3.4}$$

where $\phi(u, y)$ is the input–output injection which is bounded. This system is observable for any input, if and only if the pair (C, A) is observable in the Kalman sense (see [47]).

Then the following system:

$$\begin{cases} \dot{\widehat{\xi}} = A\widehat{\xi} + \phi(u, y) - K(C\widehat{\xi} - y) \\ \widehat{y} = C\widehat{\xi} \end{cases} \tag{3.5}$$

is an observer for system (3.4), where the gain K of the observer is chosen such that the matrix $(A - KC)$ has eigenvalues with negative real parts. The convergence of the estimation error dynamics, which is linear in the estimation error, can be directly proved. By means of a diffeomorphism, this transformation of a nonlinear system (2.7), into another given by (3.4) has been characterized in [55, 75].

The convergence of this observer is established in the following theorem.

Theorem 3.1 *Consider system* (3.4) *and the following assumptions hold:*

(1) *The system has no finite escape time;*
(2) *The nonlinear term* $\phi(u, y)$ *is bounded,*

Then the estimation error converges to zero exponentially as t tends to infinity.

The generalization for the class of nonlinear systems observable for any input is given in the following definition.

Definition 3.2 Consider the following system:

$$\begin{cases} \dot{\xi} = A\xi + \phi(u, \xi) \\ y = C\xi \end{cases} \tag{3.6}$$

where the matrix A is defined as

$$A = \begin{bmatrix} 0 & 1 & \cdots & 0 & 0 \\ & & \ddots & & \\ 0 & 0 & \cdots & 0 & 1 \\ 0 & 0 & \cdots & 0 & 0 \end{bmatrix}$$

and $C = (1, \ldots, 0)$, for any $u(t) \in U_{adm}$, the set of the admissible inputs, $y(t)$ is the measured output. The vector field $\phi(u, \xi)$ is assumed compactly supported (see [28]) and has a triangular structure (see [46] for more details). The Jacobian matrix of $\phi(u, \xi)$ is considered to be upper bounded and the vector $\phi(u, \xi)$ has the Lipschitz property, i.e.,

$$\phi(u, \xi) = (\phi_1(u, \xi_1), \phi_2(u, \xi_1, \xi_2), \ldots, \phi_n(u, \xi_1, \ldots, \xi_n))^T.$$

with the functions $\phi_j(u, \xi_1, \ldots, \xi_j)$, for $j = 1, \ldots, n$; that are locally Lipschitz functions with respect to x and uniformly with respect to u, i.e.,

$$|\phi_j(u, \widehat{\xi}_1, \ldots, \widehat{\xi}_j) - \phi_j(u, \xi_1, \ldots, \xi_j) < L||\widehat{\xi} - \xi||, \tag{3.7}$$

where L is the Lipschitz constant.

Then the *High Gain Luenberger Observer* [28] for system (3.6) is given as

$$\begin{cases} \dot{\widehat{\xi}} = A\widehat{\xi} + \phi(u, \widehat{\xi}) - \Delta_\rho^{-1} KC(\widehat{\xi} - \xi) \\ \widehat{y} = C\widehat{\xi} \end{cases} \tag{3.8}$$

where the observer gain is $\Delta_\rho K$, with $\Delta_\rho = diag(1/\rho, \ldots, 1/\rho^n)$ and K whose components are chosen in such a way that the roots of the characteristic polynomial

$$s^n + k_1 s^{n-1} + k_2 s^{n-2} + \cdots + k_n = 0 \tag{3.9}$$

have negative real parts. The parameter ρ is a positive constant for which a high value increases the convergence rate and then allows fast reconstruction of the state.

Note that the observer gain does not depend on u and is computed offline. The convergence of the High Gain Luenberger Observer is expressed in the following theorem.

Theorem 3.2 *Consider system (3.6). There is a large enough $\rho > 1$ such that for all initial conditions $(\xi_o, \widehat{\xi}_o)$ belong to $(\chi, \widehat{\chi}) \subset (\Re^n, \Re^n)$, it follows that the estimation error converges exponentially to zero, i.e.,*

$$\|\widehat{\xi}(t) - \xi(t)\|^2 < M(\rho)e^{-\rho t}\|\widehat{\xi}_o - \xi_o\|^2 \tag{3.10}$$

where $M(\rho)$ is a positive constant depending on ρ.

Proof Denoting the estimation error by $e = \widehat{\xi} - \xi$, whose dynamics is given as

$$\dot{e} = \{A - \Delta_\rho^{-1} KC\}e + \phi(u, \widehat{\xi}) - \phi(u, \xi). \tag{3.11}$$

Define the following change of coordinates: $\varepsilon = \Delta_\rho e$, where $\Delta_\rho S_1 \Delta_\rho = S_\rho$, and S_ρ is the solution of

$$\rho S_\rho + A^T S_\rho + S_\rho A - C^T C = 0 \tag{3.12}$$

and $S_1 = S_\rho|_{\rho=1}$, i.e., the evaluation of the solution of S_ρ for $\rho = 1$. Assume there exist symmetric positive definite matrices P and Q such that

$$PA + A^T P = -Q,$$

and define the following candidate Lyapunov function:

$$V = \frac{1}{\rho} e^T S_\rho e = \varepsilon^T S_1 \varepsilon.$$

The time derivative of V along the trajectories of (3.11) is

$$\dot{V} = 2\varepsilon^T S_1 \Delta_\rho [\{A - \Delta_\rho^{-1} KC\}e + \phi(u, \widehat{\xi}) - \phi(u, \xi)]. \tag{3.13}$$

Taking into account the triangular form of ϕ satisfying the Lipschitz condition, it follows that

$$\|\Delta_\rho[\phi(u, \widehat{\xi}) - \phi(u, \xi)]\| \le \eta\|\varepsilon\|.$$

On the other hand, a simple calculation gives

$$\Delta_\rho\{A - \Delta_\rho^{-1}KC\}\Delta_\rho^{-1} = \rho\{A - KC\}, \tag{3.14}$$

$$\dot{V} = 2\varepsilon^T S_1 \rho\{A - KC\}\varepsilon + \varepsilon^T S_1 \Delta_\rho[\phi(u, \widehat{\xi}) - \phi(u, \xi)]. \tag{3.15}$$

Replacing the above inequalities, it follows that

$$\dot{V} = -\rho\lambda_{min}(S_1)\lambda_{min}(Q)\|\varepsilon\|^2 + \eta\lambda_{max}(S_1)\|\varepsilon\|^2, \tag{3.16}$$

and finally, we have

$$\dot{V} = -(\rho\lambda_{min}(S_1)\lambda_{min}(Q) - \eta\lambda_{max}(S_1))\|\varepsilon\|^2 < -\delta\|\varepsilon\|^2. \tag{3.17}$$

If $\rho > \dfrac{\eta\lambda_{max}(S_1)}{\lambda_{min}(S_1)\lambda_{min}(Q)}$, then the estimation error converges exponentially to zero.

3.1.3 Kalman-Like Observers

Consider the following system:

$$\begin{cases} \dot{z}(t) = Az + Bu - K(Cz(t) - y(t)) \\ \widehat{y} = Cz. \end{cases} \tag{3.18}$$

The above system is an observer for linear system (2.1) (noted Luenberger Observer), where $z(t)$ is the estimated state and the matrix K is the gain of the observer.

Obviously, the estimation error $e(t) = x(t) - z(t)$ tends to zero as t tends to infinity if the matrix K is chosen such that the eigenvalues of the matrix $(A - BK)$ have strictly negative real parts.

The stability analysis of the closed-loop linear systems can be easily solved thanks to the separation principle, i.e., the controller and the observer can be designed independently and the resulting closed-loop system is stable.

Another solution is a time-varying gain K defined as $K(t) = P(t)^{-1}C^T R^{-1}$ where $P(t)$ is solution of the equation

$$\frac{dP(t)}{dt} = -A^T P(t) - P(t)A - P(t)QP(t) + C^T R^{-1}C. \tag{3.19}$$

Equation (3.19) is referred as the *Riccati equation*, where the matrices R and Q are symmetric definite positive matrices that are weighting matrices to tune.

Remark 3.2 The class of the nonlinear systems (3.6) that is observable for any input, is not representative of the main difficulty for the nonlinear system observer design. This is why a more general class is introduced in the following.

The Extended Kalman Filter

Now, we introduce an interesting class of nonlinear systems for which it is possible to construct an observer.

Consider the class of systems described as

$$\begin{cases} \dot{\xi} = A(u)\xi + \phi(u, y) \\ y = C\xi = \xi_1 \end{cases} \tag{3.20}$$

where the components of matrix $A(u)$ and vector $\phi(u, y)$ are continuous functions, depending on u and y and are uniformly bounded. The nonlinear term $\phi(u, y)$ has a triangular form and does not affect the observability of the system.

Then system (3.20) is observable in the rank sense if the matrix

$$d\mathcal{O} = \begin{bmatrix} C \\ CA(u) \\ \vdots \\ CA^{n-1}(u) \end{bmatrix} \tag{3.21}$$

is nonsingular.

Denote $\Psi_{u,x_0}(\tau, t)$ the transition matrix of the system

$$\begin{aligned} \dot{\xi} &= A(u)\xi \\ y &= C\xi \end{aligned} \tag{3.22}$$

where the matrices $A(u)$ and C are of the general form

$$A(u) = \begin{bmatrix} a_{11}(u) & \cdots & a_{1n}(u) \\ \vdots & \ddots & \vdots \\ a_{n1}(u) & \cdots & a_{nn}(u) \end{bmatrix}$$

and $C = (1, \ldots, 0)$.

It is clear that the structure of the matrices $A(u)$ and C is not unique.

Now, we can introduce the class of persistent inputs which will be important to design an observer for system (3.22).

Definition 3.3 [3] An input is persistent for system (3.22) if for any initial condition x_0, there exist β_1, β_2, T' positive constants and $t_0 > 0$ such that

$$\beta_1 I_d \leq \int_t^{t+T'} \Psi_{u,x_0}^T(\tau,t) C^T C \Psi_{u,x_0}^T(\tau,t) d\tau \leq \beta_2 I_d, \qquad \forall t > t_0, \quad (3.23)$$

where I_d is the identity matrix.

Notice that the input persistence is related to the observability properties of the system.

The following system noted an *Extended Kalman Observer* [41]:

$$\begin{cases} \dot{\widehat{\xi}} = A(u)\widehat{\xi} + \phi(u,y) - S^{-1}C^T(\widehat{\xi} - \xi) \\ \widehat{y} = C\widehat{\xi} \end{cases} \quad (3.24)$$

is an observer for system (3.20), where $S^{-1}C^T$ is the gain of the observer and S is a symmetric definite positive matrix, solution of the differential Riccati equation

$$\dot{S} = -\rho S(t) - A^T(u)S - SA(u) + C^T C, \quad (3.25)$$

and ρ is a positive constant, which is used to tune the convergence rate of the observer.

The convergence proof of this observer requires the following lemma:

Lemma 3.1 *Assume that v is a persistent input for the state affine system (3.20), and consider the following Lyapunov differential equation:*

$$\dot{S}(t) = -\rho S(t) - A^T(v(t))S(t) - S(t)A(v(t)) + C^T C$$

with $S(0) > 0$, then

$$\exists \rho_0 > 0, \quad \forall \rho \geq \rho_0, \quad \exists \bar{\alpha} > 0, \quad \bar{\beta} > 0, \quad t_0 > 0$$

such that

$$\bar{\alpha} I_d \leq S(t) \leq \bar{\beta} I_d, \qquad \forall t \geq t_0,$$

where I_d is the identity matrix.

The proof of this lemma is given in [4]. Then the convergence of observer (3.24) can be proved as follows.

Proof Define the estimation error as $e = \widehat{\xi} - \xi$ whose dynamics is given by

$$\begin{cases} \dot{e} = \{A(u) - S^{-1}C^T C\}e \\ \dot{S} = -\rho S(t) - A^T(u)S - SA(u) + C^T C. \end{cases} \quad (3.26)$$

If the input u is a persistent input, from Lemma 3.1, the matrix S is definite positive $\forall t \geq t_0$. Then

$$V(e) = e^T S e$$

is a well-defined Lyapunov function $V(e)$. Taking the time derivative of $V(e)$ along the trajectories of (3.26), it follows that

$$
\begin{aligned}
\dot{V}(e) = {} & e^T S\{A(u) - S^{-1}C^T C\}e + e^T\{A(u) - S^{-1}C^T C\}^T S e \\
& + e^T\{-\rho S(t) - A^T(u)S - SA(u) + C^T C\}e.
\end{aligned}
\tag{3.27}
$$

After computations, it is easy to see that

$$\dot{V}(e) < -\rho e^T S(t)e = -\rho V(e). \tag{3.28}$$

Finally, it follows that

$$\|e(t)\| < M\|e(0)\|exp(-\rho t). \tag{3.29}$$

Then the estimation error exponentially converges to zero with arbitrary rate of convergence ρ and for any initial condition $e(0)$. This ends the proof.

For general systems of the form

$$
\begin{cases}
\dot{\xi} = A(u, y, s)\xi + \phi(u, y) \\
y = C\xi
\end{cases}
\tag{3.30}
$$

with s is an external signal and where the signals (u, y, s) are assumed to be persistent inputs. An observer for system (3.30) can be designed as

$$
\begin{cases}
\dot{\widehat{\xi}} = A(u, y, s)\widehat{\xi} + \phi(u, y) - S^{-1}C^T C(\widehat{\xi} - \xi) \\
\dot{S} = -\rho S(t) - A^T(u, y, s)S - SA(u, y, s) + C^T C \\
\widehat{y} = C\widehat{\xi}.
\end{cases}
\tag{3.31}
$$

The estimation error converges exponentially to zero, with a convergence rate given by ρ provided $v = (u, y, s)$ is persistent [3].

Persistency in AC Machines

The speed sensorless control of electrical machines has been the object of intensive research during the last years. It is clear that the motivation is to reduce the cost of hardware and to increase the reliability. However, when the speed is close to zero and for low frequency voltages, some observability drawbacks appear. To overcome this difficulty, various methods have been presented where a signal is superimposed on the stator voltages or currents of the machine in order to extract sufficient information about the rotor position. Most high frequency signal injection methods have been

proposed making use of the phase inductance variation property. This approach provides rotor position information at low frequency and during standstill operation. However, a certain amount of saliency in the machine is necessary. Also, injection of high frequency signals is not desired in high speed operation. Fundamental excitation methods involve the detection of the position from the stator voltages and currents without requiring additional test signals.

The EMF was also used to estimate the rotor position by means of a state observer or a Kalman filter. This approach works well in medium and high speed applications, while this is not accurate at low speed when back EMF is weak.

General Extended Kalman Observer

Now, an observer design is introduced for the class of nonlinear systems for which it is possible to devise an Extended Kalman Observer.

Consider the following class of systems described as

$$\begin{cases} \dot{\xi} = A(u)\xi + \phi(\xi, u) \\ y = C\xi \end{cases} \tag{3.32}$$

where ξ belongs to the compact $\chi \subset \Re^n$, y belongs to $\Re^n$, u belongs to the set of the admissible input U_{adm} in $\Re^m$. The matrices $A(u)$ and C are given as

$$A(u) = \begin{bmatrix} 0 & a_1(u) & \cdots & 0 & 0 \\ & & \ddots & & \\ 0 & 0 & \cdots & a_{n-2}(u) & 0 \\ 0 & 0 & \cdots & 0 & a_{n-1}(u) \\ 0 & 0 & \cdots & 0 & 0 \end{bmatrix}$$

and $C = (1, \ldots, 0)$, with $\phi(\xi, u)$ satisfying the Lipschitz property and the elements of A are such that $0 < a_i(u) < \alpha_M$, for $i = 1, \ldots, n-1$. So, an observer for such a class of systems is given in the following definition.

Definition 3.4 High Gain Extended Kalman Filter [3]. The following system

$$\begin{cases} \dot{\widehat{\xi}} = A(u)\widehat{\xi} + \phi(\widehat{\xi}, u) - S^{-1}C^T R^{-1}(C\widehat{\xi} - y) \\ \dot{S} = -\rho S - A(u)^T S - SA(u) + C^T R^{-1}C \\ \widehat{y} = C\widehat{\xi} \end{cases} \tag{3.33}$$

is an observer for system (3.32), where S is a symmetric definite positive matrix solution of the Riccati equation, R is a symmetric definite positive matrix. The gain of the extended Kalman filter is computed online and depends on S, the solution of the Riccati equation.

The following result can be established:

Theorem 3.3 *For a large enough ρ and for all $t > 0$, system (3.33) is an extended Kalman observer for system (3.32), where the estimation error decays exponentially to zero with a rate of convergence given by ρ*

$$\|\widehat{\xi}(t) - \xi(t)\| < L(\rho)e^{-\frac{\rho}{2}t}\|\widehat{\xi}_o - \xi_o\|.$$

where $L(\rho)$ is a positive constant.

Adaptive Kalman Observer [6]

In the aforementioned observers, the system parameters are assumed exactly known. If not, under suitable assumptions, it is possible to estimate the non-measurable state and to identify the unknown parameters, simultaneously.

Consider now the case where the system is affine in the state, depends on unknown parameters in an affine form, and is represented as

$$\begin{cases} \dot{\xi} = A(u)\xi + \Psi(u, y)\vartheta + \phi(u, y) \\ y = C\xi \end{cases} \tag{3.34}$$

where ϑ is the vector of unknown parameters to be estimated and $\Psi(u, y)$ satisfies the same properties as matrix $A(u)$ and vector $\phi(u, y)$ with respect to u and y given in (3.20).

In order to design an observer for system (3.34) and to estimate simultaneously the state and parameters, the following assumptions are introduced:

Definition 3.5 Let Λ be a matrix, solution of the equation

$$\dot{\Lambda} = (A(u) - \Gamma S_\xi^{-1}C_2^T C_2)\Lambda + \Psi(u, y). \tag{3.35}$$

There exist β_3, β_4, T' positive constants and $t_0 > 0$ such that

$$\beta_3 I_d \leq \int_t^{t+T'} \Lambda^T(\tau, t)C^T C\Lambda(\tau, t)d\tau \leq \beta_4 I_d, \quad \forall t > t_0, \tag{3.36}$$

where I_d is the identity matrix.

Definition 3.5 allows to ensure the persistency of the signals which is required to identify the parameters.

Assuming that u is a persistent input and Definition 3.5 is satisfied, the following system is an *Adaptive Kalman Observer* for system (3.34) (see [6]):

$$O_{adap}: \begin{cases} \dot{\widehat{\xi}} = A(u)\widehat{\xi} + \Psi(u, y)\widehat{\vartheta} + \phi(u, y) - \{\Lambda S_\vartheta^{-1}\Lambda^T C^T + S_\xi^{-1}C^T\}C(\widehat{\xi} - \xi) \\[2mm] \dot{\widehat{\vartheta}} = -S_\vartheta^{-1}\Lambda^T C^T C(\widehat{\xi} - \xi) \\[2mm] \dot{S_\xi} = -\rho_\xi S_\xi(t) - A^T(u)S_\xi - S_\xi A(u) + C^T C \\[2mm] \dot{S_\vartheta} = -\rho_\vartheta S_\vartheta + \Lambda^T C_2^T C_2 \Lambda \\[2mm] \dot{\Lambda} = (A(u) - \Gamma S_\xi^{-1}C_2^T C_2)\Lambda + \Psi(u, y) \\[2mm] \widehat{y} = C\widehat{\xi} \end{cases} \qquad (3.37)$$

where $S_\xi^{-1}C^T$ is the gain associated to the state estimation, and $\Lambda S_\vartheta^{-1}\Lambda^T C^T$ is the parameter identification gain. S_ξ and S_ϑ are symmetric definite positive matrices solution of the Riccati equations

$$\dot{S_\xi} = -\rho_\xi S_\xi(t) - A^T(u)S_\xi - S_\xi A(u) + C^T C \qquad (3.38)$$
$$\dot{S_\vartheta} = -\rho_\vartheta S_\vartheta + \Lambda^T C_2^T C_2 \Lambda \qquad (3.39)$$

respectively, and ρ_ξ and ρ_ϑ are some positive constants sufficiently large.

Remark 3.3 Notice that the gain $\Lambda S_\vartheta^{-1}\Lambda^T C^T$ of the observer associated with the identification of the parameters depends on the solution of the S_ϑ and Λ dynamics equations, and that Assumption 3.2 is satisfied.

The convergence of the observer can be proved as follows.

Defining the state and parameter estimation errors, respectively: $e_\xi = \widehat{\xi} - \xi$ and $\epsilon_\vartheta = \widehat{\vartheta} - \vartheta$, whose dynamics are given as

$$\dot{e}_\xi = \{A(u) - \Lambda S_\vartheta^{-1}\Lambda^T C^T C - S_\xi^{-1}C^T C\}e_\xi + \Psi(u, y)\epsilon_\vartheta$$
$$\dot{\epsilon}_\vartheta = -S_\vartheta^{-1}\Lambda^T C^T C e_\xi. \qquad (3.40)$$

Now, introduce the following change of coordinates:

$$\epsilon_\xi = e_\xi - \Lambda\epsilon_\vartheta. \qquad (3.41)$$

Then taking the time derivative of (3.41) and replacing the suitable expressions, it follows that

$$\dot{\epsilon}_\xi = \{A(u) - S_\xi^{-1}C^T C\}\epsilon_\xi$$
$$\dot{\epsilon}_\vartheta = -S_\vartheta^{-1}\Lambda^T C^T C\{e_\xi - \Lambda\epsilon_\vartheta\}. \qquad (3.42)$$

Now, to prove the convergence of this observer, consider the following Lyapunov function:

$$V = \epsilon_\xi^T S_\xi \epsilon_\xi + \epsilon_\vartheta^T S_\vartheta \epsilon_\vartheta. \tag{3.43}$$

So, from the time derivative of V and substituting the suitable expression, yields:

$$
\begin{aligned}
\dot{V} = &-\rho_\xi \epsilon_\xi^T S_\xi \epsilon_\xi - \rho_\vartheta \epsilon_\vartheta^T S_\vartheta \epsilon_\vartheta \\
&- \epsilon_\xi^T C^T C \epsilon_\xi - \epsilon_\xi^T C^T C \Lambda \epsilon_\vartheta - \epsilon_\vartheta^T \Lambda^T C^T C \epsilon_\xi - \epsilon_\vartheta^T \Lambda^T C^T C \Lambda \epsilon_\vartheta.
\end{aligned}
\tag{3.44}
$$

Since

$$
\begin{aligned}
&-\epsilon_\xi^T C^T C \epsilon_\xi - \epsilon_\xi^T C^T C \Lambda \epsilon_\vartheta - \epsilon_\vartheta^T \Lambda^T C^T C \epsilon_\xi - \epsilon_\vartheta^T \Lambda^T C^T C \Lambda \epsilon_\vartheta \\
&= -\{\epsilon_\xi + \Lambda \epsilon_\vartheta\}^T C^T C \{\epsilon_\xi + \Lambda \epsilon_\vartheta\} < 0,
\end{aligned}
\tag{3.45}
$$

it follows that

$$\dot{V} = -\rho_\xi \epsilon_\xi^T S_\xi \epsilon_\xi - \rho_\vartheta \epsilon_\vartheta^T S_\vartheta \epsilon_\vartheta. \tag{3.46}$$

Choosing $\rho = min(\rho_\xi, \rho_\vartheta)$ such that

$$\dot{V} \le -\rho V \tag{3.47}$$

then, ϵ_ξ and ϵ_ϑ^T converge exponentially to zero with a rate of convergence given by ρ.

Interconnected Observers [5]

There is no systematic method to design an observer for a nonlinear system. However, if the system satisfies partially the observability property, a solution is to search if the whole system can be represented as a set of interconnected subsystems for which each one satisfies the observability property. So, the idea is to design an observer for each observable subsystem.

For instance, consider two interconnected subsystems:

$$\Sigma_1 \; : \; \begin{cases} \dot{X}_1 = A_1 X_1 + \Phi_1(u, X_1, X_2) \\ y_1 \; = C_1 X_1 \end{cases} \tag{3.48}$$

$$\Sigma_2 \; : \; \begin{cases} \dot{X}_2 = A_2 X_2 + \Phi_2(u, X_1, X_2) \\ y_2 \; = C_2 X_2. \end{cases} \tag{3.49}$$

In order to design an observer for system (3.48) and (3.49), the following assumption is needed:

Assumption 3.1

1. Φ_1 (respectively Φ_2) is a global Lipschitz function with respect to X_1 (respectively X_2), uniformly with respect to u, and globally uniformly w.r.t. X_2 (respectively X_1).
2. X_2 (respectively X_1) is considered as input of subsystems Σ_1 (respectively Σ_2).

Then, an *Interconnected Observer* [5] for subsystems (3.48) and (3.49) is given by

$$
O_{inter1} : \begin{cases}
\dot{Z}_1 = A_1 Z_1 + \Phi_1(u, Z_1, Z_2) + S_1^{-1} C_1^T (y_1 - \hat{y}_1) \\[2mm]
\dot{Z}_2 = A_2 Z_2 + \Phi_2(u, Z_1, Z_2) + S_2^{-1} C_2^T (y_2 - \hat{y}_2) \\[2mm]
\rho_{x1} S_1 + S_1 A_1 + A_1^T S_1 - C_1^T C_1 = 0 \\[2mm]
\rho_{x2} S_2 + S_2 A_2 + A_2^T S_2 - C_2^T C_2 = 0 \\[2mm]
\hat{y}_1 = C_1 Z_1 \\[2mm]
\hat{y}_2 = C_2 Z_2
\end{cases}
\tag{3.50}
$$

where Z_1 and Z_2 are the estimated state variables, respectively, of X_1 and X_2. ρ_{x1} and ρ_{x2} are positive constants, S_1 and S_2 are symmetric positive definite matrices, with $S_1(0) > 0$ and $S_2(0) > 0$ [4].

An extension of the above case is the class of systems described as

$$
\widetilde{\Sigma}_1 : \begin{cases}
\dot{X}_1 = A_1(u, y)X_1 + \Phi_1(u, X_1, X_2) \\
y_1 = C_1 X_1
\end{cases}
\tag{3.51}
$$

$$
\widetilde{\Sigma}_2 : \begin{cases}
\dot{X}_2 = A_2(u, y)X_2 + \Phi_2(u, X_1, X_2) \\
y_2 = C_2 X_2.
\end{cases}
\tag{3.52}
$$

Furthermore, the following assumption is required to design an observer for system (3.51) and (3.52):

Assumption 3.2

1. X_2 (respectively X_1) is considered as input for subsystem $\widetilde{\Sigma}_1$ (respectively $\widetilde{\Sigma}_2$).
2. The pair (u, y) is regularly persistent for $A_1(u, y)$ and $A_2(u, y)$.
3. Φ_1 (respectively Φ_2) is globally Lipschitz w.r.t. X_2 (X_1) and uniformly w.r.t. X_1 (respectively X_2) and (u, y).

So there exist ρ_{x1} and ρ_{x2} such that the following system:

$$O_{inter2} : \begin{cases} \dot{Z}_1 = A_1(u, y)Z_1 + \Phi_1(u, Z_1, Z_2) + S_1^{-1}C_1^T(y_1 - \hat{y}_1) \\ \dot{Z}_2 = A_2(u, y)Z_2 + \Phi_2(u, Z_1, Z_2) + S_2^{-1}C_2^T(y_2 - \hat{y}_2) \\ \\ \dot{S}_1 = -\rho_{x1}S_1 - A_1^T(u, y)S_1 - S_1A_1(u, y) + C_1^TC_1 \\ \dot{S}_2 = -\rho_{x2}S_2 - A_2^T(u, y)S_2 - S_2A_2(u, y) + C_2^TC_2 \\ \\ \hat{y}_1 = C_1Z_1 \\ \hat{y}_2 = C_2Z_2 \end{cases} \quad (3.53)$$

is an interconnected observer for system (3.51) and (3.52).

If the pair (u, y) is a persistent input for subsystem $\widetilde{\Sigma}_1$ (respectively $\widetilde{\Sigma}_2$), the convergence of the observer can be obtained such that for any initial condition $X_{1,0}$ (respectively $X_{2,0}$) in a compact set, the solution of the system remains bounded.

Under Assumption 3.2, the existence of the observer O_{inter2} (3.53) is ensured. Then, the following result can be established:

Theorem 3.4 *Consider the interconnected system* (3.51) *and* (3.52). *If Assumption* 3.2 *holds, the observer* O_{inter2} (3.53) *is an asymptotic observer for the interconnected system.*

To apply this theorem to real systems (AC machines in this book) the assumptions must be verified, taking into account the parameters of the systems and their operation domain.

Proof The proof can be achieved by choosing the appropriate candidate Lyapunov functions V_1 and V_2. Set $e_i = Z_i - X_i$, for $i = 1, 2$; the estimation errors of each subsystem. Then the estimation error dynamics are given by

$$\begin{cases} \dot{e}_1 = \{A_1(u, y) - S_1^{-1}C_1^TC_1\}e_1 + \Phi_1(u, Z_1, Z_2) - \Phi_1(u, X_1, X_2) \\ \dot{e}_2 = \{A_2(u, y) - S_2^{-1}C_2^TC_2\}e_2 + \Phi_2(u, Z_1, Z_2) - \Phi_2(u, X_1, X_2) \\ \\ \dot{S}_1 = -\rho_{x1}S_1 - A_1^T(u, y)S_1 - S_1A_1(u, y) + C_1^TC_1 \\ \dot{S}_2 = -\rho_{x2}S_2 - A_2^T(u, y)S_2 - S_2A_2(u, y) + C_2^TC_2. \end{cases} \quad (3.54)$$

Defining the Lyapunov functions

$$V_1 = e_1^T S_1 e_1 \quad \text{and} \quad V_2 = e_2^T S_2 e_2 \quad (3.55)$$

with

$$\lambda_{min}(S_i)\|e_i\|^2 \leq V_i = e_i^T S_i e_i \leq \lambda_{max}(S_i)\|e_i\|^2 \quad (3.56)$$

where, for $i = 1, 2$; $\lambda_{min}(S_i)$ and $\lambda_{max}(S_i)$ are the minimal and maximal eigenvalues of the matrix S_i.

Then the Lyapunov function for all estimation error dynamics is given by

$$V_{system} = V_1 + V_2$$

whose time derivative along the trajectories of system (3.51) and (3.52) is given by

$$
\begin{aligned}
\dot{V}_{system} = \\
&e_1^T S_1 \{A_1(u, y) - S_1^{-1} C_1^T C_1\} e_1 + e_1^T S_1 \{\Phi_1(u, Z_1, Z_2) - \Phi_1(u, X_1, X_2)\} \\
&+ e_1^T \{A_1(u, y) - S_1^{-1} C_1^T C_1\}^T S_1 e_1 + \{\Phi_1(u, Z_1, Z_2) - \Phi_1(u, X_1, X_2)\}^T S_1 e_1 \\
&+ e_1^T \{-\rho_{x1} S_1 - A_1^T(u, y) S_1 - S_1 A_1(u, y) + C_1^T C_1\} e_1 \qquad (3.57) \\
&+ e_2^T S_2 \{A_2(u, y) - S_2^{-1} C_2^T C_2\} e_2 + e_2^T S_2 \{\Phi_2(u, Z_1, Z_2) - \Phi_2(u, X_1, X_2)\} \\
&+ e_2^T \{A_1(u, y) - S_2^{-1} C_1^T C_2\}^T S_2 e_2 + \{\Phi_2(u, Z_1, Z_2) - \Phi_2(u, X_1, X_2)\}^T S_2 e_2 \\
&+ e_2^T \{-\rho_{x2} S_2 - A_2^T(u, y) S_2 - S_1 A_2(u, y) + C_2^T C_2\} e_2
\end{aligned}
$$

or equivalently

$$
\begin{aligned}
\dot{V}_{system} &\leq -\rho_{x1} e_1^T S_1 e_1 + 2 e_1^T S_1 \{\Phi_1(u, Z_1, Z_2) - \Phi_1(u, X_1, X_2)\} \\
&\quad - \rho_{x2} e_2^T S_2 e_2 + 2 e_2^T S_2 \{\Phi_2(u, Z_1, Z_2) - \Phi_2(u, X_1, X_2)\}.
\end{aligned} \qquad (3.58)
$$

From Assumption 3.2, the following inequalities hold:

$$\|\Phi_1(u, Z_1, Z_2) - \Phi_1(u, X_1, X_2)\| \leq K_1 \|e_2\|$$

$$\|\Phi_2(u, Z_1, Z_2) - \Phi_2(u, X_1, X_2)\| \leq K_2 \|e_1\|$$

for K_1 and K_2 positive constants. By using these inequalities, it follows that

$$
\begin{aligned}
\dot{V}_{system} &\leq -\rho_{x1} e_1^T S_1 e_1 + 2\lambda_{max}(S_1) K_1 \|e_1\| \|e_2\| \\
&\quad - \rho_{x2} e_2^T S_2 e_2 + 2\lambda_{max}(S_2) K_2 \|e_2\| \|e_1\|.
\end{aligned} \qquad (3.59)
$$

After some computation, the above equation can be expressed as follows:

$$\dot{V}_{system} \leq -\rho_{x1} V_1 - \rho_{x2} V_2 + \mu_1 \sqrt{V_1} \sqrt{V_2}, \qquad (3.60)$$

where $\mu_1 > 0$, so by using the following inequality:

$$\sqrt{V_1} \sqrt{V_2} \leq \frac{\varrho_1}{2} V_1 + \frac{1}{2\varrho_1} V_2,$$

for $\varrho_1 \in (0, 1)$. Finally,

$$\dot{V}_{system} \leq -\left(\rho_{x1} - \frac{\varrho_1 \mu_1}{2}\right) V_1 - \left(\rho_{x2} - \frac{\mu_1}{2\varrho_1}\right) V_2.$$

Choosing the gains ρ_{x1} and ρ_{x2} of the observer such that

$$\delta = min \left\{ \left(\rho_{x1} - \frac{\varrho_1 \mu_1}{2}\right), \left(\rho_{x2} - \frac{\mu_1}{2\varrho_1}\right) \right\},$$

it follows that

$$\dot{V}_{system} \leq -\delta V_{system}. \tag{3.61}$$

Then the exponential convergence of the observer to zero is obtained with a convergence rate given by δ.

Remark 3.4 It is clear that the Lyapunov functions V_1 and V_2 are definite positive if S_1 and S_2 satisfy the persistence condition, which means that the input sufficiently excites the system such that its observability is guaranteed.

Remark 3.5 Notice that this observer can be extended for n interconnected subsystems; the proof follows the same procedure presented above.

3.2 PMSM Adaptive Interconnected Observers

3.2.1 Adaptive Interconnected Observers for SPMSM

In the sequel, an adaptive interconnected observer will be designed (see [5, 6]) for the sensorless SPMSM. This observer is the combination of the adaptive observer with the interconnected observer presented in this chapter.

To design an observer for the sensorless SPMSM, it is assumed that

$$\frac{dT_l}{dt} = 0 \quad \text{and} \quad \frac{dR_s}{dt} = 0. \tag{3.62}$$

Remark 3.6 Equation (3.62) means that the load torque and the stator resistance values are assumed to be modeled by piecewise constant functions. Only the bound of the load torque is assumed to be known. Furthermore, it is clear that the stator resistance slowly changes with the temperature with respect to the other time constants of the AC machine. Other approaches can be used, for instance, singular perturbation methodology, however, as the dynamics of the SPMSM are fast with respect to the variation of the stator resistance, its dynamics could be considered constant.

Thus, the extended SPMSM model

$$
\begin{cases}
\dfrac{di_{sq}}{dt} = -\dfrac{R_s}{L_s}i_{sq} + p\Omega i_{sd} + \dfrac{v_{sq}}{L_s} - p\Omega\dfrac{\Psi_r}{L_s} \\[2mm]
\dfrac{di_{sd}}{dt} = -\dfrac{R_s}{L_s}i_{sd} - p\Omega i_{sq} + \dfrac{v_{sd}}{L_s} \\[2mm]
\dfrac{d\Omega}{dt} = -\dfrac{f}{J}\Omega + \dfrac{p\Psi_r}{J}i_{sq} - \dfrac{1}{J}T_l \\[2mm]
\dfrac{dR_s}{dt} = 0 \\[2mm]
y_1 \quad = i_{sd} \\[1mm]
y_2 \quad = i_{sq}
\end{cases}
$$

which can be seen as the interconnection between two subsystems

$$
\begin{cases}
\begin{bmatrix} \dfrac{di_{sq}}{dt} \\[2mm] \dfrac{dR_s}{dt} \end{bmatrix} = \begin{bmatrix} 0 & -\dfrac{i_{sq}}{L_s} \\[2mm] 0 & 0 \end{bmatrix}\begin{bmatrix} i_{sq} \\ R_s \end{bmatrix} + \begin{bmatrix} -p\Omega i_{sq} - p\Omega\dfrac{\Psi_r}{L_s} \\[2mm] 0 \end{bmatrix} + \begin{bmatrix} \dfrac{1}{L_s} \\[2mm] 0 \end{bmatrix}v_{sq} \\[6mm]
y_1 \quad = i_{sq},
\end{cases}
\tag{3.63}
$$

and

$$
\begin{cases}
\begin{bmatrix} \dfrac{di_{sd}}{dt} \\[2mm] \dfrac{d\Omega}{dt} \end{bmatrix} = \begin{bmatrix} 0 & -pi_{sq} \\[2mm] 0 & -\dfrac{f}{J} \end{bmatrix}\begin{bmatrix} i_{sd} \\ \Omega \end{bmatrix} + \begin{bmatrix} -\dfrac{R_s}{L_s}i_{sq} \\[2mm] \dfrac{p\Psi_r}{J}i_{sq} \end{bmatrix} + \begin{bmatrix} \dfrac{1}{L_s} \\[2mm] 0 \end{bmatrix}v_{sd} - \begin{bmatrix} 0 \\[2mm] \dfrac{1}{J} \end{bmatrix}T_l \\[6mm]
y_2 \quad = i_{sd}.
\end{cases}
\tag{3.64}
$$

The above subsystems can be represented in a general form as the interconnection between two subsystems

$$
\Sigma_1 \; : \; \begin{cases} \dot{X}_1 = A_1(y)X_1 + F_1(X_2) + \Phi_1(u) \\ y_1 \; = C_1 X_1 \end{cases}
\tag{3.65}
$$

and

$$
\Sigma_2 \; : \; \begin{cases} \dot{X}_2 = A_2(y)X_2 + F_2(X_1, X_2) + \Phi_2(u) + \Phi T_l \\ y_2 \; = C_2 X_2 \end{cases}
\tag{3.66}
$$

where $X_1 = \begin{bmatrix} i_{sq} \; R_s \end{bmatrix}^T$ and $X_2 = \begin{bmatrix} i_{sd} \; \Omega \end{bmatrix}^T$ are the state vectors of (3.65) and (3.66), respectively; $u = \begin{bmatrix} v_{sd} \; v_{sq} \end{bmatrix}^T$ is the input, and $y = \begin{bmatrix} i_{sd} \; i_{sq} \end{bmatrix}^T$ is the output, with

$$A_1(y) = \begin{bmatrix} 0 & -\dfrac{i_{sq}}{L_s} \\ 0 & 0 \end{bmatrix}, \qquad F_1(X_2) = \begin{bmatrix} -p\dfrac{\psi_f}{L_s}\Omega - p\Omega i_{sd} \\ 0 \end{bmatrix},$$

$$A_2(y) = \begin{bmatrix} 0 & pi_{sq} \\ 0 & -\dfrac{f_v}{J} \end{bmatrix}, \qquad F_2(X_1, X_2) = \begin{bmatrix} -\dfrac{R_s}{L_s}i_{sd} \\ \dfrac{p}{J}\psi_f i_{sq} \end{bmatrix},$$

$$\Phi_1 = \begin{bmatrix} \dfrac{1}{L_s} \\ 0 \end{bmatrix}, \quad \Phi_2 = \begin{bmatrix} \dfrac{1}{L_s} \\ 0 \end{bmatrix}, \quad \Phi = \begin{bmatrix} 0 \\ -\dfrac{1}{J} \end{bmatrix},$$

$$C_1 = C_2 = [1\ 0].$$

Furthermore, an operation domain for the SPMSM (and for the IPMSM) is defined as:

Definition 3.6 The PMSM physical operation domain $\mathcal{D}_{\mathcal{S}}$ is defined by the set of values

$$\mathcal{D}_{\mathcal{S}} = \{X \in \Re^5 \mid \ |i_{sd}| \le I_d{}^{max}, \ |i_{sq}| \le I_q{}^{max}, \ |\Omega| \le \Omega^{max}, \\ |T_l| \le T_l{}^{max}, \ |R_s| \le R_s{}^{max}\}$$

with $X = [i_{sd}\ i_{sq}\ \Omega\ T_l\ R_s]^T$ and $I_d{}^{max}, I_q{}^{max}, \Omega^{max}, T_l{}^{max}, R_s{}^{max}$ the actual maximum values for the stator currents, the rotor speed, the load torque and the stator resistance, respectively.

The adaptive interconnected observer, developed in the sequel for the sensorless SPMSM, is based on the interconnection between several observers satisfying some required properties, in particular the property of input persistence [4].

For designing an observer for system (3.65) and (3.66), a separate synthesis of the observer for each subsystem is required.

Remark 3.7

1. X_2 and X_1 are respectively considered as inputs for subsystems (3.65) and (3.66). From [4], solutions of $\dot{S}_1$ and $\dot{S}_2$ (used below for the observer design) are symmetric positive definite matrices.
2. When the *SPMSM* remains in the observable area, X_2 and X_1 satisfy the persistence condition: the asymptotic stability of the observer is guaranteed.
3. When the *SPMSM* remains in the unobservable area, X_2 and X_1 do not satisfy the persistence condition. The asymptotic stability of the observer is not guaranteed. This problem is solved, by using the *practical stability* introduced in the Appendix "Appendix: Practical Stability Definitions".

Remark 3.8 From (3.65) and (3.66), $A_1(y)$ is globally Lipschitz w.r.t. X_2; $A_2(y)$ is globally Lipschitz w.r.t. X_1; $F_1(X_2)$ is globally Lipschitz w.r.t. X_2 and uniformly w.r.t. (u, y) and that $F_2(X_2, X_1)$ is globally Lipschitz w.r.t. X_2, X_1 and uniformly w.r.t. (u, y).

Then an adaptive interconnected observer for subsystems (3.65) and (3.66) is given by

$$O_1 : \begin{cases} \dot{Z}_1 = A_1(y)Z_1 + F_1(Z_2) + \Phi_1(u) + S_1^{-1}C_1^T(y_1 - \hat{y}_1) \\[2mm] \dot{S}_1 = -\rho_1 S_1 - A_1^T(y)S_1 - S_1 A_1(y) + C_1^T C_1 \\[2mm] \hat{y}_1 = C_1 Z_1, \end{cases} \qquad (3.67)$$

$$O_2 : \begin{cases} \dot{Z}_2 = A_2(y)Z_2 + F_2(Z_1, Z_2) + \Phi_2(u) + \Phi \hat{T}_l \\[1mm] \quad\quad + (\varpi \Lambda S_\vartheta^{-1} \Lambda^T C_2^T + \Gamma S_x^{-1} C_2^T)(y_2 - \hat{y}_2) + K C_1^T(y_1 - \hat{y}_1) \\[2mm] \dot{\hat{T}}_l = \varpi S_\vartheta^{-1} \Lambda^T C_2^T(y_2 - \hat{y}_2) + B(y_1 - \hat{y}_1) \\[2mm] \dot{S}_x = -\rho_x S_x - A_2^T(y)S_x - S_x A_2(y) + C_2^T C_2 \\[2mm] \dot{S}_\vartheta = -\rho_\vartheta S_\vartheta + \Lambda^T C_2^T C_2 \Lambda \\[2mm] \dot{\Lambda} = (A_2(y) - \Gamma S_x^{-1} C_2^T C_2)\Lambda + \Phi \\[2mm] \hat{y}_2 = C_2 Z_2 \end{cases} \qquad (3.68)$$

with $Z_1 = \begin{bmatrix} \hat{i}_{sq} & \hat{R}_s \end{bmatrix}^T$ and $Z_2 = \begin{bmatrix} \hat{i}_{sd} & \hat{\Omega} \end{bmatrix}^T$ are the estimated state variables of X_1 and X_2 respectively. Moreover, ρ_1, ρ_x and ρ_ϑ are positive constants, S_1 and S_x are symmetric positive definite matrices [4], with

$$S_\vartheta(0) > 0, \quad B(Z_1) = k\frac{p}{J}\psi_f \hat{i}_{sq}$$

and

$$K = \begin{bmatrix} -k_{c1} \\ -k_{c2} \end{bmatrix}, \quad \Gamma = \begin{bmatrix} 1 & 0 \\ 0 & \alpha \end{bmatrix}$$

with k, k_{c1}, k_{c2}, α and ϖ are positive constants.

The second observer (3.68) is composed of two parts: the first part to estimate the state (i_{sd}, Ω) and the second part to estimate (i_{sd}, T_l). This second part depends on a differential equation representing a dynamical system described in terms of Λ (the state of this system) and Φ (the input matrix). $S_1^{-1}C_1^T$ is the gain of observer (3.67); $(\varpi \Lambda S_\vartheta^{-1} \Lambda^T C_2^T + \Gamma S_x^{-1} C_2^T)$ and $K C_1^T$ are the gains of observer (3.68).

It can be seen that the observer gain in (3.68) is split into two terms. The first one $(\Gamma S_x^{-1} C_2^T)$ is associated to the state estimation and depends on the solution of a

Ricatti equation. The second one $(\varpi \Lambda S_\vartheta^{-1} \Lambda^T C_2^T)$ is related to the parameter identification. The solutions of these equations are dependent on the persistence property (sufficient richness of the signal) with respect to the state and/or the parameter.

Remark 3.9 In Eq. (3.68), the term $B(Z_1)(y_1 - \hat{y}_1)$ can be expressed as follows:

$$B(Z_1)(y_1 - \hat{y}_1) \equiv k \left[\frac{p}{J} \psi_f (i_{sq} - \hat{i}_{sq}) \right]$$
$$\equiv k(T_e - \tilde{T}_e),$$

where T_e and $\tilde{T}_e$ are, respectively, the real electromagnetic torque and the estimated torque.

For subsystem (3.65), the input is $v = (y)$, the state X_2 and $S(t) = S_1$, and for subsystem (3.66) one has $v = (y)$, X_1 and $S(t) = S_2$.

The conditions of observability loss have been stated in Sect. 2.3: the SPMSM is unobservable for some input value such that the rotor speed is zero. In the SPMSM observability area, the inputs for subsystem (3.65) and for subsystem (3.66) respectively, are persistent and the convergence of the observer can be ensured. However, in the unobservable region of the SPMSM (zero speed), such inputs are noted "*bad input*" and the observer convergence is not guaranteed and has to be analyzed.

Stability Analysis of Observer Under Uncertain Parameters

Under indistinguishable trajectories (unobservable area), the asymptotic convergence of any observer cannot always be guaranteed because the observability properties are lost on these trajectories. In such cases, the analysis of the closed-loop system stability is necessary.

If satisfied, the practical stability property [59], allows to establish that the dynamics of the estimation error converge in a ball B_r of radius r ($x \in B_r \Rightarrow \|x\| \le r$). If $r \to 0$ at $t \to \infty$, the classical asymptotic stability is obtained.

Consider that the SPMSM parameters are uncertain bounded with well-known nominal values. Equations (3.65) and (3.66) can be rewritten as

$$\Sigma_1 : \begin{cases} \dot{X}_1 = A_1(y)X_1 + F_1(X_2) + \Phi_1(u) + \Delta A_1(y) + \Delta F_1(X_2) \\ \\ y_1 = C_1 X_1 \end{cases} \quad (3.69)$$

$$\Sigma_2 : \begin{cases} \dot{X}_2 = A_2(y)X_2 + F_2(X_1, X_2) + \Phi_2(u) + \Phi T_l + \Delta A_2(y) \\ \qquad\quad + \Delta F_2(X_1, X_2) \\ \\ y_2 = C_2 X_2 \end{cases} \quad (3.70)$$

with $\Delta A_1(y)$, $\Delta A_2(y)$, $\Delta F_1(X_2)$ and $\Delta F_2(X_1, X_2)$ are the uncertain terms of $A_1(y)$, $A_2(y)$, $F_1(X_2)$ and $F_2(X_1, X_2)$, respectively:

$$\Delta A_1(y) = \begin{bmatrix} 0 & -\dfrac{i_{sq}}{\Delta L_s} \\ 0 & 0 \end{bmatrix}, \quad \Delta F_1(X_2) = \begin{bmatrix} -p\dfrac{\Delta\psi_f}{\Delta L_s}\Omega - p\Omega i_{sd} \\ 0 \end{bmatrix}$$

and

$$\Delta A_2(y) = \begin{bmatrix} 0 & pi_{sq} \\ 0 & -\dfrac{f_v}{J} \end{bmatrix}, \quad \Delta F_2(X_1, X_2) = \begin{bmatrix} -\dfrac{\Delta R_s}{\Delta L_s}]i_{sd} \\ \dfrac{p}{\Delta J}\Delta\psi_f i_{sq} \end{bmatrix}.$$

Considering the SMPSM physical operation domain $\mathcal{D}_S$ (see Definition 3.6), then there exist positive constants $\tilde{\rho}_i > 0$, for $i = 1, \ldots, 4$; such that

$$\|\Delta A_1(y)\| \le \tilde{\rho}_1, \qquad \|\Delta A_2(y)\| \le \tilde{\rho}_2, \tag{3.71}$$

$$\|\Delta F_1(X_2)\| \le \tilde{\rho}_3, \quad \|\Delta F_2(X_1, X_2)\| \le \tilde{\rho}_4. \tag{3.72}$$

The parameters $\tilde{\rho}_i$, $i = 1, \ldots, 4$; are positive constants determined from the maximal values of $\Delta A_1(y)$, $\Delta A_2(y)$, $\Delta F_1(X_2)$ and $\Delta F_2(X_1, X_2)$ in the physical domain $\mathcal{D}_S$.

Let us define the estimation errors as

$$\epsilon_1 = X_1 - Z_1, \quad \epsilon_2' = X_2 - Z_2, \quad \epsilon_3 = T_l - \hat{T}_l. \tag{3.73}$$

From Eqs. (3.67) and (3.68) and (3.69) and (3.70), one obtains

$$\begin{aligned}
\dot{\epsilon}_1 &= \{A_1(y) - S_1^{-1}C_1^T C_1\}\epsilon_1 + \Delta A_1(y)X_2 + F_1(X_2) \\
&\quad + \Delta F_1(X_2) - F_1(Z_2) \\
\dot{\epsilon}_2' &= \{A_2(y) - \varpi\Lambda S_\vartheta^{-1}\Lambda^T C_2^T C_2 - \Gamma S_x^{-1} C_2^T C_2\}\epsilon_2' + \Phi\epsilon_3 \\
&\quad - KC_1^T C_1\epsilon_1 + \Delta A_2(y)X_2 + F_2(X_2, X_1) - F_2(Z_2, Z_1) \\
\dot{\epsilon}_3 &= -\varpi S_\vartheta^{-1}\Lambda^T C_2^T C_2\epsilon_2' - B(Z_1)C_1\epsilon_1.
\end{aligned} \tag{3.74}$$

Following the same idea as in [94], and applying the transformation $\epsilon_2 = \epsilon_2' - \Lambda\epsilon_3$, yields

$$\dot{\epsilon}_2 = \dot{\epsilon}_2' - \Lambda\dot{\epsilon}_3 - \dot{\Lambda}\epsilon_3. \tag{3.75}$$

By substituting (3.75) into (3.74), the estimation error dynamics are given by

$$\begin{aligned}
\dot{\epsilon}_1 &= \{A_1(y) - S_1^{-1}C_1^T C_1\}\epsilon_1 + \Delta A_1(y)X_2 + F_1(X_2) \\
&\quad + \Delta F_1(X_2) - F_1(Z_2) \\
\dot{\epsilon}_2 &= \{A_2(y) - \Gamma S_x^{-1}C_2^T C_2\}\epsilon_2 + (B' - K')\epsilon_1 \\
&\quad + \Delta A_2(y)X_2 + F_2(X_2, X_1) + \Delta F_2(X_2, X_1) - F_2(Z_2, Z_1) \\
\dot{\epsilon}_3 &= -\varpi S_\vartheta^{-1}\Lambda^T C_2^T C_2\Lambda\epsilon_2\varpi S_\vartheta^{-1}\Lambda^T C_2^T C_2\epsilon_3 - B'\epsilon_1
\end{aligned} \tag{3.76}$$

with $B' = B(Z_1)C_1$, $K' = KC_1^T C_1$. Since y_1 and y_2 are persistent inputs for subsystems (3.69) and (3.70), respectively; and from Lemma 3.1 there exist $t_0 \geq 0$ and real numbers $\eta_{S_i}^{max} > 0$, $\eta_{S_i}^{min} > 0$ which are independent of θ_i such that $V_i(t, \epsilon_i) = \epsilon_i^T S_i \epsilon_i$, for $i = 1, 2, 3$; (see [4])

$$\forall t \geq t_0 \quad \eta_{S_i}^{min} \|\epsilon_i\|^2 \leq V_i(t, \epsilon_i) \leq \eta_{S_i}^{max} \|\epsilon_i\|^2, \quad \text{for } i = 1, 2, 3. \tag{3.77}$$

Theorem 3.5 *Consider the extended SPMSM dynamic model represented by* (3.69) *and* (3.70)*. System* (3.67) *and* (3.68) *is an adaptive observer for system* (3.69) *and* (3.70)*. Furthermore, the strongly uniformly practically stability of estimation error dynamics* (3.76) *is established.*

The proof of Theorem 5 is given in [21].

3.2.2 Adaptive Interconnected Observers for IPMSM

In this section, from the model of the IPMSM (1.62), which was established in Chap. 1, an adaptive interconnected observer (see [4, 5]) for the IPMSM sensorless control is designed to estimate the position, rotor speed, load torque, and stator resistance.

$$\begin{cases} \dfrac{di_{sd}}{dt} = -\dfrac{R_s}{L_d}i_{sd} + p\dfrac{L_q}{L_d}\Omega i_{sq} + \dfrac{1}{L_d}v_{sd} \\[2mm] \dfrac{di_{sq}}{dt} = -\dfrac{R_s}{L_{sq}}i_{sq} - p\dfrac{L_d}{L_{sq}}\Omega i_{sd} - p\dfrac{1}{L_q}\Phi_f\Omega + \dfrac{1}{L_q}v_{sq} \\[2mm] \dfrac{d\Omega}{dt} = \dfrac{p}{J}(L_d - L_q)i_{sd}i_{sq} - \dfrac{f_v}{J}\Omega + \dfrac{p}{J}\Phi_f i_{sq} - \dfrac{1}{J}T_l \\[2mm] \dfrac{d\theta_m}{dt} = \Omega. \end{cases} \tag{3.78}$$

Similar to the SPMSM, assume that the load torque and the stator resistance are assumed piecewise constants, i.e.,

$$\frac{dT_l}{dt} = 0, \quad \frac{dR_s}{dt} = 0. \tag{3.79}$$

Thus, the extended IPMSM model (3.78) and (3.79) can be seen as the interconnection between two subsystems:

$$\begin{cases} \begin{bmatrix} \dfrac{di_{sq}}{dt} \\[2mm] \dfrac{dR_s}{dt} \end{bmatrix} = \begin{bmatrix} 0 & -\dfrac{i_{sq}}{L_q} \\[2mm] 0 & 0 \end{bmatrix} \begin{bmatrix} i_{sq} \\ R_s \end{bmatrix} + \begin{bmatrix} -\dfrac{pL_d}{L_q}\Omega i_{sq} - p\Omega\dfrac{\Psi_r}{L_q} \\[2mm] 0 \end{bmatrix} + \begin{bmatrix} \dfrac{1}{L_q} \\[2mm] 0 \end{bmatrix} v_{sq} \\[8mm] y_1 \quad = i_{sq} \end{cases}$$

(3.80)

and

$$\begin{cases} \begin{bmatrix} \dfrac{di_{sd}}{dt} \\[2mm] \dfrac{d\Omega}{dt} \end{bmatrix} = \begin{bmatrix} 0 & \dfrac{pL_q}{L_d}i_{sq} \\[2mm] 0 & -\dfrac{f_v}{J} \end{bmatrix} \begin{bmatrix} i_{sd} \\ \Omega \end{bmatrix} + \begin{bmatrix} -\dfrac{R_s}{L_d}i_{sq} \\[2mm] \dfrac{p\Psi_r}{J}i_{sq} \end{bmatrix} + \begin{bmatrix} \dfrac{1}{L_d} \\[2mm] 0 \end{bmatrix} v_{sd} - \begin{bmatrix} 0 \\[2mm] \dfrac{1}{J} \end{bmatrix} T_l \\[8mm] y_2 \quad = i_{sd} \end{cases}$$

(3.81)

To begin with, suppose that each subsystem satisfies some required properties to build an observer and assume that, for each separate observer, the state of the other is available. The system (3.80) and (3.81) can be read as:

$$\Sigma_1 : \begin{cases} \dot{X}_1 = A_1(y)X_1 + g_1(X_2) + \Phi_1 u \\ y_1 = C_1 X_1 \end{cases}$$

(3.82)

$$\Sigma_2 : \begin{cases} \dot{X}_2 = A_2(y)X_2 + g_2(X_1, X_2) + \Phi_2 u + \Phi T_l \\ y_2 = C_2 X_2 \end{cases}$$

(3.83)

where $X_1 = \begin{bmatrix} i_{sq} & R_s \end{bmatrix}^T$, $X_2 = \begin{bmatrix} i_{sd} & \Omega \end{bmatrix}^T$ are the states of each subsystem, $u = \begin{bmatrix} v_{sd} & v_{sq} \end{bmatrix}^T$ is the input, and $y = \begin{bmatrix} i_{sd} & i_{sq} \end{bmatrix}^T$ is the output of the IPMSM model. Furthermore, T_l is considered as an unknown parameter to be identified by the adaptive part of the observer, and

$$A_1(y) = \begin{bmatrix} 0 & -\dfrac{i_{sq}}{L_q} \\[2mm] 0 & 0 \end{bmatrix}, \quad g_1(X_2) = \begin{bmatrix} -p\dfrac{L_d}{L_q}\Omega i_{sd} - p\dfrac{\phi_f}{L_q}\Omega \\[2mm] 0 \end{bmatrix}, \quad \Phi_1 = \begin{bmatrix} \dfrac{1}{L_q} \\[2mm] 0 \end{bmatrix},$$

$$A_2(y) = \begin{bmatrix} 0 & p\dfrac{L_q}{L_d}i_{sq} \\[2mm] 0 & -\dfrac{f_v}{J} \end{bmatrix}, \quad g_2(X_1, X_2) = \begin{bmatrix} -\dfrac{R_s}{L_d}i_{sd} \\[2mm] \dfrac{p}{J}\Phi_f i_{sq} + \dfrac{p}{J}(L_d - L_q)i_{sq} \end{bmatrix},$$

$$\Phi = \begin{bmatrix} 0 \\[2mm] -\dfrac{1}{J} \end{bmatrix}, \quad \Phi_2 = \begin{bmatrix} \dfrac{1}{L_d} \\[2mm] 0 \end{bmatrix}, \quad C_1 = C_2 = [1\ 0],$$

where g_1 and g_2 are the interconnection terms.

The operation domain of the IPMSM is stated in Definition 3.6. In the sequel, an adaptive interconnected observer for the sensorless IPMSM represented by (3.80) and (3.81) is designed using similar results given in Theorem 3.5.

Remark 3.10

- X_2 and X_1 are considered as inputs for subsystems (3.82) and (3.83), respectively. From [6], the solutions of $\dot{S}_1$ and $\dot{S}_2$ (defined latter) are symmetric positive definite matrices.
- When the IPMSM remains in the observable area, X_1 and X_2 satisfy the persistence condition: the asymptotic stability of the observer is proved.
- If IPMSM is in the unobservable zone, X_1 and X_2 do not satisfy the persistence condition, the practical stability, introduced in the Appendix "Appendix: Practical Stability Definitions", has to be proved.

Remark 3.11 For the IPMSM,

- $A_1(y)$ is globally Lipschitz w.r.t. X_1
- $A_2(y)$ is globally Lipschitz w.r.t. X_1
- $g_1(X_2)$ is globally Lipschitz w.r.t. X_2 and uniformly w.r.t. (u, y)
- $g_2(X_1, X_2)$ is globally Lipschitz w.r.t. X_1, X_2 and uniformly w.r.t. (u, y).

Consequently, adaptive interconnected observers for (3.82) and (3.83) are given by

$$O_1 : \begin{cases} \dot{Z}_1 = A_1(y)Z_1 + g_1(Z_2) + \Phi_1(u) + S_1^{-1}C_1^T(y_1 - \hat{y}_1) \\ \dot{S}_1 = -\rho_1 S_1 - A_1^T(y)S_1 - S_1 A_1(y) + C_1^T C_1 \\ \hat{y}_1 = C_1 Z_1 \end{cases} \quad (3.84)$$

$$O_2 : \begin{cases} \dot{Z}_2 = A_2(y)Z_2 + g_2(Z_1, Z_2) + \Phi_2(u) + \Phi\hat{T}_l + KC_1^T(y_1 - \hat{y}_1) \\ \qquad + (\varpi \Lambda S_3^{-1}\Lambda^T C_2^T + \Gamma S_2^{-1}C_2^T)(y_2 - \hat{y}_2) \\ \\ \dot{\hat{T}}_l = \varpi S_3^{-1}\Lambda^T C_2^T(y_2 - \hat{y}_2) + B(Z_1)(y_1 - \hat{y}_1) + B_1(Z_1)(y_2 - \hat{y}_2) \\ \\ \dot{S}_2 = -\rho_2 S_2 - A_2^T(y)S_2 - S_2 A_2(y) + C_2^T C_2 \\ \dot{S}_3 = -\rho_3 S_3 + \Lambda^T C_2^T C_2 \Lambda \\ \\ \dot{\Lambda} = \{A_2(y) - \Gamma S_2^{-1}C_2^T C_2\}\Lambda + \Phi \\ \\ \hat{y}_2 = C_2 Z_2 \end{cases} \quad (3.85)$$

with $Z_1 = \begin{bmatrix} \hat{i}_q & \hat{R}_s \end{bmatrix}^T$ and $Z_2 = \begin{bmatrix} \hat{i}_d & \hat{\Omega} \end{bmatrix}^T$ are the estimated state variables, respectively, of X_1 and X_2, and ρ_i for $i = 1, 2, 3$; are positive constants, S_1 and S_2 are symmetric positive definite matrices [4], with $S_3(0) > 0$,

$$B(Z_1) = k\frac{p}{J}\Phi_f \hat{i}_{sq}, \quad B_1(Z_1) = k\frac{p}{J}(L_d - L_q)\hat{i}_{sq} \quad (3.86)$$

$$K = \begin{bmatrix} -k_{c1} \\ -k_{c2} \end{bmatrix}, \quad \Gamma = \begin{bmatrix} 1 & 0 \\ 0 & \alpha \end{bmatrix}$$

with k, k_{c1}, k_{c2}, α and ϖ are positive constants. Note that $S_1^{-1} C_1^T$ is the gain of observer (3.84) and $\varpi \Lambda S_3^{-1} \Lambda^T C_2^T + \Gamma S_2^{-1} C_2^T$ and $K C_1^T$ are the gains of observer (3.85).

Remark 3.12 The term $B(Z_1)(y_1 - \hat{y}_1) + B_1(Z_1)(y_2 - \hat{y}_2)$ in Eq. (3.85) can be expressed, as follows

$$B(Z_1)(y_1 - \hat{y}_1) + B_1(Z_1)(y_2 - \hat{y}_2) = k(T_e - \tilde{T}_e)$$

where T_e and $\tilde{T}_e$ are, respectively, the "real" and "estimated" electromagnetic torques.

Remark 3.13 Obviously, for subsystem (3.82): $v = (y, X_2)$ and $S(t) = S_1$, and that for subsystem (3.83) one has $v = (y, X_1)$ and $S(t) = S_2$.

Stability Analysis of the Observer Under Uncertain Parameters

Remark 3.14 All the parameters of the IPMSM are assumed uncertain but with well-known bound values.

The robustness of the observer under parametric uncertainties is analyzed and the system is rewritten in the following form:

$$\Sigma_1 : \begin{cases} \dot{X}_1 = A_1(y)X_1 + g_1(X_2) + \Phi_1(u) + \Delta A_1(y) + \Delta g_1(X_2) \\ y_1 = C_1 X_1 \end{cases} \quad (3.87)$$

$$\Sigma_2 : \begin{cases} \dot{X}_2 = A_2(y)X_2 + g_2(X_1, X_2) + \Phi_2(u) + \Phi T_l \\ \qquad + \Delta A_2(y) + \Delta g_2(X_1, X_2) \\ y_2 = C_2 X_2 \end{cases} \quad (3.88)$$

where $\Delta A_1(y)$, $\Delta A_2(X_1)$, $\Delta g_1(X_2)$ and $\Delta g_2(X_1, X_2)$ are, respectively, the uncertain terms of $A_1(y)$, $A_2(X_1)$, $g_1(X_2)$, $g_2(X_1, X_2)$:

$$\Delta A_1(y) = \begin{bmatrix} 0 & -\dfrac{i_{sq}}{\Delta L_q} \\ 0 & 0 \end{bmatrix}, \quad \Delta A_2(y) = \begin{bmatrix} 0 & p\dfrac{\Delta L_q}{\Delta L_d} i_{sq} \\ 0 & \dfrac{f_v}{\Delta J} \end{bmatrix},$$

$$\Delta g_1(X_2) = \begin{bmatrix} -p\dfrac{\Delta L_d}{\Delta L_q} \Omega i_{sd} - p\dfrac{\Delta \Phi_f}{\Delta L_q} \Omega \\ 0 \end{bmatrix},$$

$$\Delta g_2(X_1, X_2) = \begin{bmatrix} -\dfrac{R_s}{\Delta L_d} i_{sd} \\ -\dfrac{p}{\Delta J} \Omega i_{sd} \Phi_f i_{sq} - \dfrac{p}{\Delta J}(\Delta L_d - \Delta L_q) i_{sq} i_{sd} \end{bmatrix}.$$

Remark 3.15 Considering the IPMSM physical operation domain $\mathcal{D}_S$, the uncertain terms are bounded such that there exist positive constants $\varrho_i > 0$, for $i = 1, \ldots, 4$; such that

$$\|\Delta A_1\| \le \varrho_1, \quad \|\Delta A_2\| \le \varrho_2, \quad \|\Delta g_1\| \le \varrho_3, \quad \|\Delta g_2\| \le \varrho_4.$$

The parameters ϱ_i, $i = 1, \ldots, 4$; are positive constants determined from the maximal values of $\Delta A_1(\cdot)$, $\Delta A_2(\cdot)$, $\Delta g_1(\cdot)$ and $\Delta g_2(\cdot)$ in the physical domain $\mathcal{D}_S$.

Let us define the estimation errors as

$$\epsilon_1 = X_1 - Z_1, \quad \epsilon_2' = X_2 - Z_2, \quad \epsilon_3 = T_l - \hat{T}_l. \tag{3.89}$$

From Eqs. (3.84) and (3.85) and (3.87) and (3.88), the estimation error dynamics are given by

$$\dot{\epsilon}_1 = \{A_1(y) - S_1^{-1} C_1^T C_1\}\epsilon_1 + g_1(X_2) + \Delta A_1(y) X_1$$
$$+ \Delta g_1(X_2) - g_1(Z_2) \tag{3.90}$$

$$\dot{\epsilon}_2' = [A_2(y) - \varpi S_3^{-1} \Lambda^T C_2^T C_2 + \Gamma S_2^{-1} C_2^T C_2]\epsilon_2' + \Phi \epsilon_3 \tag{3.91}$$
$$- k C_1^T C_1 \epsilon_1 + \Delta A_2(y) X_2 + g_2(X_2) + \Delta g_2(X_2) - g_2(Z_2)$$

$$\dot{\epsilon}_3 = -\varpi S_3^{-1} \Lambda^T C_1^T C_1 \epsilon_1 - B_1(Z_2) C_2 \epsilon_2' - B_2(Z_2) C_1 \epsilon_1. \tag{3.92}$$

Following the same idea as in [94], and applying the transformation $\epsilon_2 = \epsilon_2' - \Lambda \epsilon_3$, the dynamics of the estimation errors are given by

$$\dot{\epsilon}_1 = \{A_1(y) - S_1^{-1} C_1^T C_1\}\epsilon_1 + \Delta A_1(y) X_1 + g_1(X_2)$$
$$+ \Delta g_1(X_2) - g_1(Z_2), \tag{3.93}$$

$$\dot{\epsilon}_2 = \{A_2(y) - \Gamma S_2^{-1} C_2^T C_2 - B_{11}\}\epsilon_2 - [B_{12} + C_{11}]\epsilon_1 + B_{22}\epsilon_3 \tag{3.94}$$
$$+ g_2(X_1, X_2) - g_2(Z_1, Z_2) + \Delta A_2(y) X_2 + \Delta g_2(X_1, X_2),$$

$$\dot{\epsilon}_3 = -B_1' \epsilon_1 - [\varpi S_3^{-1} \Lambda^T C_2^T C_2 + B_2']\epsilon_2 - [\varpi S_3^{-1} \Lambda^T C_2^T C_2 \Lambda + B_2'']\epsilon_3. \tag{3.95}$$

Since (u, y, X_2) and (u, y, X_1) are, respectively, the inputs for subsystems (3.87) and (3.88), and from Lemma 3.1, there exist $t_0 \ge 0$ and real positive numbers $\eta_{S_i}^{max}$ and $\eta_{S_i}^{min}$, which are independent of ρ_i, such that

$$V_i(t, \epsilon_i) = \epsilon_i^T S_i \epsilon_i, \quad \text{for } i = 1, 2, 3;$$

satisfying

$$\eta_{S_i}^{min} \|\epsilon_i\|^2 \le V_i(t, \epsilon_i) \le \eta_{S_i}^{max} \|\epsilon_i\|^2, \quad \forall t \ge t_0. \tag{3.96}$$

Consequently, the convergence of the observer can be established under parametric uncertainties.

Theorem 3.6 *Consider the IPMSM dynamic model* (3.87) *and* (3.88). *System* (3.84) *and* (3.85) *is an adaptive interconnected observer for system* (3.87) *and* (3.88) *with a strongly uniformly practical stability of the estimation error dynamics.*

The proof is detailed in [38].

3.3 High Order Sliding Mode Observers for PMSM

3.3.1 Sliding Mode Observers

The sliding mode observers are widely used due to their finite time convergence and to their robustness with respect to the uncertainties. Recently, various observers have been developed by using second order sliding mode, super-twisting, or high order sliding mode algorithms.

The second order sliding mode, and more recently, the High Order Sliding Mode Observers (HOSM) have been introduced in order to reduce significantly the chattering phenomenon. Contrary to the asymptotic observers which require to prove the observer-controller stability in closed-loop, for the sliding mode observers, the separation principle is automatically satisfied if the controller is started after the finite time convergence of the observer.

The first order sliding modes are restricted to systems in which the output has a relative degree 1. Besides the resulting high frequency switching, the sliding mode may cause chattering effect. On the other hand, high order sliding modes have been introduced such that the finite time convergence is preserved and the chattering effect is eliminated.

For the first order sliding mode, the stability is analyzed by means of a Lyapunov approach. However, for High Order Sliding Modes Observer, Lyapunov approaches are not often developed, and usually, upper-bound curves or homogeneity-based methods are used for convergence analysis.

The Super-Twisting Algorithm

Consider the following nonlinear system:

$$\begin{cases} \dot{x}_1 = x_2 \\ \dot{x}_2 = f(t, x_1, x_2, u) + \zeta(t, x_1, x_2, u) \\ y = x_1. \end{cases} \tag{3.97}$$

The solutions of system (3.97) are understood in the Filippov's sense (see [23] for details). The function $f(t, x_1, x_2, u)$ and the uncertainty $\zeta(t, x_1, x_2, u)$ are assumed Lebesgue-measurable and uniformly bounded in any compact region of the state-space (x_1, x_2).

The general form of the super-twisting observer is given as

$$
\begin{cases}
\dot{\hat{x}}_1 = \hat{x}_2 + \alpha_1 \left| x_1 - \hat{x}_1 \right|^{1/2} sign(x_1 - \hat{x}_1) \\
\dot{\hat{x}}_2 = f(t, x_1, \hat{x}_2, u) + \zeta(t, x_1, \hat{x}_2, u) + \alpha_2 \, sign(x_1 - \hat{x}_1) \\
y = x_1
\end{cases}
\tag{3.98}
$$

where $\hat{x}_1$ and $\hat{x}_2$ are the state estimations and α_1 and α_2 are the gains of the observers.

3.3.2 High Order Sliding Mode Observer for SPMSM

To design a high order sliding mode observer, a modified model of the SPMSM in the stationary reference frame (1.84) is introduced.

Defining the following change of variable:

$$
e_\alpha = -p\psi_f \Omega \, sin(\theta_e) \text{ and } e_\beta = p\psi_f \Omega \, cos(\theta_e),
$$

it follows that system (1.84) can be written as

$$
\begin{cases}
\dfrac{di_\alpha}{dt} = -\dfrac{R_s}{L_s} i_\alpha - \dfrac{1}{L_s} e_\alpha + \dfrac{1}{L_s} v_\alpha \\[2mm]
\dfrac{di_\beta}{dt} = -\dfrac{R_s}{L_s} i_\beta - \dfrac{1}{L_s} e_\beta + \dfrac{1}{L_s} v_\beta \\[2mm]
\dfrac{de_\alpha}{dt} = -\Omega e_\beta - \dfrac{p^2 \psi_f^2}{J} S_{\theta_e} (i_\beta C_{\theta_e} - i_\alpha S_{\theta_e}) - \dfrac{f_v}{J} e_\alpha \\[2mm]
\dfrac{de_\beta}{dt} = \Omega e_\alpha + \dfrac{p^2 \psi_f^2}{J} C_{\theta_e} (i_\beta C_{\theta_e} - i_\alpha S_{\theta_e}) - \dfrac{f_v}{J} e_\beta
\end{cases}
\tag{3.99}
$$

with $C_{\theta_e} = cos(\theta_e)$, $S_{\theta_e} = sin(\theta_e)$, $\theta_e = -\arctan(\dfrac{e_\alpha}{e_\beta})$ and
$\Omega = \dfrac{1}{p\psi_f} \sqrt{(e_\alpha{}^2 + e_\beta{}^2)}$.

Then the above system can be written in a canonical form

$$
\begin{aligned}
\dot{X}_1 &= X_2 + \Phi(U, Y) \\
\dot{X}_2 &= F(X_1, X_2)
\end{aligned}
\tag{3.100}
$$

where the state is defined as

$$
X_1 = \begin{bmatrix} x_{1,1} \\ x_{1,2} \end{bmatrix} = \begin{bmatrix} i_\alpha \\ i_\beta \end{bmatrix}, \qquad
X_2 = \begin{bmatrix} x_{2,1} \\ x_{2,2} \end{bmatrix} = \begin{bmatrix} -\dfrac{1}{L_s} e_\alpha \\[2mm] -\dfrac{1}{L_s} e_\beta \end{bmatrix},
$$

and,

$$U = \begin{bmatrix} v_\alpha \\ v_\beta \end{bmatrix}, \qquad Y = \begin{bmatrix} i_\alpha \\ i_\beta \end{bmatrix}, \qquad \Phi(U, Y) = -\frac{R_s}{L_s} X_1 + \frac{1}{L_s} U,$$

$$F(X_1, X_2) = \begin{bmatrix} -\dfrac{p^2 \psi_f^2}{J} S_{\theta_e}(i_\beta C_{\theta_e} - i_\alpha S_{\theta_e}) + \dfrac{f_v}{J} e_\beta - \Omega e_\beta \\ \dfrac{p^2 \psi_f^2}{J} C_{\theta_e}(i_\beta C_{\theta_e} - i_\alpha S_{\theta_e}) + \dfrac{f_v}{J} e_\alpha - \Omega e_\alpha \end{bmatrix}$$

with

$$S_{\theta_e} = \frac{e_\beta}{\sqrt{e_\beta^2 + e_\beta^2}} = \frac{-x_{2,2}}{\sqrt{x_{2,1}^2 + x_{2,2}^2}}, \ C_{\theta_e} = \frac{-e_\alpha}{\sqrt{e_\beta^2 + e_\beta^2}} = \frac{x_{2,1}}{\sqrt{x_{2,1}^2 + x_{2,2}^2}}.$$

3.3.2.1 High Order Sliding Modes Observer Design

A recursive scheme based on a differentiator is used to reconstruct the non-measurable variables (see [24]). The sliding mode differentiator provides an exact differentiation using a recursive method with finite-time convergence.

Now, we design a second order sliding-mode super-twisting base observer for the above interconnected system. For this, consider the following representation of the system:

$$\begin{cases} \dot{X}_1 = X_2 + \Phi(U, Y) + \Delta\xi_1 \\ \dot{X}_2 = F(X_1, X_2) + \Delta\xi_2. \end{cases} \tag{3.101}$$

The second-order super-twisting based observer is given as

$$\begin{cases} \dot{\widehat{X}}_1 = \widehat{X}_2 + \Phi(U, Y) + \alpha_2 \lambda(\widetilde{X}_1) sign(\widetilde{X}_1) \\ \dot{\widehat{X}}_2 = F(\widehat{X}_1, \widehat{X}_2) + \alpha_1 sign(\widetilde{X}_1) \end{cases} \tag{3.102}$$

where

$$\alpha_1 = diag[\alpha_{1,1}, \alpha_{1,2}] \text{ and } \alpha_2 = diag[\alpha_{2,1}, \alpha_{2,2}]$$

are the correction factors designed to imply the convergence of the estimation error

$$\widetilde{X}_1 = X_1 - \widehat{X}_1$$

with

$$\lambda(\widetilde{X}_1) = diag(|X_{1,1} - \widehat{X}_{1,1}|^{\frac{1}{2}}, |X_{2,1} - \widehat{X}_{2,1}|^{\frac{1}{2}})$$

and

$$sign(\widetilde{X}_1) = diag(sign(X_{1,1} - \widehat{X}_{1,1}), sign(X_{1,2} - \widehat{X}_{1,2})).$$

The error dynamics $\widetilde{X} = X - \hat{X}$ is given by

$$\begin{aligned}
\dot{\widetilde{X}}_1 &= \widetilde{X}_2 - \alpha_2 \lambda(\widetilde{X}_1)\, sign(\widetilde{X}_1) + \Delta\xi_1 \\
\dot{\widetilde{X}}_2 &= \widetilde{F}(X_1, X_2, \hat{X}_2) - \alpha_1\, sign(\widetilde{X}_1)
\end{aligned} \tag{3.103}$$

where $\widetilde{F}(X_1, X_2, \hat{X}_2) = F(X_1, X_2) - F(X_1, \hat{X}_2) + \Delta\xi_2$.

Let us denote f_i the ith component of $\widetilde{F}(X_1, X_2, \hat{X}_2)$ and assume that to find an upper-bound $|f_i| < f_i^+$ is possible.

Assumption 3.3 Consider that the uncertainty $\Delta\xi_1$ and its derivative are bounded such that: $\|\Delta\xi_1\| < d_1$, $\left\|\frac{d\Delta\xi_1}{dt}\right\| < d_2$, and the uncertainty $\Delta\xi_2$ is bounded, i.e. $\|\Delta\xi_2\| < d_3$, with d_1, d_2 and d_3 are positive values.

Theorem 3.7 *Suppose that the condition $|f_i| < f_i^+$ holds for system* (3.101) *and by verifying that Assumption* 3.3 *is satisfied, the parameters of the observer are selected according to*

$$\begin{aligned}
\alpha_{1,i} &> f_i^+ \\
\alpha_{2,i} &> \sqrt{\frac{2}{\alpha_{1,i} - f_i^+ - d_{2i}^+} \frac{(\alpha_{1,i} + f_i^+ + d_{2i}^+)(1 - p_i)}{1 - p_i}}
\end{aligned}$$

where p_i are constants such that $0 < p_i < 1$, $i = 1, 2$; and $\alpha_1 = diag[\alpha_{1,1}, \alpha_{1,2}]$ and $\alpha_2 = diag[\alpha_{2,1}, \alpha_{2,2}]$. So, observer (3.102) *guarantees the convergence of the estimated states $(\hat{X}, \dot{\hat{X}})$ to the real value of the states $(X, \dot{X})$ after a finite time transient, and there exists a time t_0 such that for all $t \geq t_0$, $(\hat{X}_1, \hat{X}_2) = (X_1, X_2)$.*

Proof The proof of Theorem 3.7 follows the proof given in [19, 20].
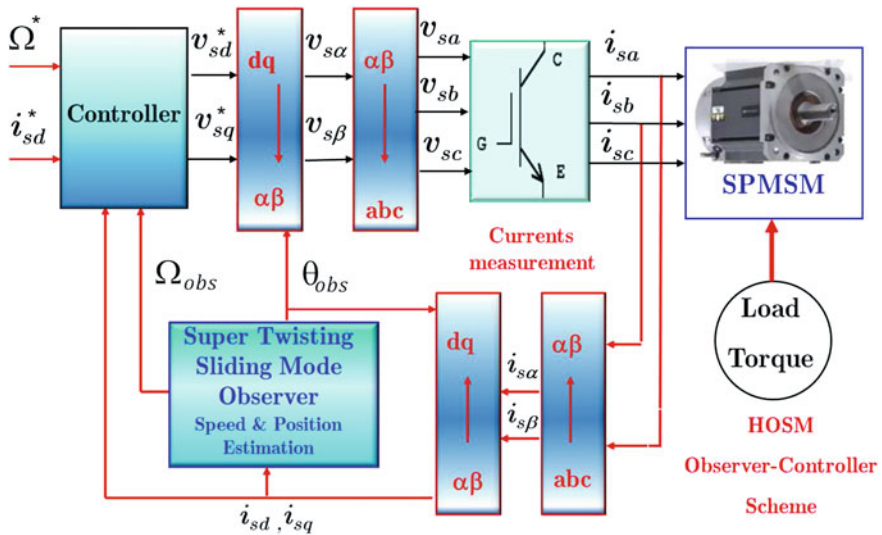
3.3.2.2 Simulation Results

By using the Simulink/MatLab software, the proposed observer scheme has been simulated, as shown in Fig. 3.1. The parameters of the tested SPMSM are given in Table 1.1. The motor is tested according to an industrial benchmark (see Chap. 1 for more details). Of course the measured rotor speed is used only for comparison purpose. The stator resistance as well as the stator inductance may be varied from their nominal values. So their deviation effects are studied.
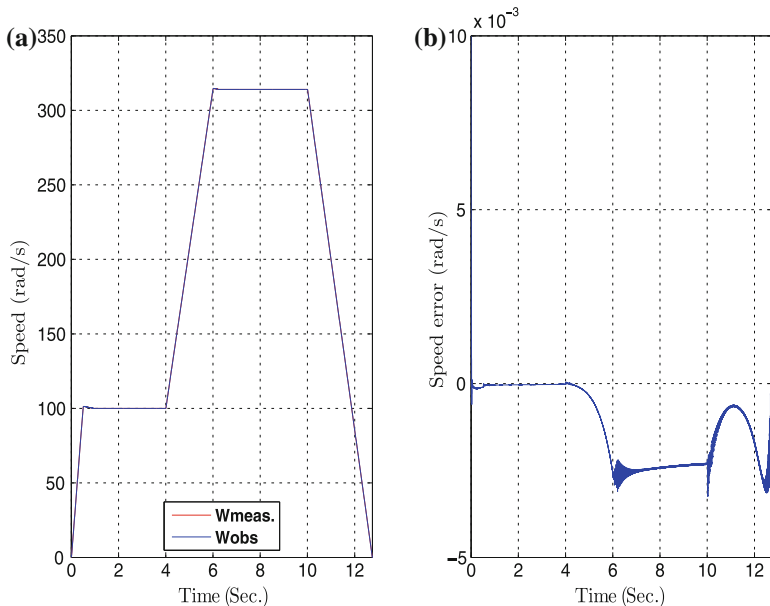
To achieve the efficiency of the proposed scheme, the tuning parameters of the observer were chosen to obtain suitable convergence and robust performance as follows:

Observer gains: $\alpha_{1,1}, = 10$, $\alpha_{1,2} = 10$ and $\alpha_{2,1} = \alpha_{2,2} = 500$.

Figure 3.2a shows the measured speed Ω and the estimated speed as well as the speed error for the nominal case (Figs. 3.2b and 3.3). It can be seen that the estimation error is very small showing the good estimation of the speed. The actual
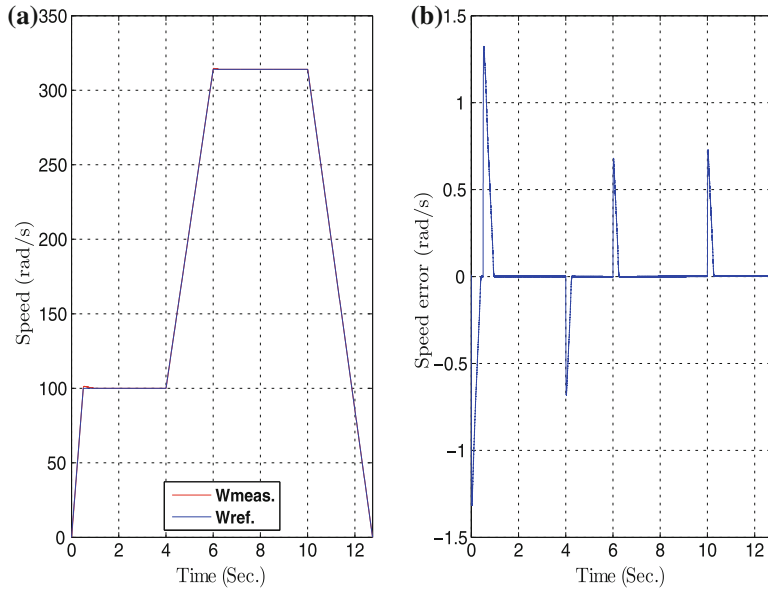
Fig. 3.1 SPMSM HOSM observer validation scheme
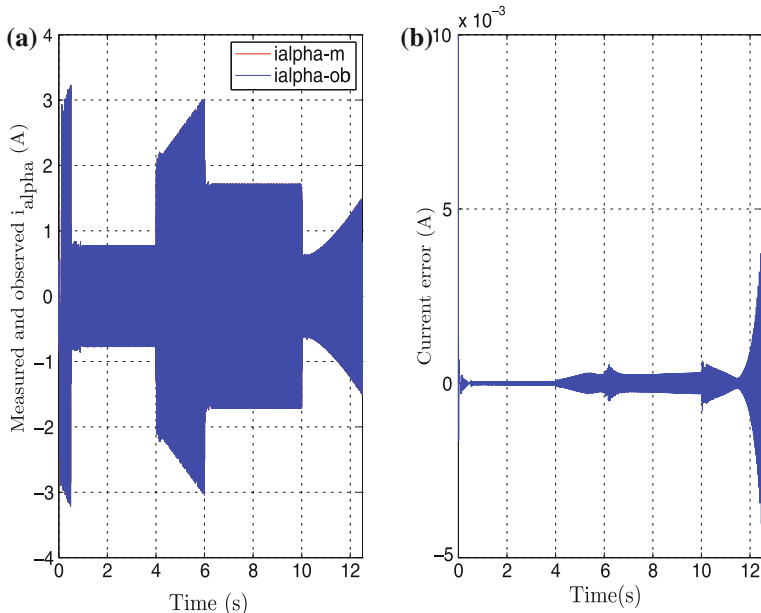
Fig. 3.2 **a** Measured and estimated speeds. **b** Observed speed error
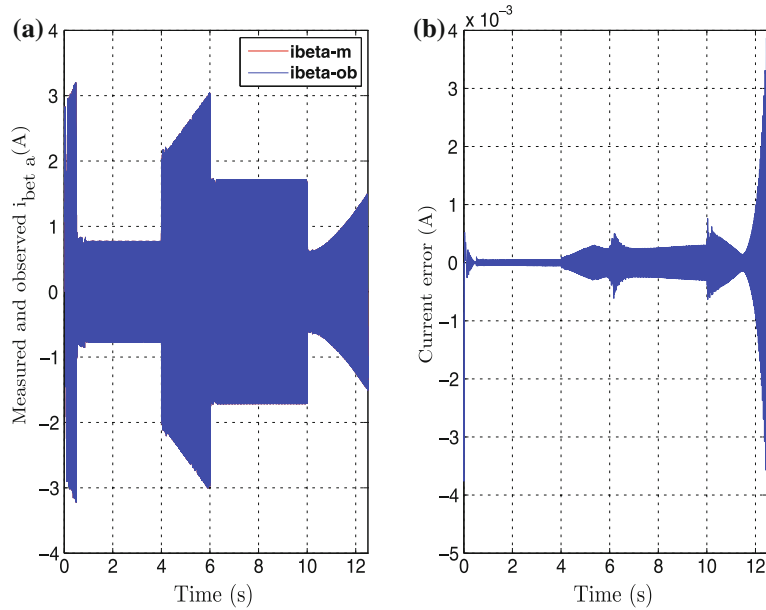
and estimated currents $(i_\alpha, \widehat{i_\alpha})$ and the estimation error are shown in Fig. 3.4a, b, respectively. Similarly, in Fig. 3.5a, b, are plotted the actual and estimated current i_β and its estimation error.

Fig. 3.3   a Measured and reference speeds. **b** Tracking speed error

Fig. 3.4   a Measured and estimated alpha currents. **b** Current error

Fig. 3.5 **a** Measured and estimated beta currents. **b** Current error

3.3.2.3 Conclusion

An observer based on sliding mode techniques of a permanent magnet synchronous motor has been presented. The observer scheme is achieved via a super-twisting sliding mode observer estimating the rotor speed. Furthermore, the observer is tested by using a specific industrial benchmark.

3.3.3 HOSM Interconnected Observers for IPMSM: Rotor Speed and Stator Resistance Estimation

Here, an interconnected high order sliding mode observer (HOSMO) for the sensorless IPMSM observation is designed to estimate the position, rotor speed, and stator resistance. The stator resistance very slowly varies with respect to time and thus its dynamics is modeled by a piecewise function. We follow the same approach as for the high order sliding mode observer design given in the previous Sect. 3.3.2.1.

The extended IPMSM model (3.78) and (3.79) can be seen as the interconnection between two subsystems and by using the following change of coordinates:

$$
\begin{bmatrix} \chi_{11} \\ \chi_{12} \end{bmatrix} = \begin{bmatrix} i_{sd} \\ -R_s \dfrac{i_{sd}}{L_d} \end{bmatrix} \quad \text{and} \quad \begin{bmatrix} \chi_{21} \\ \chi_{22} \end{bmatrix} = \begin{bmatrix} i_{sq} \\ -p\Omega \left(\dfrac{\phi_f}{L_q} + \dfrac{L_d}{L_q} i_{sd} \right) \end{bmatrix} \tag{3.104}
$$

systems (3.78) and (3.79) can be represented in the following form:

$$
\Sigma_{\chi,i} := \begin{bmatrix} \dot{\chi}_{i1} \\ \dot{\chi}_{i2} \end{bmatrix} = \begin{bmatrix} 0 & 1 \\ 0 & 0 \end{bmatrix} \begin{bmatrix} \chi_{i1} \\ \chi_{i2} \end{bmatrix} + \begin{bmatrix} \Gamma_i \\ H_i \end{bmatrix} + \begin{bmatrix} \Delta\zeta_{i1} \\ \Delta\zeta_{i2} \end{bmatrix} \tag{3.105}
$$

where χ_{i1} is the measured output and χ_{i2} is the unmeasured state, for $i = 1, 2$. T_l will be considered as a bounded non-measurable disturbance. The nonlinear terms are given as

$$
\begin{bmatrix} \Gamma_1 \\ H_1 \end{bmatrix} = \begin{bmatrix} \dfrac{1}{L_d} v_{sd} & \left(\dfrac{\chi_{12}}{\chi_{11}} \right)^2 - \dfrac{\chi_{12}}{L_d \chi_{11}} v_{sd} \end{bmatrix}^\top ,
$$

$$
\begin{bmatrix} \Gamma_2 \\ H_2 \end{bmatrix} = \begin{bmatrix} \dfrac{1}{L_q} v_{sq} \\[2em] \left\{ \left(-\dfrac{p^2}{J}(L_d - L_q)\chi_{11}\chi_{21} - \dfrac{F_v}{J} \dfrac{\chi_{22}}{\dfrac{\phi_f}{L_q} + \dfrac{L_d}{L_q}\chi_{11}} - \dfrac{p^2}{J}\phi_f \chi_{21} \right) \\[3em] + \left(\dfrac{\phi_f}{L_d} + \dfrac{L_d}{L_q}\chi_{11} \right) + \dfrac{\chi_{22}}{\dfrac{\phi_f}{L_q} + \dfrac{L_d}{L_q}\chi_{11}} \left(-\dfrac{\chi_{22}\chi_{21}}{\dfrac{\phi_f}{L_q} + \dfrac{L_d}{L_q}\chi_{11}} + \dfrac{1}{L_q} v_{sd} \right) \right\} \end{bmatrix}
$$

Furthermore, in (3.105) the terms $\Delta\zeta_{ij}$ for $i,\, j = 1, 2$; represent the interconnected terms, which will be considered as disturbances for each subsystem.

$$
\begin{bmatrix} \Delta\zeta_{11} \\ \Delta\zeta_{12} \end{bmatrix} = \begin{bmatrix} -\dfrac{L_d \chi_{22}\chi_{12}}{\Phi_f + L_d\chi_{11}} \\[1.5em] -\dfrac{\chi_{12}\chi_{22}\chi_{21}}{L_d\chi_{11}(\Phi_f + L_d\chi_{11})} \end{bmatrix}, \quad \begin{bmatrix} \Delta\zeta_{21} \\ \Delta\zeta_{22} \end{bmatrix} = \begin{bmatrix} -\dfrac{L_d\chi_{12}\chi_{21}}{L_q\chi_{11}} \\[1.5em] \dfrac{L_d\chi_{12}\chi_{22}}{\Phi_f + L_d\chi_{11}} + \dfrac{T_l}{J} \end{bmatrix}
$$

$$\tag{3.106}$$

The high order sliding mode interconnected observer for the IPMSM (3.78) and (3.79) is given as

$$
O_{\chi,i} := \left\{ \begin{bmatrix} \dot{\hat{\chi}}_{i1} \\ \dot{\hat{\chi}}_{i2} \end{bmatrix} = \begin{bmatrix} 0 & 1 \\ 0 & 0 \end{bmatrix} \begin{bmatrix} \hat{\chi}_{i1} \\ \hat{\chi}_{i2} \end{bmatrix} + \begin{bmatrix} \Gamma_i \\ \hat{H}_i \end{bmatrix} + \begin{bmatrix} \alpha_{i1} \, |\tilde{\chi}_{i1}|^{1/2} \, sign(\tilde{\chi}_{i1}) \\ \alpha_{i2} \, sign(\tilde{\chi}_{i1}) \end{bmatrix} \right. \tag{3.107}
$$

where the estimation errors $\tilde{\chi}_{i1} = \chi_{i1} - \hat{\chi}_{i1}$, for $i = 1, 2$; with $[\hat{\chi}_{i1}\ \hat{\chi}_{i2}]^T$ is the estimated state of system $\Sigma_{\chi, i}$. From (3.104), the estimates of stator resistance and speed can be obtained by

$$\hat{R}_s = -\frac{L_d \hat{\chi}_{12}}{\hat{\chi}_{11}}, \qquad \hat{\Omega} = -\frac{L_q \hat{\chi}_{22}}{p(\Phi_f + L_d \hat{\chi}_{11})}. \tag{3.108}$$

Remark 3.16 To estimate the stator resistance, the current i_{sd} (i.e., χ_{11}) has to be always nonzero. This condition is guaranteed from the Maximum Torque Per Ampere (MTPA) strategy developed in Chap. 4 (Sect. 4.2.2).

Remark 3.17 The convergence proof of observer (3.107), is given in [39].

3.4 Adaptive Interconnected Observer for the Induction Motor

An adaptive interconnected observer (see [5]) will be designed for the sensorless IM to estimate the rotor speed, flux, and load torque. The details are given in [85]. First, we define the operation domain of the IM.

Definition 3.7 The IM physical operation domain $\mathcal{D}_{\mathcal{IM}}$ is defined by the set of values

$$\mathcal{D}_{IM} = \{X \in \mathfrak{R}^6 \mid |\phi_{rd}| \le \Phi_d{}^{max}, |\phi_{rq}| \le \Phi_q{}^{max}, |i_{sd}| \le I_d{}^{max},$$
$$|i_{sq}| \le I_q{}^{max}, |\Omega| \le \Omega^{max}, |R_s| \le R_s{}^{max}\}$$

where $X = (\phi_{rd}, \phi_{rq}, i_{sd}, i_{sq}, \Omega, T_l, R_s)$, and $\Phi_d{}^{max}, \Phi_q{}^{max}, I_d{}^{max}, I_q{}^{max}, \Omega^{max}, T_l{}^{max}, R_s{}^{max}$ are the actual maximum values for the fluxes, stator currents, rotor speed, torque load, and stator resistance, respectively.

The IM Model can be represented in the following interconnected form:

$$\Sigma : \begin{cases} \dot{X}_1 = A_1(X_2)X_1 + g_1(u, y, X_2, X_1) \\ y_1 = C_1 X_1 \\ \dot{X}_2 = A_2(X_1)X_2 + g_2(u, y, X_1, X_2) \\ y_2 = C_2 X_2 \end{cases} \tag{3.109}$$

where

$$A_1(X_2) = \begin{pmatrix} 0 & bp\phi_{rq} & 0 \\ 0 & 0 & -\frac{1}{J} \\ 0 & 0 & 0 \end{pmatrix}, \qquad A_2(X_1) = \begin{pmatrix} -\gamma & -bp\Omega & ab \\ 0 & -a & -p\Omega \\ 0 & p\Omega & -a \end{pmatrix}$$

$$g_1(u, y, X_2, X_1) = \begin{pmatrix} -\gamma i_{sd} + ab\phi_{rd} + m_1 u_{sd} + \omega_s i_{sq} \\ m(\phi_{rd} i_{sq} - \phi_{rq} i_{sd}) - c\Omega \\ 0 \end{pmatrix}$$

$$g_2(u, y, X_1, X_2) = \begin{pmatrix} -\omega_s i_{sd} + m_1 u_{sq} \\ \omega_s \phi_{rq} + a M_{sr} i_{sd} \\ -\omega_s \phi_{rd} + a M_{sr} i_{sq} \end{pmatrix}$$

and $X_1 = \left(i_{sd}, \Omega, T_l\right)^T$, $X_2 = \left(i_{sq}, \phi_{rd}, \phi_{rq}\right)^T$ are the states, $u = \left(u_{sd}, u_{sq}\right)^T$ are the inputs, and $y = \left(i_{sd}, i_{sq}\right)^T$ are the output of the IM model. $C_1 = C_2 = \left(1\ 0\ 0\right)$.

Remark 3.18 From the model (1.119), we can easily verify that the matrix $A_1(X_2, y)$ is globally Lipschitz w.r.t. X_2, and the matrix $A_2(X_1)$ is globally Lipschitz w.r.t. X_1. The terms $g_1(u, y, X_2, X_1)$ and $g_2(u, y, X_2, X_1)$ are globally Lipschitz w.r.t. X_2, X_1 and uniformly w.r.t. (u, y), as long as the *IM* state remains in $\mathcal{D}_{\mathcal{IM}}$.

By verifying first the conditions on the IM observability and from Remark 3.18, a nominal observer for the interconnected systems (3.109) is given as:

$$O: \begin{cases} \dot{Z}_1 = A_1(Z_2)Z_1 + g_1(u, y, Z_2, Z_1) \\ \qquad + (\Gamma S_1^{-1} C_1^T + B_2(Z_2))(y_1 - \hat{y}_1) + (B_1(Z_2) + K C_2^T)(y_2 - \hat{y}_2) \\ \dot{S}_1 = -\rho_1 S_1 - A_1^T(Z_2)S_1 - S_1 A_1(Z_2) + C_1^T C_1 \\ \hat{y}_1 = C_1 Z_1 \\ \\ \dot{Z}_2 = A_2(Z_1)Z_2 + g_2(u, y, Z_1, Z_2) + S_2^{-1} C_2^T(y_2 - \hat{y}_2) \\ \dot{S}_2 = -\rho_2 S_2 - A_2^T(Z_1)S_2 - S_2 A_2(Z_1) + C_2^T C_2 \\ \hat{y}_2 = C_2 Z_2. \end{cases} \qquad (3.110)$$

Remark 3.19 Owing to the persistency property of the inputs, it is worth noticing that $\|S_1\|$ and $\|S_2\|$ are bounded for ρ_1 and ρ_2 large enough (see details in [31]).

The stability analysis of the observer under parameters uncertainties is given in [85] by using a Lyapunov function.

IM Interconnected Observer Design: Conclusions

An observer design for the IM drive without mechanical sensors (speed and load torque sensor) is given. The major contributions of this section are as follows:

(1) The design of an adaptive interconnected observer that estimates the rotor speed and position, rotor fluxes, and load torque;
(2) Based on the Lyapunov theory, sufficient conditions allow to prove the practical stability of the estimation error even under or near unobservability conditions [85].

3.5 Conclusions

In this chapter, several observer designs have been presented to estimate the unmeasurable state components of dynamical systems. More precisely, from the machines mathematical models introduced in Chap. 1, suitable transformations have been defined so that observers can be designed. Here, the representations of the PMSM and IM have been considered as state affine system plus nonlinear interconnected terms, or more generally, as interconnected subsystems plus nonlinear terms affined in the parameters. The asymptotic convergence of the adaptive interconnected observers and of the finite-time observer based on sliding mode techniques have been analyzed and applied to the PMSM and IM machines with robustness properties.

These observers will be applied in closed-loop with the controller designed in the following chapters for the control of the PMSM and the IM machines.

3.6 Bibliographical Notes

When considering the nonlinear systems, even if the observability property is satisfied, the construction of an observer is not an easy task [4, 30, 42]. For the nonlinear systems, the observer design specifically depends on the class of the concerned models.

For example, in [46] for SISO case and in [75] for MIMO case, it concerns nonlinear systems that can be transformed into either a linear system, or a linear system plus an output injection by means of a diffeomorphism. For that class of systems, a linear observer, called the *General Luenberger Observer*, can be designed.

Furthermore, when this transformation does not exist, it is possible to search to transform the nonlinear system into a linear time variant system plus an input–output injection for which a Kalman-like observer can be designed [83].

A more general class of nonlinear systems observable for any input is given by system

$$\begin{cases} \dot{\xi} = A\xi + \phi(\xi, u) \\ y = C\xi \end{cases} \tag{3.111}$$

with some conditions given in terms of the matrices A and C, and for any $u(t) \in U_{adm}$, set of the admissible inputs. The vector field $\phi(\xi, u)$ is assumed compactly supported. This term has a triangular structure and does not affect the observability of the system (see [41]). So, a High Gain Luenberger Observer for this class of systems has be defined in [28].

An interesting class of nonlinear systems for which it is possible to construct an Extended Kalman Observer is characterized by the dynamics:

$$\begin{cases} \dot{\xi} = A(u)\xi + \phi(u, y) \\ y = C\xi = \xi_1 \end{cases} \tag{3.112}$$

where the components of matrix $A(u)$ and vector $\phi(u, y)$ are continuous functions, depending on u and y, uniformly bounded. The nonlinear term $\phi(u, y)$ does not affect the observability of the system.

Another interesting class of system adapted to the design of an observer is described by

$$\begin{cases} \dot{\xi} = A(u)\xi + \phi(\xi, u) \\ y = C(u)\xi \end{cases} \tag{3.113}$$

where ξ belongs to the compact $\chi \subset \Re^n$, y belongs to $\Re$, u belongs to the set of the admissible input U_{adm} in $\Re^m$. For this class of systems, a High Gain Extended Kalman Filter can be designed [3].

In the aforementioned observers, the parameters of the system are assumed exactly known. If not, under suitable assumptions, the estimation of the non-measurable state is possible and, moreover, simultaneously the identification of the unknown parameters, by using Adaptive Kalman Filter [6].

Another way to observe a nonlinear system when the parameters are not well known is by using robust sliding mode observers as introduced in [19, 24]. However, if the system satisfies partially the observability property, a solution is to search if the whole system can be represented as a set of interconnected subsystems for which each subsystem satisfies the observability property. The idea is to design an observer for each observable subsystem. These interconnected observers are introduced in [5].

All the above-mentioned, observers have been applied for the AC machines observation problem, due to the intrinsic observability difficulty of these machines under their operation domain.

For the SPMSM, adaptive interconnected observers have been introduced in [21].[1] This class of Adaptive Interconnected Observers has also been used for the IPMSM in [38][2] and for the induction motor in [85].

For robustness purpose, High Order sliding Mode Observer can be designed as in [20][3] via a Super-Twisting Algorithm. For the IPMSM case, an interconnected High Order Sliding Mode Observer (HOSMO) is designed to estimate the position, rotor speed, and stator resistance in [39].[4]

---

[1] This chapter includes excerpts of [21], originally published in the proceedings of IFAC world Congress, Milano, Italy, IFAC-PapersOnLine IFAC 2011.

[2] This chapter includes excerpts reprinted from Journal of the Franklin Institute, 349(5):1734–1757, Hamida M, Glumineau A, De Leon J (2012) Robust integral backstepping control for sensorless IPM synchronous motor controller. Copyright (2012), with permission from Elsevier.

[3] This chapter includes excerpts of [20], (2010) IEEE. Reprinted, with permission, from Ezzat M, De Leon J, Gonzalez N, Glumineau A, Observer-controller scheme using high order sliding mode techniques for sensorless speed control of permanent magnet synchronous motor. In: Decision and Control (CDC), 49th IEEE Conference on Decision Control.

[4] This chapter includes an excerpt of [39]: "Hamida M, De Leon J, Glumineau A (2013) High order sliding-mode observers and integral backstepping sensorless control of IPMS motor. International Journal of Control DOI: 10.1080/00207179.2014.904523" reprinted by permission of the publisher Taylor & Francis Ltd, http://www.tandf.co.uk/journals.

Appendix: Practical Stability Definitions

This part is devoted to introduce some concepts and results of practical stability properties using in terms of Lyapunov functions [59].

Theory of stability is the basis of the control systems study. Moreover, the concept of practical stability allows to study the properties of a nonlinear system when the state of this system is bringing close to a set instead of the equilibrium point. From a practical point of view, a system will be considered stable if the deviations remain bounded around the equilibrium point. This is clear that, in practice, asymptotic stability towards a domain whose the size has to be determined, for performance checking, is sufficient. If the behavior of the system can be bounded by certain bounds, the notion of practical stability becomes useful. For example, for AC machines the stability towards a domain with specified bounds during a fixed time interval is a concept equivalent to a finite time stability.

Now, we introduce definitions which are useful for to guarantee the practical stability, in terms of Lyapunov functions.

Define the following class of function:

$$\mathbf{W} = \{d_1 \in C[\Re^+, \Re^+] :$$

$$d_1(l) \text{ is strictly increasing in } l \text{ and}$$

$$d_1(l) \to \infty \text{ as } l \to \infty\}.$$

Let $B_r = \{e \in \Re^n : \|e\| \le r\}$. Consider the dynamical system

$$\dot{e} = f(t, e), \quad e(t_0) = e_0, t_0 \ge 0, \tag{3.114}$$

System (3.114) is said to be

Definition 3.8   UPS Uniformly practically stable if, given $(\hbar_1, \hbar_2)$ with $0 < \hbar_1 < \hbar_2$, one has

$$\|e_0\| \le \hbar_1 \Rightarrow \|e(t)\| \le \hbar_2, \quad \forall t \ge t_0. \tag{3.115}$$

Definition 3.9   UPQS Uniformly practically quasi-stable if, given $\hbar_1 > 0$, $\Im > 0$, $T > 0$ and $\forall t_0 \in \Re^+$, one has

$$\|e_0\| \le \hbar_1 \Rightarrow \|e(t)\| \le \Im, \quad t \ge t_0 + T. \tag{3.116}$$

Definition 3.10   SUPS Strongly uniformly practically stable, if (**UPS**) and (**UPQS**) hold together.

A result of the practical stability in terms of Lyapunov-like functions is presented

Theorem 3.8 [59] *Assume that*

(i) *$\hbar_1$ and $\hbar_2$ are given such that $0 < \hbar_1 < \hbar_2$,*
(ii) *$V \in C[\mathfrak{R}^+ \times \mathfrak{R}^n, R^+]$ and $V(t, e)$ is locally Lipschitz in e,*
(iii) *for $(t, e) \in \mathfrak{R}^+ \times B_{\hbar_2}, d_1(\|e\|) \le V(t, e) \le d_2(\|e\|)$ and*

$$\dot{V}(t, e) \le \wp(t, V(t, e)) \tag{3.117}$$

where $d_1, d_2 \in \textbf{W}$ and $\wp \in C[\mathfrak{R}^{+,2}, \mathfrak{R}]$,
(iv) *$d_2(\hbar_1) < d_1(\hbar_2)$ holds.*

Consequently, the practical stability properties of

$$\dot{l} = \wp(t, l), \quad l(t_0) = l_0 \ge 0, \tag{3.118}$$

implies the corresponding practical stability properties of system (3.114).

From the above theorem, the following criteria can be established

Corollary 3.1 [59] *In Theorem* 3.8, *if $\wp(t, l) = -\alpha_1 l + \alpha_2$, with α_1 and $\alpha_2 > 0$, it implies strong uniform practical stability (SUPS) of system* (3.114).

We can see that the solution of equation

$$\dot{l}(t) = -\alpha_1 l(t) + \alpha_2 \tag{3.119}$$

is of the form

$$l(t) = l_0 e^{-\alpha_1 t - t_0} + \frac{\alpha_2}{\alpha_1} \left[1 - e^{-\alpha_1(t - t_0)} \right], \quad t \ge t_0 \tag{3.120}$$

The strong uniform practical stability of (3.119) is obtained.

Chapter 4
Robust Synchronous Motor Controls Designs (PMSM and IPMSM)

Abstract In this chapter, two robust control strategies for the synchronous motor are designed. In this preliminary phase, it is assumed all the variables are measurable and that all the parameters are known or bounded (and their bounds are known). The estimation of the nonmeasured state and of some sensitive parameters has been studied in Chap. 3. The sensitivity with respect to the variations of these parameters will be studied in Chap. 6. First, integral backstepping control strategies for the PMSM and the IPMSM are designed to track the desired trajectories of the rotor speed (defined in Chap. 1). Sufficient conditions are obtained to ensure the exponential convergence of the tracking error. Next, control strategies based on sliding mode techniques are designed to track the desired trajectories. Since the chattering phenomenon is a drawback of the classical sliding mode control and represents a limitation for its implementation, then in order to reduce these effects, a quasi-continuous sliding mode controller and a high-order sliding mode controller are designed for the PMSM and the IPMSM.

4.1 Backstepping Control

Recently, several approaches have been proposed for the design of nonlinear control systems. Among these controllers, the backstepping control constitutes a major design methodology.

The backstepping technique is a systematic and recursive design for nonlinear feedback control (see [53]). Backstepping control principle is based on select recursively some appropriate functions of state variables as virtual control input for a subsystem of order one. The virtual control is designed to obtain the stability of this subsystem via a Lyapunov function. After each backstepping stage, it results a new virtual control obtained from the previous step. Backstepping procedure terminates when the real input appears. A whole Lyapunov function is defined by summing all the previous Lyapunov functions introduced at each design step.

For a large class of nonlinear systems, the backstepping procedure provides a powerful framework for the design of tracking and regulation strategies.

In this chapter, the robustness of the classical backstepping control is improved by adding integral control at each step of the design. This allows to reject unknown terms due to parameters uncertainties or disturbances. This approach can also be extended to handle systems with unknown parameters via adaptive backstepping by using parameters estimation (see Chap. 6).

For a nominal system (without uncertainties), the integral backstepping controllers achieve an asymptotic tracking. Thus, the main objectives of this section are to design a controller based on a classical backstepping technique for the SPMSM and an integral backstepping controller for the IPMSM, ensuring that the speed asymptotically tracks the desired reference.

4.1.1 Backstepping Control of SPMSM

The purpose of this section is to design a backstepping controller for the SPMSM that is robust under parametric uncertainties in order to achieve the control objectives, i.e., the rotor speed tracks the desired reference and the controller regulates the stator currents.

Consider the mathematical model of the PMSM in the (d, q) frame (1.65), introduced in Chap. 1. This model will be used to design the control strategy in order to achieve the following control objective.

Control Objective

The objective is to design a controller in order to track the desired rotor speed reference, (i.e., $\Omega \to \Omega^*$) despite the unknown and bounded load torque and under a bad knowledge of the system parameters. Furthermore, by applying a vector control strategy, the stator current i_{sd} is forced to zero, (i.e., $i_{sd} \to 0$). For sensorless purpose, the rotor position and speed will be estimated by an observer (see Chap. 6).

The controller design will be performed in three steps.

Step 1: Speed loop

To solve the rotor speed tracking problem, the design process starts by introducing the tracking error

$$z_1 = \Omega - \Omega^* \tag{4.1}$$

and the new variables,

$$\xi_1 = \Omega, \qquad \alpha_0 = \Omega^* \tag{4.2}$$

where Ω^* is the speed reference. Taking the time derivative of z_1, we have

$$\dot{z}_1 = \frac{p\psi_f}{J} i_{sq} - \frac{f_v}{J} \Omega - \frac{T_l}{J} - \dot{\Omega}^*$$

with the new variables

$$\xi_2 = \frac{p\psi_f}{J} i_{sq}, \qquad \beta_1 = -\frac{f_v}{J}\Omega - \frac{T_l}{J} - \dot{\alpha}_0. \tag{4.3}$$

The dynamics of z_1 is described by

$$\dot{z}_1 = \xi_2 + \beta_1$$

To analyze the dynamics of the tracking error z_1, consider the following Lyapunov function candidate, $V_1 = \frac{1}{2}z_1^2$, and define the following new variables

$$\alpha_1 = -k_\Omega z_1 - \beta_1, \qquad z_2 = \xi_2 - \alpha_1. \tag{4.4}$$

Then, taking the time derivative of V_1, and substituting $\dot{z}_1 = \xi_2 + \beta_1 = z_2 - k_\Omega z_1$, where k_Ω is a positive constant, it follows that

$$\dot{V}_1 = z_2 z_1 - k_\Omega z_1^2.$$

Step 2: Current i_{sq} loop

The next step is to design the speed control input v_{sq}, following the systematic design procedure of the backstepping algorithm.

We start the second step by taking the time derivative of $z_2 = \xi_2 - \alpha_1$, then

$$\dot{z}_2 = \beta_2 + K v_{sq}$$

where $\beta_2 = \frac{p\psi_f}{J}\{-\frac{p\psi_f}{L_s}\Omega - p\Omega i_{sd} - \frac{R_s}{L_s}i_{sq}\} - \dot{\alpha}_1$ and $K = \frac{p\psi_f}{JL_s}$.

Defining the following candidate Lyapunov function

$$V_2(z_1, z_2) = V_1 + \frac{1}{2}z_2^2, \tag{4.5}$$

whose time derivative is given by

$$\dot{V}_2 = -k_\Omega z_1^2 + z_2(z_1 + \beta_2 + K v_{sq}), \tag{4.6}$$

to ensure that the right side of (4.6) becomes a negative definite function of the state vector, the control input v_{sq} is selected as

$$v_{sq} = \frac{1}{K}\left[-k_q\left\{ \frac{p\psi_f}{J}i_{sq} + (k_\Omega + 1)(\Omega - \Omega^*) - \frac{f_v}{J}\Omega - \frac{T_l}{J} - \dot{\alpha}_0 \right\} \right. \\ \left. - \left\{ \frac{p\psi_f}{J}\left\{ -\frac{p\psi_f}{L_s}\Omega - p\Omega i_d - \frac{R_s}{L_s}i_{sq} \right\} - \dot{\alpha}_1 \right\} \right] \tag{4.7}$$

where k_q is a positive control parameter to be tuned.

$$\dot{V}_2 = -k_\Omega z_1^2 - k_q z_2^2 < 0. \tag{4.8}$$

Thus, under the action of the control input v_{sq}, the rotor speed Ω tracks the desired rotor speed reference Ω^*.

Step 3: Current i_{sd} loop

As mentioned above, to eliminate a residual reluctance torque, the stator current reference is fixed to zero, i.e., $i_{sd}^* = 0$. Introduce the following variable $z_3 = i_{sd}$, whose dynamics is given by

$$\dot{z}_3 = -\frac{R_s}{L_s}i_{sd} + p\Omega i_{sq} + \frac{1}{L_s}v_{sd}.$$

Define the Lyapunov function

$$V_3 = V_2 + \frac{1}{2}z_3^2, \tag{4.9}$$

whose time derivative is given by

$$\dot{V}_3 = -k_\Omega z_1^2 - k_q z_2^2 + z_3 \left\{ -\frac{R_s}{L_s}i_d + p\Omega i_{sq} + \frac{1}{L_s}v_{sd} \right\}. \tag{4.10}$$

Since $i_{sd}^* = 0$, the control input v_d is choosing as follows

$$v_{sd} = -L_s k_d i_{sd} + R_s i_{sd} - pL_s\Omega i_{sq} \tag{4.11}$$

where k_d is a positive control parameter, such that

$$\dot{V}_3 = -k_\Omega z_1^2 - k_q z_2^2 - k_d z_3^2 < 0.$$

This implies that under the action of the control v_{sd} the stator current i_{sd} tracks the desired reference i_{sd}^*. The control design is achieved.

Summary 4.1.1 SPMSM Backstepping Control

$$v_{sd} = -L_s k_d i_{sd} + R_s i_{sd} - pL_s\Omega i_{sq}$$

$$v_{sq} = \frac{1}{K}\left[-k_q \left\{ \frac{p\psi_f}{J}i_{sq} + (k_\Omega + 1)(\Omega - \Omega^*) - \frac{f_v}{J}\Omega - \frac{T_l}{J} - \dot{\Omega}^* \right\} \right.$$

$$\left. -\left\{ \frac{p\psi_f}{J} \left\{ -\frac{p\psi_f}{L_s}\Omega - p\Omega i_{sd} - \frac{R_s}{L_s}i_{sq} \right\} - \dot{\alpha}_1 \right\} \right]$$

with $\alpha_1 = -k_\Omega(\Omega - \Omega^*) + \frac{f_v}{J}\Omega + \frac{T_l}{J} + \dot{\Omega}^*$

and k_Ω, k_q, k_d are the tuning positive parameters.

Remark 4.1 For sensorless control, since the mechanical variables are not available by measurement, the rotor speed and the load torque will be replaced by their estimates provided by an observer.

4.1.2 Integral Backstepping Control of IPMSM

The aim is to design an improved backstepping controller for the IPMSM ($L_d \neq L_q$). The advantage of this improved backstepping control design is obtained by an integral term added to the classical backstepping procedure to increase the robustness of the controller under uncertainties and disturbances. To design such a controller, the (d, q) frame model of the IMPSM (1.62) will be used.

Control Objective

The design of a controller such that the rotor speed tracks a desired reference (Ω^*) and overcomes the effects of the parametric uncertainties or disturbance (mainly due to the rotor resistance variation and the load torque).

Furthermore, to achieve the above control objective, the direct axis component of the current reference is chosen equal to zero, (i.e., $i_{sd}^* = 0$), to apply a vector control and to avoid the reluctance effect (as $L_d \neq L_q$).

Regarding the classical backstepping control [53], the control robustness under uncertain parameters and the performance are highly improved by adding integral terms at each step of the procedure. In this section, we assume that all variables are available for measurement, i.e., the rotor angular position and the rotor speed are measurable. The analysis of the closed-loop stability when the angular position and rotor speed, the load torque are not available and under a bad knowledge of the rotor resistance, will be considered in Chap. 6.

The control synthesis is carried out in three steps.

Step 1: Speed loop

We start the control design to solve the rotor speed tracking problem, by defining the tracking error variable as

$$z_\Omega = \Omega^* - \Omega + k'_\Omega \int_0^t (\Omega^* - \Omega)dt \tag{4.12}$$

where $k'_\Omega \int_0^t (\Omega^* - \Omega)dt$ is the integral term added to the rotor speed tracking error and k'_Ω is a positive constant, used to improve the performance of the controller.

Next, to design the speed control, v_{sq} is computed to force the quadrature axis component of the stator current i_{sq} to track the reference i_{sq}^*. Then, taking the time derivative of (4.12) and replacing i_{sq} by i_{sq}^*, it follows that

$$\dot{z}_\Omega = \dot{\Omega}^* - \frac{p}{J}(L_d - L_q)i_{sd}i_{sq}^* + \frac{f_v}{J}\Omega - \frac{p}{J}\Phi_f i_{sq}^* + \frac{1}{J}T_l + k'_\Omega(\dot{\Omega}^* - \Omega). \tag{4.13}$$

Note that the reference i_{sq}^* will be considered as a new input for the resulting closed-loop system.

Choosing the following candidate Lyapunov function

$$V_\Omega = \frac{1}{2}z_\Omega^2$$

and by taking the time derivative along the trajectories of (4.13), we obtain

$$\dot{V}_\Omega = z_\Omega \left\{ \dot{\Omega}^* - \frac{p}{J}(L_d - L_q)i_{sd}i_{sq}^* + \frac{f_v}{J}\Omega - \frac{p}{J}\Phi_f i_{sq}^* + \frac{1}{J}T_l + k'_\Omega(\dot{\Omega}^* - \Omega) \right\}. \tag{4.14}$$

Following the backstepping methodology, and in order to the derivative of the Lyapunov function $\dot{V}_\Omega$ becomes definite negative, the virtual control input i_{sq}^* is choosing as

$$i_{sq}^* = \frac{J}{p\Phi_f + \frac{p}{J}(L_d - L_q)i_{sd}}[k_\Omega z_\Omega + \dot{\Omega}^* + \frac{f_v}{J}\Omega + k'_\Omega(\Omega^* - \Omega) + \frac{1}{J}T_l], \tag{4.15}$$

and by substituting in (4.14), we obtain

$$\dot{V}_\Omega = -k_\Omega z_\Omega^2.$$

It follows that z_Ω converges to zero exponentially with an arbitrary rate of convergence $k_\Omega > 0$.

Step 2: Current i_{sq} loop

It is clear that the virtual input i_{sq}^* is synthesized to stabilize the dynamics (4.13). Now, to design the control input v_{sq}, we introduce the following tracking error:

$$z_q = i_{sq}^* - i_{sq} + z'_q \tag{4.16}$$

where $z'_q = k'_q \int_0^t (i_{sq}^* - i_{sq})dt$ is the integral action, and k'_q is a positive control parameter.

Consider the total Lyapunov function

$$V_q = V_\Omega + \frac{1}{2}z_q^2 + \frac{1}{2}z'^2_q. \tag{4.17}$$

Taking the time derivative of V_q, and replacing the suitable terms, it follows that

$$\dot{V}_q = -k_\Omega z_\Omega^2 + z_q \left\{ \frac{di_{sq}^*}{dt} + \frac{R_s}{L_q}i_{sq} + p\frac{L_d}{L_q}\Omega i_{sd} + p\frac{1}{L_q}\Phi_f \Omega - \frac{1}{L_q}v_{sq} \right. \tag{4.18}$$
$$\left. + k'_q(i_{sq}^* - i_{sq}) \right\} + z'_q k'_q(i_{sq}^* - i_{sq}).$$

By choosing the control input v_{sq} as

$$v_{sq} = L_q \left[k_q z_q + 2\frac{p}{J}\Phi_f z_\Omega + p\frac{\Phi_m}{L_q}\Omega + \frac{R_s}{L_q}i_{sq} + \frac{di_{sq}^*}{dt} \right], \tag{4.19}$$

and substituting in (4.18),

$$\dot{V}_q = -k_\Omega z_\Omega^2 - k_q z_q^2 + \{z_q + z_q'\}k_q'(i_{sq}^* - i_{sq}). \tag{4.20}$$

Since $i_{sq}^* - i_{sq} = z_q - z_q'$, then (4.20) becomes

$$\dot{V}_q = -k_\Omega z_\Omega^2 - \{k_q - k_q'\}z_q^2 - k_q' z_q'^2 \tag{4.21}$$

such that

$$\dot{V}_q \leq -\overline{K}_q V_q$$

where $\overline{K}_q = min\{k_\Omega, \{k_q - k_q'\}, k_q'\}$ is a positive constant. Then, under the control action v_{sq}, the quadrature axis component of the stator current i_{sq} tracks the desired current reference i_{sq}^*, i.e., $i_{sq} \to i_{sq}^*$; and since i_{sq}^* is designed such that the rotor speed tracks the desired reference, i.e., $(\Omega \to \Omega^*)$, the first control objective is achieved.

Step 3: Current i_{sd} loop

The last step of the integral backstepping algorithm is focused on eliminating the reluctance torque. Then, to achieve this objective, the current reference is fixed to zero, i.e., $(i_{sd}^* = 0)$. To apply the vector control method, let us define the following tracking: error

$$z_d = i_{sd}^* - i_{sd} + z_d'$$

where $z_d' = k_d' \int_0^t (i_{sd}^* - i_{sd})dt$ is the integral action and k_d' a positive constant to be tuned. Define the following candidate Lyapunov function:

$$V_d = \tfrac{1}{2}z_d^2 + \tfrac{1}{2}z_d'^2, \tag{4.22}$$

whose time derivative is

$$\dot{V}_d = z_d \left\{ -\frac{di_{sd}}{dt} - k_d' i_{sd} \right\} + z_d' \left\{ -k_d' i_{sd} \right\}.$$

Since $i_{sd}^* = 0$, and by replacing $i_{sd} = z_d - z_d'$ in the above equation, it follows that

$$\dot{V}_d = z_d \left\{ \frac{R_s}{L_d}i_{sd} - p\frac{L_q}{L_d}\Omega i_{sq} - \frac{1}{L_d}v_{sd} \right\} + k_d'\{z_d + z_d'\}\{z_d - z_d'\}. \tag{4.23}$$

In order to force $\dot{V}_d$ to be a definite negative function, the control input v_{sd} is defined as follows:

$$v_{sd} = L_d k_d(i_{sd}^* - i_d) + L_d k_d' \int_0^t (i_{sd}^* - i_{sd})dt + R_s i_{sq} - pL_q i_{sq}\Omega, \tag{4.24}$$

and substituting (5.2) in (4.23), we obtain

$$\dot{V}_d = -\{k_d - k_d'\}z_d^2 - k_d' z_d'^2.$$

By choosing a positive constant: $\overline{K}_d = min\{\{k_d - k'_d\}, k'_d\}$, it follows that

$$\dot{V}_d \leq -\overline{K}_d V_d.$$

This implies that under the action of the control v_{sd}, the d-axis component of the stator current i_{sd} tracks exponentially the desired reference, i.e., $i_{sd} \rightarrow i^*_{sd}(= 0)$.

The full control design is now completed. Finally, combining the action of the control inputs v_{sq}, i^*_{sq} and v_{sd}, the control objectives are achieved.

Summary 4.1.2 *IPMSM Backstepping Control*

$$v_{sd} = L_d \left[k_d \left(i^*_{sd} - i_{sd} + k'_d \int_0^t (i^*_d - i_{sd})dt \right) + \frac{R_s}{L_d} i_{sq} - p\frac{L_q}{L_d} i_{sq}\Omega \right].$$

$$v_{sq} = L_q \left[k_q z_q + 2\frac{p}{J}\Phi_f z_\Omega + p\frac{\Phi_m}{L_q}\Omega + \frac{R_s}{L_q} i_{sq} + \frac{di^*_{sq}}{dt} \right],$$

$$i^*_{sq} = \frac{J}{p\Phi_f + \frac{p}{J}(L_d - L_q)i_{sd}} \left[k_\Omega z_\Omega + \dot{\Omega}^* + \frac{f_v}{J}\Omega \right.$$

$$\left. + k'_\Omega(\Omega^* - \Omega) + \frac{1}{J}T_l \right]$$

where $k_d, k'_d, k_q, k'_q, k_\Omega$ are the positive tuning parameters.

4.2 High-Order Sliding Mode Control

In this section, another robust control methodology based on the sliding mode techniques is introduced. The main characteristics of these controllers are to achieve the control objectives with a finite-time convergence, in spite of parameter uncertainties and some classes of disturbances.

Regarding sliding mode technique, by using the classical sliding mode techniques, a discontinuous input is obtained, yielding on the system the so-called *chattering phenomenon*. This problem is one of the most important limitations of such controllers.

Recently, several works have addressed the problem on how to reduce this phenomenon. For instance, the high-order sliding mode controllers have been proposed, thanks to its attractive properties: the robustness, the finite-time convergence, and the chattering reduction (see [61]).

The aim of this section is to design sliding mode control strategies for a robust tracking of the desired trajectories defined by an industrial benchmark (see Sect. 1.6). In order to reduce the effects of the chattering phenomenon, a quasi-continuous sliding mode controller will be proposed and applied to the SPMSM. Furthermore, for the same purpose, a high-order sliding mode controller will be designed for the IPMSM.

4.2.1 High-Order Sliding Mode Control of SPMSM

4.2.1.1 Quasi-Continuous High-Order Sliding Mode Controller

In the previous section, it has been introduced a rotor speed controller based on an improved backstepping algorithm allowing to track a desired reference. Now, a quasi-continuous high-order sliding mode controller will be designed to achieve the following control objective.

Control Objective

The objective is to design a control algorithm in order to the SPMSM rotor speed (Ω) tracks in finite time a desired reference Ω^* in the presence of uncertainties on the rotor resistance, the inductance, and despite of the unknown load torque.

For achieving this objective, some assumptions must be formulated. First, it is assumed that the stator currents, the voltages, the rotor speed, and the angular position are available (by sensors). If the rotor speed and the angular position are not measured, it is necessary to estimate them by means of an observer. This case has been studied in Chap. 3.

Consider the following nonlinear system with a smooth output function σ

$$\begin{aligned} \dot{x} &= f(t, x) + g(t, x)u \\ y &= \sigma(t, x) \end{aligned} \tag{4.25}$$

where $x \in \Re^n$ is the state vector, f and g and $\sigma : \Re^{n+1} \to \Re$ are unknown smooth functions, $u \in \Re$ is the input, y is the new output of the system which is equal to the sliding surface σ.

Introducing a new change of coordinates of the form $\xi_1 = \sigma, \xi_2 = \dot{\sigma}, \ldots, \xi_r = \sigma^{(r-1)}$, where r is the relative degree of the system with respect to the output $y = \sigma(t, x)$. r is assumed to be constant and known, i.e.,

$$\sigma^{(r)} = F(t, x) + G(t, x)u \tag{4.26}$$

where $F(t, x) = \sigma^{(r)}|_{u=0}$ and $G(t, x) = \frac{\partial \sigma^{(r)}}{\partial u}| \neq 0$.

It is supposed that for some C, K_m, K_M positive constants, the following inequalities hold at least locally

$$|\sigma^{(r)}|_{u=0}| \le C, \qquad 0 < K_m \le \frac{\partial \sigma^{(r)}}{\partial u} \le K_M. \tag{4.27}$$

The sliding mode controller is a continuous function of $\sigma, \dot{\sigma}, \ldots, \sigma^{(r-1)}$, except on a r-sliding mode manifold defined by $\sigma = \dot{\sigma} = \cdots = \sigma^{(r-1)} = 0$.

The construction of the controller that stabilizes system (4.25) at the origin in finite time is established in the following:

Theorem 4.1 ([62]) *Assuming that the constants* $\beta_1, \beta_2, \ldots, \beta_{r-1}, \alpha > 0$ *are chosen sufficiently large in the lexicographic order, the controller*

$$u = \Psi_{r-1,r}(\sigma, \dot{\sigma}, \ldots, \sigma^{(r-1)}) \tag{4.28}$$

is a r-sliding homogeneous controller and provides for the finite-time stability of (4.25) *and* (4.28)*, where*

$$
\begin{aligned}
\varphi_{0,r} &= \sigma, \\
N_{0,r} &= |\sigma|, \\
\Psi_{0,r} = \frac{\varphi_{0,r}}{N_{0,r}} &= \mathrm{sign}(\sigma), \\
\varphi_{i,r} &= \sigma^{(i)} + \beta_i N_{(i-1,r)}^{(r-i)/(r-i+1)} \Psi_{i-1,r} \\
N_{i,r} &= |\sigma^{(i)}| + \beta_i N_{(i-1,r)}^{(r-i)/(r-i+1)} \Psi_{i-1,r} \\
\Psi_{i,r} &= \frac{\varphi_{i,r}}{N_{i,r}}.
\end{aligned}
\tag{4.29}
$$

Furthermore, for $i = 1, \ldots, r - 1$, $N_{i,r}$ *is positive definite,* ($N_{i,r} = 0$ *if and only if* $\sigma = \dot{\sigma} = \cdots = \sigma^{(r-1)} = 0$). *The inequality* $|\Psi_{r-1,r}(\sigma, \dot{\sigma}, \ldots, \sigma^{(r-1)})| \leq 1$ *holds whenever* $N_{i,r} > 0$. *The function* $\Psi_{r-1,r}(\sigma, \dot{\sigma}, \ldots, \sigma^{(r-1)})$ *is continuous everywhere except for the r-sliding mode* $\sigma = \dot{\sigma} = \cdots = \sigma^{(r-1)} = 0$.

The choice of the parameters $\beta_1, \beta_2, \ldots, \beta_{r-1}$ and α, which are positive constants, determines a controller family applicable to system (4.25) of relative degree r. The parameter α is chosen specifically for any fixed C, K_m and K_M, most conveniently by computer simulation, avoiding redundantly large estimations of C, K_m, and K_M.

The controller (4.28) for systems having a relative degree equal to $r = 1$ and $r = 2$ are given by

$$
\begin{aligned}
r = 1: \quad & u = -\alpha\mathrm{sign}(\sigma) \\
r = 2: \quad & u = -\alpha \frac{\left\{\dot{\sigma} + |\sigma|^{\frac{1}{2}}\mathrm{sign}(\sigma)\right\}}{|\dot{\sigma}| + |\sigma|^{\frac{1}{2}}}.
\end{aligned}
\tag{4.30}
$$

Notice that these controllers are discontinuous and they are only tuning by means of the parameter α.

4.2.1.2 PMSM Control Design

Now, the above robust sliding mode control algorithm will be applied to the PMSM in order to force the tracking errors converge to zero in finite time, i.e., the rotor speed tracking error $\sigma_1 = \Omega - \Omega^* \to 0$ and the d-axis component of the stator current i_{sd} to zero, i.e., $\sigma_2 = i_{sd} \to 0$.

Considering the new outputs to be controlled $\sigma_1 = \Omega - \Omega^*$ and $\sigma_2 = i_{sd}$, where the relative degrees of the system associated to these new outputs are $r_1 = 2, r_2 = 1$, respectively. These relative degrees are assumed to be constant

Taking the first and second time derivatives of the output σ_1, yields

$$
\dot{\sigma}_1 = \frac{p\psi_f}{J}i_{sq} - \frac{f_v}{J}\Omega - \dot{\Omega}^*
$$

$$
\ddot{\sigma}_1 = \frac{p\psi_f}{J}\left\{-\frac{p\psi_f}{L_s}\Omega - p\Omega i_{sd} - \frac{R_s}{L_s}i_{sq} + \frac{1}{L_s}v_{sq}\right\} - \frac{f_v}{J}\left\{\frac{p\psi_f}{J}i_{sq} - \frac{f_v}{J}\Omega\right\} - \ddot{\Omega}^*,
$$

$$(4.31)$$

where the nonlinear terms obtained from the second derivative of σ_1 can be written in the form of (4.26), i.e.,

$$
F(t, x) = \frac{p\psi_f}{J}\left\{-\frac{p\psi_f}{L_s}\Omega - p\Omega i_{sd} - \frac{R_s}{L_s}i_{sq}\right\} - \frac{f_v}{J}\left\{\frac{p\psi_f}{J}i_{sq} - \frac{f_v}{J}\Omega\right\} - \ddot{\Omega}^*,
$$

$$
G(t, x) = \frac{p\psi_f}{JL_s}.
$$

Using these expressions, the inequalities (4.27) can be easily verified.

Similarly, taking the time derivative of σ_2, we have

$$
\dot{\sigma}_2 = -\frac{R_s}{L_s}i_{sd} + p\Omega i_{sq} + \frac{1}{L_s}v_{sd}, \tag{4.32}
$$

where $F(t, x) = -\dfrac{R_s}{L_s}i_{sd} + p\Omega i_{sq}$, and $G(t, x) = \dfrac{1}{L_s}$.

Finally, following the procedure to design a quasi-continuous high-order sliding mode controller, as it was introduced in Theorem 4.1, it follows that the controllers are given by

Summary 4.2.1 *SPMSM Quasi-continuous HOSM Control*

$$
v_{sd} = L_s\left\{\frac{R_s}{L_s}i_{sd} - p\Omega i_{sq} - \alpha_2\text{sign}(i_{sd})\right\}
$$

$$
v_{sq} = \frac{JL_s}{p\psi_f}\left\{-\frac{p\psi_f}{J}\left\{-\frac{p\psi_f}{L_s}\Omega - p\Omega i_{sd} - \frac{R_s}{L_s}i_{sq}\right\} - \frac{f_v}{J}\left\{\frac{p\psi_f}{J}i_{sq} - \frac{f_v}{J}\Omega\right\}\right.
$$

$$
\left. - \alpha_1\frac{\left\{\frac{p\psi_f}{J}i_{sq} - \frac{f_v}{J}\Omega - \dot{\Omega}^* + |\Omega - \Omega^*|^{\frac{1}{2}}\text{sign}(\Omega - \Omega^*)\right\}}{|\frac{p\psi_f}{J}i_{sq} - \frac{f_v}{J}\Omega - \dot{\Omega}^*| + |\Omega - \Omega^*|^{\frac{1}{2}}}\right\}
$$

where α_1 and α_2 are the tuning positive control parameters.

Remark 4.2 The control parameters α_1 and α_2 are, respectively, chosen regarding the mechanical and electrical time constants of the machine.

4.2.2 MTPA Current Reference for IPMSM

Now, a control strategy will be designed to avoid the reluctance effect (when $L_d \neq L_q$) and by using the maximum torque per ampere (MTPA) control method (see [90]). From the MTPA strategy, current references are designed in order to increase the efficiency of the IPMSM.

The electromagnetic torque of the IPMSM can be expressed as follows:

$$T_e = p\Phi_r i_{sq} + p(L_d - L_q)i_{sd}i_{sq}. \tag{4.33}$$

The first term of (4.33) is the magnetic torque owing to the rotor permanent magnet flux Φ_r and the second term is the reluctance torque due to the complex interaction of dq-axis currents and inductances of the IPMSM.

However, the approach that forces the d-axis component of the stator current i_{sd} to 0 does not efficiently utilize the electromagnetic torque of an IPMSM. Then, to ensure the full use of the reluctance torque and to operate the motor with optimum efficiency, the d-axis component of the stator current reference i_{sd}^* is determined based on the MTPA control strategy. The reference of i_{sd} is obtained by differentiating (4.33) with respect to i_{sd} and by setting the resulting expression to zero. The optimal torque is then obtained for the given d-axis stator current reference.

More precisely, the relation between the stator currents i_{sd}, i_{sq}, and the stator phase current I_a is given by

$$I_a^2 = i_{sq}^2 + i_{sd}^2. \tag{4.34}$$

Using (4.34) and replacing i_{sq} into the torque equation (4.33), the following expression is obtained

$$T_e = p[\Phi_r + (L_d - L_q)i_{sd}]\sqrt{I_a^2 - i_{sd}^2}. \tag{4.35}$$

The torque variation with respect to the d-axis stator current is given by

$$\frac{\partial T_e}{\partial i_{sd}} = p\frac{[-\Phi_r i_{sd} + (L_d - L_q)(I_a^2 - i_{sd}^2) - (L_d - L_q)i_{sd}^2]}{\sqrt{I_a^2 - i_{sd}^2}}. \tag{4.36}$$

Then, the maximum of the torque can be obtained from $\dfrac{\partial T_e}{\partial i_{sd}} = 0$, i.e.,

$$2i_{sd}^2 + \frac{\Phi_r}{(L_d - L_q)}i_{sd} - I_a^2 = 0. \tag{4.37}$$

Finally, from (4.34) and (4.37), the reference i_{sd}^* can be computed as follows:

$$i_{sd}^* = -\frac{\Phi_r}{2(L_d - L_q)} - \sqrt{\frac{\Phi_r^2}{4(L_d - L_q)^2} + i_{sq}^2}. \tag{4.38}$$

Notice that the reference i_{sd}^* depends on the inductances and the q-axis component of the stator current reference i_{sq}. In this way, the optimal torque of the machine can be determined and will be used in the control algorithms.

4.2.3 High-Order Sliding Mode Control of IPMSM

Despite the many advantageous features of an interior permanent magnet synchronous motor, the control at high-speed conditions remains an engineering challenge [90].

The aim of this section is to design a robust nonlinear controller for the interior permanent magnet synchronous motor (IPMSM) to track a desired reference, using a maximum torque per ampere strategy (MTPA). The proposed controller is used to ensure finite-time convergence of sliding variables despite parameter uncertainties and the unknown load torque.

Defining the following tracking errors as follows:

$$\begin{pmatrix} \sigma_\Omega, & \sigma_{i_{sd}} \end{pmatrix}^T = \begin{pmatrix} \Omega - \Omega^*, & i_{sd} - i_{sd}^* \end{pmatrix}^T \tag{4.39}$$

that will be considered as the new outputs.

It is easy to see that the relative degrees associated to the outputs σ_Ω and $\sigma_{i_{sd}}$ are $r_\Omega = 2$ and $r_{i_{sd}} = 1$, respectively. Furthermore, it is assumed that they are constant and the associated zero dynamics is stable.

Now, we show the procedure how to design a HOSM controller for the IPMSM that attenuates the chattering phenomenon.

For this purpose, to avoid the direct switch of the input, the relative degrees are increased and chosen as $r_\Omega = 3$ and $r_{i_{sd}} = 2$, respectively; which is equivalent to derive once more the outputs. It yields that the discontinuous control is acting on the first time derivative of the control inputs.

Taking the second and first time derivatives of σ_Ω and $\sigma_{i_{sd}}$, respectively; we obtain

$$\begin{pmatrix} \sigma_\Omega^{(2)} \\ \sigma_{i_{sd}}^{(1)} \end{pmatrix} = \begin{pmatrix} \Psi_{\alpha;1} \\ \Psi_{\alpha;2} \end{pmatrix} + \begin{pmatrix} \Psi_{\beta;11} & \Psi_{\beta;12} \\ \Psi_{\beta;21} & \Psi_{\beta;22} \end{pmatrix} \begin{pmatrix} u_{sd} \\ u_{sq} \end{pmatrix} := \Psi_\alpha + \Psi_\beta u \tag{4.40}$$

where the components of the vector Ψ_α and the matrix Ψ_β are given by

$$\Psi_{\alpha;1} = L_f^{r_\Omega} \sigma_\Omega, \qquad \Psi_{\alpha;2} = L_f^{r_{i_{sd}}} \sigma_{i_{sd}}, \tag{4.41}$$

$$\Psi_{\beta;11} = L_{g_1} L_f^{r_\Omega - 1} \sigma_\Omega, \qquad \Psi_{\beta;12} = L_{g_1} L_f^{r_{i_{sd}} - 1} \sigma_{i_{sd}}, \tag{4.42}$$

$$\Psi_{\beta;21} = L_{g2} L_f^{r_\Omega -1} \sigma_\Omega, \qquad \Psi_{\beta;22} = L_{g2} L_f^{r_{i_{sd}} -1} \sigma_{i_{sd}}, \tag{4.43}$$

and expressed in terms of the motor dynamics

$$\Psi_{\alpha;1} = +k_1 i_q (k_4 i_{sd} + k_5 \Omega i_{sq}) + k_3 [(k_1 i_{sd} + k_2) i_{sq} + k_3 \Omega]$$
$$- \Omega^{*2} + (k_1 i_{sd} + k_2)(k_7 \Omega + k_8 \Omega i_{sd} + k_9 i_{sq}) \tag{4.44}$$
$$\Psi_{\alpha;2} = k_4 i_{sd} + k_5 \Omega i_{sq} - 2k_{11} i_{sq}$$

and

$$\Psi_\beta = \begin{pmatrix} \Psi_{\beta;11} & \Psi_{\beta;12} \\ \Psi_{\beta;21} & \Psi_{\beta;22} \end{pmatrix} = \begin{pmatrix} k_1 k_6 i_{sq} & (k_1 i_{sd} + k_2) k_{10} \\ k_6 & 0 \end{pmatrix}. \tag{4.45}$$

Its inverse is given by

$$\Psi_\beta^{-1} = \begin{pmatrix} 0 & \dfrac{1}{k_6} \\ \dfrac{1}{(k_1 i_{sd} + k_2) k_{10}} & -\dfrac{k_1 i_q}{(k_1 i_{sd} + k_2) k_{10}} \end{pmatrix} \tag{4.46}$$

with

$$k_1 = \frac{p}{J}(L_d - L_q), k_2 = \frac{p}{J}\phi_f, k_3 = -\frac{\phi_f}{J}, k_4 = -\frac{R_s}{L_d}, k_5 = p\frac{L_q}{L_d},$$
$$k_6 = \frac{1}{L_d}, k_7 = -p\frac{\phi_f}{L_q}, k_8 = -p\frac{L_d}{L_q}, k_9 = -\frac{R_s}{L_q}, k_{10} = \frac{1}{L_q}, k_{11} = \frac{(L_d - L_q)}{\phi_f}.$$

Remark 4.3 Using the parameter values and applying the MTPA strategy, it is easy to verify that the matrix Ψ_β is nonsingular.

It is clear that in practice the functions $\Psi_{\alpha;i}$ and $\Psi_{\beta,ij}$, for $i = 1, 2; j = 1, 2;$ are not well known. Then, it is necessary to take into account the uncertain terms. Thus we define $\Psi_{\alpha;i}$ and Ψ_β as follows:

$$\begin{cases} \Psi_{\alpha;i} = \Psi_{\alpha;i}^{nom} + \Delta\Psi_{\alpha;i}, & \text{for } i = 1, 2; \\ \Psi_\beta = \Psi_\beta^{nom} + \Delta\Psi_\beta \end{cases} \tag{4.47}$$

such that $\Psi_{\alpha;1}^{nom}, \Psi_{\alpha;2}^{nom}$ and Ψ_β^{nom} are the known nominal terms whereas $\Delta\Psi_{\alpha;1}, \Delta\Psi_{\alpha;2}$ and $\Delta\Psi_\beta$ represent all the uncertainties due to parameter variations and disturbance. Furthermore, in practice, the uncertainties $\Delta\Psi_{\alpha;1}, \Delta\Psi_{\alpha;2}$ and $\Delta\Psi_\beta$ are bounded.

Then, system (4.40) can be expressed in terms of uncertainties as follows:

$$\left(\sigma_\Omega^{(2)} \quad \sigma_{i_{sd}}^{(1)} \right)^T = \left(\Psi_\alpha^{nom} + \Delta\Psi_\alpha \right) + \left(\Psi_\beta^{nom} + \Delta\Psi_\beta \right) u. \tag{4.48}$$

Applying the following decoupling feedback control

$$u = \begin{pmatrix} u_{sd} \\ u_{sq} \end{pmatrix} = (\Psi_\beta^{nom})^{-1} \left\{ -\Psi_\alpha^{nom} + \nu \right\} \tag{4.49}$$

where $\nu := (\nu_d \ \nu_q)^T$ is the new control vector, then the closed-loop system is given by

$$\left(\sigma_\Omega^{(2)} \quad \sigma_{i_{sd}}^{(1)} \right)^T = \widetilde{\Psi}_\alpha + \widetilde{\Psi}_\beta \nu \tag{4.50}$$

where the uncertain terms are given by

$$\widetilde{\Psi}_\alpha = \Psi_\alpha - \left\{ I + \Delta\Psi_\beta (\Psi_\beta^{nom})^{-1} \right\} \Psi_\alpha^{nom} \tag{4.51}$$

and

$$\widetilde{\Psi}_\beta = \left\{ I + \Delta\Psi_\beta (\Psi_\beta^{nom})^{-1} \right\}. \tag{4.52}$$

Now, by using the uncertain nonlinear system (4.50), we design a 3rd order (for the speed loop) and a 2nd order (for the current loop) sliding mode controllers for system (4.50) in order to attenuate the chattering effect and to improve the robustness under uncertainties. Notice that we shall design a discontinuous control of $\sigma_\Omega^{(3)}$ and $\sigma_{i_{sd}}^{(2)}$, through the derivative of the inputs $\dot{\nu} = (\dot{\nu}_d \ \dot{\nu}_q)^T$.

Computing the time derivatives of $\sigma_\Omega^{(2)}$ and $\sigma_{i_{sd}}^{(1)}$, it yields

$$\begin{pmatrix} \sigma_\Omega^{(3)} \\ \sigma_{i_{sd}}^{(2)} \end{pmatrix} = \underbrace{\dot{\widetilde{\Psi}}_\alpha + \dot{\widetilde{\Psi}}_\beta \begin{pmatrix} \nu_d \\ \nu_q \end{pmatrix}}_{\varphi_1} + \underbrace{\widetilde{\Psi}_\beta \begin{pmatrix} \dot{\nu}_d \\ \dot{\nu}_q \end{pmatrix}}_{\varphi_2}, \tag{4.53}$$

thus

$$\left(\sigma_\Omega^{(3)} \quad \sigma_{i_{sd}}^{(2)} \right)^T := \varphi_1 + \varphi_2 \cdot \dot{\nu}. \tag{4.54}$$

Notice that system (4.54) can be represented in the form (4.26) where $F(t, x) = \varphi_1$, $G(t, x) = \varphi_2$ and $u = \dot{\nu}$.

The functions φ_1 and φ_2 must satisfy the following assumptions:

Assumption 4.1 Let be $\mathcal{U}$ the set of bounded inputs, then $\dot{\nu} \in \mathcal{U}$ is a bounded discontinuous vector and system (4.53) with discontinuous right-hand side admits solutions in the Filippov's sense.

Assumption 4.2 The components of the vector φ_1 and matrix φ_2 are bounded uncertain functions. Furthermore, there exist positive constants $C_{0;i}$, $K_{m;i,j}$ and $K_{M;i,j}$, for $i = 1, 2$ and $j = 1, 2$, such that

$$|\varphi_{1,i}| \le C_{0;i}, \quad \forall x \in R^n, \tag{4.55}$$
$$0 \le K_{m;i,j} \le \varphi_{2,ij} \le K_{M;i,j}, \quad \text{for } i = 1, 2; j = 1, 2.$$

Notice that, after straightforward computations, it is possible to determine the values of $C_{0;i}$, $K_{m;i,j}$ and $K_{M;i,j}$, for $i = 1, 2$; and $j = 1, 2$, in terms of the machine parameters. It is clear that they represent the bounds which allow to design the sliding mode controller.

The main advantage of this controller is that the discontinuous function "sign" is acting now on the time derivative of the control input, then attenuates the chattering phenomenon. Regarding the new control $\dot{\nu}$ and the outputs σ_Ω and σ_{i_d}, system (4.53) admits a relative degree vector (3, 2).

Remark 4.4 The bounded functions $\varphi_{1;i}$ and $\varphi_{2;ij}$ for $i = 1, 2$; and $j = 1, 2$; represent the time derivative of the smooth functions describing the uncertainties of the system. Thus, the bounds in $\varphi_{1;i}$ and $\varphi_{2;ij}$ for $i = 1, 2$; and $j = 1, 2$, are easily determined in terms of the operation domain $\mathcal{D}_S$ of the IPMSM as introduced by Definition 3.6. This implies that the terms $\varphi_{1;i}$ and $\varphi_{2;ij}$ are uncertain bounded C^1 functions and thus for a given motor and its operation domain, Assumption 4.2 is easy to verify.

The discontinuous control in (4.54) is determined as follows:

$$\dot{\nu} = \begin{pmatrix} \dot{\nu}_d \\ \dot{\nu}_q \end{pmatrix} = \begin{pmatrix} -\alpha\text{sign}(S_\Omega) \\ -\alpha\text{sign}(S_{i_{sd}}) \end{pmatrix} \tag{4.56}$$

where α is positive control parameter.

This control design can be established by the following lemma:

Lemma 4.1 *Consider the IPMSM model* (1.62)*, the tracking errors* (4.39) *and the associated dynamics given by*

$$\begin{pmatrix} \sigma_\Omega^{(2)} & \sigma_{i_d}^{(1)} \end{pmatrix}^T = \left(\Psi_\alpha^{nom} + \Delta\Psi_\alpha \right) + \left(\Psi_\beta^{nom} + \Delta\Psi_\beta \right) u, \tag{4.57}$$

with the control action

$$u = \begin{pmatrix} u_{sd} \\ u_{sq} \end{pmatrix} = (\Psi_\beta^{nom})^{-1} \left\{ -\begin{pmatrix} \Psi_{\alpha;1}^{nom} \\ \Psi_{\alpha;2}^{nom} \end{pmatrix} + \begin{pmatrix} \nu_d \\ \nu_q \end{pmatrix} \right\} \tag{4.58}$$

and the discontinuous control law

$$\dot{\nu} = \begin{pmatrix} \dot{\nu}_d \\ \dot{\nu}_q \end{pmatrix} = \begin{pmatrix} -\alpha\text{sign}(S_\Omega) \\ -\alpha\text{sign}(S_{i_{sd}}) \end{pmatrix} \tag{4.59}$$

where α is a positive constant. Then, the tracking error converges to zero in finite time, where $t_f = max(t_{\Omega,f}, t_{i_d,f})$ is the desired time of convergence.

Then, it allows the establishment of a sliding mode, i.e.,

$$\dot{S}_\Omega S_\Omega \leq -\eta_\Omega |S_\Omega|, \qquad \dot{S}_{i_d} S_{i_d} \leq -\eta_{i_d} |S_{i_d}|$$

for positive constants η_{i_d} and η_Ω (see [77, 86]). Then, the finite-time convergence of tracking errors is ensured. The details of the proof can be found in [37].

Summary 4.2.3 *IPMSM HOSM Controller*

$$\begin{pmatrix} u_{sd} \\ u_{sq} \end{pmatrix} = (\Psi_\beta^{nom})^{-1} \left\{ - \begin{pmatrix} \Psi_{\alpha;1}^{nom} \\ \Psi_{\alpha;2}^{nom} \end{pmatrix} + \begin{pmatrix} \nu_d \\ \nu_q \end{pmatrix} \right\}$$

where

$$\Psi_{\alpha;1}^{nom} = +k_1 i_{sq}(k_4 i_{sd} + k_5 \Omega i_{sq}) + k_3[(k_1 i_{sd} + k_2)i_{sq} + k_3 \Omega]$$
$$- \Omega^{*2} + (k_1 i_{sd} + k_2)(k_7 \Omega + k_8 \Omega i_{sd} + k_9 i_{sq})$$
$$\Psi_{\alpha;2}^{nom} = k_4 i_{sd} + k_5 \Omega i_{sq} - 2k_{11} i_q,$$

$$(\Psi_\beta^{nom})^{-1} = \begin{pmatrix} 0 & \dfrac{1}{k_6} \\ \dfrac{1}{(k_1 i_{sd} + k_2)k_{10}} & -\dfrac{k_1 i_{sq}}{(k_1 i_{sd} + k_2)k_{10}} \end{pmatrix}$$

and

$$\begin{pmatrix} \dot{\nu}_d \\ \dot{\nu}_q \end{pmatrix} = \begin{pmatrix} -\alpha \mathrm{sign}(S_\Omega) \\ -\alpha \mathrm{sign}(S_{i_{sd}}) \end{pmatrix}.$$

4.3 Conclusions

In this chapter, two approaches have been presented to design robust controllers for the SPMSM and the IPMSM. These approaches are based on integral backstepping and high-order sliding mode techniques. Both control designs are robust with respect to perturbation and parameters uncertainties. Furthermore, a design procedure is given and control gains can be easily tuned.

For the sensorless purpose, these controllers in conjunction with the observers designed in Chap. 3, will be implemented, and an analysis of the closed-loop system stability will be presented in Chap. 6.

4.4 Bibliographical Notes

The principles of modern AC machines control can be found in the classical books [17, 60], where the field-oriented control algorithm appears as a seminal control strategy [7]. Nevertheless the sensorless control is a very difficult problem that requires robustness properties because the mechanical variables are not available by measurement. If the observability property is satisfied (see Chap. 2) some unmeasured variables can be reconstructed (observed) as the position, the speed, the rotor resistance, and the load torque. The basic control designs use these observers associated with linear controllers: field-oriented control with PI regulator [25, 78], or state feedback control [96].

Owing to the difficulty to precisely reconstruct these variables and the bad knowledge on some parameters, the robustness of the controllers is a required property. Thus, new robust nonlinear controllers can be employed, thanks to their intrinsic properties. That is why, backstepping control [48] and high-order sliding mode Control [18] were designed for sensorless control.

In this chapter, robust nonlinear controls are presented and applied to the permanent magnet synchronous motor, without using any mechanical sensors.

The synchronous motors can be controlled with efficiency if the control strategies are judiciously chosen. The maximum torque per ampere (MTPA) control strategy provides a maximum torque/current ratio [90], and will be used to characterize the current references.

First, among techniques of the robust nonlinear control design, the backstepping technique has been introduced as a systematic and recursive design methodology for nonlinear feedback control (see [53]). This approach has been improved to reject some classes of disturbances and applied for the SPMSM control in [21][1] and for the IPMSM in [38][2]. Regarding the controllers designed using sliding mode techniques, the quasi-continuous high-order sliding mode controller has been presented (see [61]) as well as the high-order sliding mode controller that allows the establishment of a sliding mode with a fixed *a priori* finite-time convergence of the tracking errors [77, 86]. These HOSM techniques are applied to the control design of the SPMSM in [20][3] and in [37][4] for the IPMSM.

Appendix: A HOSM algorithm

Now, the synthesis of a HOSM control is recalled. The advantage of this methodology [74] is such that the time of convergence t_f is stated *a priori* and the robustness is ensured during the entire response of the system.

The synthesis of the high-order sliding mode controller is designed in two steps:

(1) A linear continuous finite-time convergent control law is used in order to *induce reference trajectories* for system (4.60), which defines the sliding manifold on which the system evolves as early as $t = 0$.

---

[1] This chapter includes excerpts of [21], originally published in the proceedings of IFAC World Congress, Milano, Italy, IFAC-PapersOnLine IFAC 2011.

[2] This chapter includes excerpts reprinted from "Journal of the Franklin Institute, 349(5):1734–1757, Hamida M, Glumineau A, De Leon J (2012) Robust integral backstepping control for sensorless IPM synchronous motor controller." Copyright (2012), with permission from Elsevier.

[3] This chapter includes excerpts of [20], Copyright (2010) IEEE. Reprinted, with permission, from "Ezzat M, De Leon J, Gonzalez N, Glumineau A, Observer-controller scheme using high-order sliding mode techniques for sensorless speed control of permanent magnet synchronous motor. In: Decision and Control (CDC), 49th IEEE Conference on Decision Control, Atlanta, USA".

[4] This chapter includes excerpts of [37], originally published in the proceedings of IFAC Power Plant and Power System Control conference (PPPSC), Toulouse, France, IFAC-PapersOnLine IFAC 2012.

(2) A discontinuous control law is designed in order to maintain the system trajectories on the sliding manifold which ensures the establishment a rth order sliding mode.

Consider an uncertain nonlinear system of the form

$$\dot{x} = f(x) + g(x)u \tag{4.60}$$

with $x \in \mathcal{X} \subset \Re^n$ the state variable and $u \in \Re$ the input control. For a sake of clarity, only single input–single output case is considered in the sequel.

Let $\sigma_c(x, t)$ the sliding variable with a relative degree equal to r.

Assumption 4.3 The relative degree r of (4.60) with respect to σ_c is assumed to be constant and known, and the associated zero dynamics are stable.

The control objective is to fulfill the constraint $\sigma_c(x, t) = 0$ in finite time and to keep it exactly by some feedback.

The rth order sliding mode control approach allows the finite-time stabilization to zero of the sliding variable σ_c and its $r - 1$ first time derivatives by defining a suitable discontinuous control function. Then, the output σ_c satisfies equation

$$\sigma_c^{(r)} = \varphi_1(x, t) + \varphi_2(x)u \tag{4.61}$$

with $\varphi_2(x) = L_g L_f^{r-1} \sigma_c$ and $\varphi_1(x) = L_f^r \sigma_c$. System (4.60) has to satisfy:

Assumption 4.4 The solutions are understood in the Filippov sense [23], and system trajectories are supposed to be infinitely extendible in time for any bounded Lebesgue measurable input.

Assumption 4.5 Functions $\varphi_1(x, t)$ and $\varphi_2(x)$ are bounded uncertain functions, and, without loss of generality, let also the sign of $\varphi_2(x)$ be strictly positive. Thus, there exist positive constants $K_m > 0$, $K_M > 0$, and $C_0 \geq 0$ such that $0 < K_m < \varphi_2(x) < K_M$ and $|\varphi_1(x, t)| \leq C_0$ for $x \in \mathcal{X} \subset \Re^n$, $\mathcal{X}$ being a bounded open subset of $\Re^n$ within which the boundedness of the system dynamics is ensured, and $t > 0$.

Then, the rth order sliding mode control of (4.60) with respect to the sliding variable σ_c is equivalent to the finite-time stabilization of

$$\dot{Z}_{c1} = A_{11} Z_{c1} + A_{12} Z_{c2}, \quad \dot{Z}_{c2} = \varphi_1 + \varphi_2 u \tag{4.62}$$

with $Z_{c1} := [\sigma_c \ \dot{\sigma}_c \ \cdots \ \sigma_c^{(r-2)}]^T$ and $Z_{c2} = \sigma_c^{(r-1)}$. $A_{11(r-1)\times(r-1)}$ and $A_{12(r-1)\times 1}$ are such that Z_{c1} dynamics reads as linear Brunovsky form.

Controller synthesis

The synthesis of a high-order sliding mode controller for (4.60) consists of two steps.

- Design of the sliding manifold on which the system evolves as early as $t = 0$.
- Design of the discontinuous control law u in order to maintain the system trajectories on the sliding manifold.

Step 1: Switching variable design

Let S denote the switching variable defined as

$$S = \sigma_c^{(r-1)} - \mathcal{F}^{(r-1)}(t) + \lambda_{r-2}\left[\sigma_c^{(r-2)} - \mathcal{F}^{(r-2)}(t)\right] \tag{4.63}$$
$$+ \cdots + \lambda_0\left[\sigma_c(x,t) - \mathcal{F}(t)\right],$$

with $\lambda_{r-2}, \ldots, \lambda_0$ defined such that $P(z) = z^{(r-1)} + \lambda_{r-2}z^{(r-2)} + \cdots + \lambda_0$ is a Hurwitz polynomial in the complex variable z. The function $\mathcal{F}(t)$ is a C^r– one defined such that $S(t = 0) = 0$ and $\sigma_c^{(k)}(x(t_f), t_f) - \mathcal{F}^{(k)}(t_f) = 0$ $(0 \leq k \leq r-1)$. Then, from initial and final conditions the problem consists in finding the function $\mathcal{F}(t)$ such that

$$\sigma_{c,t=0} = \mathcal{F}(0), \sigma_{c,t=t_f} = \mathcal{F}(t_f) = 0, \dot{\sigma}_{c,t=0} = \dot{\mathcal{F}}(0),$$

$$\dot{\sigma}_{c,t=t_f} = \dot{\mathcal{F}}(t_f) = 0, \ldots, \sigma_{c,t=0}^{(r-1)} = \mathcal{F}^{(r-1)}(0),$$

$$\sigma_{c,t=t_f}^{(r-1)} = \mathcal{F}^{(r-1)}(t_f) = 0.$$

A solution for $\mathcal{F}(t)$ for $(1 \leq j \leq r)$ [77], is given by

$$\mathcal{F}(t) = K_c T e^{Ft} \sigma_c^{(r-j)}(0) \tag{4.64}$$

with F being a $2r \times 2r$-dimensional stable matrix (strictly negative eigenvalues), T being a $2r \times 1$-dimensional vector, and K_c is a $1 \times 2r$-dimensional gain matrix such system (4.64) is fulfilled.

Assumption 4.6 There exists an integer j such that $\sigma_c^{(r-j)}(0) \neq 0$ and bounded.

Now, we have the following lemma:

Lemma 4.2 *From Assumption* 4.6 *and assuming that* $t_f > 0$ *is bounded, there exists a Hurwitz matrix* $F_{2r \times 2r}$ *and a matrix* $T_{2r \times 1}$ *such that matrix* $\mathcal{K}$ *defined as*

$$\mathcal{K} = \left[F^{r-1}T\sigma_c^{(r-j)}(0) \quad F^{r-1}e^{Ft_f}T \quad F^{r-2}T\sigma_c^{(r-j)}(0)\right.$$
$$\left. F^{r-2}e^{Ft_f}T \quad \cdots \quad T\sigma_c^{(r-j)}(0) \quad e^{Ft_f}T\right] \tag{4.65}$$

is invertible.

Then, the gain matrix K_c is given by

$$K_c = \left[\sigma_c^{(r-1)}(0) \, 0 \, \sigma_c^{(r-2)}(0) \, 0 \, \cdots \, \sigma_c(0) \, 0\right]\mathcal{K}^{-1}. \tag{4.66}$$

Furthermore, the switching variable S is expressed as

$$
\begin{aligned}
S = \ & \sigma_c^{(r-1)} - K_c T F^{(r-1)} e^{Ft} \sigma_c^{(r-j)}(0) \\
& + \lambda_{r-2} \left[\sigma_c^{(r-2)} - K_c T F^{(r-2)} e^{Ft} \sigma_c^{(r-j)}(0) \right] \\
& + \cdots + \lambda_0 \left[\sigma_c(x,t) - K_c T e^{Ft} \sigma_c^{(r-j)}(0) \right].
\end{aligned}
\tag{4.67}
$$

Assumption 4.7 There exists a finite positive constant $\Theta > 0$ such that

$$
\begin{aligned}
|K_c T F^r e^{Ft} \sigma_c^{(r-j)}(0) & - \lambda_{r-2}[\sigma_c^{(r-1)} - K_c T F^{r-1} e^{Ft} \sigma_c^{(r-j)}(0)] \\
& - \cdots - \lambda_0[\dot{\sigma}_c(x,t) - K_c T F e^{Ft} \sigma_c^{(r-j)}(0)]| < \Theta
\end{aligned}
\tag{4.68}
$$

Equation $S = 0$ describes the desired dynamics which satisfy the finite time stabilization of $[\sigma_c^{(r-1)} \sigma_c^{(r-2)} \cdots \sigma_c]^T$ to zero. The *switching manifold* on which system (4.62) is forced to slide, via a discontinuous control υ, is defined as

$$
\mathcal{S} = \{x | S = 0\}.
\tag{4.69}
$$

Given Eq. (4.66), one gets $S(t=0) = 0$, at the initial time, the system still evolves on the switching manifold which implies that there is no reaching phase.

Step 2: Discontinuous control design

The attention is now focused on the design of the discontinuous control law u which forces the system trajectories of (4.62) to slide on $\mathcal{S}$ in order to reach the origin in finite time and so to maintain the system at the origin.

Theorem 4.2 ([77]) *Consider system* (4.60) *of relative degree r with respect to* $\sigma_c(x,t)$. *Assume that system* (4.60) *is minimum phase with respect to* $\sigma_c(x,t)$ *and that Assumptions* 4.3, 4.4, 4.5 *and* 4.6 *are fulfilled. Let r be the sliding mode order and t_f $(0 < t_f < \infty)$ the desired convergence time. Let $S \in \Re^n$ define by* (4.67) *with K_c being the single solution* (4.66) *and suppose that Assumption* 4.7 *is fulfilled. Then, the control input u defined by*

$$
u = -\alpha_c \text{sign}(S)
$$

with

$$
\alpha_c \geq \frac{C_0 + \Theta + \eta}{K_m},
\tag{4.70}
$$

C_0, K_m *defined in Assumption* 4.5, Θ *defined by* (4.68), *leads to the establishment of a rth order sliding mode with respect to σ_c, and the time of convergence fixed a priori is t_f.*

Proof See [77].

Condition (4.70) allows to satisfy the attractivity condition

$$\dot{S} S \leq -\eta |S|$$

with $\eta > 0$. By using the same procedure established in Theorem 4.2, there exist gains α_c such that for the Lyapunov function

$$W = \frac{1}{2} S^T S$$

whose time derivative satisfy the inequality

$$\dot{W} = \dot{S} S \leq -\eta |S| \leq -\eta \sqrt{W}. \tag{4.71}$$

Integrating the above inequality, we have

$$\sqrt{W(t)} \leq \sqrt{W(t_0)} - \frac{\eta}{2} t. \tag{4.72}$$

Let $\sqrt{W(t_0)} - \frac{\eta}{2} t_f = 0$, then the time of convergence is given by

$$t_f = \frac{2\sqrt{W(t_0)}}{\eta}. \tag{4.73}$$

Then, the convergence in finite time of the tracking dynamics is guarantee.

Chapter 5
Robust Induction Motor Controls Design (IM)

Abstract In this chapter, three control strategies for the induction motor (IM) are studied, thanks to their robustness properties, their implementation simplicity, and their time computation cost. To compare the performance of the control strategies, specific trajectories have been defined by a so-called control benchmark (see Sect. 1.6 in Chap. 1). For the control design, it is assumed that all the variables are measurable and all parameters are known (or known except bounded uncertainties). Firstly, a classical field-oriented control [7] is introduced. Next, a robust backstepping controller is designed. However, the robustness of the classical backstepping controller is improved, thanks to integral terms that are added at each step of the iterative procedure. Finally, another robust control design for the IM is introduced, based on sliding mode control techniques. For the classical sliding mode control design, the chattering effect phenomenon is a drawback that involves a limited implementation of such a controller. Thus, to reduce the effects of this phenomenon, a high-order sliding mode controller (HOSM) is designed to track the desired rotor speed and the modulus flux references.

5.1 Field-Oriented Control

It is well known that there are several algorithms to guarantee the asymptotic tracking of a reference for the induction motor control. These algorithms must work under different operating conditions and in uncertain parameter context. Regarding the parameters of the induction machine, the rotor resistance and the load torque are usually unknown and time varying. Strategies have been introduced to improve the performance of the machine under uncertainties. One of these strategies is based on adaptive techniques to online identify some parameters. Another strategy is the passivity control design which has been proposed for the induction machine control and will be used in this chapter.

On the other hand, regarding classical control strategies, the direct field-oriented controller (FOC) and the indirect field oriented controller are the most implemented in practice.

The field-oriented control (FOC) was introduced in [7], where the three-phase AC induction motor is controlled under all operating conditions similarly to a separately excited DC motor. The three-phase sinusoidal system is first projected using the three-to-two phase Clarke transformation, i.e., from a fixed (a, b, c) frame to a fixed (α, β) frame. Thanks to the two-to-two phase (α, β)-to-(d, q) rotating Park transformation, the original sinusoidal system can be defined in a rotating (d, q) coordinate system frame (see details in Sect. 1.2 of Chap. 1). Consequently, it can be obtained that the field flux linkage component of current is aligned along the d-axis and the torque component of current is aligned along the q-axis. The AC motor behaves like a DC motor in which the field flux linkage and the armature flux linkage created by the respective field and armature currents are orthogonal such that when the torque is controlled, the field flux linkage is not affected. By using the IM model in the (d, q) frame (1.108), the FOC strategy is presented.

5.1.1 Speed and Flux References

Now, we introduce the direct field-oriented control (DFOC), which is a basis of the IM control. Furthermore, for the control design, it will be assumed that all state variables are measurable. This assumption is introduced only to illustrate the potential performance of the developed control algorithms. In the subsequent chapters, this assumption will be no longer necessary due to the implementation of an observer (soft sensor). The observer–controller schemes will be studied in Chap. 7.

First, denoting Ω^* and ϕ^* as the smooth-bounded reference signals for the output variables the rotor speed Ω and the rotor flux modulus $\sqrt{\phi_{rd}^2 + \phi_{rq}^2}$, respectively.

Following the strategy of the field-oriented control [7], and using the IM model in the rotating (d, q) frame oriented according to the rotor flux (see (1.115)), the flux control goal is to force ϕ_{rq} toward zero. Then, the electromagnetic torque is proportional to the product of two state variables: the d-component of the rotor flux ϕ_{rd} and the q-component of the stator current i_{sq}

$$T_e = \frac{pM_{sr}}{L_r}\phi_{rd}i_{sq}. \tag{5.1}$$

From (5.1), it is clear that by holding constant the magnitude of the rotor flux ϕ_{rd}, it follows that there is a linear relationship between the q-axis component of the stator current i_{sq} and the electromagnetic torque.

Notice that i_{sd}^* and i_{sq}^* are the references for the (d, q)-components of the stator current. Next, the voltage controls (v_{sd}, v_{sq}) can be defined by using PI current controllers

$$v_{sd} = K_{Ivd}\int_0^t (i_{sd}^* - i_{sd})dt + K_{Pvd}(i_{sd}^* - i_{sd}) \tag{5.2}$$

$$v_{sq} = K_{Ivq}\int_0^t (i_{sq}^* - i_{sq})dt + K_{Pvq}(i_{sq}^* - i_{sq}) \tag{5.3}$$

where $K_{Ivd}, K_{Pvd}, K_{Ivq}, K_{Pvq}$ are positive constants to be tuned. These control loops have to be tuned so fast to force i_{sd} and i_{sq} to quickly track their references i_{sd}^* and i_{sq}^*, respectively. Then, the PI current loops result in fast responses.

The resulting IM system in closed loop with the control actions (5.2) and (5.3) is given by

$$\begin{pmatrix} \dot{\Omega} \\ \dot{\phi}_{rd} \end{pmatrix} = \begin{pmatrix} m\phi_{rd}i_{sq}^* - c\Omega - \frac{T_l}{J} \\ -a\phi_{rd} + aM_{sr}i_{sd}^* \end{pmatrix} \qquad (5.4)$$

where the references i_{sd}^* and i_{sq}^* are considered as *new inputs* for system (5.4).

For system (5.4), a decoupling multivariable controller can be designed as follows:

$$i_{sq}^* = \frac{1}{m\phi_{rd}} \left(K_{P\Omega}(\Omega^* - \Omega) + \dot{\Omega}^* + c\Omega + \frac{T_l}{J} \right), \qquad (5.5)$$

$$i_{sd}^* = \frac{1}{aM_{sr}}\dot{\phi}^* + \frac{1}{M_{sr}}\phi^*$$

where Ω^* and ϕ^* are the reference signals.

As introduced previously, at this step, it is assumed that the load torque T_l and all the parameters of the machine are known. This hypothesis will be released by using observers in Chap. 7, where the load torque is estimated by an observer.

Furthermore, in order to avoid singularities in controller (5.5), the initial condition $\phi_{rd}(0)$ must be greater than zero, such that the d-axis component of the rotor flux $\phi_{rd}(t)$ be different to zero (for example, $\phi_{rd} > 0$, for all $t > 0$). This is trivially a physical constraint as it can be easily seen in (5.1).

It is worth mentioning that, in case of parameter uncertainties, the robustness of this decoupling multivariable feedback controller (5.5) has an unsatisfactory performance. Controller (5.5) achieves the control objective at the exception of a singularity at $\phi_{rd} = 0$, which may imply very large currents, when ϕ_{rd} tends to zero. A classical strategy to avoid this difficulty is to modify the direct field-oriented control by replacing ϕ_{rd} by its reference ϕ^*, so that the resulting control becomes

$$i_{sq}^* = \frac{1}{m\phi^*} \left(K_{P\Omega}(\Omega^* - \Omega) + \dot{\Omega}^* + c\Omega + \frac{T_l}{J} \right), \qquad (5.6)$$

$$i_{sd}^* = \frac{1}{aM_{sr}}\dot{\phi}^* + \frac{1}{M_{sr}}\phi^*.$$

This controller is well known as the *indirect field-oriented controller*. Finally, the indirect field-oriented controller can be summarized as follows:

- Let $(\Omega^*, \phi^*, 0)$ be the reference signals of $(\Omega, \phi_{rd}, \phi_{rq})$.
- Design a controller so that the tracking errors $(\tilde{\Omega}, \tilde{\phi}_{rd}, \tilde{\phi}_{rq})$ tend exponentially to zero from any initial condition, assuming the measurement of the rotor speed, the load torque T_l, and the rotor resistance R_s and all parameters of the induction machine are available.

The advantages and the limitations of each controller depend on the requirements to implement them, the operation conditions as well as the speed–torque range of operation. For instance, the direct FOC requires the rotor speed and the rotor flux d-axis component knowledge. On the contrary, the indirect FOC only requires the rotor speed measurement. However, in both controllers it is necessary to know or to estimate the load torque T_l and if possible all the bad known parameters of the machine. For example, the stator resistance R_s is time varying with respect to the temperature variation.

5.1.2 Flux Controller Design

Taking into account the requirements of the FOC strategy, which can be modified to improve its performance, a PI controller is introduced in the controller design (5.5). Then, following the FOC strategy for the induction motor, the reference of the stator current d-component i_{sd} is designed using a PI controller

$$
\begin{aligned}
i_{sd}^* = K_{I\phi_{rd}} \int_0^t (\phi^* - \phi_{rd})d\tau + K_{P\phi_{rd}}(\phi^* - \phi_{rd}) \\
+ \frac{1}{aM_{sr}}\dot{\phi}^* + \frac{1}{M_{sr}}\phi^*
\end{aligned}
\tag{5.7}
$$

where $K_{I\phi_{rd}}$ and $K_{P\phi_{rd}}$ are positive constants to tune. Defining the rotor flux d-component tracking error as $e_\phi = \phi^* - \phi_{rd}$, and replacing reference current i_{sd}^* given by (5.7) in (5.4), then, the dynamics of the rotor flux d-component tracking error e_ϕ is given by

$$
\dot{e}_\phi = (-a - aM_{sr}K_{P\phi_{rd}})e_\phi - aM_{sr}K_{I\phi_{rd}} \int_0^t e_\phi(\tau)d\tau.
\tag{5.8}
$$

By choosing the following change of coordinates

$$
\chi_\phi = T_\phi(e_\phi) = \left(\int_0^t e_\phi(\tau)d\tau, e_\phi\right)^T
\tag{5.9}
$$

equation (5.8) can be written, in a state-space representation, as follows:

$$
\dot{\chi}_\phi = \bar{A}_\phi \chi_\phi
\tag{5.10}
$$

where $\bar{A}_\phi = \begin{pmatrix} 0 & 1 \\ \alpha_{1\phi} & \alpha_{2\phi} \end{pmatrix}$, $\alpha_{1\phi} = -aM_{sr}K_{I\phi_{rd}}$ and $\alpha_{2\phi} = -a - M_{sr}K_{P\phi_{rd}}$.

Note that the tuning parameters $K_{I\phi_{rd}}$ and $K_{P\phi_{rd}}$ are positive to force the matrix $\bar{A}_\phi$ to be stable.

5.1.3 Speed Control Design

If the flux controller forces the d-component of flux ϕ_{rd} to track its reference ϕ^* and assuming the flux is properly established in the motor, the electromagnetic torque (5.1) can be expressed as

$$T_e = K_T i_{sq} \tag{5.11}$$

where $K_T = (p M_{sr}/L_r)\phi^*$. Thus, as planned by the FOC strategy, there is a linear relationship between the stator current q-component i_{sq} and the IM torque.

Now, the reference current i_{sq}^* is designed for dealing with the speed control problem, and forcing the rotor speed Ω to track the desired reference Ω^*. To achieve this objective, the reference current i_{sq}^* is designed as follows:

$$
i_{sq}^*(t) = \frac{1}{K_T}\left(K_{I\Omega}\int_0^t (\Omega^*(\tau) - \Omega(\tau))d\tau + K_{P\Omega}(\Omega^* - \Omega) \right)
$$
$$
+ \frac{1}{m\phi_{rd}}\left(\dot{\Omega}^* + c\Omega + \frac{\hat{T}_l}{J} \right) \tag{5.12}
$$

where $e_\Omega(t) := \Omega - \Omega^*$ is the speed tracking error and $\hat{T}_l$ is the estimation of the load torque, (see Chap. 3). The term $[K_{I\Omega}\int_0^t (\Omega^*(\tau) - \Omega(\tau))d\tau + K_{P\Omega}(\Omega^* - \Omega)]$ is equivalent to a PI controller.

If the load torque is not available, the PI controller has to reject this disturbance. Replacing (5.12) in (5.4), then the dynamics of the speed tracking error e_Ω is given by

$$\dot{e}_\Omega = -\frac{K_{P\Omega}}{J}e_\Omega - \frac{K_{I\Omega}}{J}\int_0^t e_\Omega(\tau)d\tau. \tag{5.13}$$

Consider the following change of coordinates

$$\chi_\Omega = T_\Omega(e_\Omega) = \left(\int_0^t e_\Omega(\tau)d\tau, e_\Omega \right)^T. \tag{5.14}$$

It follows that (5.13) can be written, in a state-space representation, as follows:

$$\dot{\chi}_\Omega = \bar{A}_\Omega \chi_\Omega \tag{5.15}$$

where $\bar{A}_\Omega = \begin{pmatrix} 0 & 1 \\ \alpha_{1\Omega} & \alpha_{2\Omega} \end{pmatrix}$, with $\alpha_{1\Omega} = -\dfrac{K_{I\Omega}}{J}$ and $\alpha_{2\phi} = -\dfrac{K_{P\Omega}}{J}$.

Remark 5.1 For simulation and experimental tests, the proportional-integral (PI) controller, which has been widely used for the speed control, can be replaced by an integral-proportional (IP) controller to limit transient phenomena. This is an important industrial requirement if the reference is a step signal.

Proposition 5.1 *Consider the reduced induction motor model* (5.4) *under the action of the flux controller* (5.7) *and the speed controller* (5.12). *The rotor speed tracking error and the flux tracking error converge to zero exponentially as t tends to ∞.*

Proof Let us consider the following candidate Lyapunov function

$$V_c = \chi_\phi^T P_\phi \chi_\phi + \chi_\Omega^T P_\Omega \chi_\Omega. \tag{5.16}$$

where $P_\phi^T = P_\phi > 0$ and $P_\Omega^T = P_\Omega > 0$, are definite positive, respectively, solutions of

$$P_\phi \bar{A}_\phi + \bar{A}_\phi^T P_\phi = -Q_\phi \text{ and } P_\Omega \bar{A}_\Omega + \bar{A}_\Omega^T P_\Omega = -Q_\Omega.$$

with Q_Ω and Q_ϕ suitable positive definite matrices. The time derivative of (5.16) along with (5.10) and (5.15), yields

$$\begin{aligned}
\dot{V}_c &= \chi_\phi^T (P_\phi \bar{A}_\phi + \bar{A}_\phi^T P_\phi) \chi_\phi + \chi_\Omega^T (P_\Omega \bar{A}_\Omega + \bar{A}_\Omega^T P_\Omega) \chi_\Omega \\
&= -\chi_\phi^T Q_\phi \chi_\phi - \chi_\Omega^T Q_\Omega \chi_\Omega.
\end{aligned}$$

This implies

$$\dot{V}_c \le -\eta_\phi \chi_\phi^T P_\phi \chi_\phi - \eta_\Omega \chi_\Omega^T P_\Omega \chi_\Omega$$

where $\eta_\phi = \dfrac{\lambda_{min} Q_\phi}{\lambda_{max} P_\phi}, \eta_\Omega = \dfrac{\lambda_{min} Q_\Omega}{\lambda_{max} P_\Omega}$. Choosing $\delta_c = min(\eta_\phi, \eta_\Omega)$, then

$$\dot{V}_c \le -\delta_c V_c.$$

This shows that the tracking error exponentially converges to zero.

Remark 5.2 Our controller is a classical high-gain PI controller with additional terms (see (5.7) and (5.12)) to improve the tracking performance. Its purpose is to guarantee the boundedness of the state. The assumption that the IM state is bounded is not required for the closed-loop system.

Summary 5.1 field-oriented control

$$v_{sd} = K_{Ivd} \int_0^t (i_{sd}^* - i_{sd}) dt + K_{Pvd}(i_{sd}^* - i_{sd})$$

$$v_{sq} = K_{Ivq} \int_0^t (i_{sq}^* - i_{sq}) dt + K_{Pvq}(i_{sq}^* - i_{sq})$$

where

$$i_{sd}^* = K_{I\phi rd} \int_0^t (\phi^* - \phi_{rd})(\tau)d\tau + K_{P\phi rd}(\phi^* - \phi_{rd})$$

$$+ \frac{1}{aM_{sr}}\dot{\phi}^* + \frac{1}{M_{sr}}\phi^*$$

$$i_{sq}^* = \frac{1}{K_T}\left[K_{I\Omega}\int_0^t (\Omega^* - \Omega)(\tau)d\tau + K_{P\Omega}(\Omega^* - \Omega)\right]$$

$$+ \frac{1}{m\phi_{rd}}\left[\dot{\Omega}^* + c\Omega + \frac{\hat{T}_l}{J}\right],$$

with

   Ω^* *and* ϕ^* *the speed and flux references,* $a = R_r/L_r$, $c = f_v/J$

and

   $K_{Ivd}, K_{Pvd}, K_{I\phi rd}, K_{P\phi rd}, K_{I\Omega}, K_{P\Omega}$ *are the parameters to tune with respect to the time constants of the motor.*

5.2 Integral Backstepping Control and Field-Oriented Control

The aim of this section is to design a control law combining the advantages of the field-oriented controller strategy with the robustness properties of the backstepping control, in order to track the desired reference (see the benchmark references defined in Chap. 1, Sect. 1.6).

   The proposed controller is designed to regulate the rotor speed and the flux by using the backstepping technique. This synthesis is carried out in two steps:

- First step: Speed and flux loops design
- Second step: Currents loops design.

   It is well known that the control performance of the induction motor is still affected by the uncertainties such as mechanical parameter uncertainties, external load disturbance, nonideal field orientation in a transient state and unmodeled dynamics. The speed/flux controllers and the current controllers are designed using an improved backstepping strategy, which increases the robustness of the field-oriented control for high-performance applications. In particular, in the sequel, the robustness of the control law is increased with respect to the load disturbance by designing a new integral backstepping algorithm.

5.2.1 Speed and Flux Loops

Let us consider the reduced model of the induction motor given by

$$\begin{bmatrix} \dot{\Omega} \\ \dot{\phi}_{rd} \end{bmatrix} = \begin{bmatrix} m\phi_{rd}i_{sq} - c\Omega - \frac{T_l}{J} \\ -a\phi_{rd} + aM_{sr}i_{sd} \end{bmatrix}. \tag{5.17}$$

This model is obtained using current controllers (defined later) and tuned to force the stator currents i_{sd} and i_{sq} to quickly track their corresponding references i_{sd}^* and i_{sq}^*. Consequently, references i_{sd}^* and i_{sq}^* can be considered as the *new inputs* of the reduced model (5.17).

To solve the speed and flux tracking problems, define the tracking errors as

$$z_\Omega = \Omega^* - \Omega + K_\Omega' \int_0^t (\Omega^* - \Omega)dt$$

$$z_\phi = \phi^* - \phi_{rd} + K_\phi' \int_0^t (\phi^* - \phi_{rd})dt.$$

Next, replacing the stator currents i_{sq} and i_{sd} by their respective desired references i_{sq}^* and i_{sd}^* in (5.17), it follows that the dynamics of z_Ω and z_ϕ are

$$\begin{cases} \dot{z}_\Omega = \dot{\Omega}^* - m\phi_{rd}i_{sq}^* + c\Omega + \dfrac{T_l}{J} + K_\Omega'(\Omega^* - \Omega) \\[2mm] \dot{z}_\phi = \dot{\phi}^* + a\phi_{rd} - aM_{sr}i_{sd}^* + K_\phi'(\phi^* - \phi_{rd}). \end{cases} \tag{5.18}$$

Choosing the virtual control inputs i_{sq}^* and i_{sd}^* in (5.18) as follows:

$$\begin{cases} i_{sq}^* = \dfrac{1}{m\phi_{rd}}\left[\dot{\Omega}^* + c\Omega + K_\Omega z_\Omega + K_\Omega'(\Omega^* - \Omega) + \dfrac{T_l}{J}\right] \\[4mm] i_{sd}^* = \dfrac{1}{aM_{sr}}\left[\dot{\phi}^* + a\phi_{rd} + K_\phi z_\phi + K_\phi'(\phi^* - \phi_{rd})\right] \end{cases} \tag{5.19}$$

where K_Ω, K_Ω', K_ϕ, K_ϕ' are positive parameters to be tuned, so (5.18) in closed loop with the control actions (5.19) becomes

$$\dot{z}_\Omega = -K_\Omega z_\Omega \quad \text{and} \quad \dot{z}_\phi = -K_\phi z_\phi$$

It is easy to see that using the following candidate Lyapunov functions

$$V_{z\Omega} = \frac{1}{2}z_\Omega^2, \quad \text{and} \quad V_{z\phi} = \frac{1}{2}z_\phi^2,$$

their time derivatives along the trajectories of (5.18) are

$$\dot{V}_{z\Omega} = -K_\Omega z_\Omega^2, \quad \text{and} \quad \dot{V}_{z\phi} = -K_\phi z_\phi^2$$

which implies the exponential convergence to zero of the tracking errors with, respectively, arbitrary time constants K_Ω^{-1} and K_ϕ^{-1}.

5.2.2 Current Loops

Now, we show how to design a controller such that the stator currents, the rotor speed, and the d-axis component of the rotor flux converge to the desired references.

Since in the first step, we have designed the virtual inputs (i_{sq}^* and i_{sd}^*) to stabilize the reduced model, now we shall design the control laws for the complete model.

We start the control design by introducing the following change of variable

$$
\begin{aligned}
z_{iq} &= i_{sq}^* - i_{sq} + z_{iq}' \\
z_{id} &= i_{sd}^* - i_{sd} + z_{id}' \\
z_{iq}' &= K_{iq}'' \int_0^t (i_{sq}^* - i_{sq}) dt \\
z_{id}' &= K_{id}'' \int_0^t (i_{sd}^* - i_{sd}) dt
\end{aligned}
\tag{5.20}
$$

where K_{iq}'' and K_{id}'' are tuning positive constants.

Consider the following candidate Lyapunov functions

$$
\begin{cases}
V_{z_{iq}} = V_{z\Omega} + \dfrac{1}{2} z_{iq}^2 + \dfrac{1}{2} z_{iq}'^2 \\[2mm]
V_{z_{id}} = V_{z\phi} + \dfrac{1}{2} z_{id}^2 + \dfrac{1}{2} z_{id}'^2.
\end{cases}
\tag{5.21}
$$

Taking the time derivative along the trajectories of (5.18) and replacing the currents (i_{sq}, i_{sd}), it follows that

$$
\begin{cases}
\dot{V}_{z\Omega} = z_\Omega \left[\dot{\Omega}^* - m\phi_{rd} i_{sq} + c\Omega + \dfrac{T_l}{J} + K_\Omega'(\Omega^* - \Omega) \right] \\[3mm]
\dot{V}_{z\phi} = z_\phi \left[\dot{\phi}^* + a\phi_{rd} - aM_{sr} i_{sd} + K_\phi'(\phi^* - \phi_{rd}) \right].
\end{cases}
\tag{5.22}
$$

Since $i_{sq} = -z_{iq} + z'_{iq} + i^*_{sq}$ and $i_{sd} = -z_{id} + z'_{id} + i^*_{sd}$, then (5.22) becomes

$$
\begin{cases}
\dot{V}_{z\Omega} = z_\Omega \left(\dot{\Omega}^* + m\phi_{rd}z_{iq} - m\phi_{rd}z'_{iq} - m\phi_{rd}i^*_{sq} \right) \\
\quad\quad + z_\Omega \left(c\Omega + \frac{T_l}{J} + K'_\Omega(\Omega^* - \Omega) \right) \\
\dot{V}_{z\phi} = z_\phi \left(\dot{\phi}^* + a\phi_{rd} + aM_{sr}z_{id} - aM_{sr}z'_{id} \right) \\
\quad\quad - z_\phi \left(aM_{sr}i^*_{sd} + K'_\phi(\phi^* - \phi_{rd}) \right).
\end{cases}
\tag{5.23}
$$

Substituting equation (5.19) into (5.23), it follows that

$$
\begin{cases}
\dot{V}_{z\Omega} = -K_\Omega z_\Omega^2 + m\phi_{rd}z_\Omega z_{iq} - m\phi_{rd}z'_{iq}z_\Omega \\
\dot{V}_{z\phi} = -K_\phi z_\phi^2 + aM_{sr}z_\phi z_{id} - aM_{sr}z'_{id}z_\phi.
\end{cases}
\tag{5.24}
$$

Replacing (5.24) in $\dot{V}_{z_{iq}}$ and $\dot{V}_{z_{id}}$, we have

$$
\begin{cases}
\dot{V}_{z_{iq}} = -K_\Omega z_\Omega^2 + z_{iq}(m\phi_{rd}z_\Omega + \dot{z}_{iq}) + z'_{iq}(-m\phi_{rd}z_\Omega + \dot{z}'_{iq}) \\
\dot{V}_{z_{id}} = -K_\phi z_\phi^2 + z_{id}(aM_{sr}z_\phi + \dot{z}_{id}) + z'_{id}(-aM_{sr}z_\phi + \dot{z}'_{id}).
\end{cases}
\tag{5.25}
$$

Choosing the following equalities

$$
\begin{cases}
m\phi_{rd}z_\Omega + \dot{z}_{iq} = -K_{iq}z_{iq} \\
-m\phi_{rd}z_\Omega + \dot{z}'_{iq} = -K'_{iq}z'_{iq} \\
aM_{sr}z_\phi + \dot{z}_{id} = -K_{id}z_{id} \\
-aM_{sr}z_\phi + \dot{z}'_{id} = -K'_{id}z'_{id}
\end{cases}
\tag{5.26}
$$

where $K_{iq}, K'_{iq}, K_{id},$ and K'_{id} are positive constants, satisfying the following inequalities $K_{iq} > K'_{iq}$ and $K_{id} > K'_{id}$; it implies that

$$
\dot{V}_{z_{iq}} \le 0 \quad \text{and} \quad \dot{V}_{z_{iq}} \le 0.
$$

From the FOC strategy, with $\phi_{rq} = 0$, and since

$$
\dot{z}_{iq} = \dot{i}^*_{sq} - \dot{i}_{sq} + \dot{z}'_{iq} \quad \text{and} \quad \dot{z}_{id} = \dot{i}^*_{sd} - \dot{i}_{sd} + \dot{z}'_{id},
$$

the following dynamics are obtained

$$
\begin{cases}
\dot{z}_{iq} = \dot{i}^*_{sq} - \dot{i}_{sq} - K'_{iq}z'_{iq} + m\phi_{rd}z_\Omega \\
\dot{z}_{id} = \dot{i}^*_{sd} - \dot{i}_{sd} - K'_{id}z'_{id} + aM_{sr}z_\phi.
\end{cases}
\tag{5.27}
$$

According to (1.128), (5.26), and (5.27), the controllers are defined as

$$
\begin{cases}
u_{sq} = \dfrac{1}{m_1}\left(K_{iq}z_{iq} - K'_{iq}z'_{iq} + 2m\phi_{rd}z_\Omega + bp\Omega\phi_{rd} + \gamma i_{sq} + \omega_s i_{sd} + \dot{i}^*_{sq}\right) \\[2mm]
u_{sd} = \dfrac{1}{m_1}\left(K_{id}z_{id} - K'_{id}z'_{id} + 2aM_{sr}z_\phi - ba\phi_{rd} + \gamma i_{sd} - \omega_s i_{sq} + \dot{i}^*_{sd}\right).
\end{cases}
\tag{5.28}
$$

with the reference currents given by

$$
\begin{cases}
i^*_{sq} = \dfrac{1}{m\phi_{rd}}\left[\dot{\Omega}^* + c\Omega + K_\Omega z_\Omega + K'_\Omega(\Omega^* - \Omega) + \dfrac{T_l}{J}\right] \\[2mm]
i^*_{sd} = \dfrac{1}{aM_{sr}}\left[\dot{\phi}^* + a\phi_{rd} + K_\phi z_\phi + K'_\phi(\phi^* - \phi_{rd})\right].
\end{cases}
\tag{5.29}
$$

The above procedure can be summarized by the following proposition:

Proposition 5.2 *Consider the reduced order model of the induction motor represented by (5.17) with the reference signals i^*_{sq}, i^*_{sd}, Ω^*, and ϕ^*, and assume that they are differentiable and bounded. Then, system (5.17) in closed loop with the rotor speed, rotor flux, and the current tracking laws (5.19)–(5.28) is asymptotically stable.*

This proposition can be proved by considering the following Lyapunov candidate function

$$
\begin{aligned}
V_c &= V_{z\Omega} + V_{z\phi} + V_{z_{iq}} + V_{z_{id}} \\
&= z_\Omega^2 + z_\phi^2 + \frac{1}{2}z_{iq}^2 + \frac{1}{2}z_{iq}'^2 + \frac{1}{2}z_{id}^2 + \frac{1}{2}z_{id}'^2.
\end{aligned}
\tag{5.30}
$$

Taking the time derivative of (5.30), and replacing the suitable terms, we obtain
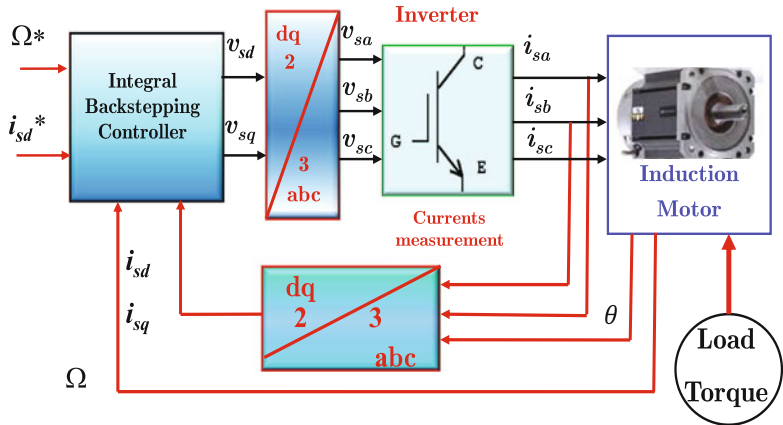
$$
\dot{V}_c = -2K_\Omega z_\Omega^2 - 2K_\phi z_\phi^2 - K_{iq}z_{iq}^2 - K'_{iq}z_{iq}'^2 - K_{id}z_{id}^2 - K'_{id}z_{id}'^2 < 0.
$$

This implies that the tracking errors asymptotically converge to zero as t tends to ∞. Hence, the stator currents, rotor speed, and the d-axis component of the rotor flux converge to the desired references.

In Fig. 5.1 is shown the integral backstepping control scheme. This can be summarized as follows:

Summary 5.2 Integral Backstepping Control

$$
\begin{aligned}
u_{sq} = \frac{1}{m_1}\Big(&K_{iq}z_{iq} - K'_{iq}z'_{iq} + 2m\phi_{rd}z_\Omega + bp\Omega\phi_{rd} \\
&+ \gamma i_{sq} + \omega_s i_{sd} + \dot{i}^*_{sq}\Big)
\end{aligned}
$$

Fig. 5.1 Integral backstepping controller diagram

$$u_{sd} = \frac{1}{m_1} \left(K_{id}z_{id} - K'_{id}z'_{id} + 2aM_{sr}z_\phi - ba\phi_{rd} \right.$$
$$\left. + \gamma i_{sd} - \omega_s i_{sq} + \dot{i}^*_{sd} \right)$$

where

$$z_\Omega = \Omega^* - \Omega + K'_\Omega \int_0^t (\Omega^* - \Omega)dt$$

$$z_\phi = \phi^* - \phi_{rd} + K'_\phi \int_0^t (\phi^* - \phi_{rd})dt$$

$$z_{iq} = i^*_{sq} - i_{sq} + z'_{iq}, \qquad z_{id} = i^*_{sd} - i_{sd} + z'_{id}$$

$$z'_{iq} = K''_{iq} \int_0^t (i^*_{sq} - i_{sq})dt, \qquad z'_{id} = K''_{id} \int_0^t (i^*_{sd} - i_{sd})dt$$

with

$$a = R_r/L_r, \quad b = M_{sr}/\sigma L_s L_r, \quad c = f_v/J, \quad \gamma = \frac{L_r^2 R_s + M_{sr}^2 R_r}{\sigma L_s L_r^2},$$

$$\sigma = 1 - (M_{sr}^2/L_s L_r), \quad m = pM_{sr}/JL_r, \quad m_1 = 1/\sigma L_s$$
$$i^*_{sq} \text{ and } i^*_{sd} \text{ from (5.29)}$$

and

$$K_{iq}, K'_{iq}, K''_{iq}, K_{id}, K'_{id}, K''_{id} \text{ are the parameters to tune with}$$
respect to the electrical time constants of the motor.

Notice that, the above control scheme to be implemented requires not only the rotor speed, the d-axis component of the rotor flux, and the stator currents measurements, but also the knowledge of the torque load T_l and the rotor resistance R_r. As we

shall see in Chap. 7, using an adaptive interconnected observer, the estimation of these variables/parameters will be used to guarantee the stability of the observer–controller scheme in closed loop in spite of the uncertainties and sudden changes of the load torque.

5.3 High-Order Sliding Mode Control

5.3.1 Introduction

The purpose of this section is to design high-order sliding mode (HOSM) based rotor speed and flux controllers for the induction motor (Fig. 5.2). One of the problems of the sliding mode control (or observer) of order 1 is the effect of the chattering phenomenon. This is described as the appearance of oscillations of finite frequency and finite amplitude. These oscillations are caused by the high-frequency switching of the first-order sliding mode control that can excite unmodeled dynamics, like sensors and actuators dynamics, which are generally neglected in the system modeling. These dynamics are generally faster than the system dynamics. The chattering phenomenon is also induced by the uncertainties and the perturbations that force the system dynamics to leave the sliding mode (i.e., to leave the sliding reference surface), inducing a discontinuous control action.

Taking into account the chattering problem, a solution to avoid these effects is the use of a high-order sliding mode (HOSM) control, where the chattering effect is considerably reduced in the control action.

5.3.2 Application to the Induction Motor Control

The speed and current controllers based on the backstepping methodology, presented in the previous sections, have an exponential convergence with arbitrary rate
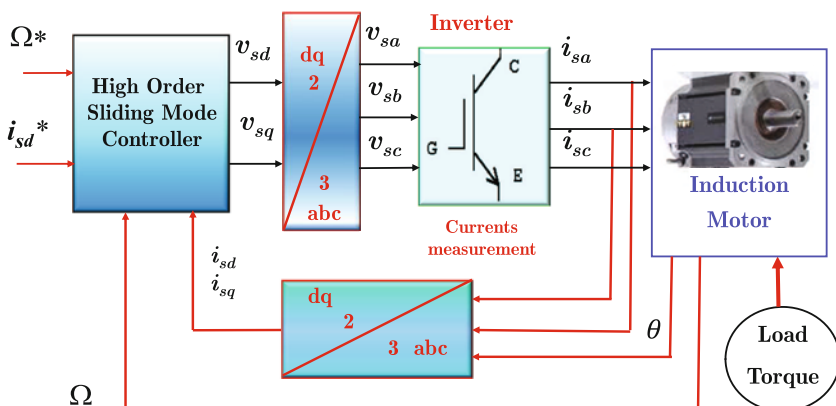
Fig. 5.2 High-order sliding mode controller diagram

convergence. We show how to design a robust rotor flux and speed controller based
on the sliding mode techniques for the induction motor, in presence of uncertain-
ties and disturbances. At this step, it is assumed that all the variables are available
by measurement, and that all the parameters are known. This strategy implies that
the controlled variables convergence to the desired references is in finite time. Con-
trary to the other controls design based on the sliding mode techniques, the time of
convergence of the proposed controller is determined a priori by the designer.

We begin the design by following the FOC strategy previously introduced. Define
the following sliding variables σ_ϕ and σ_Ω as:

$$\sigma_\phi = \phi_{rd} - \phi^* \quad \text{and} \quad \sigma_\Omega = \Omega - \Omega^*.$$

From the IM model (1.108), the relative degrees of the two new outputs σ_ϕ and σ_Ω
with respect to the input u (the voltages u_{sd} and u_{sq}) are equal to 2 ($r = 2$), which
implies that at least a second-order sliding mode controller can be designed for the
flux and speed tracking.

Regarding the chattering problem, to improve the robustness of the controller and
to reduce these effects, we start the procedure according to the HOSM algorithm,
given in Appendix "Appendix: A HOSM Algorithm", where third-order HOSM
controllers are designed for the two new outputs σ_ϕ and σ_Ω.

This means that through the discontinuous control $\dot{u}$, which will be applied, the
chattering effect on the system will be reduced.

Furthermore, by forcing $\sigma_\phi^{(3)}$ and $\sigma_\Omega^{(3)}$ to track the reference trajectories $\mathcal{F}_\phi$ and
$\mathcal{F}_\Omega$, (defined in Appendix "Appendix: A HOSM Algorithm"), implies that $\sigma_\phi^{(2)}$ and
$\sigma_\Omega^{(2)}$ tend to zero in a pre-fixed finite time t_f, in spite of uncertainties and disturbances.

Then, the dynamics of $\phi_{rd}^{(2)}$ and $\Omega^{(2)}$ are given by

$$\begin{bmatrix} \phi_{rd}^{(2)} \\ \Omega^{(2)} \end{bmatrix} = \begin{bmatrix} \varphi_{\alpha_1} \\ \varphi_{\alpha_2} \end{bmatrix} + \varphi_\beta \begin{bmatrix} u_{sd} \\ u_{sq} \end{bmatrix} \tag{5.31}$$

where φ_{α_1} and φ_{α_2} are expressed as

$$\varphi_{\alpha_1} = -a\dot{\phi}_{rd} + (\omega_s - p\Omega)\dot{\phi}_{rq}$$

$$+ \frac{aM_{sr}\left((ba\phi_{rq} - bp\Omega\phi_{rd} - \gamma i_{sq} - \omega_s i_{sd})\phi_{rd} - i_{sq}\dot{\phi}_{rd}\right)}{\phi_{rd}^2}\phi_{rq}$$

$$+ aM_{sr}(ba\phi_{rd} + bp\Omega\phi_{rq} - \gamma i_{sd} + \omega_s i_{sq}), \tag{5.32}$$

$$\varphi_{\alpha_2} = m\left[\dot{\phi}_{rd}i_{sq} + \phi_{rd}(ba\phi_{rq} - bp\Omega\phi_{rd} - \gamma i_{sq} - \omega_s i_{sd})\right.$$

$$\left. - \dot{\phi}_{rq}i_{sd} - \phi_{rq}(ba\phi_{rd} + bp\Omega\phi_{rq} - \gamma i_{sd} + \omega_s i_{sq})\right] - c\dot{\Omega} - \frac{\dot{T}_l}{J},$$
$$\tag{5.33}$$

and the matrix φ_β

$$\varphi_\beta = \begin{bmatrix} aM_{sr}m_1 & aM_{sr}m_1\dfrac{\phi_{rq}}{\phi_{rd}} \\[2mm] -mm_1\phi_{rq} & mm_1\phi_{rd} \end{bmatrix}. \tag{5.34}$$

Following the flux-oriented control strategy, the q-axis component of the rotor flux is forced to zero, i.e., $\phi_{rq} = 0$, then φ_{α_1}, φ_{α_2}, and φ_β are given by

$$\begin{aligned}
\varphi_{\alpha_1} &= -a^2 M_{sr} i_{sd} + a^2 \phi_{rd} - a(\omega_s - p\Omega)\phi_{rq} \\
&\quad + aM_{sr}(ba\phi_{rd} - \gamma i_{sd} + \omega_s i_{sq}) \\
\varphi_{\alpha_2} &= m\big[(aM_{sr}i_{sd} - a\phi_{rd} + (\omega_s - p\Omega)\phi_{rq})i_{sq} \\
&\quad - \phi_{rd}(bp\Omega\phi_{rd} + \gamma i_{sq} + \omega_s i_{sd})\big] - c\dot{\Omega} - \dfrac{\dot{T_l}}{J}
\end{aligned}$$

and

$$\varphi_\beta = \begin{bmatrix} aM_{sr}m_1 & 0 \\ 0 & mm_1\phi_{rd} \end{bmatrix}.$$

Remark 5.3 As recalled previously, it is clear that no torque can be obtained as long as the IM rotor flux is zero. This physical constraint induces the singularity for the IM control.

Taking into account the parameters uncertainties, the functions φ_{α_1}, φ_{α_2}, and φ_β can be written as

$$\varphi_{\alpha 1} = \varphi_{\alpha 1}^{Nom} + \Delta\varphi_{\alpha 1} \tag{5.35}$$

$$\varphi_{\alpha 2} = \varphi_{\alpha 2}^{Nom} + \Delta\varphi_{\alpha 2} \tag{5.36}$$

$$\varphi_\beta = \varphi_\beta^{Nom} + \Delta\varphi_\beta \tag{5.37}$$

where $\varphi_{\alpha 1}^{Nom}$, $\varphi_{\alpha 2}^{Nom}$, and φ_β^{Nom} are the well-known nominal terms whereas $\Delta\varphi_{\alpha 1}$, $\Delta\varphi_{\alpha 2}$ (including $\dot{T_l}/J$), and $\Delta\varphi_\beta$ contain all the uncertainties due to the parameters variations and the torque disturbance. In practice, these uncertainties are bounded. As the matrix φ_β^{Nom} is invertible on the operation domain ($\phi_{rd} \neq 0$), then the control input u is given by[1]

$$\begin{bmatrix} u_{sd} \\ u_{sq} \end{bmatrix} = \left(\varphi_\beta^{Nom}\right)^{-1}\left[-\begin{bmatrix} \varphi_{\alpha 1}^{Nom} \\ \varphi_{\alpha 2}^{Nom} \end{bmatrix} + \begin{bmatrix} \nu_{sd} \\ \nu_{sq} \end{bmatrix}\right]. \tag{5.38}$$

From (5.31) to (5.38), switching variables dynamics are defined by

---

[1] The interest of a such feedback, which has been detailed in [13], is that it allows to minimize gain values of the control discontinuous function.

$$\begin{bmatrix} \phi_{rd}^{(2)} \\ \Omega^{(2)} \end{bmatrix} = \Psi_\alpha + \Psi_\beta \begin{bmatrix} \nu_{sd} \\ \nu_{sq} \end{bmatrix}. \tag{5.39}$$

It is clear that functions $\varphi_{\alpha_1}^{Nom}$, $\varphi_{\alpha_1}^{Nom}$ and the components of the matrix φ_β^{Nom} are bounded C^1-functions in the operation domain $\mathcal{D}_{\mathcal{IM}}$ of IM (Definition 3.7). This implies that the components of the vector Ψ_α and the matrix Ψ_β are uncertain bounded C^1-functions.

Taking the time derivative of $\sigma_\phi^{(3)}$ and $\sigma_\Omega^{(3)}$, it follows that

$$\begin{bmatrix} \sigma_\phi^{(3)} \\ \sigma_\Omega^{(3)} \end{bmatrix} = \underbrace{\dot{\Psi}_\alpha + \dot{\Psi}_\beta \begin{bmatrix} \nu_{sd} \\ \nu_{sq} \end{bmatrix} - \begin{bmatrix} \phi^{*(3)} \\ \Omega^{*(3)} \end{bmatrix}}_{\varphi_1} + \underbrace{\Psi_\beta}_{\varphi_2} \begin{bmatrix} \dot{\nu}_{sd} \\ \dot{\nu}_{sq} \end{bmatrix} \tag{5.40}$$

$$= \varphi_1 + \varphi_2 \cdot \dot{\nu}. \tag{5.41}$$

Note that previous system has the same form that system (4.26). As mentioned in previous subsection, the HOSM control synthesis is made in two steps.

Step 1. Switching vector

To design the switching vector, we follow the procedure given in Appendix "Appendix: A HOSM Algorithm". First, define the finite time of convergence t_f, and from (4.67) and Theorem 4.2, the switching vector is defined as

- For $t \leq t_f$, the switching variables are

$$S_\phi = \sigma_\phi^{(2)} - \chi_\phi$$

$$S_\Omega = \sigma_\Omega^{(2)} - \chi_\Omega$$

where

$$\chi_\phi = K_\phi F^2 e^{Ft} T \sigma_\phi(0) - 2\zeta_\phi \omega_{n\phi} (\dot{\sigma}_\phi - K_\phi F e^{Ft} T \sigma_\phi(0))$$
$$- \omega_{n\phi}^2 (\sigma_\phi - K_\phi e^{Ft} T \sigma_\phi(0)) \tag{5.42}$$

and

$$\chi_\Omega = K_\Omega F^2 e^{Ft} T \sigma_\Omega(0) - 2\zeta_\Omega \omega_{n\Omega} (\dot{\sigma}_\Omega - K_\Omega F e^{Ft} T \sigma_\Omega(0))$$
$$- \omega_{n\Omega}^2 (\sigma_\Omega - K_\Omega e^{Ft} T \sigma_\Omega(0)). \tag{5.43}$$

- For $t > t_f$, the resulting switching variables are given by

$$S_\phi = \sigma_\phi^{(2)} + 2\zeta_\phi \omega_{n\phi} \dot{\sigma}_\phi + \omega_{n\phi}^2 \sigma_\phi \tag{5.44}$$

and

$$S_\Omega = \sigma_\Omega^{(2)} + 2\zeta_\Omega\omega_{n\Omega}\dot\sigma_\Omega + \omega_{n\Omega}^2\sigma_\Omega \tag{5.45}$$

where

$$K_\phi = \left[\sigma_\phi^{(2)}(0)\ 0\ \dot\sigma_\phi(0)\ 0\ \sigma_\phi(0)\ 0\right](\mathcal{K}_\phi)^{-1}, \tag{5.46}$$

$$K_\Omega = \left[\sigma_\Omega^{(2)}(0)\ 0\ \dot\sigma_\Omega(0)\ 0\ \sigma_\Omega(0)\ 0\right](\mathcal{K}_\Omega)^{-1}, \tag{5.47}$$

and

$$\mathcal{K}_\phi = \begin{bmatrix} F^2 T\sigma_\phi(0) \\ F^2 e^{Ft_f}T \\ FT\sigma_\phi(0) \\ Fe^{Ft_f}T \\ T\sigma_\phi(0) \\ e^{Ft_f}T \end{bmatrix}^T, \quad \mathcal{K}_\Omega = \begin{bmatrix} F^2 T\sigma_\Omega(0) \\ F^2 e^{Ft_f}T \\ FT\sigma_\Omega(0) \\ Fe^{Ft_f}T \\ T\sigma_\Omega(0) \\ e^{Ft_f}T \end{bmatrix}^T. \tag{5.48}$$

Notice that these matrices depend on the initial value of $\sigma_\phi(0)$ and $\sigma_\Omega(0)$. Furthermore, according to Lemma 4.2 (see [77] for more details) the matrix F and the vector T are choosen as follows:

$$T = \begin{bmatrix} 1 \end{bmatrix}_{6\times 1}, \quad F = Diag\left[-(1+i)\right]_{6\times 6}, \quad \text{for} \quad 0 \le i \le 5.$$

Step 2. Discontinuous Input Design

The discontinuous control $\dot\nu$ is

$$\begin{bmatrix} \dot\nu_{sd} \\ \dot\nu_{sq} \end{bmatrix} = \begin{bmatrix} -\alpha_\phi\text{sign}(S_\phi) \\ -\alpha_\Omega\text{sign}(S_\Omega) \end{bmatrix}, \tag{5.49}$$

where α_ϕ and α_Ω are the controller gains to tune.

Then, replacing the discontinuous control (5.49) in (5.40), we obtain

$$\begin{bmatrix} \dot S_\phi \\ \dot S_\Omega \end{bmatrix} = \varphi_1 + \varphi_2\dot\nu - \begin{bmatrix} \chi_\phi \\ \chi_\Omega \end{bmatrix}. \tag{5.50}$$

By using the same procedure established in Theorem 4.2 (see Appendix "Appendix: A HOSM Algorithm"), there exist gains α_ϕ and α_Ω such that the time derivatives of the Lyapunov function

$$W_\phi = S_\phi^T S_\phi \text{ and } W_\Omega = S_\Omega^T S_\Omega$$

satisfy the inequalities

$$\dot W_\phi = \dot S_\phi S_\phi \le -\eta_\phi|S_\phi| \le -\eta_\phi\sqrt{W_\phi} \tag{5.51}$$

and

$$\dot{W}_\Omega = \dot{S}_\Omega S_\Omega \leq -\eta_\Omega |S_\Omega| \leq -\eta_\Omega \sqrt{W_\Omega}. \tag{5.52}$$

Integrating the above inequalities gives

$$\sqrt{W_\phi(t)} \leq \sqrt{W_\phi(t_0)} - \frac{\eta_\phi}{2}t \tag{5.53}$$

and

$$\sqrt{W_\Omega(t)} \leq \sqrt{W_\Omega(t_0)} - \frac{\eta_\Omega}{2}t. \tag{5.54}$$

Let $\sqrt{W_\phi(t_0)} - \dfrac{\eta_\phi}{2}t_{f,\phi} = 0$ and $\sqrt{W_\Omega(t_0)} - \dfrac{\eta_\Omega}{2}t_{f,\Omega} = 0$, then the convergence time is given by

$$t_{f,\phi} = \frac{2\sqrt{W_\phi(t_0)}}{\eta_\phi} \tag{5.55}$$

and

$$t_{f,\Omega} = \frac{2\sqrt{W_\Omega(t_0)}}{\eta_\Omega}. \tag{5.56}$$

Choosing $t_f = max(t_{f,\phi}, t_{f,\Omega})$, then the convergence in finite time of the tracking dynamics is guaranteed.

Remark 5.4 The terms $(-c\dot{\Omega} - \dot{T}_l/J)$ can be added in $\varphi_{\alpha_2^{Nom}}$ if they are estimated, thanks to an observer. Otherwise, these terms are added to the uncertainties $\Delta\varphi_{\alpha 2}$ (5.36) to reject by the controller.

Summary 5.3 IM high-order sliding mode control

$$\begin{bmatrix} u_{sd} \\ u_{sq} \end{bmatrix} = (\varphi_\beta^{Nom})^{-1}\left[-\begin{bmatrix} \varphi_{\alpha_1}^{Nom} \\ \varphi_{\alpha_2}^{Nom} \end{bmatrix} + \begin{bmatrix} \nu_{sd} \\ \nu_{sq} \end{bmatrix}\right]$$

where

$$\varphi_{\alpha_1^{Nom}} = -a^2 M_{sr}i_{sd} + a^2\phi_{rd} - a(\omega_s - p\Omega)\phi_{rq}$$
$$+ aM_{sr}(ba\phi_{rd} - \gamma i_{sd} + \omega_s i_{sq})$$
$$\varphi_{\alpha_2^{Nom}} = m[(aM_{sr}i_{sd} - a\phi_{rd} + (\omega_s - p\Omega)\phi_{rq})i_{sq}$$
$$- \phi_{rd}(bp\Omega\phi_{rd} + \gamma i_{sq} + \omega_s i_{sd})]$$
$$\varphi_\beta = \begin{bmatrix} aM_{sr}m_1 & 0 \\ 0 & mm_1\phi_{rd} \end{bmatrix}$$

and

$$\begin{bmatrix} \dot{\nu}_{sd} \\ \dot{\nu}_{sq} \end{bmatrix} = \begin{bmatrix} -\alpha_\phi.\text{sign}(S_\phi) \\ -\alpha_\Omega.\text{sign}(S_\Omega) \end{bmatrix},$$

with

$$a = R_r/L_r, \quad b = M_{sr}/\sigma L_s L_r, \quad c = f_v/J, \quad \gamma = \frac{L_r^2 R_s + M_{sr}^2 R_r}{\sigma L_s L_r^2},$$

$$\sigma = 1 - (M_{sr}^2/L_s L_r), \quad m = p M_{sr}/J L_r, \quad m_1 = 1/\sigma L_s$$

and

$$\alpha_\phi, \alpha_\Omega \text{ are parameters to be tuned following (4.70)}. \quad\quad (5.57)$$

Notice that the implementation of the HOSM controller requires the knowledge of the rotor speed, the stator currents, the d-axis component of the rotor flux, the load torque, and the rotor resistance. As we shall see in Chap. 7, the adaptive interconnected observer given in Chap. 3 can be used to replace the unmeasured variables by its estimates. Furthermore, a stability analysis of the closed-loop system will be presented in order to ensure the convergence to the reference variables without these measurements.

5.4 Conclusions

Two control methodologies for designing IM machines robust controllers are presented in this chapter. One of these designs is based on an improved version of the classical backstepping control design, and the second one is based on high-order sliding mode techniques. It is clear that there is a trade-off between the performance and the complexity of the controller. However, as it will be introduced in the following chapters, the requirements to implement it, the computational cost, and the simplicity to tune the controllers are the keys to select the better controller.

Furthermore, the control algorithms which have been presented have assumed that all variables are measurable. However, if they are not available, they can be replaced by their estimates given by an observer including the unknown load torque. It is clear that the properties of the tracking convergence (asymptotic or in finite time) can be ensured locally if the observer estimation errors decay (asymptotically or in finite time) to zero. This problem will be studied in Chap. 7.

5.5 Bibliographical Notes

As noted in Chap. 4, the principles of modern AC machines control can be found in the classical books [17, 60], where the field-oriented control algorithm appears as a seminal control strategy [7].

Owing to the intrinsic difficulty to precisely reconstruct the unmeasured variables of the AC machines, the robustness of the controllers is a required property. Thus, new robust nonlinear controllers can be employed, thanks to their high-performance properties.

A brief outline of the main research directions for the robust control of the induction motor is given in the following:

The field-oriented control strategy has been improved by many papers among them [85][2] partially used in this chapter and where nonlinear compensation terms complete the classical PI controllers.

Control methods based on the approximate linearization around an equilibrium point have been studied in [49]. These methods are not adapted to the trajectory tracking in the whole working domain of the controlled machine. The more complete method of the exact input–output linearization technique has been developed in [8, 15, 16, 17].

The IM adaptive control is proposed in [56, 68, 82]. The backstepping control algorithm [53] has been carried out in [63, 79]. Recently the FOC strategy has been combined with the backstepping control. Furthermore, an integral term has been added, at each step of the backstepping algorithm, to increase the robustness of the above combination of controllers [88].[3]

The sliding mode control has also been applied in [1, 2, 57, 58, 81, 95]. An extended approach is the high-order sliding mode control. This strategy allows finite time control, and moreover, significantly reduces the "chattering phenomenon" induced by the basic sliding mode. The chattering implies finite frequency and finite amplitude oscillations appearing when the basic sliding mode algorithm is implemented. In [77], an high-order sliding mode control algorithm has been introduced that allows a priori choice of the finite time of convergence. In [86],[4] for the induction motor, this algorithm is applied to design a high-order sliding mode (HOSM) based rotor speed and flux controllers.

---

[2] This chapter includes excerpts of "Traore D, De Leon J, Glumineau A, Loron L (2007) Speed sensorless field-oriented control of induction motor with interconnected observers: experimental tests on low frequencies benchmark. IET control theory applications, 1–6(10):1681–1692, DOI 10.1049/iet-cta.2009.0648" with permission from IET.

[3] This chapter includes excerpts of "Traore D, De Leon J, Glumineau A (2010) Sensorless induction motor adaptive observer-backstepping controller: experimental robustness tests on low frequencies benchmark. IET Control Theory Applications 4(10):1989–2002, DOI 10.1049/iet-cta.2009.0648" with permission from IET.

[4] This chapter includes excerpts of [86], (2008) IEEE. Reprinted, with permission, from "Traore D, Plestan F, Glumineau A, de Leon J (2008) Sensorless induction motor: High-order sliding mode controller and adaptive interconnected observer. IEEE Transactions on Industrial Electronics, 55(11):3818–3827".

Chapter 6
Sensorless Output Feedback Control for SPMSM and IPMSM

Abstract In this chapter, the observers previously designed in Chap. 3 are associated with the control strategies proposed in Chap. 4, in order to achieve the SPMSM and the IPMSM sensorless controls. These observer-control schemes assume that only the currents and the voltages are available from measurements. Furthermore, these schemes are tested on the benchmarks specified in Chap. 1, Sect. 1.6. The first part of this chapter is devoted to the observer-control scheme where the control is designed using the backstepping techniques, and in the second part, the controller is designed using high order sliding mode techniques. For the backstepping control case, an observer-controller scheme applied to the SPMSM is constituted by a backstepping controller combined with an adaptive interconnected observer. Next, for the IPMSM, an adaptive interconnected observer combined with an integral backstepping controller is introduced. For both control-observer schemes, sufficient conditions are obtained to ensure the tracking stability of the closed-loop systems. For the high order sliding mode control case, first for the SPMSM, a sliding mode observer is associated with a quasi continuous high order sliding mode controller. Next, for the IPMSM, an observer-control scheme constituted of an adaptive observer combined with a finite time convergence high order sliding mode controller, by following a Maximum Torque Per Ampere (MTPA) strategy, is analyzed. Thanks to the benchmark trajectories previously introduced in Chap. 1, Sect. 1.6, significant simulation results illustrate the robustness and performance of all these observer-controller schemes.

6.1 Robust Adaptive Backstepping Sensorless Control

6.1.1 SPMSM Case

In this section, we present on how to implement a robust sensorless speed observer-controller scheme for a Surface Permanent Magnet Synchronous Motor (SPMSM). This observer-controller strategy combines an adaptive high gain interconnected observer (see Sect. 3.2) with a nonlinear backstepping controller (see Sect. 4.1.1). Furthermore, the advantages of the proposed scheme are shown.

In the proposed scheme, the adaptive high gain interconnected observer only requires the supply of the electrical measurements, the stator currents and the stator voltages, and provides the estimation of the rotor speed, the stator resistance, and the load torque as well. In this section, the stability of the whole closed-loop system is analyzed, taking into account that the rotor speed and the load torque are replaced in the control law by their estimated values. The tracking dynamics convergence of the complete scheme is analyzed using the Lyapunov theory, and sufficient conditions are given to ensure the stability of the closed-loop system.
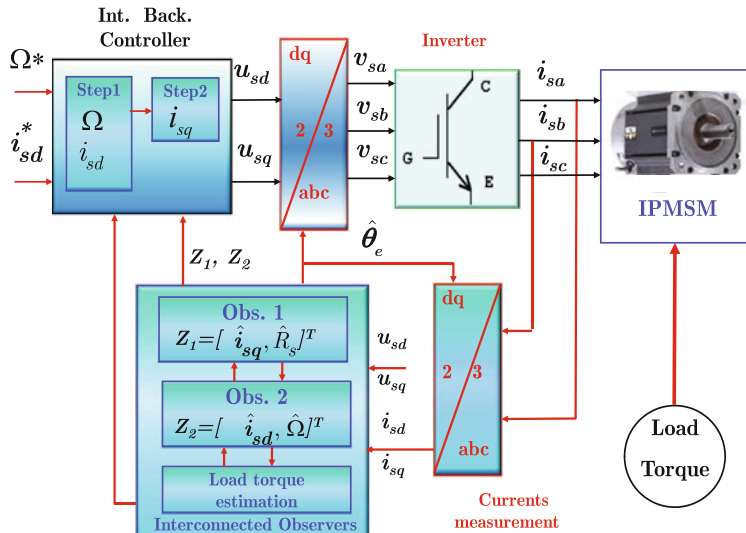
This observer-controller scheme is implemented to control the motor with load (see Fig. 6.1) and tested via simulation on an industrial benchmark in order to illustrate its performance. The trajectories of the benchmark were chosen to test the motor under unobservability conditions. Some robustness tests are carried out to show the robustness of the observer-controller scheme.

To analyze the stability of the closed-loop system, consider the following Lyapunov function candidate:

$$V_{oc} = V_o + V_c \tag{6.1}$$

which is composed of the Lyapunov function V_c associated with the backstepping controller (Chap. 4, Sect. 4.1.1), and V_o for the adaptive interconnected observer, as shown in Chap. 3, Sect. 3.2, which are given by

$$
\begin{aligned}
V_o &= \epsilon_1^T S_{x_1} \epsilon_1 + \epsilon_2^T S_{x_2} \epsilon_2 + \epsilon_3^T S_\tau \epsilon_3, \\
V_c &= \tfrac{1}{2} z_1^2 + \tfrac{1}{2} z_2^2 + \tfrac{1}{2} z_3^2.
\end{aligned}
\tag{6.2}
$$

Fig. 6.1 Adaptive high gain observer and backstepping controller for SPMSM

Notice that the time derivative of V_o associated with the observer (see [22]) is given by

$$\dot{V}_o \leq -\delta V_o + \mu\psi\sqrt{V_o}. \tag{6.3}$$

On the other hand, taking the time derivative of V_{oc} and replacing the state estimates $(\widehat{X})$ provided by the adaptive interconnected observer in the control inputs v_{sq} and v_{sd} design, we obtain

$$\begin{aligned}
\dot{V}_{oc} &= -w_1 z_1^2 + z_2\{z_1 + \beta_2 + K v_{sq}(\widehat{X})\} \\
&\quad + z_3\{-\frac{R_s}{L_s}i_{sd} + p\Omega i_{sq} + \frac{1}{L_s}v_{sd}(\widehat{X})\}.
\end{aligned} \tag{6.4}$$

Adding the terms $\pm v_{sq}(X)$ and $\pm v_{sd}(X)$ in (6.4), and after straightforward computations, it follows that

$$\begin{aligned}
\dot{V}_{oc} &\leq -w_1 z_1^2 - w_2 z_2^2 - w_3 z_3^2 + K|z_2||v_{sq}(\widehat{X}) - v_{sq}(X)| \\
&\quad + \frac{1}{L_s}|z_3||v_{sd}(\widehat{X}) - v_{sd}(X)|.
\end{aligned}$$

On the practical domain $\mathcal{D}_\mathcal{S}$ (see Definition 3.6 in Chap. 3) it is easy to see that the terms $|v_{sq}(\widehat{X}) - v_{sq}(X)|$ and $|v_{sd}(\widehat{X}) - v_{sd}(X)|$ satisfy the Lipschitz conditions, i.e.,

$$\begin{aligned}
|v_{sq}(\widehat{X}) - v_{sq}(X)| &\leq L_1\{\|\epsilon_1\|_{S_{\rho_{x1}}} + \|\epsilon_2\|_{S_{\rho_{x2}}} + \|\epsilon_3\|_{S_{\rho_\tau}}\} \\
|v_{sd}(\widehat{X}) - v_{sd}(X)| &\leq L_2\{\|\epsilon_1\|_{S_{\rho_{x1}}} + \|\epsilon_2\|_{S_{\rho_{x2}}} + \|\epsilon_3\|_{S_{\rho_\tau}}\}
\end{aligned} \tag{6.5}$$

where L_1 and L_2 are the associated Lipschitz constants. Using the following inequalities:

$$\begin{aligned}
|z_j| \, \|\epsilon_1\|_{S_{\rho_{x1}}} &\leq \frac{\xi_{j1}}{2} \|\epsilon_1\|^2_{S_{\rho_{x1}}} + \frac{1}{2\xi_{j1}}z_j^2 \\
|z_j| \, \|\epsilon_2\|_{S_{\rho_{x2}}} &\leq \frac{\xi_{j2}}{2} \|\epsilon_2\|^2_{S_{\rho_{x2}}} + \frac{1}{2\xi_{j2}}z_j^2 \\
|z_j| \, \|\epsilon_3\|_{S_{\rho_\tau}} &\leq \frac{\xi_{j3}}{2} \|\epsilon_3\|^2_{S_{\rho_\tau}} + \frac{1}{2\xi_{j3}}z_j^2,
\end{aligned} \tag{6.6}$$

for $j = 2, 3$; it follows that the time derivative of V_{oc} satisfies

$$\begin{aligned}
\dot{V}_{oc} &\leq -\delta V_o + \mu\psi\sqrt{V_o} + \vartheta_1 \|\epsilon_1\|^2_{S_{\rho_{x1}}} + \vartheta_2 \|\epsilon_2\|^2_{S_{\rho_{x2}}} \\
&\quad + \vartheta_3 \|\epsilon_3\|^2_{S_{\rho_\tau}} - \vartheta_4 z_1^2 - \vartheta_5 z_2^2 - \vartheta_6 z_3^2
\end{aligned} \tag{6.7}$$

where

$$\vartheta_1 = \left(\frac{L_1 K}{2} + \frac{L_2}{2L_s}\right)\{\xi_{21} + \xi_{31}\}, \qquad \vartheta_2 = \left(\frac{L_1 K}{2} + \frac{L_2}{2L_s}\right)\{\xi_{22} + \xi_{32}\},$$

$$\vartheta_3 = \left(\frac{L_1 K}{2} + \frac{L_2}{2L_s}\right)\{\xi_{23} + \xi_{33}\}, \qquad \vartheta_4 = w_1,$$

$$\vartheta_5 = w_2 - \frac{L_1 K}{2}\left\{\frac{1}{\xi_{21}} + \frac{1}{\xi_{22}} + \frac{1}{\xi_{23}}\right\}, \quad \vartheta_6 = w_3 - \frac{L_2}{2L_s}\left\{\frac{1}{\xi_{31}} + \frac{1}{\xi_{32}} + \frac{1}{\xi_{33}}\right\}.$$

Taking $\vartheta_O = max(\vartheta_1, \vartheta_2, \vartheta_3)$ and $\vartheta_C = min(\vartheta_4, \vartheta_5, \vartheta_6)$, the inequality (6.7) can be expressed as

$$\dot{V}_{oc} \leq -(\delta - \vartheta_O)V_o + \mu\psi\sqrt{V_o} - \vartheta_C(z_1^2 + z_2^2 + z_3^2) \tag{6.8}$$

and choosing $\eta = min(\delta - \vartheta_O, \vartheta_C)$, we obtain

$$\dot{V}_{oc} \leq -\eta V_{oc} + \mu\psi\sqrt{V_{oc}}. \tag{6.9}$$

It is easy to see that after the following change of variable $v_{oc} = 2\sqrt{V_{oc}}$, and taking the time derivative of v_{oc}, we obtain

$$\dot{v}_{oc} \leq -\eta v_{oc} + \psi\mu. \tag{6.10}$$

From the solution of (6.10), i.e.,

$$v_{oc} = v_{oc}(t_0)e^{-\eta(t-t_0)} + \frac{\psi\mu}{\eta}\left(1 - e^{-\eta(t-t_0)}\right), \tag{6.11}$$

and applying Corollary 3.1 (Chap. 3), the estimation and tracking errors of the closed-loop system converge toward a ball $B_{\hbar_{oc}}$ of radius $\hbar_{oc}$ with $\hbar_{oc} = \frac{\psi\mu}{\eta}$. This ensures the strong uniform practical stability of the closed-loop system.

The performance of the closed-loop error system is summarized in the following theorem.

Theorem 6.1 *The adaptive high gain interconnected observer* (3.110) *combined with the backstepping controller* (*Summary* 4.1.1) *is a sensorless adaptive observer-controller for the extended model of the SPMSM* (1.119)*, where the estimation errors and the tracking error dynamics are strongly uniformly practically stable.*

6.1.1.1   Simulation Results

Now, the observer-controller scheme is applied to control the SPMSM and tested in simulation, using the Simulink/MatLab software, in order to show the performance of this strategy.

The parameters of the SPMSM are given in Table 6.1.

The observer gains are tuned to satisfy the convergence conditions, as in [86]. The controller gains are chosen with respect to the open-loop time constants of the mechanical and the electrical dynamics.

Table 6.1 SPMS motor parameters

Current	9.67 A	Torque	9 Nm
Speed	3,000 rpm	Ψ_r	0.1814 Wb
R_s	0.45 ohm	L_s	3.425 mH
J	0.00679 kg m^2	f_v	0.0034 kg m^2/s
p	3		

Summary 6.1.1 Tuning parameters

    Adaptive Interconnected Observer
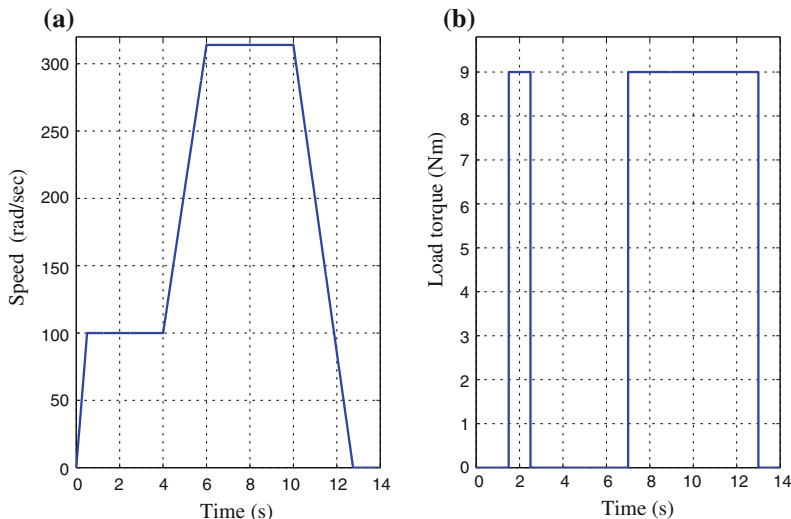
        $\varpi = 80$, $k = 0.05$, $k_{c1} = 0.001$, $k_{c2} = 0.1$, $\rho_1 = 2{,}500$,
        $\rho_x = 6{,}000$, $\rho_\theta = 100$, $k_{c2} = 0.01$, $\alpha = 0.1$.

    Backstepping Controller
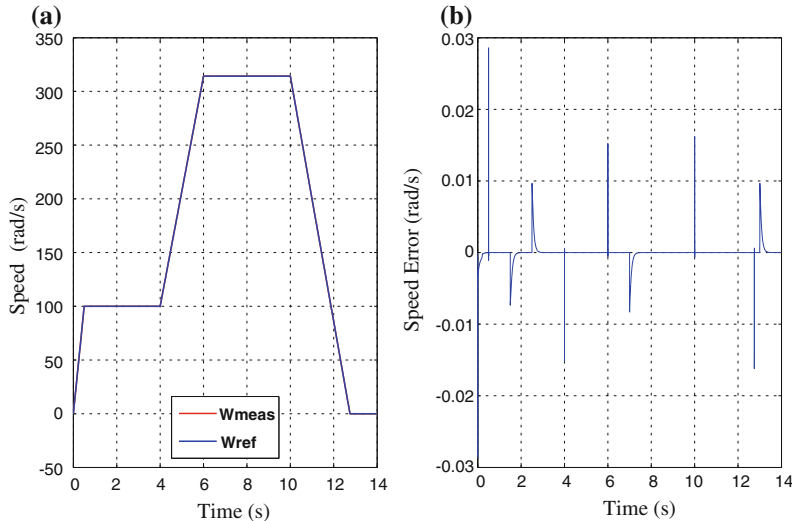
        $w_1 = 1{,}000$ rad/s, $w_2 = 1{,}000$ rad/s and $w_3 = 1{,}500$ rad/s.

The SPMSM model controlled by the observer-controller scheme has been tested according to a sensorless industrial benchmark introduced in Chap. 1 (see Sect. 1.6). The rotor speed and the load torque references are plotted: see Fig. 6.2.
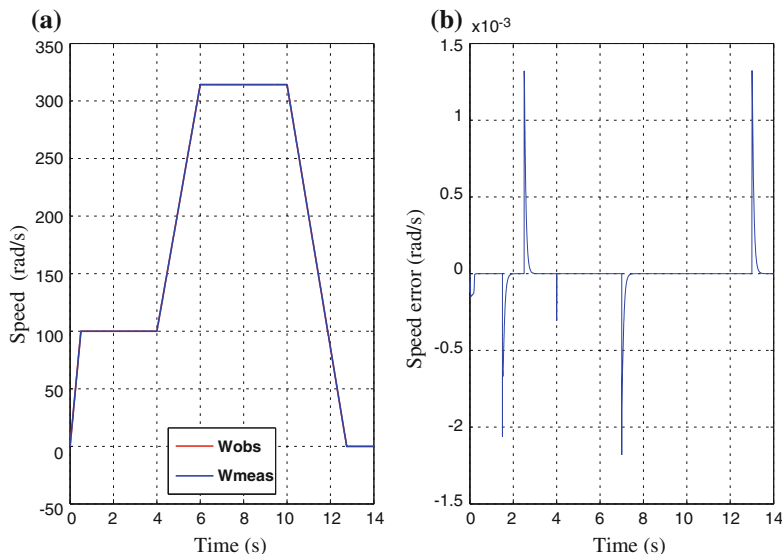
In this section, nominal case means that the controller and the observer are designed by using the same parameters as the motor model parameters but the initial conditions can be selected arbitrarily in the operation domain $\mathcal{D}_\mathcal{S}$. In Fig. 6.3a is displayed the rotor speed and its reference for the nominal case, and the motor is loaded following the benchmark trajectories.

Fig. 6.2 Reference trajectories of the sensorless industrial benchmark. **a** Speed reference. **b** Load torque

(a)

(b)
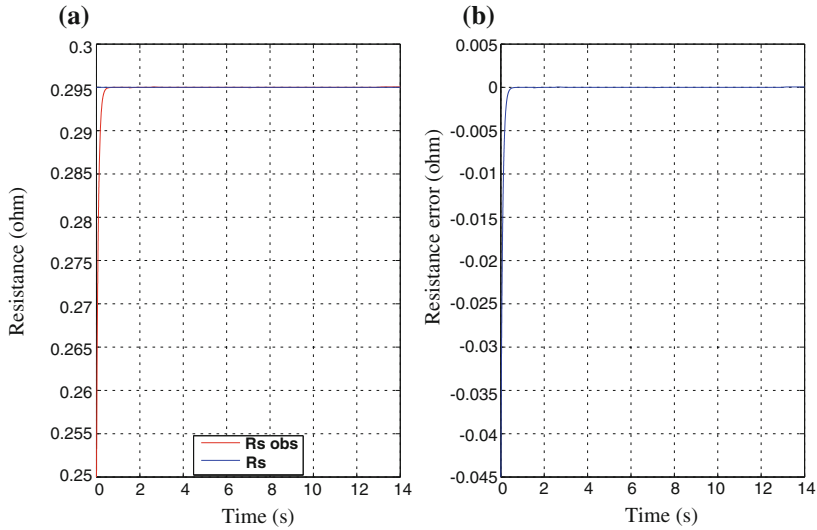
Fig. 6.3 Tracking control. **a** Reference speed and measured speed. **b** Speed error

(a)

(b) x10⁻³
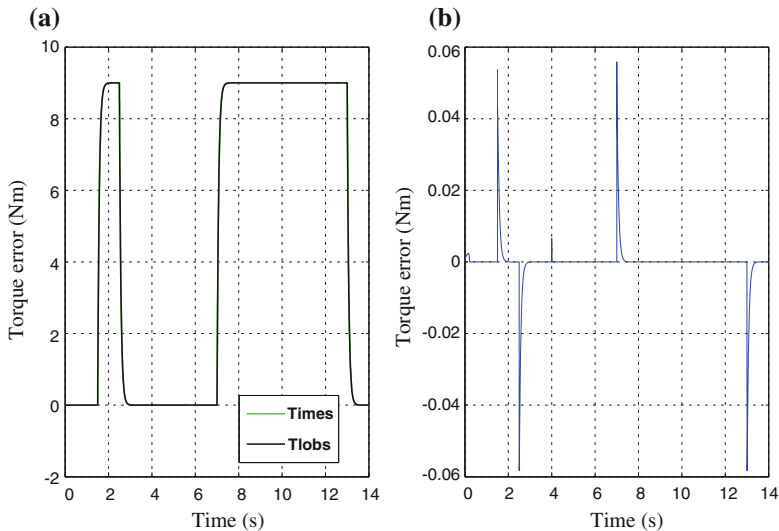
Fig. 6.4 Nominal case. **a** Estimated speed. **b** Speed estimation error

The rotor speed tracking is very efficient as displayed by Fig. 6.3b, which shows the speed error (speed reference-measured speed). The measured rotor speed is used in simulations only for comparison purpose. Of course, only the estimated rotor speed is supplied to the controller. In addition, Fig. 6.4a shows the estimated and the measured speeds. The speed error is shown in Fig. 6.4b. From simulation results, it is

(a)   **(b)**
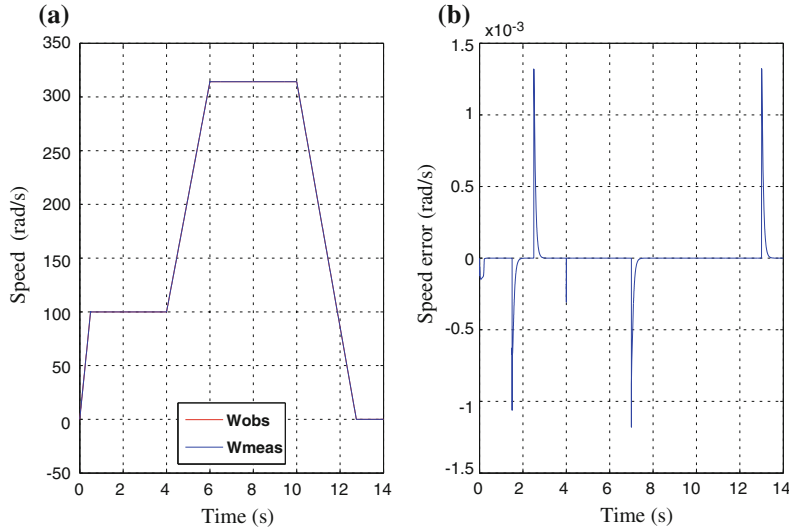
Fig. 6.5 Resistance estimation. **a** Estimated resistance. **b** Resistance estimation error

(a)   **(b)**
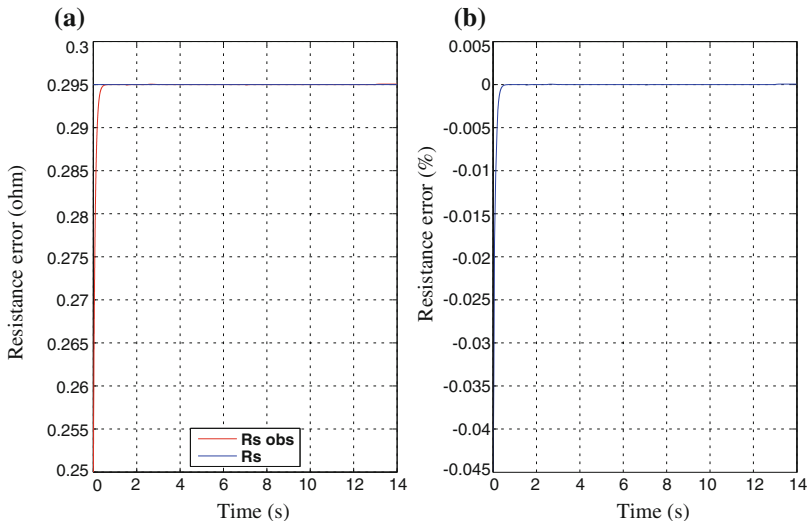
Fig. 6.6 Load torque estimation. **a** Estimated and applied load torques. **b** Load torque estimation error

clear that the observer has good performance. Figures 6.5 and 6.6 display the stator resistance and load torque estimation, respectively, for the nominal case.

Now, in order to illustrate the robustness of the sensorless control scheme, the influence of parameter deviations is investigated. Parameter deviations are intentionally introduced in the observer-controller scheme. First, a resistance variation of +50 % with full load torque application is carried out. The results for this case are

(a)

(b)
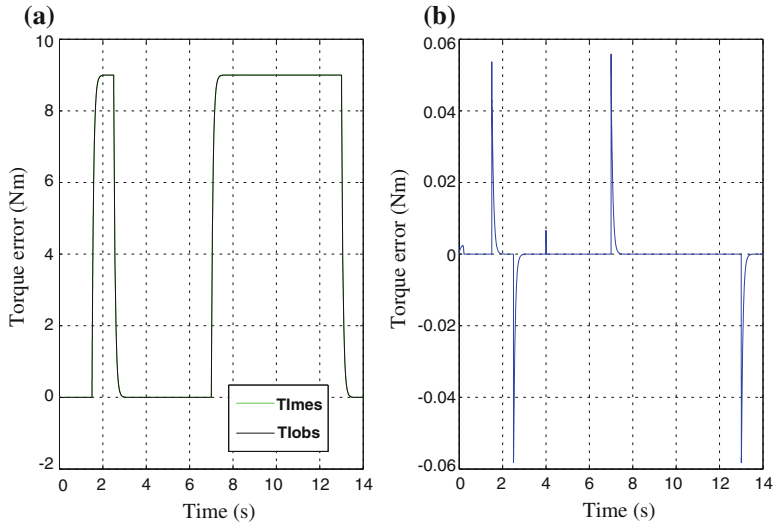
Fig. 6.7 Case $+50\,\%R_s$. **a** Estimated and real speeds. **b** Speed estimation error

(a)

(b)
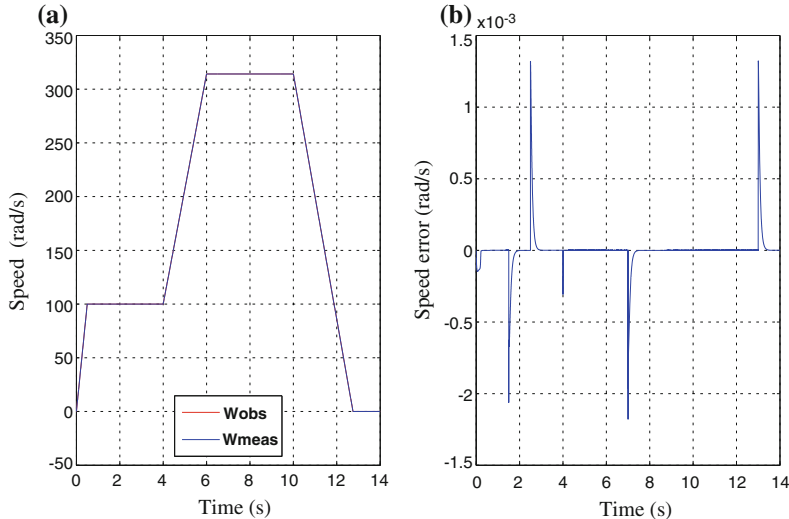
Fig. 6.8 Case $+50\,\%\ R_s$. **a** Estimated and real resistances. **b** Resistance estimation error

displayed in Figs. 6.7, 6.8 and 6.9 showing the speed, resistance, and load torque estimation, respectively.

Figure 6.10 shows the estimated speed for a variation of $-50\,\%$ introduced in the resistance value with fully loaded motor. Furthermore, the resistance and load torque estimation are exhibited in Figs. 6.11 and 6.12, respectively. The results reveal the efficiency of the proposed observer-controller scheme.
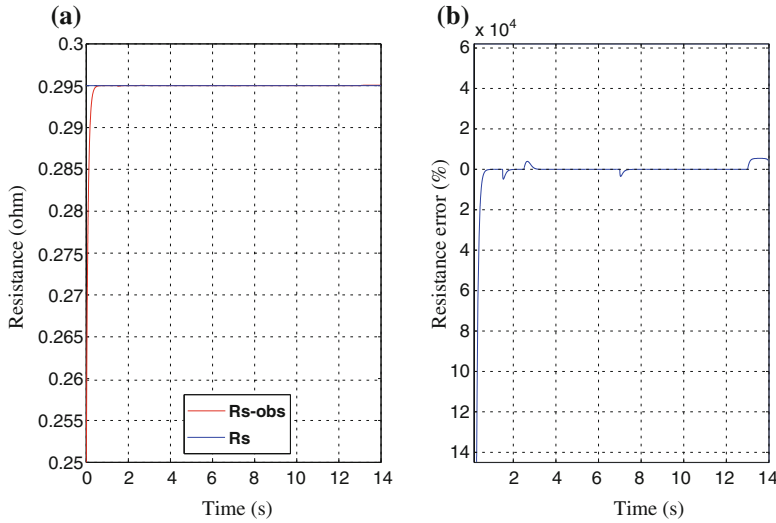
Fig. 6.9 Load torque estimation, case $+50\%$ R_s. **a** Estimated and applied load torques. **b** Load torque estimation error
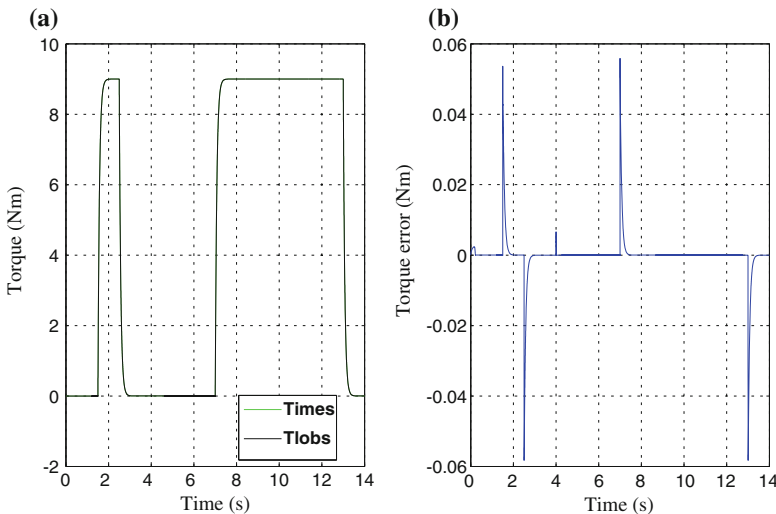
Fig. 6.10 Case -50% R_s. **a** Estimated and real speeds. **b** Speed estimation error

Conclusions

A robust sensorless speed observer-control scheme for a surface PMSM has been designed by combining an adaptive high gain interconnected observer that estimates the rotor speed and the position, and that identifies the stator resistance and the load

Fig. 6.11 Case -50% R_s. **a** Estimated and model resistances. **b** Resistance estimation error

Fig. 6.12 Load torque estimation, case -50% R_s. **a** Estimated and applied load torques. **b** Load torque estimation error

torque simultaneously, with a backstepping controller forcing the rotor speed and the stator currents to track the desired references. Sufficient conditions have been given to ensure the practical stability of the estimation and the tracking errors. The closed-loop system has been tested by simulation on an industrial benchmark, where the proposed controller-observer scheme shows good performance in spite of the uncertainties and the unknown load torque.

6.1.2 IPMSM Case

In this section, a sensorless speed control for the IPMSM is designed by combining an adaptive interconnected observer, proposed in Sect. 3.2.2, and a robust backstepping controller with integral actions, introduced in Sect. 4.1.2. The total observer-controller-system scheme is shown in Fig. 6.13.

The stability of the closed-loop system with the observer-controller scheme is analyzed and sufficient conditions are given to guarantee the practical stability. The performance of the proposed scheme under parametric uncertainties, the unknown load torque and at low speed, are illustrated via simulation results. Furthermore, a comparative study is considered where the proposed integral backstepping control is compared with the classical backstepping controller.
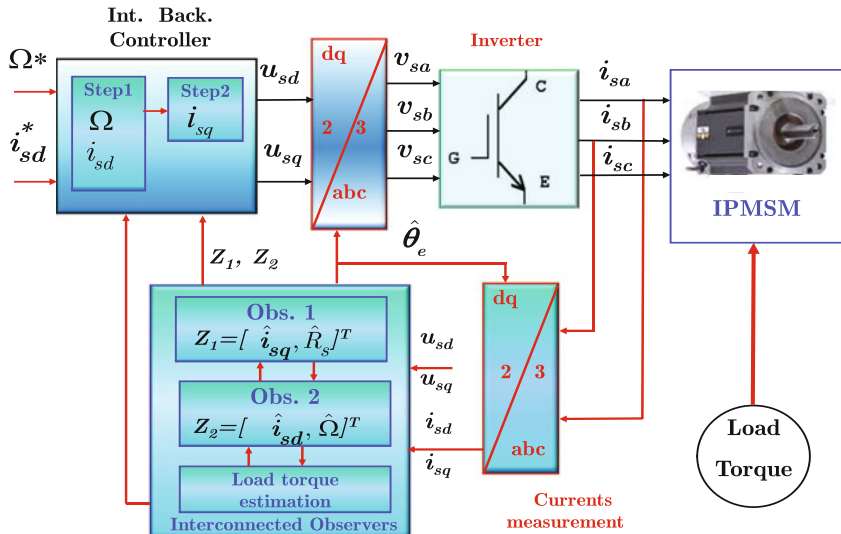
Stability Analysis of Observer-Controller in Spite of Uncertain Parameters and Unknown Load Torque

We start the stability analysis of the system in closed-loop with the observer-controller scheme, by considering the following candidate Lyapunov function:

$$V_{oc} = V_o + V_c \tag{6.12}$$

where V_c is the Lyapunov function of the controlled system defined as

$$\begin{aligned} V_c &= V_d + V_q \\ &= \frac{1}{2}\left[z_\Omega^2 + z_q^2 + z_q'^2 + z_d^2 + z_d'^2\right] \end{aligned} \tag{6.13}$$

Fig. 6.13 Adaptive interconnected observer and integral backstepping controller

and V_o is the Lyapunov function associated to the observer dynamics given by

$$V_o = \epsilon_1^T S_1 \epsilon_1 + \epsilon_2^T S_2 \epsilon_3 + \epsilon_3^T S_3 \epsilon_3. \tag{6.14}$$

The time derivative of V_o is given by

$$\dot{V}_o \leq -\delta V_o + \mu \psi_o \sqrt{V_o}, \tag{6.15}$$

for suitable positive constants coefficients δ, μ, ψ_o (see [38]).

Taking into account that the control laws are function of the estimates provided by the observer, the time derivative of V_c is

$$\dot{V}_c = -k_\Omega z_\Omega^2 + z_q \left\{ \frac{di_{sq}^*}{dt} + \frac{R_s}{L_q} i_{sq} + p \frac{L_d}{L_q} \Omega i_d + p \frac{1}{L_q} \Phi_f \Omega \right.$$
$$\left. - \frac{1}{L_q} v_{sq}(\widehat{X}) + k_q'(i_{sq}^* - i_{sq}) + k_q'(i_{sq}^* - i_{sq}) \right\} + z_q' k_q'(i_q^* - i_{sq})$$
$$+ z_d \left\{ \frac{R_s}{L_d} i_{sd} - p \frac{L_q}{L_d} \Omega i_{sq} - \frac{1}{L_d} v_{sd}(\widehat{X}) \right\} + k_d'\{z_d + z_d'\}\{z_d - z_d'\}. \tag{6.16}$$

Adding the terms $\pm v_{sq}(X)$ and $\pm v_{sd}(X)$ in the above equation, it follows that

$$\dot{V}_c = -k_\Omega z_\Omega^2 - \{k_q - k_q'\}z_q^2 - k_q' z_q'^2 - \frac{1}{L_q} z_q \{v_{sq}(\widehat{X}) - v_{sq}(X)\}$$
$$- \{k_d - k_d'\}z_d^2 - k_d' z_d'^2 - \frac{1}{L_d} z_d \{v_{sd}(\widehat{X}) - v_{sd}(X)\}. \tag{6.17}$$

Introducing the following inequalities:

$$|z_j| \, \|\epsilon_1\|_{s_1} \leq \frac{\xi_{j1}}{2} \|\epsilon_1\|_{s_1}^2 + \frac{1}{2\xi_{j1}} |z_j|^2$$

$$|z_j| \, \|\epsilon_2\|_{s_2} \leq \frac{\xi_{j2}}{2} \|\epsilon_2\|_{s_2}^2 + \frac{1}{2\xi_{j2}} |z_j|^2$$

$$|z_j| \, \|\epsilon_3\|_{s_3} \leq \frac{\xi_{j3}}{2} \|\epsilon_3\|_{s_3}^2 + \frac{1}{2\xi_{j3}} |z_j|^2 \tag{6.18}$$

$$|v_{sq}(\widehat{X}) - v_{sq}(X)| \leq L_1\{\|\epsilon_1\|_{s_1} + \|\epsilon_2\|_{s_2} + \|\epsilon_3\|_{s_3}\}$$

$$|v_{sd}(\widehat{X}) - v_{sd}(X)| \leq L_2\{\|\epsilon_1\|_{s_1} + \|\epsilon_2\|_{s_2} + \|\epsilon_3\|_{s_3}\}$$

$\forall \, \xi_{j1}, \, \xi_{j2}, \, \xi_{j3} \in \,]0 \; 1[$; for $j = q, d$; where L_1 and L_2 are the Lipschitz constants. Taking the time derivative of (6.12), and substituting (6.15)–(6.18) yields

$$\dot{V}_{oc} \leq -\delta V_o + \mu \psi_o \sqrt{V_o} + \vartheta_1 \|\epsilon_1\|_{s_1}^2 + \vartheta_2 \|\epsilon_2\|_{s_2}^2 + \vartheta_3 \|\epsilon_3\|_{s_3}^2$$
$$- \vartheta_4 z_\Omega^2 - \vartheta_5 z_q^2 - \vartheta_6 z_q'^2 - \vartheta_7 z_d^2 - \vartheta_8 z_d'^2 \tag{6.19}$$

where

$$\vartheta_1 = \frac{L_1\xi_{q1}}{2L_q} + \frac{L_2\xi_{d1}}{2L_d}, \qquad\qquad\qquad \vartheta_2 = \frac{L_1\xi_{q2}}{2L_q} + \frac{L_2\xi_{d2}}{2L_d},$$

$$\vartheta_3 = \frac{L_1\xi_{q3}}{2L_q} + \frac{L_2\xi_{d3}}{2L_d}, \qquad\qquad\qquad \vartheta_4 = k_\Omega,$$

$$\vartheta_5 = \{k_q - k'_q\} - \frac{L_1}{2L_q}\left\{\frac{1}{\xi_{q1}} + \frac{1}{\xi_{q2}} + \frac{1}{\xi_{q3}}\right\}, \qquad \vartheta_6 = k'_q,$$

$$\vartheta_7 = \{k_d - k'_d\} - \frac{L_2}{2L_d}\left\{\frac{1}{\xi_{d1}} + \frac{1}{\xi_{d2}} + \frac{1}{\xi_{d3}}\right\}, \qquad \vartheta_8 = k'_d.$$

By selecting $\vartheta_O = max(\vartheta_1, \vartheta_2, \vartheta_3)$ and $\vartheta_C = min(\vartheta_4, \vartheta_5, \vartheta_6, \vartheta_7, \vartheta_8)$, then the inequality (6.19) becomes

$$\dot{V}_{oc} \leq -(\delta - \vartheta_O)V_o + \mu\psi_o\sqrt{V_o} - \vartheta_C(z_\Omega^2 + z_q^2 + z_q'^2 + z_d^2 + z_d'^2). \qquad (6.20)$$

Choosing $\eta = min(\delta - \vartheta_O, \vartheta_C)$, from (6.20) it is obtained that

$$\dot{V}_{oc} \leq -\eta V_{oc} + \mu\psi_o\sqrt{V_{oc}}. \qquad (6.21)$$

Define the following change in variable $v_{oc} = 2\sqrt{V_{oc}}$, and taking the time derivative of v_{oc}, we obtain

$$\dot{v}_{oc} \leq -\eta v_{oc} + \psi_o\mu$$

whose solution is given as

$$v_{oc} \leq v_{oc}(t_0)e^{-\eta(t-t_0)} + \frac{\psi_o\mu}{\eta}\left(1 - e^{-\eta(t-t_0)}\right). \qquad (6.22)$$

Following the same procedure as the proof given for the observer (see Sect. 3.2.2), the strongly uniformly practical stability of the observer-controller scheme can be ensured. Hence, the estimation and tracking errors of the closed-loop system converge toward a ball $B_{\hbar_{oc}}$ of radius $\hbar_{oc}$ with $\hbar_{oc} = \frac{\psi_o\mu}{\eta}$.

Then, the above result can be summarized in the following theorem.

Theorem 6.2 *Consider the IPMSM dynamic model (1.70) with a reference signal Ω^* assumed to be differentiable and bounded. Then, by using the estimates provided by the adaptive interconnected observer (3.84) and (3.85) for the integral backstepping controller designed in Sect. 4.1.2, the closed-loop system tracking error is strongly uniformly practically stable.*

Simulation Results

The performance of the proposed IPMSM sensorless controller is investigated thanks to simulations. Simulations are carried out following the observer-controller scheme shown in Fig. 6.13.

Table 6.2 IPMSM nominal parameters

Current	6 A	Torque	5.3 Nm
Speed	3,000 rpm	Ψ_r	0.341 Wb
R_s	3.25 ohm	p	3
L_d	18 mH	L_q	34 mH
J	0.00417 kg m^2	f_v	0.0034 kg m^2 s^{-1}

Table 6.2 gives the nominal parameters of the IPMSM that are used for the simulation tests. The simulation has been carried out using Matlab/Simulink software. The motor is tested according to industrial test trajectories (see Chap. 1 for more details).

As usual for industrial applications, the stator resistance as well as the stator inductance is known with some uncertainties with respect to their nominal values. So it is important to study their deviation effects with respect to the sensorless control scheme performance. The gain tuning design is given below (for more details see Appendix A.2 of [38]).

Summary 6.2.1 Tuning parameters

Controller
$$k_\Omega = 120, k'_\Omega = 12, k_q = 150, k'_q = 10, k_d = 100, k'_d = 8.$$

Observer
$$\rho_1 = 900, \rho_2 = 800, \rho_3 = 15, \varpi = 80, k_{c1} = 0.1,$$
$$k_{c2} = 0.01, \alpha = 0.1.$$

Observer initial conditions
$$\hat{\Omega} = 10 \,\text{rad/s}, \hat{\theta}_m = 0.6 \,\text{rad}, \hat{T}_l = 0 \,\text{Nm}, \hat{R}_s = 2 \,\text{ohm}.$$
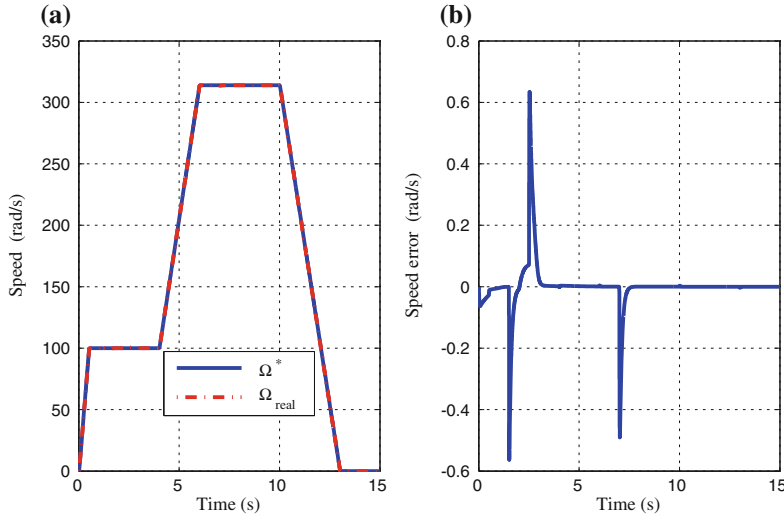
The IPMSM nominal parameter values are given in Table 6.2.
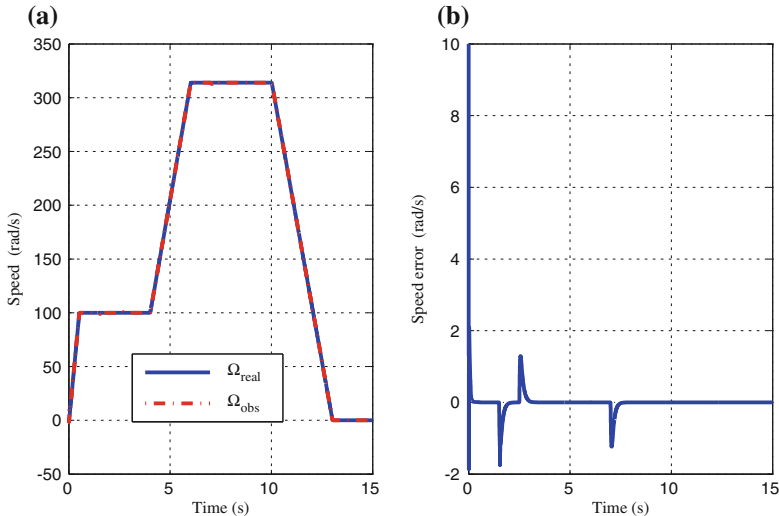
The simulation results of the IPMSM sensorless control are given in Figs. 6.14, 6.15, 6.16, 6.17, 6.18, 6.19 and 6.20 for the nominal parameters case: the controller and the observer are designed using the same parameters as the motor model parameters. The motor is initially running under no-load condition. Full-load torque is applied in the time intervals from $t = 1.5$ to 2.5 s, and from $t = 7$ to 15 s.

Figure 6.14a shows the reference and the measured rotor speeds. The speed error due to the perturbation is very small and quickly converges to zero after the transients that are induced by the load torque application (see Fig. 6.14b).

Figure 6.15a shows the estimated and measured speeds. The speed error is displayed in Fig. 6.15b. These responses are detailed in Fig. 6.16. The estimated speed tracks the actual speed very well. Figure 6.17 gives the measured and estimated positions. By Figs. 6.18 and 6.19, the resistance and load torque estimations are

(a)

(b)
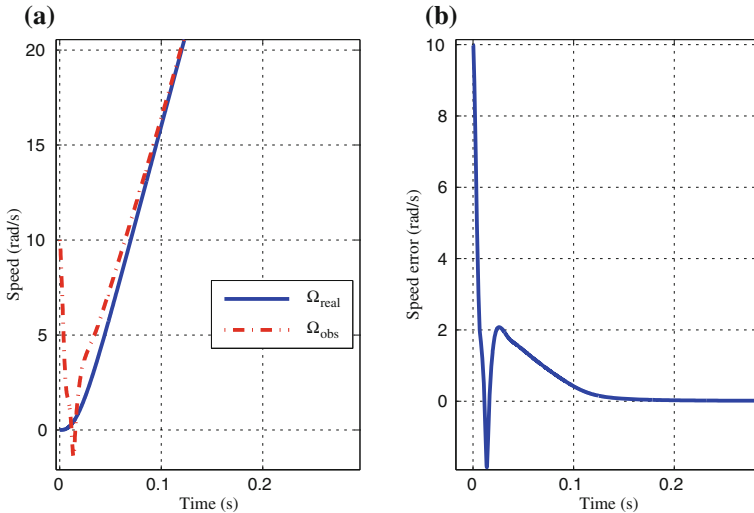
Fig. 6.14   Speed tracking: nominal case. **a** Reference and measured speeds, **b** speed error

(a)

(b)
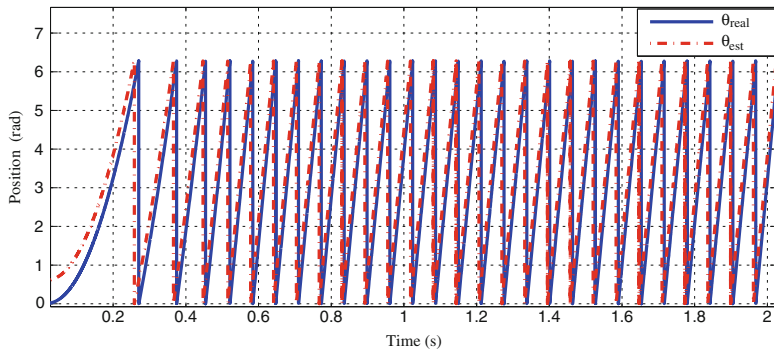
Fig. 6.15   Speed tracking: nominal case. **a** Real and estimated speeds, **b** speed error

respectively displayed. Figure 6.18 shows the estimation of the stator resistance with a voluntary quick change from 1.9 to 3.25 Ω. The estimated resistance converges very well to the actual value. The torque estimation is displayed by Fig. 6.20. It is clear that the observer has good performance for these estimations.

(a)

(b)

Fig. 6.16 Zoom of Speed tracking: nominal case. **a** Real and estimated speeds, **b** speed error
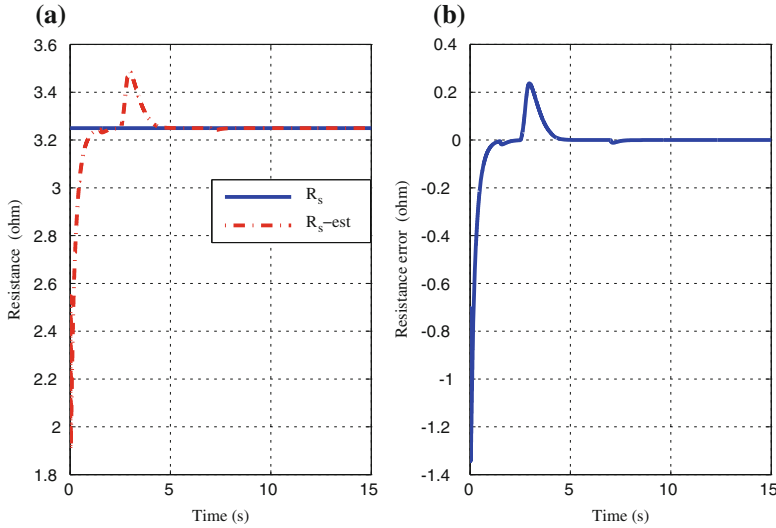
Fig. 6.17 Measured and estimated positions w.r.t. time (s): nominal case
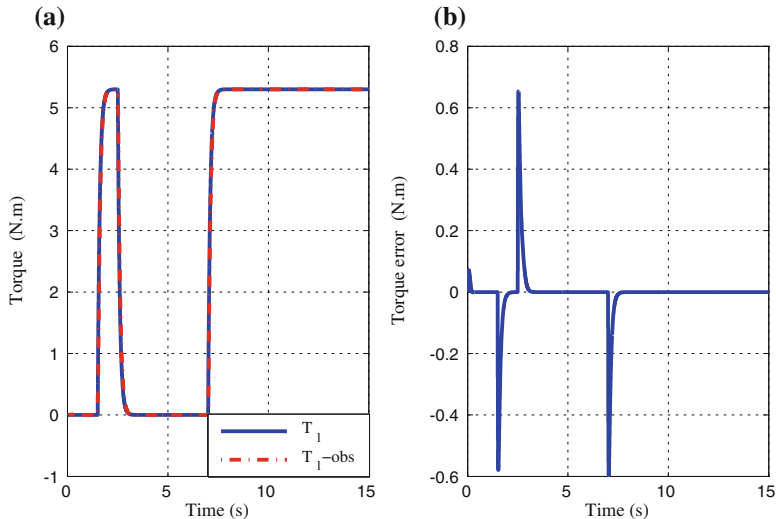
Now, in order to illustrate the robustness of the sensorless control scheme, the influence of parameter deviations is investigated. Parameter deviations are intentionally introduced in the observer-controller scheme. First, Figs. 6.21, 6.22 and 6.23 show the responses for a +50 % variation of the stator resistance value.

Secondly, the robustness with respect to the inductances is tested. Figures 6.24, 6.25 and 6.26 show the responses for a +20 % change of the (d, q) axes stator inductances.

Figures 6.27 and 6.28 show the responses for a +25 % deviation of the rotor inertia J. A zoom is given on the speed error to display that, for uncertain case, only practical stability is obtained (no asymptotic stability). However, the response on the speed tracking is satisfactory.
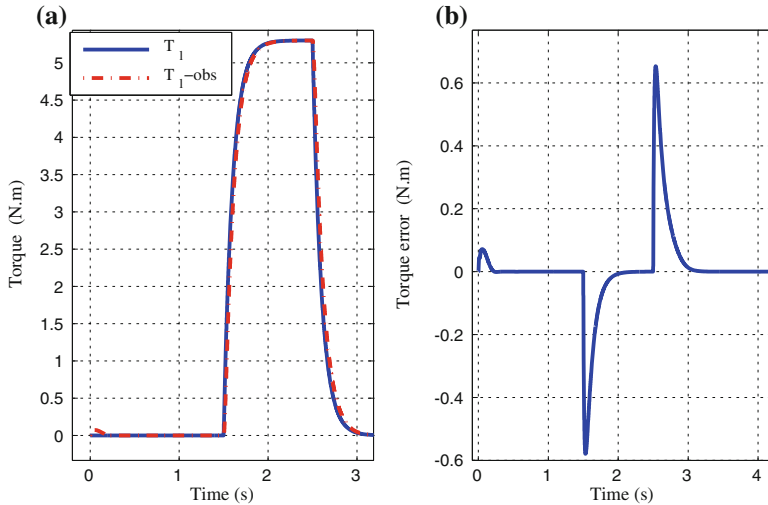
Fig. 6.18 R_s estimation: nominal case. **a** Real and estimated resistances, **b** resistance error
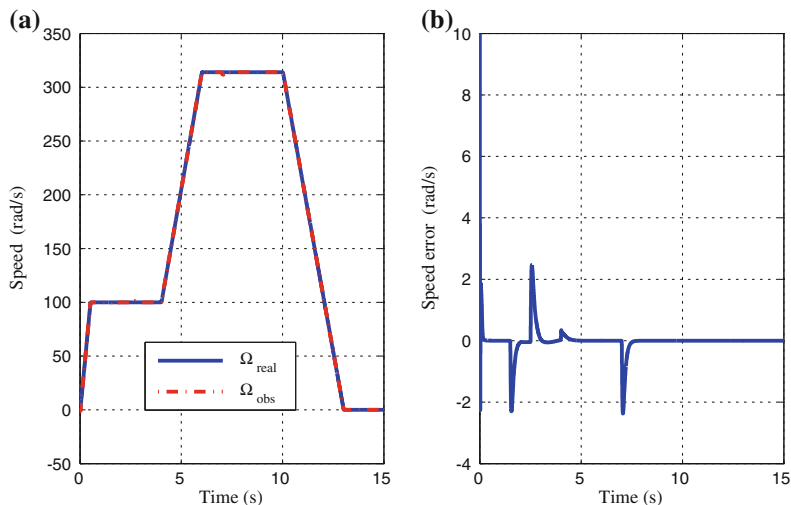
Fig. 6.19 Torque estimation: nominal case. **a** Real and estimated torques, **b** torque error

For all these cases, the robustness and the efficiency of the proposed sensorless control under parameter variations and the load torque variation clearly has been illustrated.

Finally, to compare the performance of a Classical Backstepping Controller (CBC) with respect to the new Integral Backstepping Controller (IBC), it is shown in

(a)

(b)
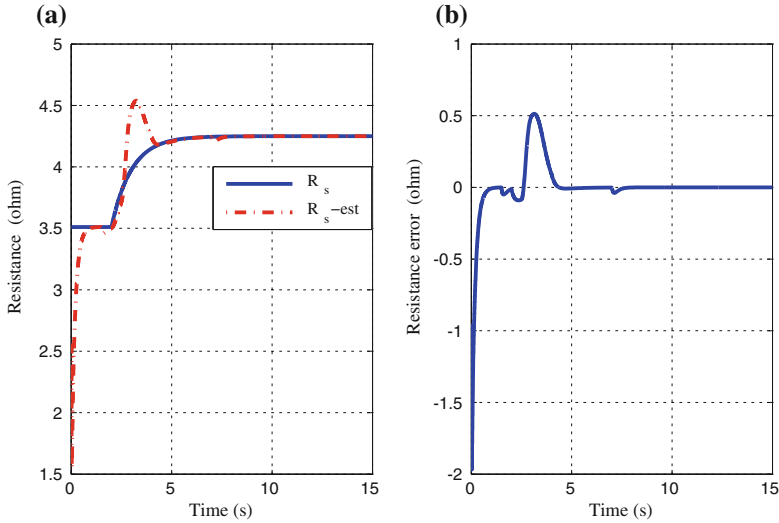
Fig. 6.20 Zoom of torque estimation: nominal case. **a** Real and estimated torques, **b** torque error

(a)

(b)
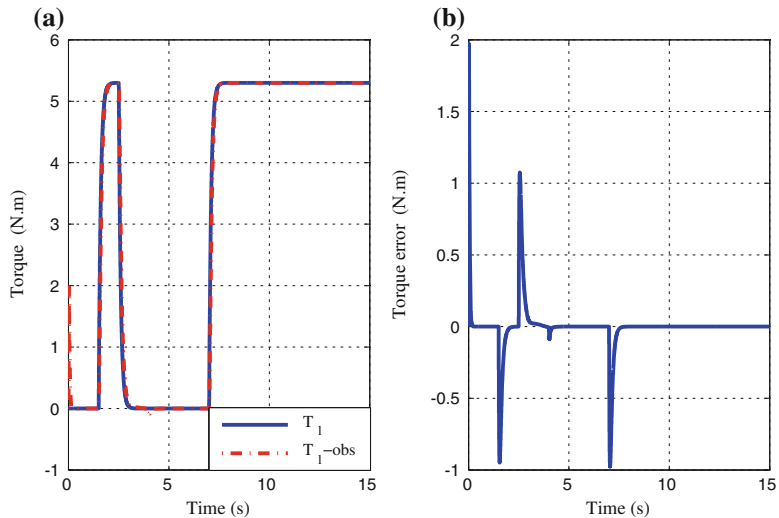
Fig. 6.21 Speed tracking: robustness w.r.t. $+50\%$ R_s deviation. **a** Real and estimated speeds, **b** speed error

Fig. 6.29 the speed errors for a $+20\%$ $L_d - L_q$ deviation, and in Fig. 6.30 the speed errors for a -20% $L_d - L_q$ deviation. These two latter figures clearly show the benefits of the integral backstepping algorithm with respect to the classical backstepping control.
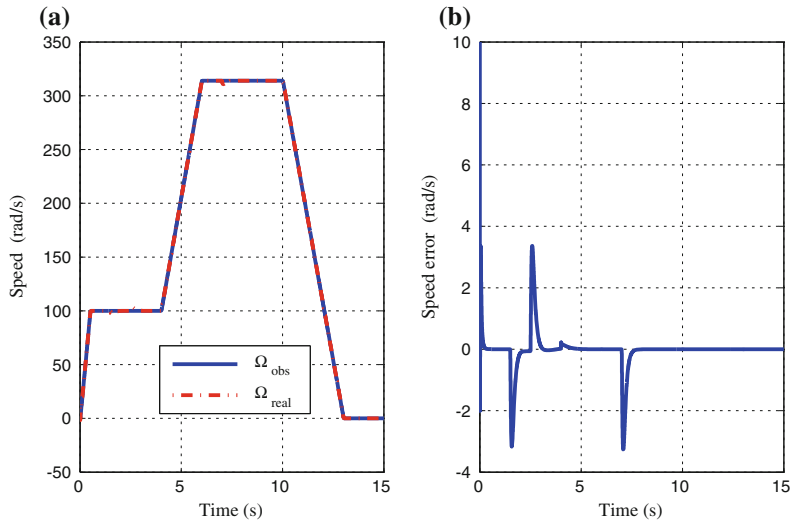
Fig. 6.22 Resistance estimation: robustness w.r.t. $+50\%$ R_s deviation. **a** Real and estimated resistances, **b** resistance error
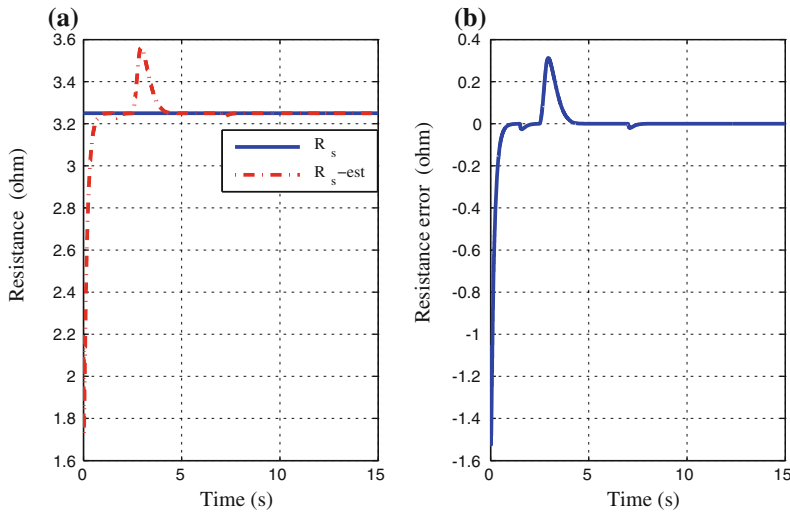
Fig. 6.23 Torque estimation: robustness w.r.t. $+50\%$ R_s deviation. **a** Real and estimated torques, **b** torque error

Conclusions
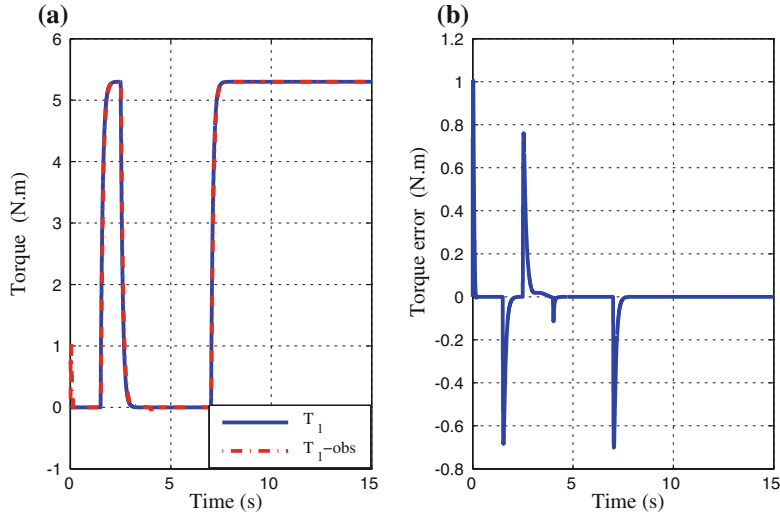
A robust sensorless control for the salient-pole IPMSM combining a robust backstepping controller plus an integral action with an adaptive interconnected observer has been presented. Based on Lyapunov stability analysis, sufficient conditions have
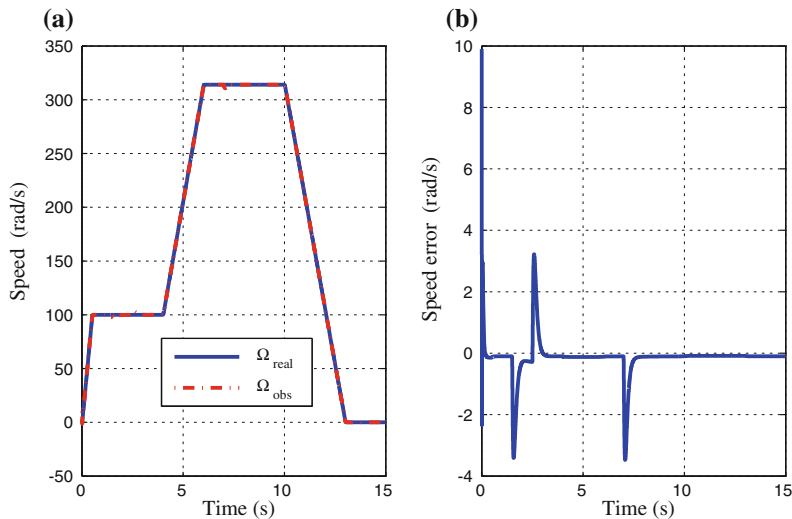
Fig. 6.24 Speed tracking: robustness w.r.t. $+20\%$ $L_d - L_q$ deviation. **a** Real and estimated speeds, **b** speed error
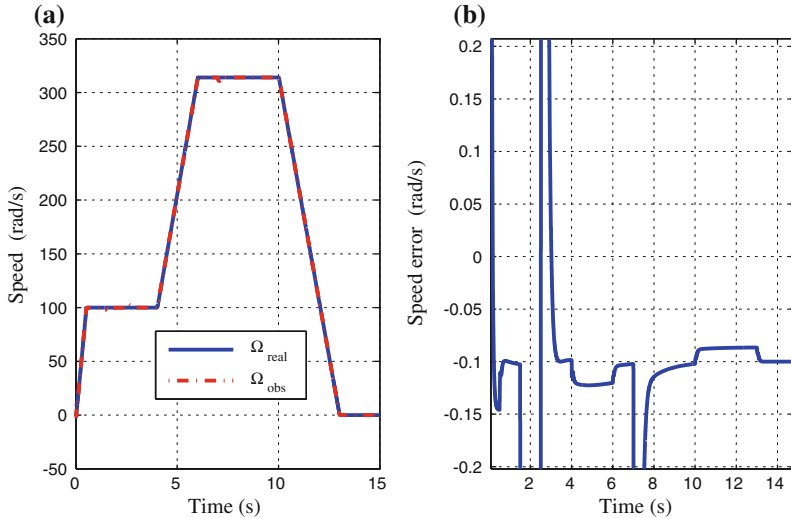
Fig. 6.25 Resistance estimation: robustness w.r.t. $+20\%$ $L_d - L_q$ deviation. **a** Real and estimated resistances, **b** resistance error
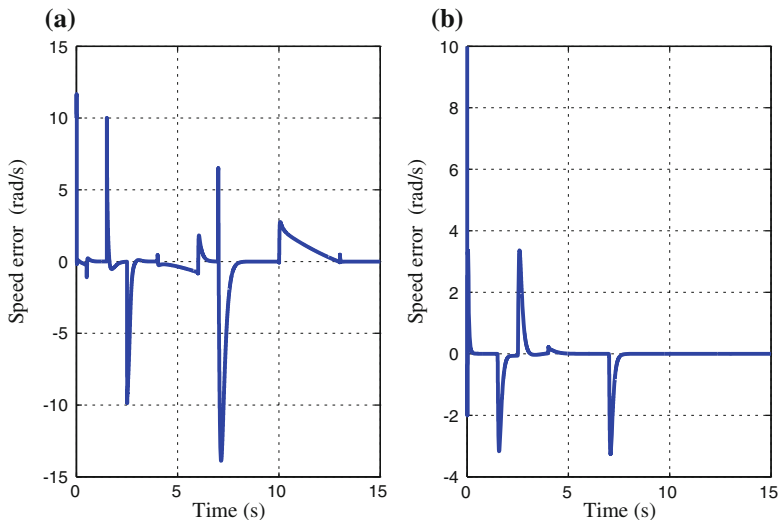
Fig. 6.26 Torque estimation: robustness w.r.t. $+20\%$ $L_d - L_q$ deviation. **a** Real and estimated torques, **b** torque error

Fig. 6.27   Speed tracking: robustness w.r.t. $+25\%$ J deviation. **a** Real and estimated speeds, **b** speed error

(a)

(b)
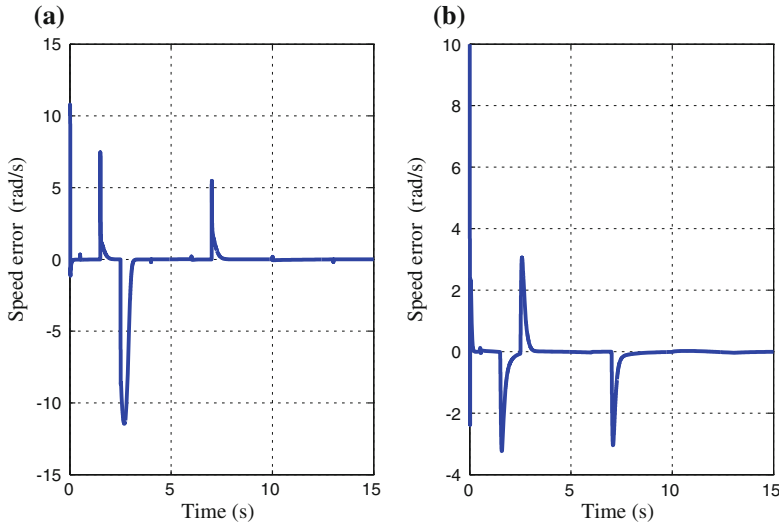
Fig. 6.28 Zoom of speed tracking: robustness w.r.t. $+25\%$ J deviation. **a** Real and estimated speeds, **b** speed error

(a)

(b)

Fig. 6.29 Speed errors w.r.t. -20% $L_d - L_q$ deviation with: **a** backstepping control, **b** integral backstepping control

been obtained to ensure the practical stability of the system in closed-loop with the proposed observer-controller.

Notice that the tuning of the observer-controller is simple and easy. The computational effort is not important, and for all the cases tested by simulation, it can be concluded that this control strategy is robust under parametric uncertainties and unknown load torque.

Fig. 6.30   Speed errors w.r.t. -20% $L_d - L_q$ deviation with: **a** backstepping control, **b** integral backstepping control

6.2 Robust Adaptive High Order Sliding Mode Control
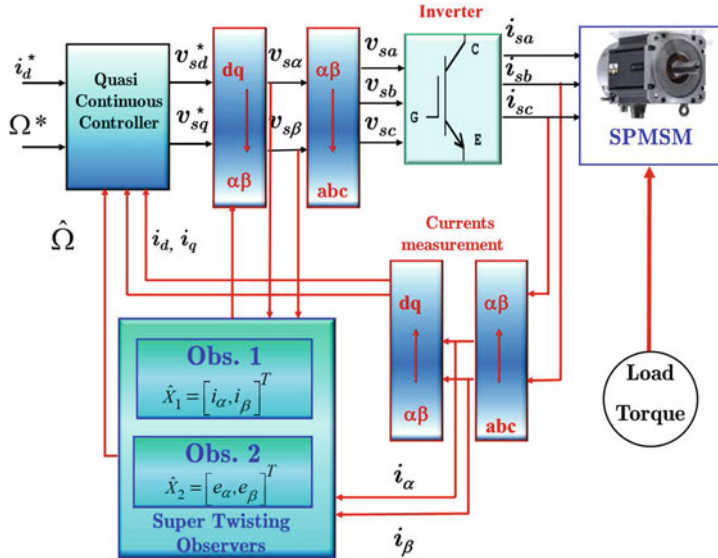
6.2.1 SPMSM Case

This section deals with the sensorless Surface Permanent Magnet Synchronous Motor (SPMSM) control by using a super-twisting algorithm observer (designed in Sect. 3.3.2) combined with the high order sliding mode control designed in Sect. 4.2.1. The advantage of these algorithms is based on the attractive property of the sliding mode technique: the robustness. Moreover, thanks to the finite time convergence of the super-twisting algorithm, the estimation of non-measurable variables can be done before to apply the control action to the motor. Thus, the separation principle is easy to satisfy in this case. Furthermore, the super-twisting observer is implemented to estimate the speed and the position of the motor from the stator currents and voltages, which are available from measurements. The observer-controller scheme is shown in Fig. 6.31.

Using an industrial benchmark for the SPMSM, introduced in Chap. 1, simulation results are shown to illustrate the performance of the proposed scheme. The results are obtained in presence of parameter uncertainties on stator resistance and on stator inductance.

Convergence of the Observer-Controller Scheme

Since the observer has a finite-time convergence, as established in [19], there is no difficulty to prove the convergence of the observer-controller scheme. Then, it is

Fig. 6.31 Super-twisting observer and quasi-continu HOSM controller

only necessary to tune the gains of the observer such that the observer converges sufficiently fast in finite-time and once the observer convergence is ensured, the controller can be then started, i.e., the observer-controller scheme can be successfully applied without stability problem.

Simulation Results

The proposed observer-controller scheme has been simulated in closed-loop with the SPMS motor to evaluate the robustness performance. The parameters of the SPMSM are given in Table 6.1 (Sect. 6.1.1). This motor is coupled to another synchronous machine that is torque controlled. The motor is tested according to an industrial benchmark (see Chap. 1 for more details). Of course the measured speed is used only for comparison purpose. The stator resistance and the stator inductance are varied from their nominal values, and then the resulting effects are studied.
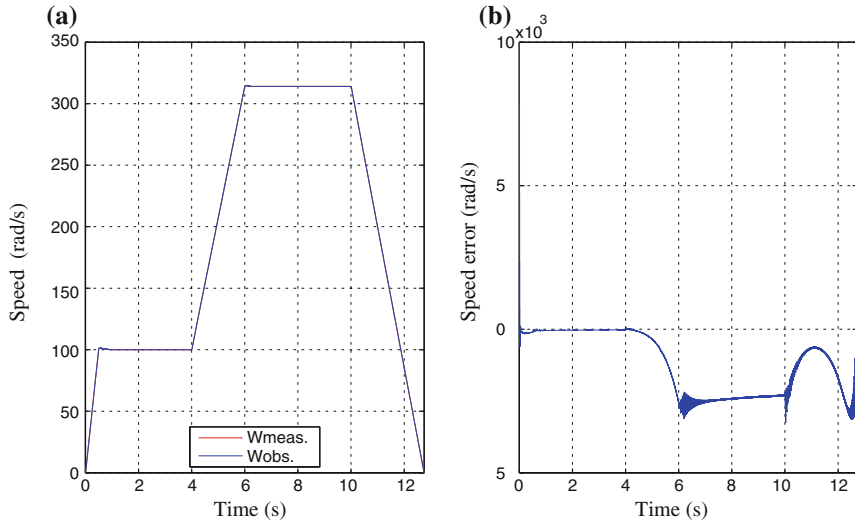
   Better performance of the proposed scheme is achieved, when the parameters of the controller and of the observer are chosen as follows:
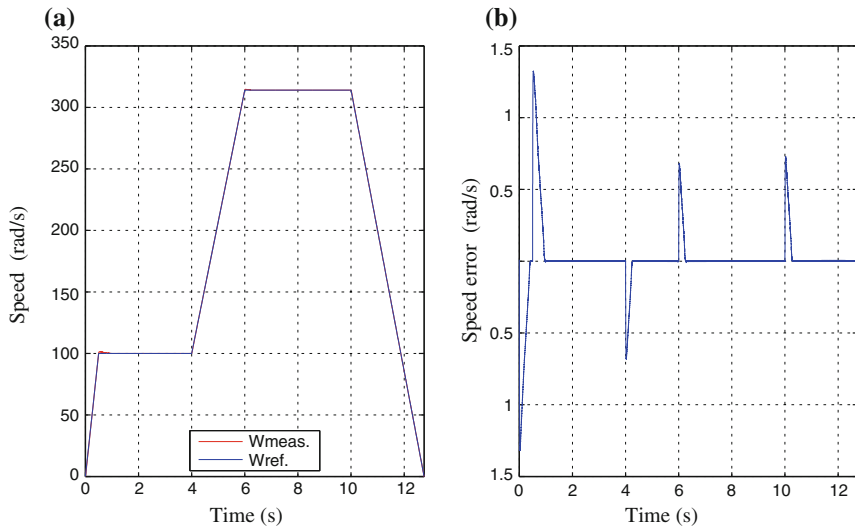
> *Summary* 6.2.1 Tuning parameters
> *Controller:* $\alpha_1 = 9 * 10^4$, $\alpha_2 = 3 * 10^3$
> *Observer:* $\alpha_{1,1} = 10$, $\alpha_{1,2} = 10$, $\alpha_{2,1} = 500$, $\alpha_{2,2} = 500$.

   Figure 6.32a shows the measured speed Ω and the estimated speed as well as the speed error for the nominal case in Fig. 6.32b. It can be seen that the estimation error is very small showing the speed estimation quality.
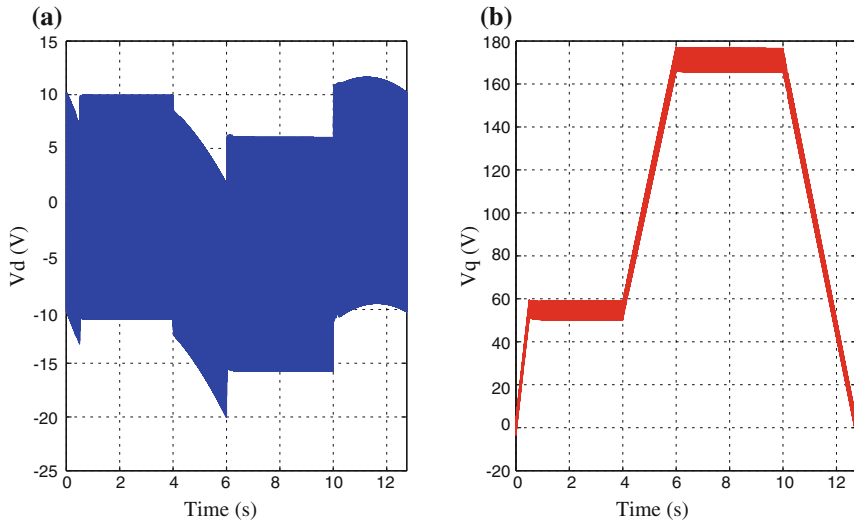
Fig. 6.32 **a** Measured and estimated speeds. **b** Observed speed error
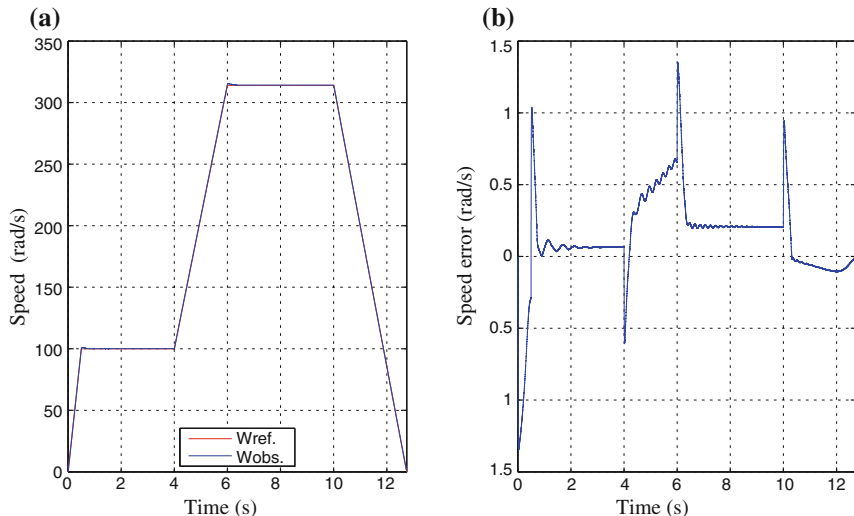
Fig. 6.33 **a** Measured and reference speeds. **b** Tracking speed error

Figure 6.33a displays the measured and the reference speeds, whereas the tracking error is plotted in Fig. 6.33b. This result attests the good tracking of the observer-controller scheme.

Figure 6.34 shows the control inputs (v_{sd}, v_{sq}) applied to the motor.

(a)

(b)
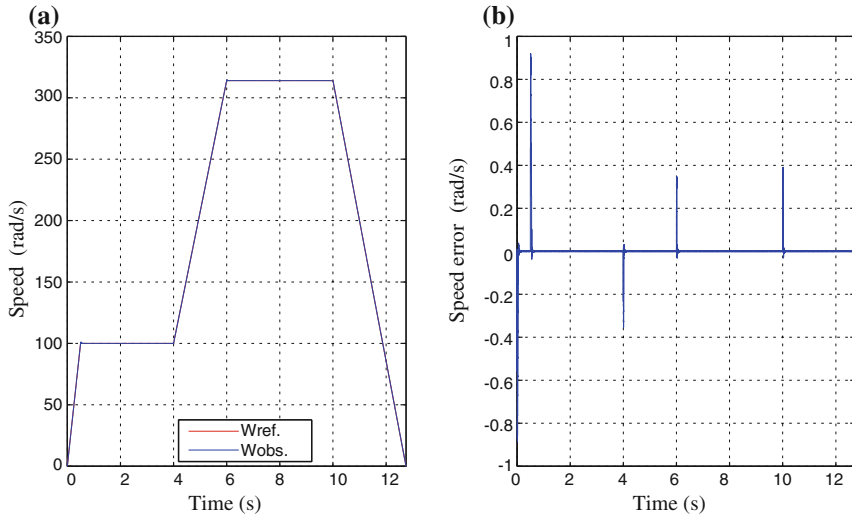
Fig. 6.34   Control inputs v_{sd}, v_{sq}

(a)

(b)
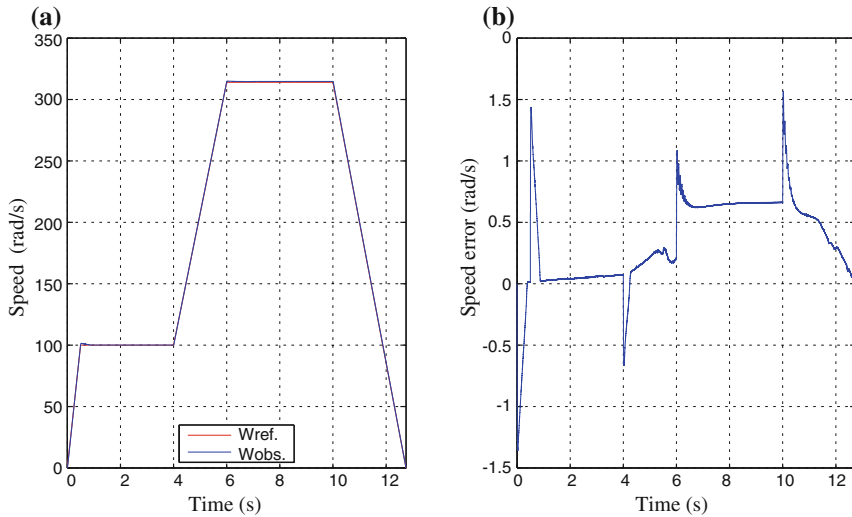
Fig. 6.35   **a** Reference and estimated speeds for $+50\,\%\,R_s$. **b** Speed error

Robustness tests

Now, in order to test the robustness of the proposed scheme, variations of $+50$ and $-50\,\%$ in the stator resistance value are introduced in the observer-controller scheme parameters. In Figs. 6.35 and 6.36 are plotted the corresponding responses.

Fig. 6.36 **a** Reference and estimated speeds for $-50\,\%R_s$. **b** Speed error
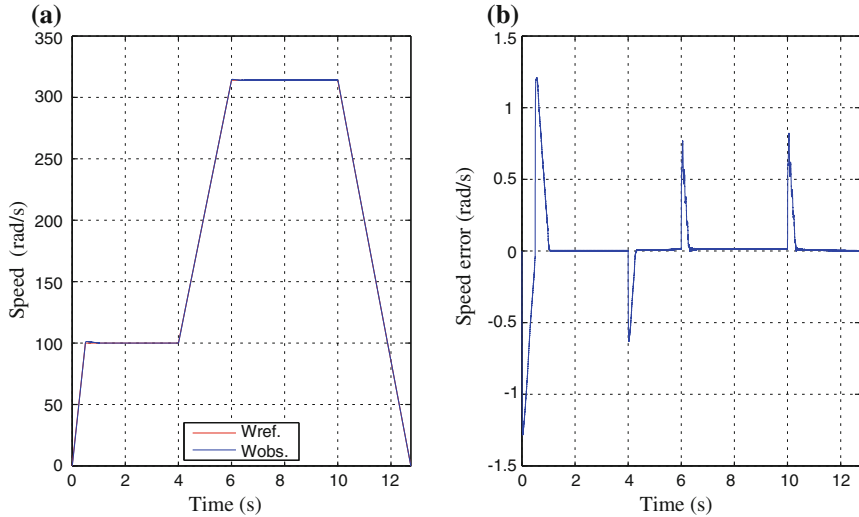
Fig. 6.37 **a** Reference and estimated speeds for $+20\,\%L_s$. **b** Speed error
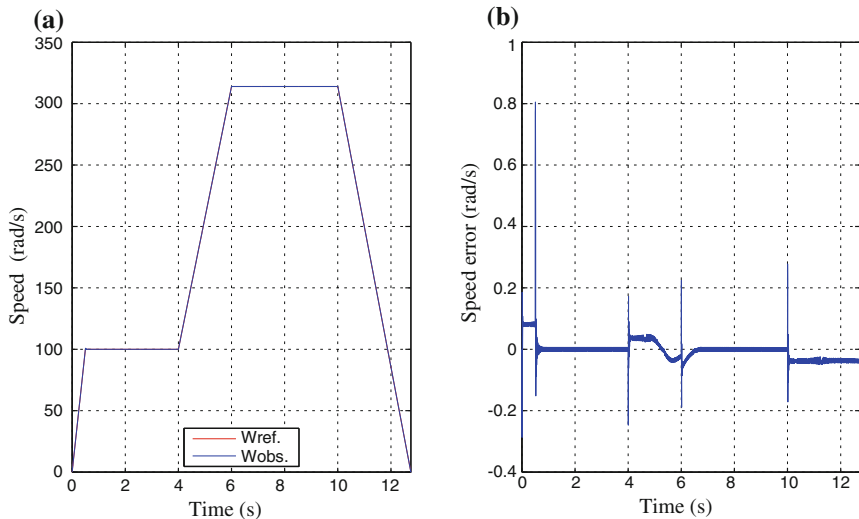
The following test results consider stator inductance variations of $+20\,\%$ given in Fig. 6.37 and of $-20\,\%$ variation which is plotted in Fig. 6.38 .

Finally, the results considering a $+50\,\%$ variation of the total inertia are shown in Fig. 6.39.

All these tests clearly show the robustness of the proposed observer-controller scheme.

(a)

(b)

Fig. 6.38 **a** Reference and estimated speeds for $-20\,\%L_s$. **b** Speed error

(a)

(b)

Fig. 6.39 **a** Reference and estimated speeds for $+50\,\%J$. **b** Speed error

Conclusion

A sensorless robust control of a surface permanent magnet synchronous motor is achieved via a super-twisting sliding mode observer which estimates the rotor position and the rotor speed of the SPMSM. Furthermore, the controller is designed applying higher order sliding mode techniques, to achieve a robust and precise control. Moreover, the system in closed-loop with the observer-based controller has

been tested by using a specific industrial benchmark. Significant robustness tests are implemented and simulation results illustrate the efficiency of the proposed sensorless observer-controller scheme.

6.2.2 IPMSM Case

In Sect. 4.2.3, a high order sliding mode control with finite time convergence, fixed *a priori*, has been designed assuming the perfect knowledge of the state of the system.

For sensorless purpose, the controller is now designed by replacing the state variables by their estimates provided by the observer designed in Sect. 3.2.2. Then, in order to guarantee the correct behavior of the system in closed-loop with the observer-controller scheme, an analysis of stability is necessary. Sufficient conditions ensuring the stability of the closed-loop system are obtained (see also Lemma 2.1 in [80]), which can be summarized as follows (see [37] for details):

Lemma 6.1 *Consider the IPMSM model* (1.70) *in closed-loop with the high order sliding mode controller given in Summary* 4.2.3 *with gains defined by* (4.68)*,* (4.70)*, and using the estimations given by the interconnected observer* (3.84) *and* (3.85)*. Then, there exist* ϵ^**,* $K_{\Omega,i}$*,* $K_{i_{sd},i}$ *and* $\lambda_{\Omega,i}$*,* $\lambda_{i_{sd},i}$*, for* $i = 1, 2$*; such that the rotor speed and the current tracking errors satisfy*
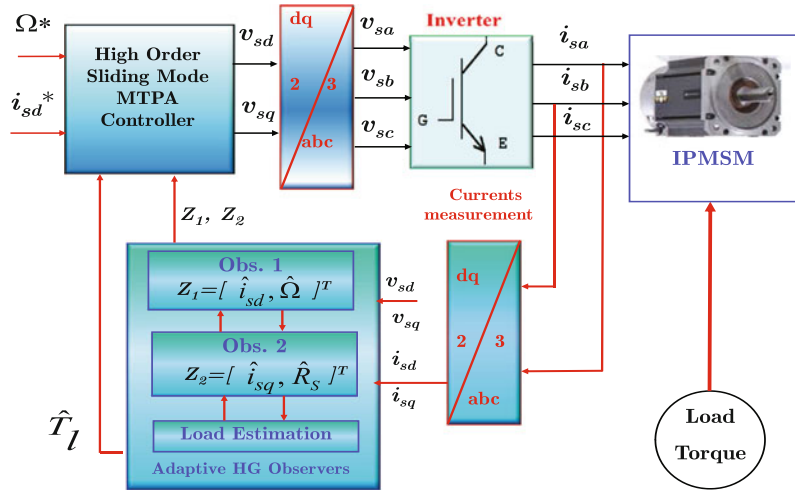
$$|\Omega - \Omega^*| \leq \frac{1}{\lambda_{\Omega,2}}(K_{\Omega,1}\epsilon^* + K_{\Omega,2})$$

$$|i_{sd} - i_{sd}^*| \leq \frac{1}{\lambda_{i_{sd},1}}(K_{i_{sd},1}\epsilon^* + K_{i_{sd},2}). \tag{6.23}$$

Remark 6.1 Two cases can be distinguished:

(1) *Nominal case* (*no parameter variations*) and unloaded drive, an asymptotic stability result of the closed-loop system is obtained under the action of the controller using the estimates provided by the observer. More precisely, the estimated and tracking errors tend to zero.
(2) *Uncertain case* (*with parameter variations and bounded load torque*). Then, a strong uniform practical stability condition of the closed-loop system is obtained, i.e., the convergence of the tracking error to a ball whose radius depends on the bounds of the parameter uncertainties and of the observer and controller gains.

Simulation Results

The sensorless control diagram of the observer-controller scheme with the MTPA strategy for the IPMSM is shown in Fig. 6.40. The proposed sensorless scheme has been tested by using Matlab/Simulink software following the specification of the industrial benchmark defined in Chap. 1. The trajectories of this benchmark are chosen to test the motor under different operation conditions, including when the

Fig. 6.40 Adaptive observer and HOSM controller scheme for IPMSM

motor works in the non-observable condition. At initial time, the speed and the load torque values are zero. Then, the reference speed is carried to 100 rad/s, and in the time interval from 1.5 to 2.5 s the load torque is applied. This first step allows to test the performance and the robustness of the observer at low speed. Following the possible acceleration on the setup, from 4 to 6 s, the speed is carried out to 314 rad/s and remains constant until 10 s with the load torque applied from 7 s. This second step is defined to test the observer during a great speed transient and to check its robustness at high speed. Then, the motor is driven to reach zero speed from 13 to 15 s when the load torque is applied. The system in closed-loop with the controller-observer scheme is then tested at zero speed. The motor parameters used in this simulation are given in Table 6.2 (Sect. 6.1.2).

Summary 6.2.1 Tuning parameters

   Observer

$$\rho_1 = 900, \rho_2 = 800, \rho_\eta = 15, \varpi = 80,$$
$$k_{c1} = 0.1, k_{c2} = 0.01, \alpha = 0.1, K_{\theta_m} = 40.$$

   Controller the convergence time t_f is fixed to 50 ms

      For $t \leq 50$ ms

$$\zeta_\Omega = 0.32, \ \omega_{n\Omega} = 250 \text{ rad/s}, \ \omega_{ni_d} = 32 \text{ rad/s}, \ \alpha = 5.10^4$$

      For $t > 50$ ms
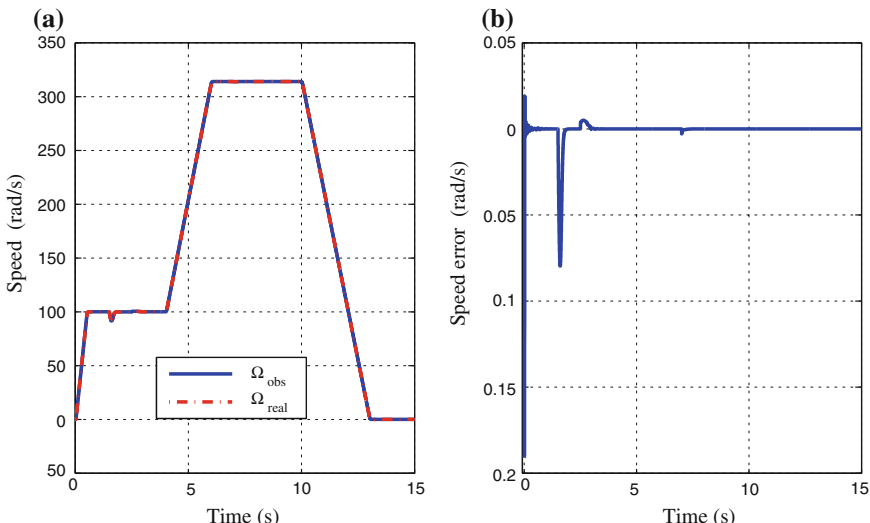
$$\zeta_\Omega = 0.35, \ \omega_{n\Omega} = 325 \text{ rad/s}, \ \omega_{ni_d} = 85 \text{ rad/s}, \ \alpha = 6.10^6$$

$$F_\Omega = \begin{bmatrix} -1 & 0 & 0 & 0 & 0 & 0 \\ 0 & -1.1 & 0 & 0 & 0 & 0 \\ 0 & 0 & -1.2 & 0 & 0 & 0 \\ 0 & 0 & 0 & -1.3 & 0 & 0 \\ 0 & 0 & 0 & 0 & -1.4 & 0 \\ 0 & 0 & 0 & 0 & 0 & -1.5 \end{bmatrix}, \quad J_\Omega = \begin{bmatrix} 1 \\ 1 \\ 1 \\ 1 \\ 1 \\ 1 \end{bmatrix},$$
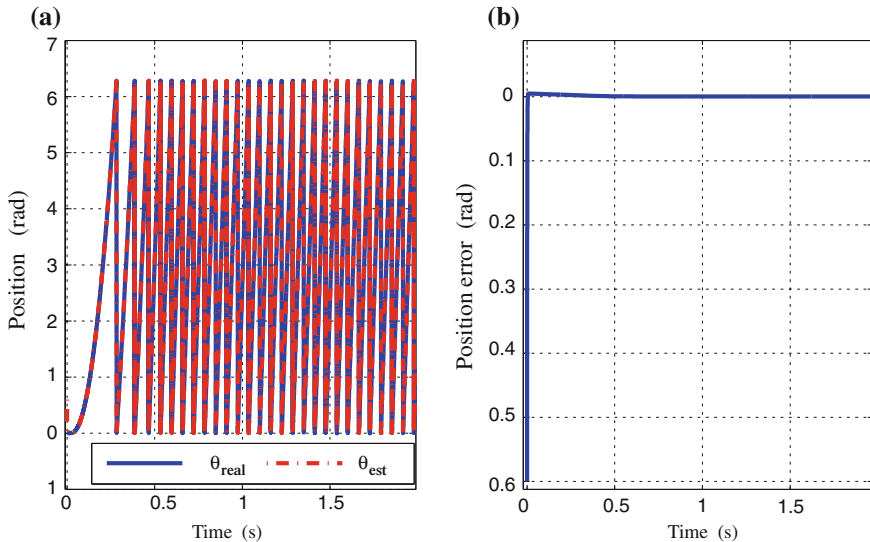
$$F_{i_d} = \begin{bmatrix} -1 & 0 & 0 & 0 \\ 0 & -1.1 & 0 & 0 \\ 0 & 0 & -1.2 & 0 \\ 0 & 0 & 0 & -1.3 \end{bmatrix}, \quad J_{i_{sd}} = \begin{bmatrix} 1 \\ 1 \\ 1 \\ 1 \end{bmatrix}.$$

The stator resistance can vary from its nominal value, and then its effect is studied.
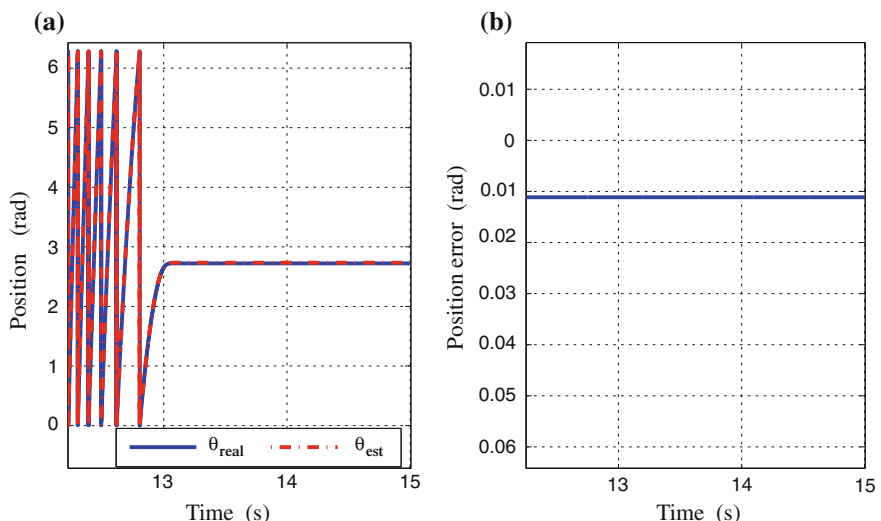
First, for the nominal case, Fig. 6.41a shows the estimated and measured speeds. The speed error owing to the torque perturbation is very small and quickly converges to zero (see Fig. 6.41b). For the nominal case, the measured and observed positions are given at the beginning of the test (Fig. 6.42) and at the end (Fig. 6.43). When the speed is equal to zero (with non-identical initial conditions for the observer and the motor) the estimated and real resistances and the load torque estimation are given by Figs. 6.44 and 6.45, respectively. The sensorless control is capable of non-persistent zero-speed operation with full load torque with very small errors. The inputs voltages and $d-q$ currents are shown in Fig. 6.46. The current i_q increases with the increase of the load torque. The d-axis current tracks its reference designed by using the MTPA

Fig. 6.41 Nominal case, **a** observed and measured speeds, **b** speed estimation error

(a)

(b)
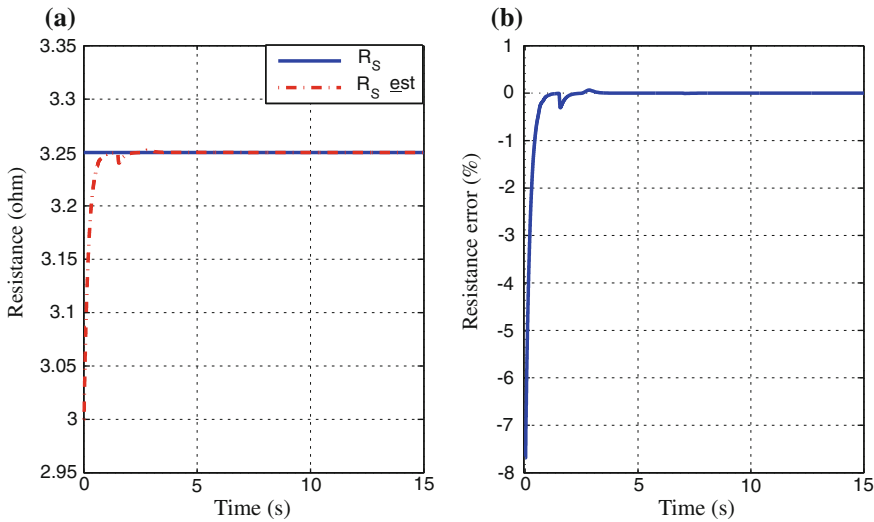
Fig. 6.42 Nominal case, observed and real position

(a)

(b)
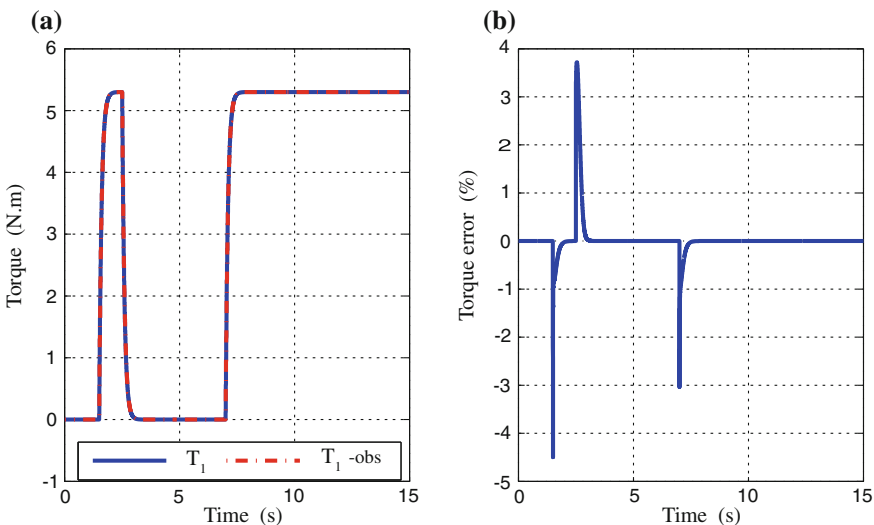
Fig. 6.43 Nominal case, observed and real position at zero speed

strategy. The MTPA strategy shares the load torque rejection to the two axis currents (d and q). The amount of the developed torque using MTPA strategy depends on the saliency of the IPMSM.

Next, in order to illustrate the robustness of the sensorless control scheme, resistance deviations are intentionally introduced. First, Figs. 6.47 and 6.48 show the

Fig. 6.44 Nominal case, **a** estimated and real resistance, **b** resistance estimation error
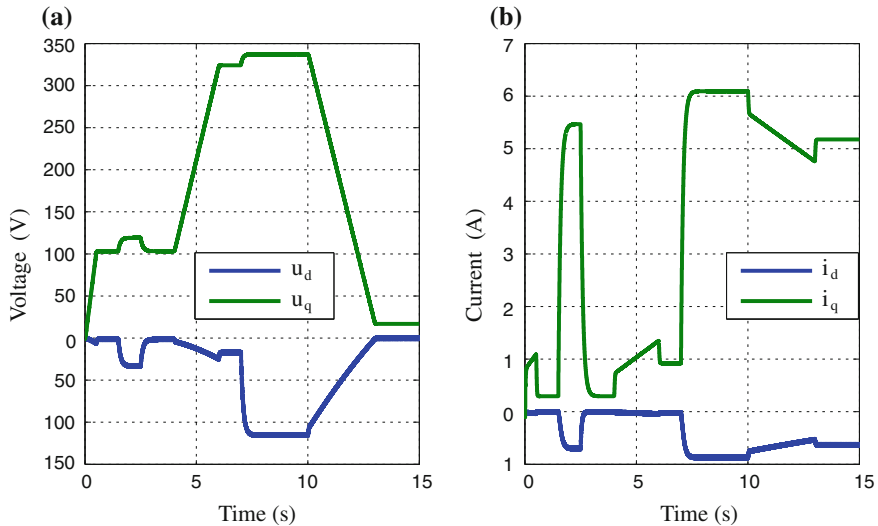
Fig. 6.45 Nominal case, **a** estimated and real load torque, **b** load torque estimation error
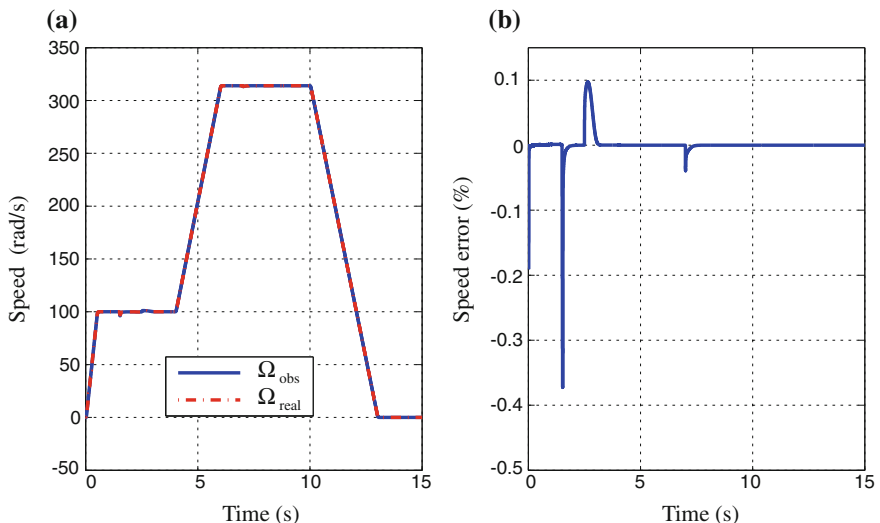
tracking and estimation responses for a $+50\%$ variation of the nominal value of the stator resistance.

The case when a -50% deviation is introduced in the stator resistance is displayed in Fig. 6.49.

The robustness and the efficiency of the proposed sensorless control under parameter variations and load torque clearly appear.

(a)

(b)
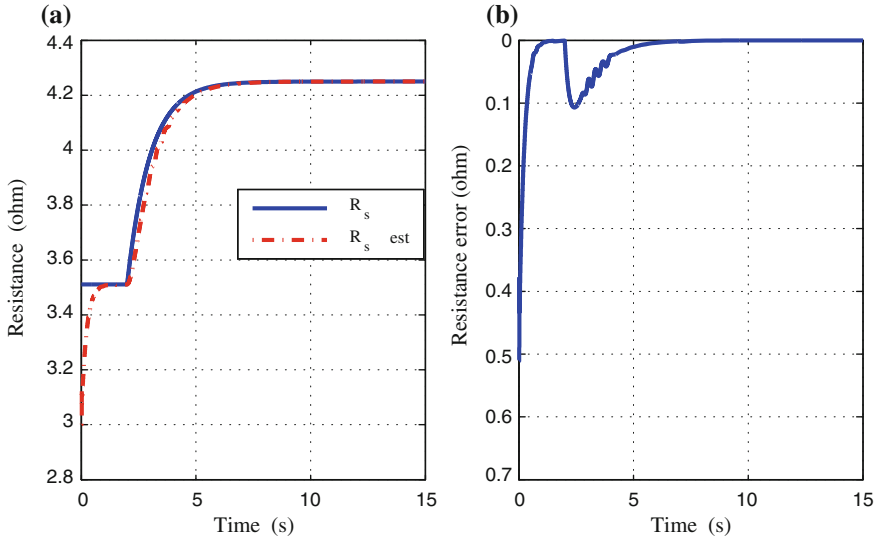
Fig. 6.46 Nominal case, dq Voltages and Currents

(a)

(b)
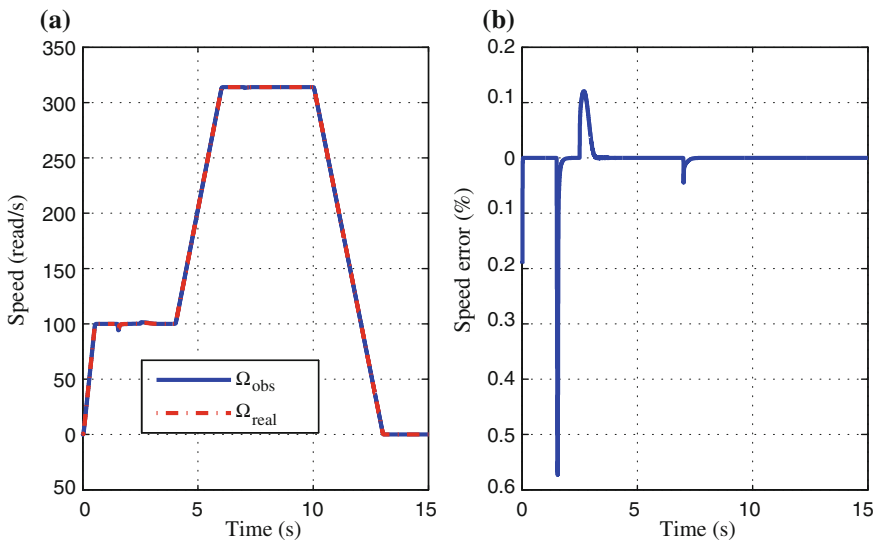
Fig. 6.47 Robustness w.r.t. $+50\%$ R_s, **a** observed and measured speeds, **b** speed estimation error

Conclusion

An adaptive interconnected observer combined with a high order sliding mode controller for sensorless control of the IPMSM has been introduced. The adaptive interconnected observer simultaneously estimates the state variables (the position and the speed), an unknown parameter (the stator resistance) and a disturbance (the load

(a)

(b)

Fig. 6.48   Robustness w.r.t. $+50\%$ R_s, **a** estimated and real resistance, **b** resistance estimation error

(a)

(b)

Fig. 6.49   Robustness w.r.t. -50% R_s, **a** observed and measured speeds, **b** speed estimation error

torque). A stability analysis of the closed-loop system has been given, where sufficient conditions have been obtained to guarantee the strong uniform practical stability of the estimation error. The whole system is tested by using a specific industrial benchmark. Significant robustness tests are implemented and simulation results illustrate the efficiency of the proposed sensorless observer-controller scheme.

6.3 Conclusions

Robust observer-control schemes for the SPMSM and the IPMSM have been presented in this chapter. Sufficient conditions to guarantee the closed-loop stability of these schemes are given.

The robustness of the proposed observer schemes have been presented and tested on an industrial benchmark. From the obtained responses, the efficiency of these schemes shows the advantages of these sensorless control strategies.

6.4 Bibliographical Notes

For the SPMSM sensorless control purpose, different approaches based mainly on electromotrive force [14, 69, 73], adaptive observers [12, 25], and extended Kalman filter [10, 52] have been studied to estimate both the speed and the position of the PMSM.

When analyzing all these results, it is clear that previous results have rarely evaluated robustness of the closed-loop system with respect to parameter variations, while this is a key point to get a robust performance for sensorless control. Moreover, these studies never investigate the robustness of the observer-controller scheme when the observability of the SPMSM is lost. The published observers have been tested with classical vector control using a proportional-integral controller. From this point of view, more adapted nonlinear robust controls as high order sliding mode and backstepping [72, 76] could be more efficient. But all of them use the speed measurement. In [48], an angular velocity observer is proposed to estimate the speed but the measurement of the position is required.

For the PMSM case, the drawbacks mentioned above were treated in [21][1], where it is proposed a robust sensorless observer-based control scheme such that the motor speed tracks a desired reference by using only the measurement of the motor currents and voltages. The observer-controller scheme combines a backstepping controller and an adaptive interconnected observer. The proposed scheme is verified according to the framework of a specific industrial benchmark. A good sensorless tracking is obtained in spite of uncertainties in the stator resistance, which usually is bad known while the nominal (unknown) load torque is applied.

The same approach for the IPMSM case is given in [38][2], where a sensorless speed control for the IPMSM is designed by combining an adaptive interconnected observer and a robust backstepping controller with integral actions.

---

[1] This chapter includes excerpts of [21], originally published in the proceedings of IFAC world Congress, Milano, Italy, IFAC-PapersOnLine IFAC 2011.

[2] This chapter includes excerpts reprinted from Journal of the Franklin Institute, 349(5):1734–1757, Hamida M, Glumineau A, De Leon J (2012) Robust integral backstepping control for sensorless IPM synchronous motor controller. Copyright (2012), with permission from Elsevier.

In [20][3], another Observer-Controller scheme deals with the sensorless SPMSM control problem by using a super-twisting based observer combined with a high order sliding mode control.

In [37][4], the case of the IPMSM is treated by combining an adaptative interconnected observer with a high order sliding mode control. An analysis of stability is given based on previous results Lemma 6.1 (see also Lemma 2.1 in [80]).

For some of these algorithms, the initial value of the rotor position can be necessary. This problem has been treated in [10, 50, 51].

---

[3] This chapter includes excerpts of [20], Copyright (2010) IEEE. Reprinted, with permission, from "Ezzat M, De Leon J, Gonzalez N, Glumineau A, Observer-controller scheme using high order sliding mode techniques for sensorless speed control of permanent magnet synchronous motor. In: Decision and Control (CDC), 49th IEEE Conference on Decision Control, Atlanta, USA".

[4] This chapter, includes excerpts of [37], originally published in the proceedings of IFAC Power Plant and Power System Control conference (PPPSC), Toulouse, France, IFAC-PapersOnLine IFAC 2012.

Chapter 7
Sensorless Output Feedback Control for Induction Motor

Abstract In this chapter, the IM sensorless control problem is considered, where observer-control schemes are combinations of the observers designed in Chap. 3, with the control strategies proposed in Chap. 5. These observer-controller schemes take into account that the mechanical variables are not measurable (rotor position, rotor speed, and load torque), and only the currents and the voltages are available by measurement. For the induction motor, first an observer-controller scheme is constituted by combining an adaptive interconnected observer with a backstepping controller. The observer is designed to estimate the rotor speed, the fluxes, the load torque, and simultaneously to identify a sensitive parameter: the rotor resistance. The controller is designed to track the reference trajectories of the rotor speed and of the flux modulus. Finally, an observer-controller constituted by an adaptive interconnected observer combined with a high order sliding mode controller is designed. Sufficient conditions are given to ensure the stability of the closed-loop system. Furthermore, the tracking errors convergence of these schemes is analyzed in presence of parametric uncertainties, and a strong uniform practical stability condition is obtained. All these control strategies are experimentally tested on a motor setup using the control benchmark trajectories introduced in Chap. 1 (Sect. 1.6), with parametric uncertainties robustness tests and a non-measured load torque. For all the cases, the Field-Oriented Control (FOC) strategy will be the basis of the control algorithms.

7.1 Classical Sensorless Field-Oriented Control

7.1.1 Trajectory Tracking for Sensorless Field-Oriented Control

For the IM sensorless control problem, the speed and the flux are not measurable. Moreover, the load torque is assumed to be an unknown bounded perturbation.

Denote Ω^* and ϕ^* the smooth bounded reference signals of the rotor speed Ω and the rotor flux modulus $\sqrt{\phi_{rd}^2 + \phi_{rq}^2}$, respectively. Following the strategy of the Field-Oriented Control [7] (i.e., $\phi_{rq} = 0$,), the resulting electromagnetic torque is

given by

$$T_e = \frac{pM_{sr}}{L_r}\phi_{rd}i_{sq} \tag{7.1}$$

which is proportional to the product of ϕ_{rd} and i_{sq}. Notice that by holding constant the magnitude of the rotor flux in (7.1), there is a linear relationship between the variable i_{sq} and the electromagnetic torque T_e.

For the FOC strategy, an important step is to estimate the stator frequency ω_s and the (d, q) frame angular position. For flux-oriented field control design, the stator frequency is given by

$$\omega_s = \dot{\rho} = p\Omega + a\frac{M_{sr}}{\phi_{rd}}i_{sq}$$

(see [70]). Then, a robust observer of the (d, q) frame angular position is designed as

$$\dot{\hat{\rho}} = p\hat{\Omega} + a\frac{M_{sr}}{\hat{\phi}_{rd}}i_{sq} - k_{\omega_s}\frac{(i_{sq} - \hat{i}_{sq})}{\beta_1\hat{\phi}_{rd}} \tag{7.2}$$

with $\beta_1 = M_{sr}/(\sigma L_s L_r)$ and $k_{\omega_s} > 0$.

Thus, to apply the FOC strategy, it is necessary to replace the speed and the flux measurements by their estimations in the controllers: i.e., in the control equations i_{sd}^* (5.7), and i_{sq}^* (5.12). Then, the new controllers, in terms of the estimated variables, are

$$i_{sd}^*(t) = Ki_{\phi_{rd}}\int_0^t (\phi^* - \hat{\phi}_{rd})(\tau)d\tau + Kp_{\phi_{rd}}(\phi^* - \hat{\phi}_{rd})$$
$$+ \frac{1}{aM_{sr}}\dot{\phi}^* + \frac{1}{M_{sr}}\phi^* \tag{7.3}$$

$$i_{sq}^*(t) = \frac{1}{K_T}\left(Ki_\Omega\int_0^t (\Omega^* - \hat{\Omega})(\tau)d\tau + Kp_\Omega(\Omega^* - \hat{\Omega})\right)$$
$$+ \frac{1}{m\hat{\phi}_{rd}}\left(\dot{\Omega}^* + c\hat{\Omega} + \frac{\hat{T}_l}{J}\right). \tag{7.4}$$

Remark 7.1 Notice that in order to avoid a singularity in (7.4), the observer must be initialized with a rotor flux value different from zero, so that controller (7.4) is well defined. This condition represents a physical condition for the induction motor: no rotor flux implies no torque (see [17]). Moreover, the flux controller (7.3) allows to guarantee that ϕ_{rd} reaches its reference ϕ^*. Before the motor is fluxed, (i.e., $\phi_{rd} < \phi^*$), the speed reference is kept to 0 without load torque. As soon as the motor is fluxed, there is no more singularity for the controller (7.4) for all $t \geq 0$.

The stator current $i_{sd}^*(\phi_{rd})$, which is expressed in terms of ϕ_{rd}, is replaced by its estimate $i_{sd}^*(\hat{\phi}_{rd})$ (7.3), and similarly $i_{sq}^*(\Omega, \phi_{rd})$, which depends on Ω and ϕ_{rd}, is replaced by its estimate $i_{sq}^*(\hat{\Omega}, \hat{\phi}_{rd})$ (7.4).

The reduced model of the induction motor (5.4) can be rewritten in closed-loop as follows:

$$\begin{pmatrix} \dot{\Omega} \\ \dot{\phi}_{rd} \end{pmatrix} = \begin{pmatrix} m\phi_{rd}i_{sq}^*(\hat{\Omega}, \hat{\phi}_{rd}) - c\Omega - \frac{T_l}{J} \\ -a\phi_{rd} + aM_{sr}i_{sd}^*(\hat{\phi}_{rd}) \end{pmatrix}. \tag{7.5}$$

Now, adding the terms $\pm m\phi_{rd}i_{sq}^*(\Omega, \phi_{rd})$ and $\pm aM_{sr}i_{sd}^*(\phi_{rd})$ in reduced model (7.5), it follows that

$$\begin{cases} \dot{\Omega} = m\phi_{rd}i_{sq}^*(\Omega, \phi_{rd}) - c\Omega - \frac{T_l}{J} + m\phi_{rd}[i_{sq}^*(\hat{\Omega}, \hat{\phi}_{rd}) - i_{sq}^*(\Omega, \phi_{rd})] \\ \dot{\phi}_{rd} = -a\phi_{rd} + aM_{sr}i_{sd}^*(\phi_{rd}) + aM_{sr}[i_{sd}^*(\hat{\phi}_{rd}) - i_{sd}^*(\phi_{rd})]. \end{cases} \tag{7.6}$$

Define the rotor flux and the speed tracking errors as $e_\phi = \phi^* - \phi_{rd}$ and $e_\Omega = \Omega - \Omega^*$, whose dynamics are given by

$$\begin{cases} \dot{e}_\phi = \left(-a - aM_{sr}Kp_{\phi_{rd}}\right)e_\phi - aM_{sr}Ki_{\phi_{rd}}\int_0^t e_\phi(\tau)d\tau \\ \qquad -aM_{sr}\left(Ki_{\phi_{rd}}\int_0^t \epsilon_\phi(\tau)d\tau + Kp_{\phi_{rd}}\epsilon_\phi\right) \\ \dot{e}_\Omega = -\frac{Kp_\Omega}{J}\left(1 + \frac{\epsilon_\phi}{\hat{\phi}_{rd}}\right)e_\Omega - \frac{Ki_\Omega}{J}\left(1 + \frac{\epsilon_\phi}{\hat{\phi}_{rd}}\right)\int_0^t e_\Omega(\tau)d\tau \\ \qquad + \left(\frac{Kp_\Omega}{J}\left[1 + \frac{\epsilon_\phi}{\hat{\phi}_{rd}}\right] - c\right)\epsilon_\Omega \\ \qquad + \frac{Ki_\Omega}{J}\left(1 + \frac{\epsilon_\phi}{\hat{\phi}_{rd}}\right)\int_0^t \epsilon_\Omega(\tau)d\tau + \frac{\epsilon_\phi}{\hat{\phi}_{rd}}\left(\Omega^* + c\hat{\Omega} + \frac{e_{T_l}}{J}\right) \end{cases} \tag{7.7}$$

where the rotor flux and speed estimation errors are expressed by $\epsilon_\phi = \phi_{rd} - \hat{\phi}_{rd}$ and $\epsilon_\Omega = \Omega - \hat{\Omega}$.

Now, by using the following change of coordinates:

$$\chi_\Omega = \left(\int_0^t e_\Omega(\tau)d\tau, \ e_\Omega\right)^T, \tag{7.8}$$

$$\chi_\phi = \left(\int_0^t e_\phi(\tau)d\tau, \ e_\phi\right)^T, \tag{7.9}$$

then, Eq. (7.7) becomes

$$\begin{cases} \dot{\chi}_\phi = \bar{A}_\phi\chi_\phi + B_\phi\Gamma_\phi(\epsilon_\phi) \\ \dot{\chi}_\Omega = \bar{A}_\Omega\chi_\Omega + B_\Omega\Gamma_\Omega(\epsilon_\Omega) \end{cases} \tag{7.10}$$

where

$$\bar{A}_\Omega = \begin{pmatrix} 0 & 1 \\ \alpha_{1\Omega} & \alpha_{2\Omega} \end{pmatrix}, \text{ with } \alpha_{1\Omega} - \frac{K_{I\Omega}}{J} \text{ and } \alpha_{2\phi} = -\frac{K_{P\Omega}}{J},$$

$$\bar{A}_\phi = \begin{pmatrix} 0 & 1 \\ \alpha_{1\phi} & \alpha_{2\phi} \end{pmatrix}, \text{ with } \alpha_{1\phi} = -a M_{sr} K_{I\phi rd} \text{ and } \alpha_{2\phi} = -a - M_{sr} K_{P\phi rd},$$

$$B_\phi = B_\Omega = \begin{pmatrix} 0 \\ 1 \end{pmatrix},$$

$$\Gamma_\phi(\epsilon_\phi) = -a M_{sr} \left[K p_{\phi rd} \epsilon_\phi + K_{I\phi} \int_0^t \epsilon_\phi(\tau)d\tau \right],$$

$$\Gamma_\Omega = \Gamma_1(\epsilon_\Omega) + \Gamma_2(\epsilon_\phi) + \Gamma_3(\epsilon_\Omega, \epsilon_\phi), \text{ where}$$

$$\Gamma_1(\epsilon_\Omega) = \frac{K i_\Omega}{J} \int_0^t \epsilon_\Omega(\tau)d\tau + \left[\frac{K p_\Omega}{J} - c \right] \epsilon_\Omega,$$

$$\Gamma_2(\epsilon_\phi) = \frac{\epsilon_\phi}{\hat{\phi}_{rd}} \left[\Omega^* + c\hat{\Omega} + \frac{e_{T_l}}{J} \right] - \frac{K p_\Omega}{J} \left(\frac{\epsilon_\phi}{\hat{\phi}_{rd}} \right) e_\Omega - \frac{K i_\Omega}{J} \left(\frac{\epsilon_\phi}{\hat{\phi}_{rd}} \right) \int_0^t e_\Omega(\tau)d\tau,$$

$$\Gamma_3(\epsilon_\Omega, \epsilon_\phi) = \frac{\epsilon_\phi}{\hat{\phi}_{rd}} \left[\frac{K p_\Omega}{J} \epsilon_\Omega + \frac{K i_\Omega}{J} \int_0^t \epsilon_\Omega(\tau)d\tau \right].$$

Then, the rotor flux and speed trackings and the estimation error dynamics are given as

$$
\begin{cases}
\dot{\chi}_\phi = \bar{A}_\phi \chi_\phi + B_\phi \Gamma_\phi(\epsilon_\phi) \\
\dot{\chi}_\Omega = \bar{A}'_\Omega \chi_\Omega + B_\Omega \Gamma_\Omega(\epsilon_\Omega) \\
\dot{\epsilon}_1 = \left[A_1(Z_2) - S_1^{-1} \Gamma C_1^T C_1 - B_1 C_1 \right] \epsilon_1 \\
\quad + g_1(u, y, X_2) + \Delta g_1(u, y, X_2, X_1) - g_1(u, y, Z_2, Z_1) \\
\quad + [A_1(X_2) + \Delta A_1(X_2) - A_1(Z_2)]X_1 - (B_2 C_2 + K C_2^T C_2)\epsilon_2 \\
\dot{\epsilon}_2 = [A_2(Z_1) - S_2^{-1} C_2^T C_2]\epsilon_2 + [A_2(X_1) + \Delta A_2(X_1) - A_2(Z_1)]X_2 \\
\quad + g_2(u, y, X_1, X_2) + \Delta g_2(u, y, X_1, X_2) - g_2(u, y, Z_1, Z_2).
\end{cases}
\tag{7.11}
$$

To show how the stator currents and rotor speed trackings are achieved by using the estimates provided by the observer, define the candidate Lyapunov function for the overall error dynamics (7.11)

$$
\begin{aligned}
V_{oc} &= V_o + V_c \\
&= \epsilon_1^T S_1 \epsilon_1 + \epsilon_2^T S_2 \epsilon_2 + \chi_\phi^T P_\phi \chi_\phi + \chi_\Omega^T P_\Omega \chi_\Omega,
\end{aligned}
\tag{7.12}
$$

where $V_o = \epsilon_1^T S_1 \epsilon_1 + \epsilon_2^T S_2 \epsilon_2 = \|\epsilon\|_{S_\theta}^2$ and $V_c = \chi_\phi^T P_\phi \chi_\phi + \chi_\Omega^T P_\Omega \chi_\Omega$ are the Lyapunov functions of the estimated errors and of the tracking errors, respectively.

Defining $\delta_o = (1 - \varsigma)\delta$, and taking the time derivative of V_o, after straightforward computations the following inequality is satisfied:

$$\dot{V}_o \leq -(1-\varsigma)\delta V_o \leq -\delta_o V_o.$$

Now, computing the time derivative of V_{oc} (7.12) along the dynamics of system (7.11), yields

$$\dot{V}_{oc} \leq -\delta_o V_o + \chi_\phi^T(P_\phi \bar{A}_\phi + \bar{A}_\phi^T P_\phi)\chi_\phi + 2\chi_\phi^T P_\phi B_\phi \Gamma_\phi(\epsilon_\phi)$$
$$+ \chi_\Omega^T(P_\Omega \bar{A}_\Omega + \bar{A}_\Omega^T P_\Omega)\chi_\Omega + 2\chi_\Omega^T P_\Omega B_\Omega \Gamma_\Omega(\epsilon_\Omega).$$

After some computations, it follows that

$$\dot{V}_{oc} \leq -\delta_o \|\epsilon\|_{S_\theta}^2 - \chi_\phi^T Q_\phi \chi_\phi + 2l_1 \|\chi_\phi\|_{P_\phi} \|\epsilon\|_{S_\theta}$$
$$- \chi_\Omega^T Q_\Omega \chi_\Omega + 2l_2 \|\chi_\Omega\|_{P_\Omega} \|\epsilon\|_{S_\theta}$$

where the nonlinear terms $\Gamma_\phi(\epsilon_\phi)$ and $\Gamma_\Omega(\epsilon_\Omega)$ satisfy the following inequalities $\|\Gamma_\phi(\epsilon_\phi)\| \leq l_1 \|\epsilon\|_{S_\theta}$, $\|\Gamma_\Omega(\epsilon_\Omega)\| \leq l_2 \|\epsilon\|_{S_\theta}$, where l_1 and l_2 are positive constants.
By using the following inequalities:

$$\|\epsilon\|_{S_\theta} \|\chi_\phi\|_{P_\phi} \leq \frac{\xi_1}{2} \|\chi_\phi\|_{P_\phi}^2 + \frac{1}{2\xi_1} \|\epsilon\|_{S_\theta}^2,$$

$$\|\epsilon\|_{S_\theta} \|\chi_\Omega\|_{P_\Omega} \leq \frac{\xi_2}{2} \|\chi_\Omega\|_{P_\Omega}^2 + \frac{1}{2\xi_2} \|\epsilon\|_{S_\theta}^2,$$

$\forall \xi_1, \xi_2 \in]0, 1[$, and by substituting the above inequalities in $\dot{V}_{oc}$, it follows that

$$\dot{V}_{oc} \leq -\left(\delta_o - \frac{l_1}{\xi_1} - \frac{l_2}{\xi_2}\right) \|\epsilon\|_{S_\theta}^2 - (\eta_\phi - l_1\xi_1) \|\chi_\phi\|_{P_\phi}^2 - (\eta_\Omega - l_2\xi_2) \|\chi_\Omega\|_{P_\Omega}^2.$$

Let us define the following constants:

$$\vartheta_1 = (\eta_\phi - l_1\xi_1) > 0, \quad \vartheta_2 = (\eta_\Omega - l_2\xi_2) > 0, \quad \vartheta_3 = \left(\delta - \frac{l_1}{\xi_1} - \frac{l_2}{\xi_2}\right) > 0.$$

Then, it follows that

$$\dot{V}_{oc} \leq -\vartheta V_{oc}.$$

where $\vartheta = min(\vartheta_1, \vartheta_2, \vartheta_3)$.

Hence, the estimation and the tracking errors of the overall system converges asymptotically to zero with arbitrary rate of convergence ϑ. This proves that controller (7.4) is well defined for all $t \geq 0$.

Then, with the assumption of persistent inputs the system is not in the unobservability area, we can establish the following result about the stability of the closed-loop system under parametric uncertainties.

Lemma 7.1 *Consider*: (*a*) *System* (1.119) *that satisfies conditions given in Remark* 3.17 *and for which an interconnected observer* (3.110) *can be designed*; (*b*) *System*
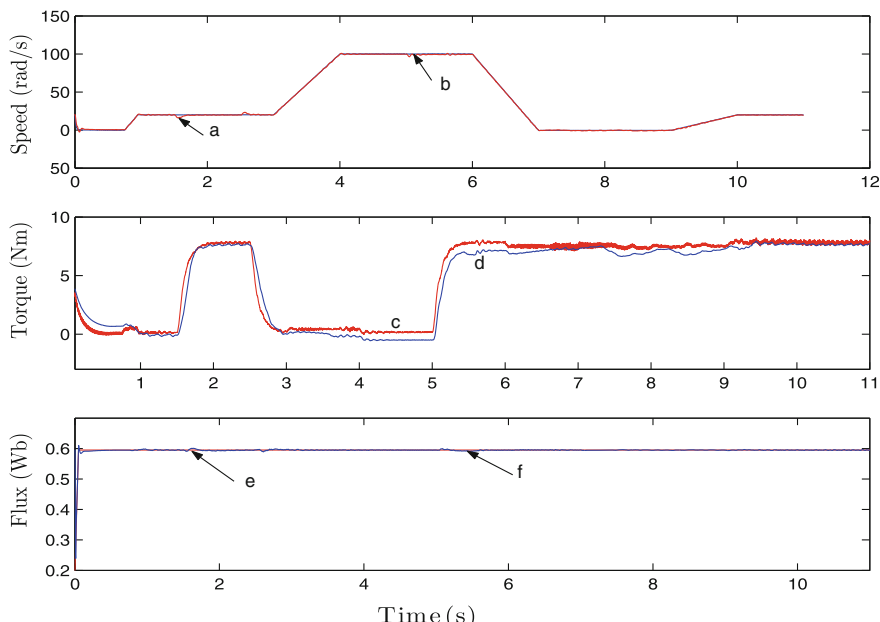
(5.4) *controlled by* (7.3) *and* (7.4). *Then, by using estimations provided by the inter-connected observer* (3.110), *the speed and flux tracking errors converge asymptotically to zero.*

Remark 7.2 For the case of non-persistent inputs, a complementary analysis is necessary that is detailed in Appendix "Appendix: Stability of the Observer-Controller Scheme".

7.1.2 Experimental Results

Experimental results of the above observer-controller are now given. To test robustness conditions, we take a $+30\%$ variation of R_s for the design of the observer-controller. For the experiment, only the stator currents are measured. The speed and the flux amplitude are provided by the observer. The experimental results for the nominal case, i.e., when the parameters (except stator resistance) are known, are shown in Fig. 7.1.

These figures show the good performance of both system "observer + controller" for the trajectory tracking problem and for the perturbation rejection. In terms of tracking trajectory, we note that the estimated rotor speed (see Fig. 7.1b) converges to the measured speed (Fig. 7.1a) near and under unobservable conditions. The same
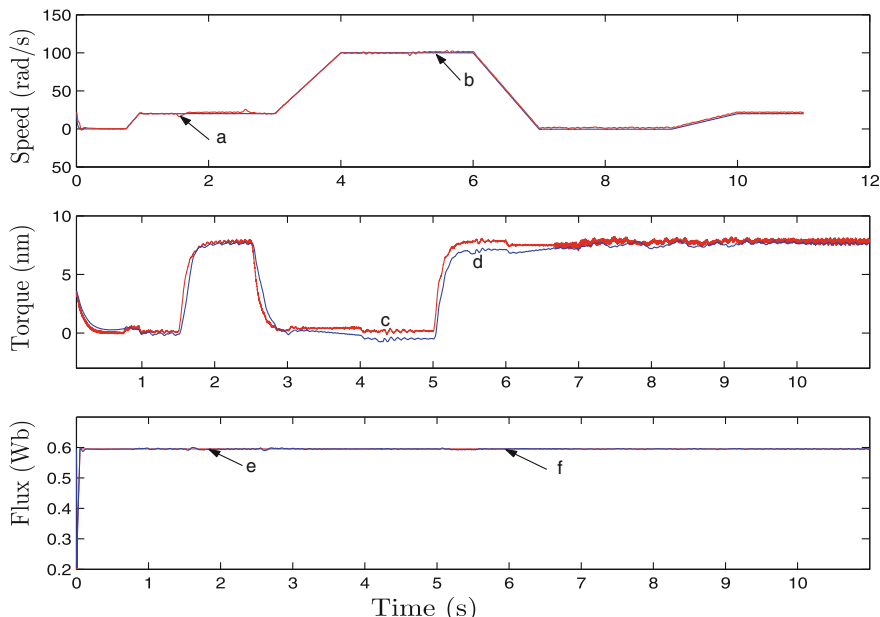
Fig. 7.1 Experimental result in nominal case
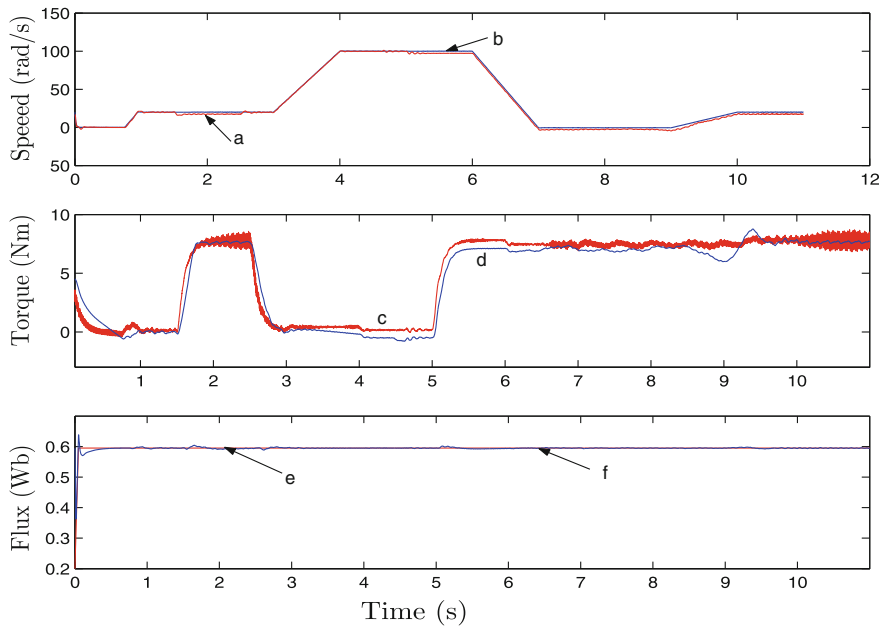
conclusion is obtained for the estimated flux (Fig. 7.1f) with respect to the reference flux (see Fig. 7.1e). The estimated load torque (Fig. 7.1d) converges to the measured load torque (Fig. 7.1c), except under unobservable conditions (from 7 to 9 s). Nevertheless, it appears a small static error when the rotor speed increases (from 3 to 6 s). In terms of perturbation rejection, we have noted that the load torque is well rejected excepted at the time when it is applied: see Fig. 7.1a–b, e–f at time 1.5 and 5 s, and when it is removed (Fig. 7.1a–b, e–f at time 2.5 s).

The robustness of the observer-controller scheme is confirmed by the results obtained in presence of rotor resistance variations, i.e. a variation of +50 % on the rotor resistance is introduced for the observer-controller scheme design, see Fig. 7.2. It is obtained similar experimental results for the rotor resistance at the nominal case under observable conditions. We can see that a static error appears when the motor is under unobservable condition: during the time interval from 7 to 9 s, see Fig. 7.2a–b. However, the static error increases a little when the load torque is applied at time 1.5 and 5 s, see Fig. 7.2a–b. In conclusion, the increase in the rotor resistance value slightly affects the performance of the speed trajectories tracking.

A second test is made with a −50 % variation on the rotor resistance value. The experimental results are given in Fig. 7.3. For the speed, flux, and load torque estimation, the conclusion is the same as for the +50 % variation case (see Fig. 7.2). But for this robustness test, the control induces noise. This can be seen on the measured torque (see Fig. 7.3c).

Fig. 7.2 Experimental result with rotor resistance variation: +50 %
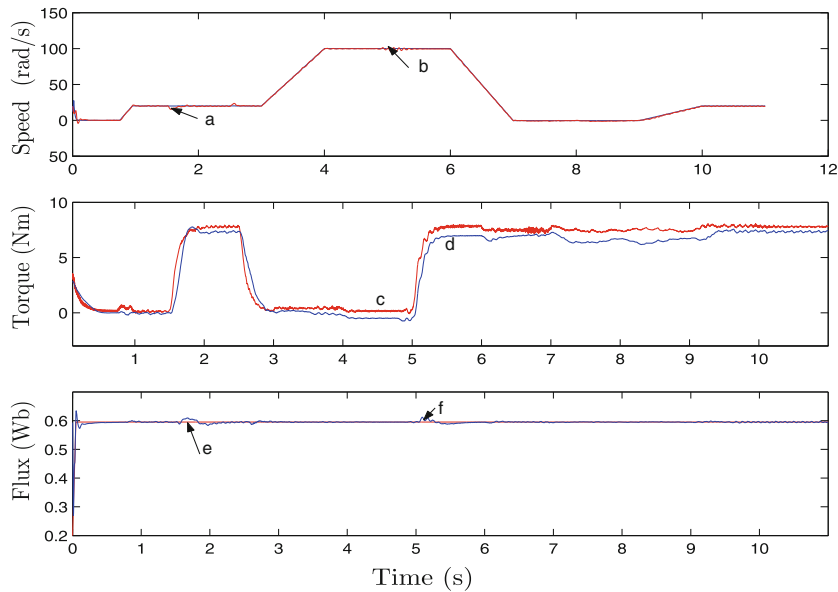
Fig. 7.3 Experimental result with rotor resistance variation: $-50\,\%$

A new robustness test is made by introducing a variation of $+10\,\%$ on rotor self-inductance value. The results of this test are shown in Fig. 7.4. By analyzing Fig. 7.4, we can see that the rotor self-inductance variation does not affect the performances of both "control $+$ observer" scheme. Nevertheless, a small oscillation appears at the time when the load torque is applied (see Fig. 7.4a–b).
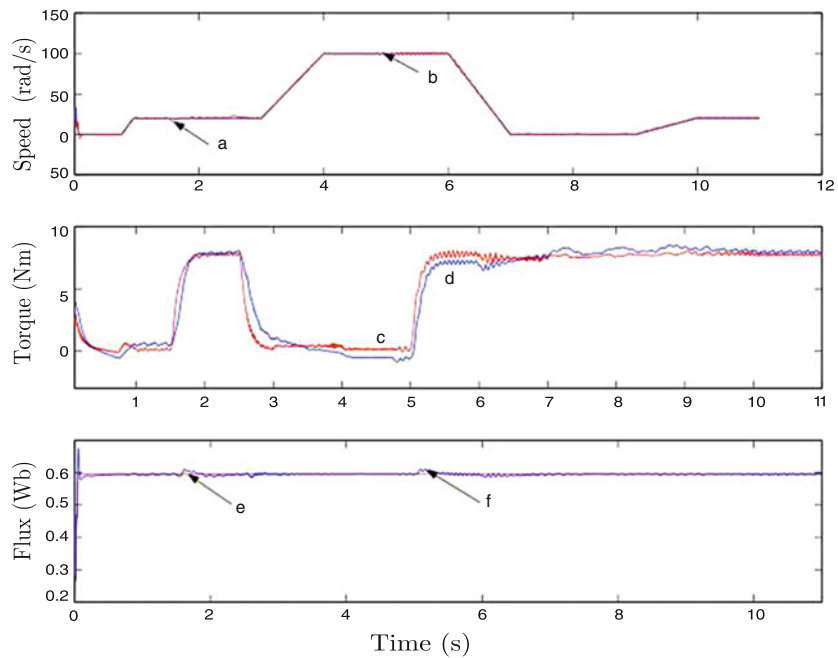
A last robustness test is to introduce a $+10\,\%$ variation of the stator self-inductance value. The results of this test are shown in Fig. 7.5. Comparing this result with the rotor self-inductance variation case yields the same conclusion except the oscillations that become important at time 5 s when the load torque is applied: see Fig. 7.5a–b.

7.1.3 Conclusion

In this section, the field-oriented control of the IM without mechanical sensors (position, speed, and load torque sensors) is investigated. An interconnected observer provides a good estimation of the load torque even when nominal load is applied. Furthermore, a control strategy composed of a field-oriented control plus a high-gain PI controller achieves a good speed and flux tracking for IM without mechanical sensors. Moreover, the proposed "observer $+$ controller" scheme has been tested and evaluated on experimental setup with a significant "Sensorless Control Benchmark."

Fig. 7.4 Experimental result with rotor self-inductance variation: $+10\,\%$

Fig. 7.5 Experimental result with stator self-inductance variation: $+10\,\%$

The trajectories of this benchmark are defined in the operation region where the speed and the torque are in opposite directions (generator mode).

The stability of the system in closed-loop with the "controller + observer" scheme has been proved by the Lyapunov theory, where sufficient conditions have been obtained.

Finally, the robustness of the "controller + observer" scheme is confirmed by the good performances under parameter variations.

7.2 Robust Adaptive Observer-Backstepping Sensorless Control

7.2.1 Sensorless Observer-Controller Scheme Stability Analysis

To implement the controller (5.7)–(5.12), it is necessary to replace the rotor speed, flux measurements, load torque, stator resistance, and the stator frequency by their estimated values. Then, the speed, flux controllers, and reference control inputs are expressed as follows:

$$
\begin{cases}
i_{sq}^*(\hat{\Omega}, \widehat{T}_l, \hat{\phi}_{rd}, \widehat{R}_s) = \dfrac{1}{m\hat{\phi}_{rd}}\Big[\dot{\Omega}^* + c\hat{\Omega} + \dfrac{\widehat{T}_l}{J} + (K_\Omega + K_\Omega')(\Omega^* - \hat{\Omega}) \\
\qquad\qquad\qquad\qquad + K_\Omega K_\Omega' \int_0^t (\Omega^* - \hat{\Omega})dt\Big] \\
i_{sd}^*(\hat{\phi}_{rd}, \widehat{R}_s) \quad = \dfrac{1}{aM_{sr}}\Big[\dot{\phi}_{rd}^* + a\hat{\phi}_{rd} + (K_\phi + K_\phi')(\phi_{rd}^* - \hat{\phi}_{rd}) \\
\qquad\qquad\qquad\qquad + K_\phi K_\phi' \int_0^t (\phi_{rd}^* - \hat{\phi}_{rd})dt\Big]
\end{cases}
\tag{7.13}
$$

$$
\begin{cases}
u_{sq} = \dfrac{1}{m_1}\Big[K_{iq}(i_{sq}^* - i_{sq}) + K_{iq}'' K_{iq} \int_0^t (i_{sq}^* - i_{sq})dt \\
\qquad\qquad - ab\hat{\phi}_{rq} + bp\hat{\Omega}\hat{\phi}_{rd} + \widehat{\gamma}(\widehat{R}_s)i_{sq} + \tilde{\omega}_s i_{sd} + i_{sq}^*\Big] \\
u_{sd} = \dfrac{1}{m_1}\Big[K_{id}(i_{sd}^* - i_{sd}) + K_{id}'' K_{id} \int_0^t (i_{sd}^* - i_{sd})dt \\
\qquad\qquad - ab\hat{\phi}_{rd} - bp\hat{\Omega}\hat{\phi}_{rq} + \widehat{\gamma}(\widehat{R}_s)i_{sd} - \tilde{\omega}_s i_{sq} + i_{sd}^*\Big].
\end{cases}
\tag{7.14}
$$

where

$$
\tilde{\omega}_s = p\hat{\Omega} + a\frac{M_{sr}}{\hat{\phi}_{rd}}i_{sq} - \frac{(i_{sq} - \hat{i}_{sq})}{\beta_1 \hat{\phi}_{rd}}k_{\omega_s}
\tag{7.15}
$$

is the estimation of ω_s, $\beta_1 = \frac{M_{sr}}{\sigma L_s L_r}$ and k_{ω_s} is a positive constant. The closed-loop system with the controls (7.13) and (7.14) is given by

$$
\begin{bmatrix} \dot{\Omega} \\ \dot{\phi}_{rd} \end{bmatrix} = \begin{bmatrix} m\phi_{rd} i_{sq}^*(\hat{\Omega}, \widehat{T}_l, \hat{\phi}_{rd}) - c\Omega - \dfrac{T_l}{J} - \Delta\Gamma_\Omega \\[2mm] -a\phi_{rd} + aM_{sr} i_{sd}^*(\hat{\phi}_{rd}) - \Delta\Gamma_{\phi_{rd}} \end{bmatrix}. \tag{7.16}
$$

To analyze the closed-loop system stability, first by expressing (7.16) in terms of the speed and flux tracking error dynamics, respectively, z_Ω and $z_{\phi_{rd}}$, it follows that system (7.16) can be rewritten in the following form:

$$
\begin{cases} \dot{z}_\Omega = -K_\Omega z_\Omega + \Lambda_1(\epsilon_\Omega, \epsilon_{T_l}, \epsilon_\phi, \epsilon_{R_s}) - \Delta\Gamma_\Omega \\[2mm] \dot{z}_{\phi_{rd}} = -K_\phi z_{\phi_{rd}} - \Lambda_2(\epsilon_\phi, \epsilon_{R_s}) - \Delta\Gamma_{\phi_{rd}} \end{cases} \tag{7.17}
$$

where $\epsilon_\Omega = \Omega - \hat{\Omega}$, $\epsilon_{T_l} = T_l - \widehat{T}_l$, $\epsilon_\phi = \phi_{rd} - \hat{\phi}_{rd}$, $\epsilon_{R_s} = R_s - \hat{R}_s$, are the estimation errors, and

$$
\Lambda_1(\epsilon_\Omega, \epsilon_{T_l}, \epsilon_\phi, \epsilon_{R_s}) = m\phi_{rd}\{i_{sq}^*(\hat{\Omega}, \widehat{T}_l, \hat{\phi}_{rd}, \widehat{R}_s) - i_{sq}^*(\Omega, T_l, \phi_{rd}, R_s)\}
$$

$\Lambda_2(\epsilon_\phi, \epsilon_{R_s}) = aM_{sr}\{i_{sd}^*(\hat{\phi}_{rd}, \widehat{R}_s) - i_{sd}^*(\phi_{rd}, R_s)\}$, $\Delta\Gamma_{\phi_{rd}}$ and $\Delta\Gamma_\Omega$ are the uncertain terms.

Notice that $\Lambda_1(\epsilon_\Omega, \epsilon_{T_l}, \epsilon_{R_s}, \epsilon_\phi)$ is Lipschitz with respect to $\epsilon_\Omega, \epsilon_{T_l}, \epsilon_{R_s}, \epsilon_\phi$, and $\Lambda_2(\epsilon_\phi, \epsilon_{R_s})$ is Lipschitz with respect to ϵ_ϕ, and ϵ_{R_s}. Then the stability of the closed-loop system (7.17) associated to the observer dynamics can be established by the following theorem.

Theorem 7.1 *Consider system (7.16) with the reference signals Ω^* and ϕ_{rd}^* assumed to be differentiable and bounded. Then the closed-loop system given by system (7.16) with the speed, flux, and current tracking laws (7.13) and (7.14) using the estimates provided by the adaptive interconnected observer (3.110), has strongly uniformly practically stable tracking errors.*

The proof follows a similar procedure as Proposition 5.2 in Chap. 5.

7.2.2 Experimental Results

The proposed observer-controller scheme shown in Fig. 7.6 has been tested using a 1.5 kW induction motor (see the setup characteristics in Sect. 1.6).

The parameters of the observer-controller scheme are chosen as follows.

Summary 7.2.2 Tuning parameters

   Observer

$\alpha = 5, \varpi = 10, k = 0.16, k_{c1} = 450, K_{c2} = 0.5$

$\theta_1 = 5000, \theta_2 = 7000$ and $\theta_3 = 10^{-9}$

   Controller

$K_\Omega = 200\,\mathrm{s}^{-1}, K'_\Omega = 0.001s^{-1}, K_\phi = 1100\,\mathrm{s}^{-1}$
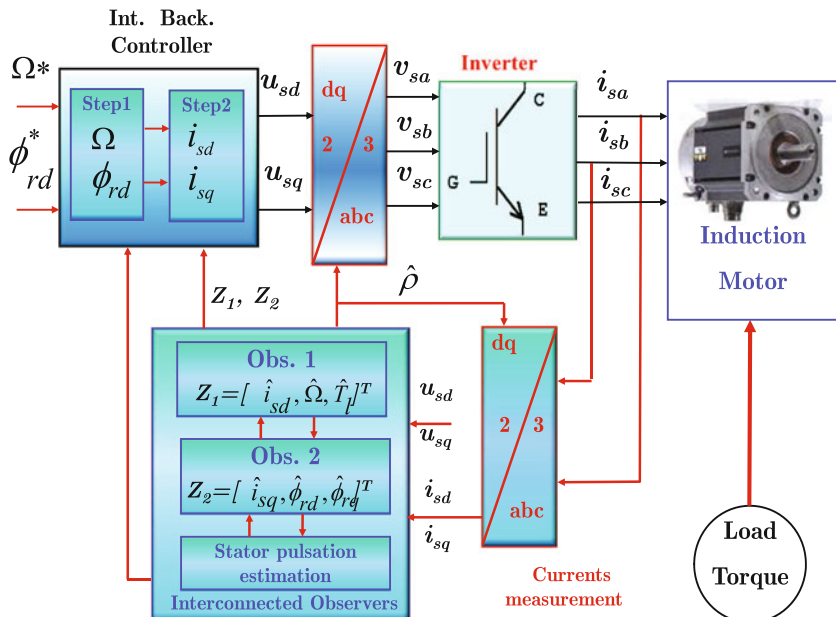
$K'_\phi = 0.012\,\mathrm{s}^{-1}, K_{id} = 550\,\mathrm{s}^{-1}, K'_{id} = 20\,\mathrm{s}^{-1}, K''_{id} = 34\,\mathrm{s}^{-1}$

$K_{iq} = 1200\,\mathrm{s}^{-1}, K'_{iq} = 10\,\mathrm{s}^{-1}, K''_{iq} = 35s^{-1}, K_{\omega_s} = 90\,\mathrm{rad.m}^4\,\mathrm{s}^5\,\mathrm{kg}^2\,\mathrm{A}^4$

The identified parameters of the IM were previously obtained offline and they are assumed to be close to the real values of the IM. It is clear that they are not exactly the actual values. However in the sequel, these identified parameters are used for the so-called *nominal system* and they will be used to start the performance test of the proposed scheme.
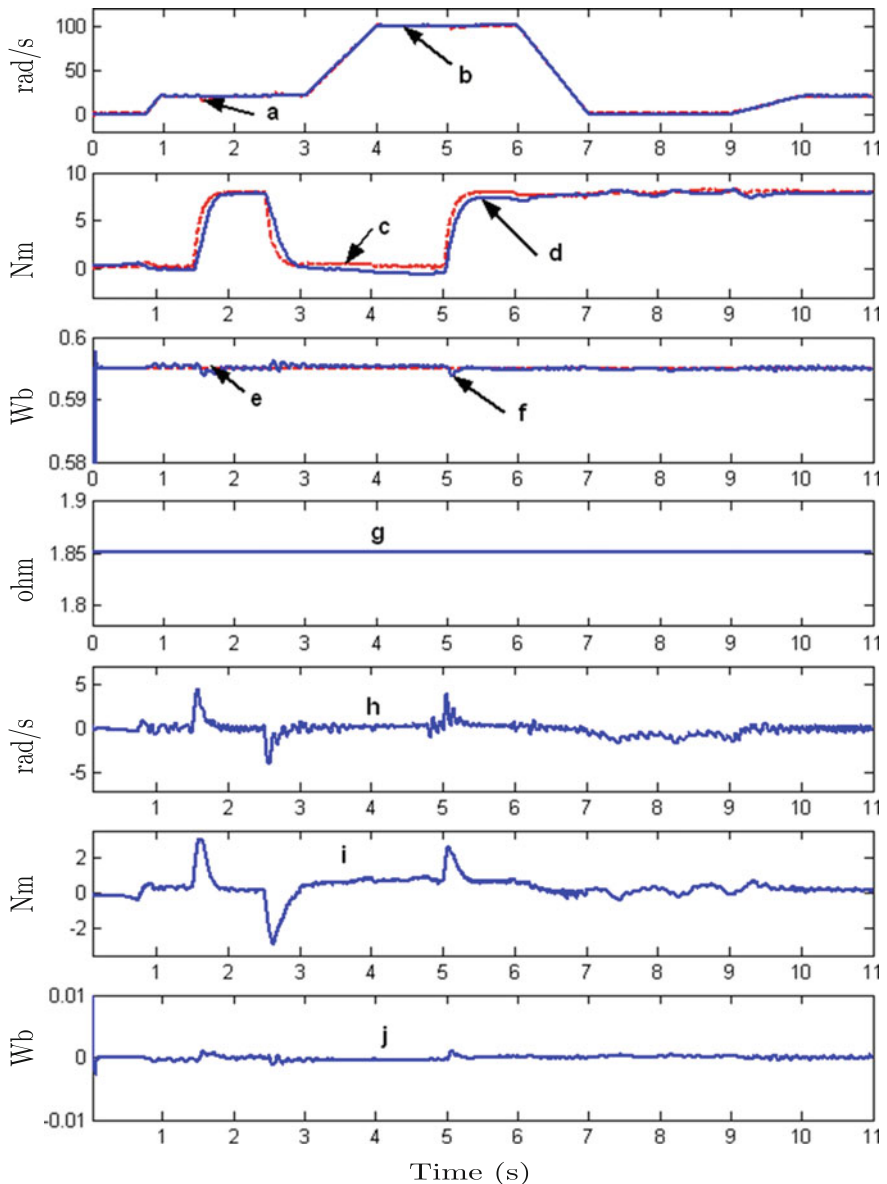
The proposed observer and controller are implemented using the stator resistance $R_{s0} = 1.9\,\Omega$ as the initial value of stator resistance estimation in the observer.

The experimental test is achieved by a significant benchmark (see Chap. 1, Sect. 1.6 for details); the time-varying reference trajectories are defined such that, at initial time, the rotor speed and load torque values are zero until the flux reaches its nominal value.

Fig. 7.6 Adaptive interconnected observer and integral backstepping control scheme

Figures 7.7 and 7.8 show the responses obtained from the experimental results by considering the nominal case with identified parameters. Notice the good performance of the proposed scheme, where the control action maintains the rotor speed and load torque close to the desired references even though in presence of the disturbance

Fig. 7.7 Experimental results in nominal case

(load torque). It is worth mentioning that on the experimental setup, the load torque is measured as a reference to compare with the estimated value provided by the observer.
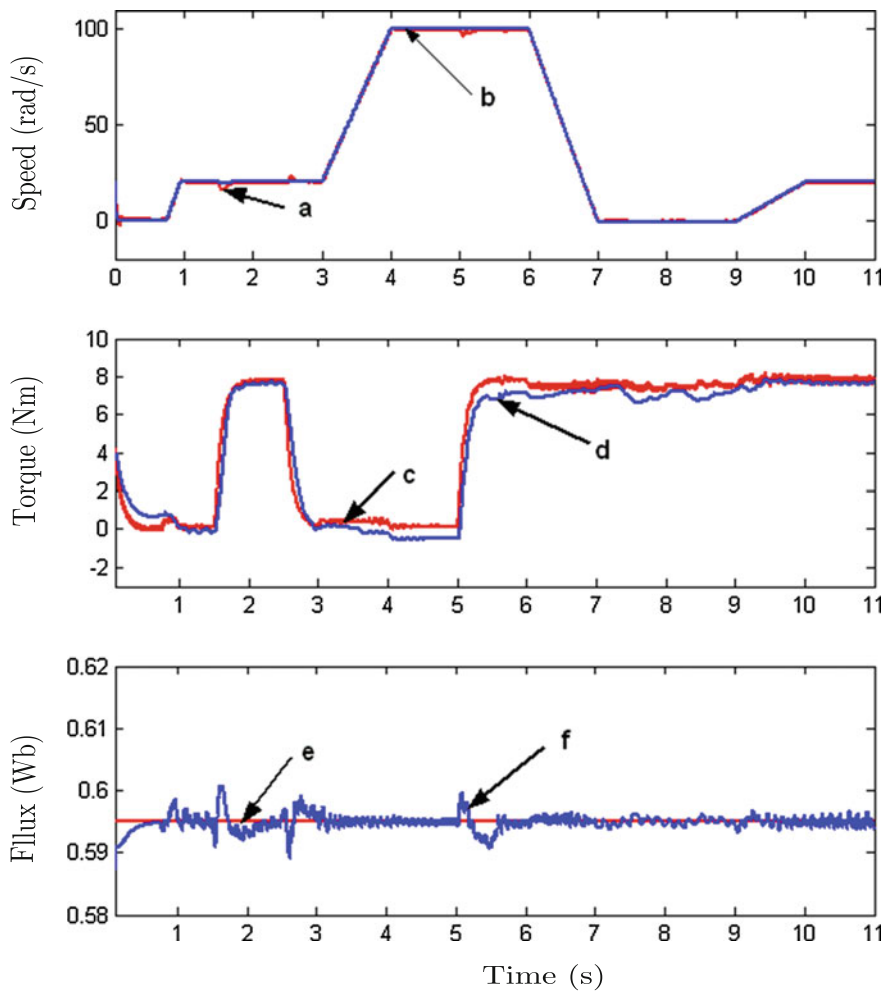
In terms of trajectory tracking, notice that the estimated rotor speed (Fig. 7.7b) converges to the measured speed (Fig. 7.7a) near and under conditions of unobservability. A similar conclusion is obtained for the estimated flux (Fig. 7.7f) with respect to the reference flux (Fig. 7.7e). The estimated load torque (Fig. 7.7d) converges to the measured load torque (Fig. 7.7c), under conditions of observability and at very low frequency (conditions of unobservability) from 7 to 9 s. Nevertheless, a small static error appears when the rotor speed increases (from 4 to 6 s). In terms of disturbance rejection, it is noted that the load torque is well rejected except at its application times (1.5 and 5 s), see Fig. 7.7h, j, and when it is removed (2.5 s) (Fig. 7.7h, j).

A comparison with the results obtained by a field-oriented control based on PI controllers and a non-adaptive observer, developed in [85], on the same setup and with the same experimental conditions is now developed. It has been shown that this observer is sensitive with respect to variation of the stator resistance. This problem clearly appears for the estimation of the flux, and more particularly, at low speed. This is an important point when a sensorless field-oriented control strategy is implemented.

Now, using an adaptive observer, the robustness with respect to the variation of the stator resistance is more confident. This can be seen in Fig. 7.9 which shows the responses of the stator resistance estimation (Fig. 7.10). This is also clear for the flux and speed tracking, by comparing the results obtained in the nominal case by our observer-controller with a FOC/IP controller (see respectively Figs. 7.7 and 7.8) and for the case of a rotor resistance variation: -50% (see Figs. 7.10 and 7.11).

In addition, in Fig. 7.12 is shown the responses obtained when a rotor resistance variation of -50 and $+50\%$ is considered for the observer-controller test. The robustness of the observer-controller scheme with respect to this parameter changes is clearly shown. From these responses, one concludes that the rotor resistance changes do not affect the performance of the speed trajectories tracking, when the conditions of observability are verified for the IM. When the motor is under conditions of unobservability, from 7 to 9 s, only a relatively small steady-state error comes out (Figs. 7.10a, b and 7.12a, b). Moreover, large peaks appear in the responses when the load torque is applied at time 1.5 and 5 s (Fig. 7.10h, j and Fig. 7.12h, j).

The last experiment first introduces a variation of $+10\%$ on the rotor self-inductance, and in the second experiment, a variation of $+10\%$ on the stator self-inductance value. This amplitude is realistic with the uncertainties on inductance values for electric motors. The responses of the system under the observer-controller action are, respectively, shown in Figs. 7.13 and 7.14 where one can see that the rotor and the stator self-inductance variation do not affect the performances of the system in closed-loop with the observer-controller algorithm. Nevertheless, small oscillations appear when the load torque is applied at time 5 s: Figs. 7.13a, b and 7.14a, b. Finally, in all cases one can see that the speed and the flux track in the desired references despite different changes in the parameters. This shows that the proposed scheme is robust under the parametric uncertainties and the load torque disturbance.
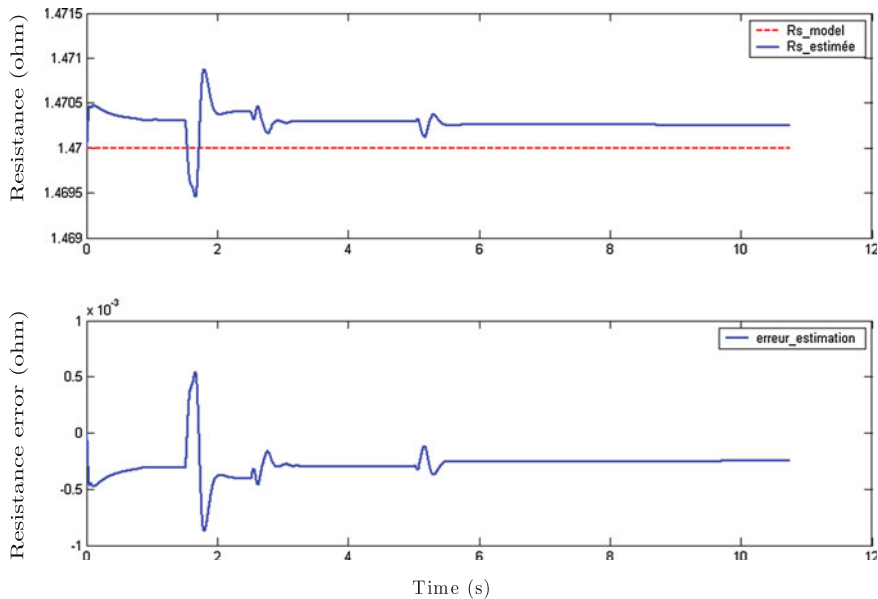
Fig. 7.8 FOC/IP controller: Experimental results in nominal case

7.2.3 Conclusions

A field-oriented controller combined with an integral backstepping technique is designed for the IM drive without mechanical sensors.

The major contributions of this study are summarized as follows:

(1) An adaptive interconnected observer to estimate the speed, fluxes, and load torque, whose performances are tested under disturbances and parametric uncertainties.
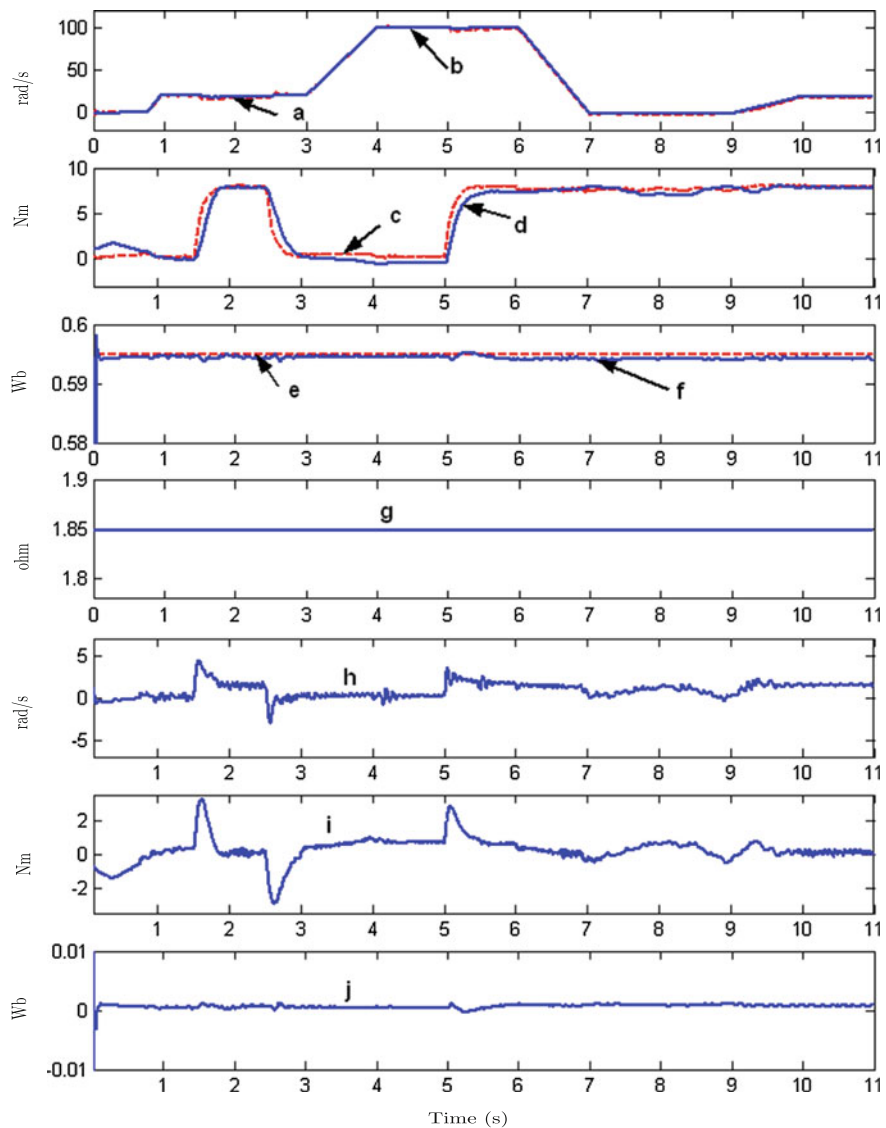
Fig. 7.9 Rs estimation with initial error: $+50\%$

(2) A field-oriented control combined with a robust integral backstepping technique to achieve a good speed and flux tracking for the IM without mechanical sensor under different operating conditions, particularly at low speed. These results are obtained thanks to an improved backstepping design using integral terms that eliminate the static errors in inner and outer loops to increase the robustness of the scheme.

(3) Sufficient conditions to guarantee the practical stability based on Lyapunov theory for the observer and for the "observer-controller" schemes.

(4) The successful application of the observer-controller scheme on an experimental setup with a significant sensorless control benchmark dealing with the low frequencies case.

(5) The robustness of the observer-controller scheme under significant parameters variations and unknown perturbation are shown for different operation conditions.

7.3 Robust Adaptive High Order Sliding Mode Control

In this section, the control of the IM without mechanical sensors (position, speed and load torque sensors) is designed by associating the adaptive interconnected observer, introduced in Chap. 3 (Sect. 3.4), with the HOSM controller, introduced in Chap. 5

Fig. 7.10 Experimental results with rotor resistance variation: $-50\,\%$
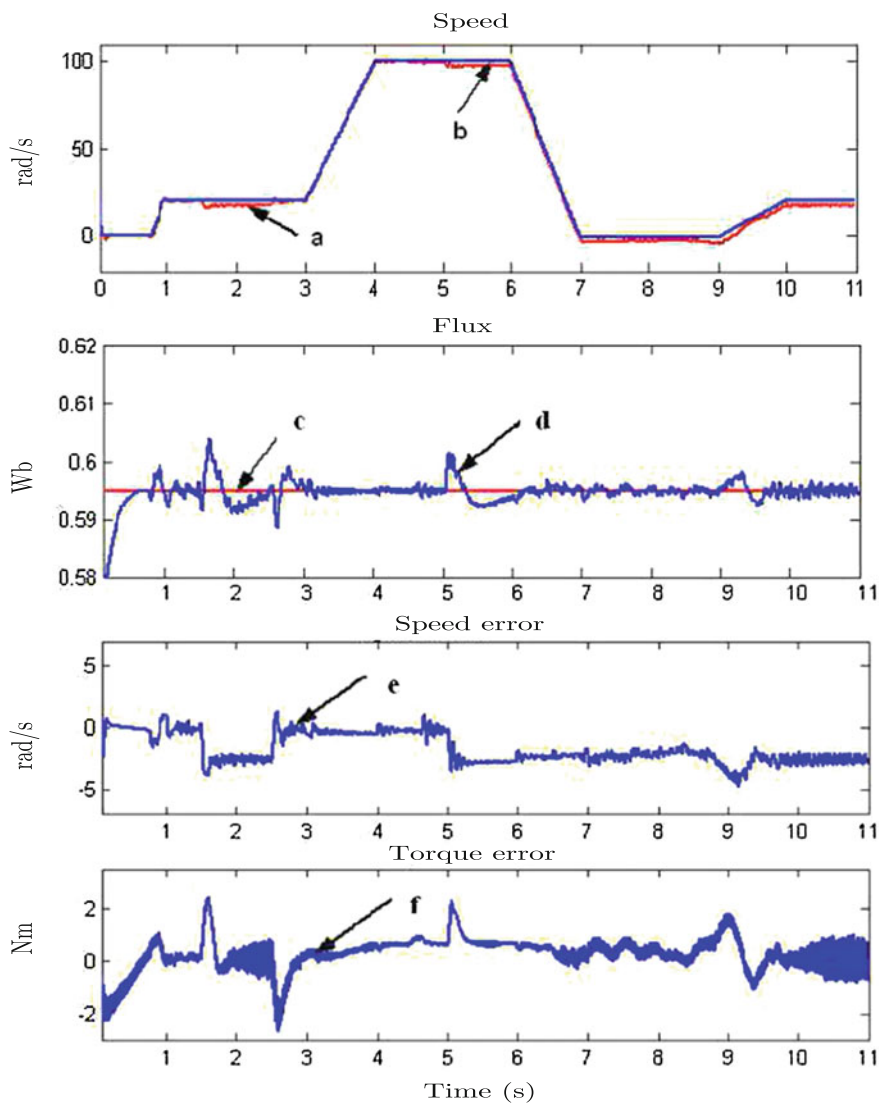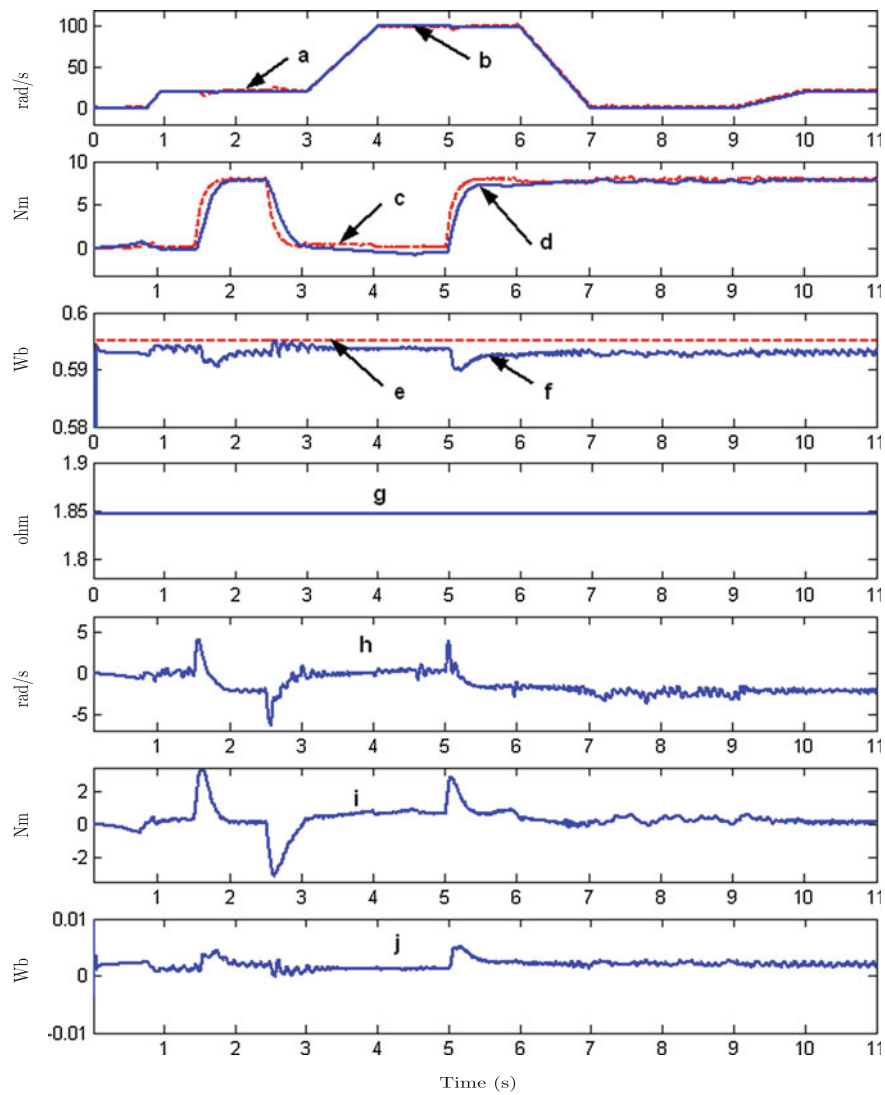
Fig. 7.11 FOC/IP controller: Experimental results with rotor resistance variation: -50%

Fig. 7.12 Experimental results with rotor resistance variation: $+50\,\%$
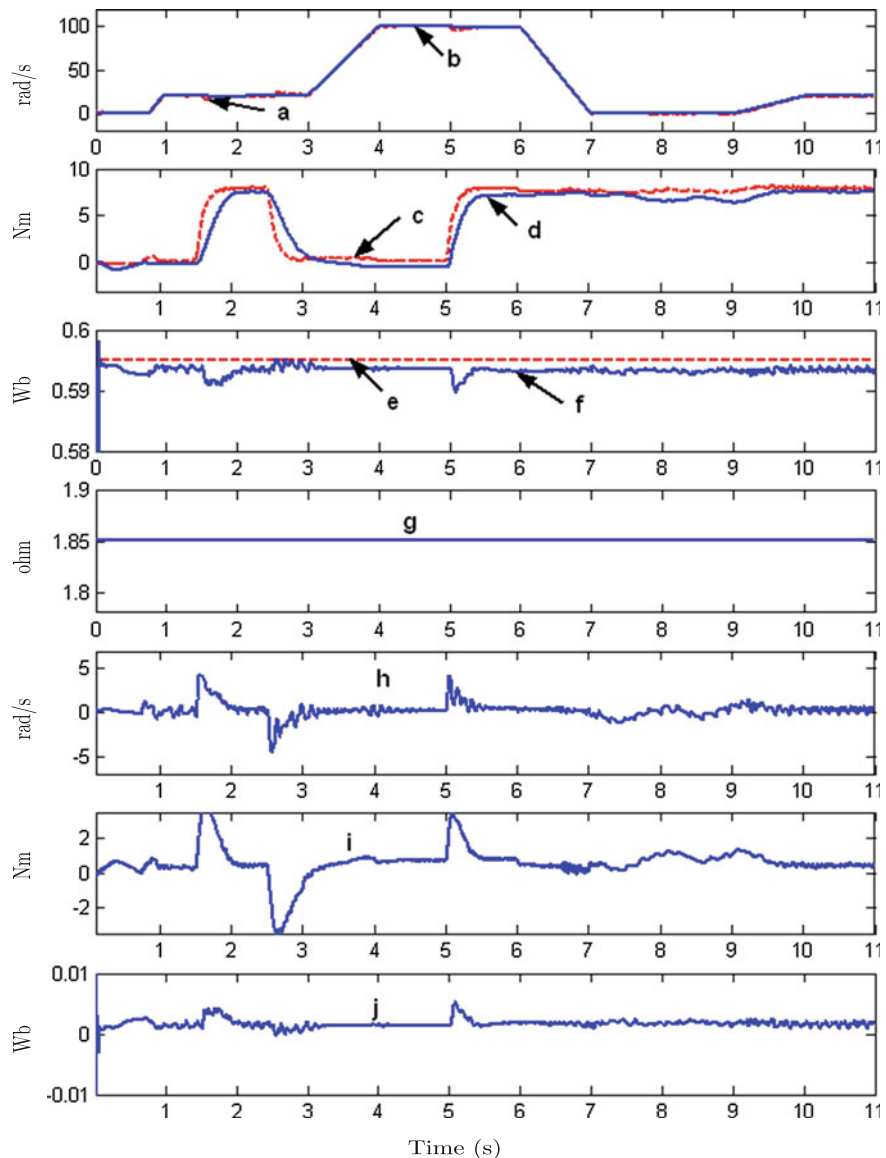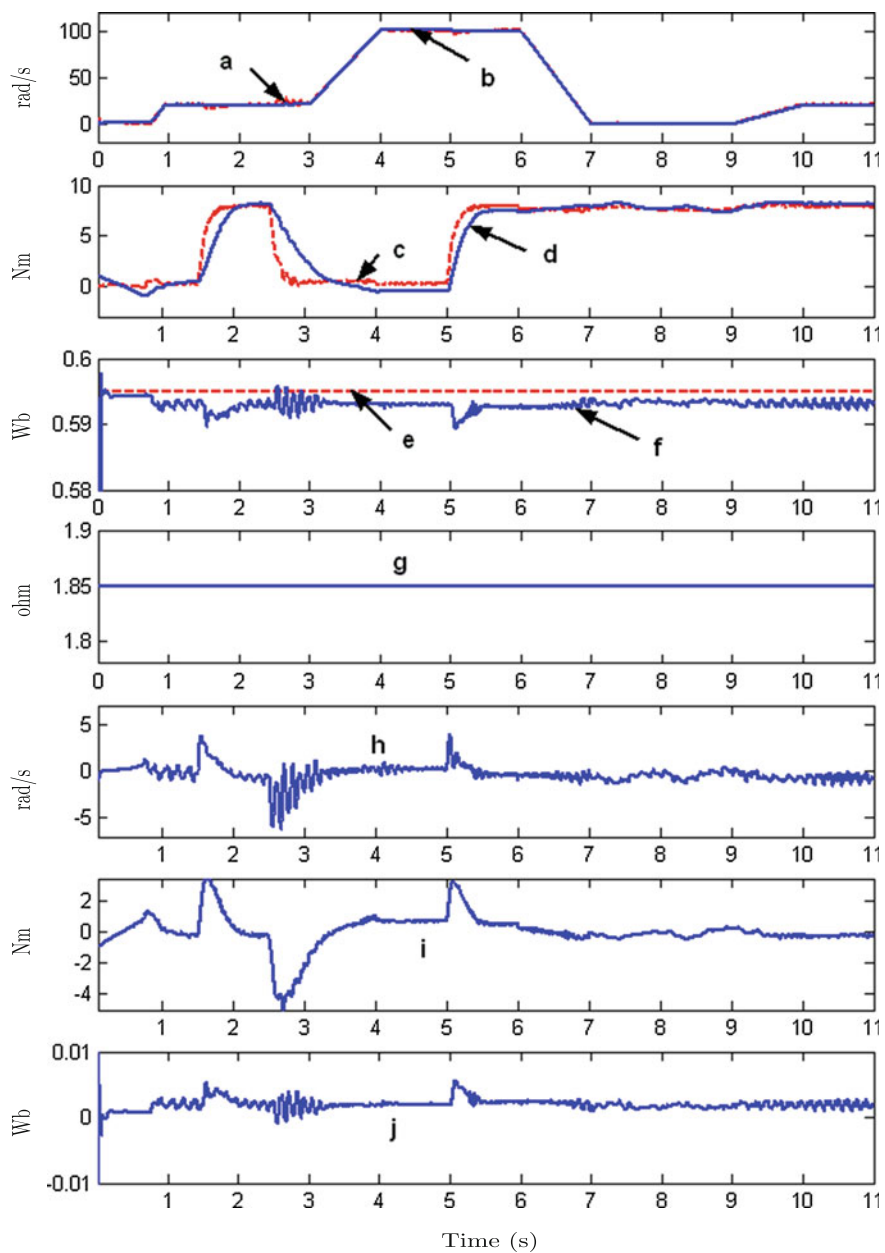
Fig. 7.13 Experimental results with rotor self-inductance variation: $+10\%$

Fig. 7.14 Experimental results with stator self-inductance variation: $+10\,\%$

(Sect. 5.3). The stability of the system in closed-loop with the controller + observer scheme is proved. Finally, the robustness of this scheme is evaluated experimentally showing its performances under parameter variations.

7.3.1 Analysis of the Closed-Loop System

As introduced previously, the position, speed, flux measurements and the stator resistance values are replaced by their estimated values in the control algorithm.

Next, define the new sliding variable as

$$\sigma_{\hat{\phi}} = \hat{\phi}_{rd} - \phi^*, \quad \sigma_{\hat{\Omega}} = \hat{\Omega} - \Omega^*.$$

Then the control input (5.38) given by

$$\begin{bmatrix} u_{sd} \\ u_{sq} \end{bmatrix} = (\hat{\varphi}_{\beta}^{Nom})^{-1} \left[- \begin{bmatrix} \hat{\varphi}_{\alpha_1}^{Nom} \\ \hat{\varphi}_{\alpha_2}^{Nom} \end{bmatrix} + \begin{bmatrix} \nu_{sd} \\ \nu_{sq} \end{bmatrix} \right] \tag{7.18}$$

with $\hat{\varphi}_{\beta}^{Nom}$, $\hat{\varphi}_{\alpha_1}^{Nom}$ and $\hat{\varphi}_{\alpha_2}^{Nom}$, the *estimated* values of φ_{β}^{Nom}, $\varphi_{\alpha_1}^{Nom}$ and $\varphi_{\alpha_2}^{Nom}$ (given by observer (3.110)).

By using the same design procedure as for control (5.31)–(5.38), the switching variables dynamics read as

$$\begin{bmatrix} \sigma_{\hat{\phi}}^{(3)} \\ \sigma_{\hat{\Omega}}^{(3)} \end{bmatrix} = \underbrace{\dot{\hat{\Psi}}_{\alpha} + \dot{\hat{\Psi}}_{\beta} \begin{bmatrix} \nu_{sd} \\ \nu_{sq} \end{bmatrix} - \begin{bmatrix} \phi^{*(3)} \\ \Omega^{*(3)} \end{bmatrix}}_{\hat{\varphi}_1} + \underbrace{\hat{\Psi}_{\beta}}_{\hat{\varphi}_2} \begin{bmatrix} \dot{\nu}_{sd} \\ \dot{\nu}_{sq} \end{bmatrix} \tag{7.19}$$

with $\begin{bmatrix} \dot{\nu}_{sd} & \dot{\nu}_{sq} \end{bmatrix}^T = \begin{bmatrix} -\alpha_{\phi}\mathrm{sign}(S_{\hat{\phi}}) & -\alpha_{\Omega}\mathrm{sign}(S_{\hat{\Omega}}) \end{bmatrix}^T$.

From (7.19) and the definition of switching vector (5.50), it yields

$$\begin{bmatrix} \dot{S}_{\hat{\phi}} & \dot{S}_{\hat{\Omega}} \end{bmatrix}^T = \hat{\varphi}_1 + \hat{\varphi}_2 \cdot \dot{\nu} - \begin{bmatrix} \chi_{\hat{\phi}} & \chi_{\hat{\Omega}} \end{bmatrix}^T. \tag{7.20}$$

By using the same design procedure introduced in Theorem 4.2. (Appendix "Appendix: A HOSM Algorithm"), there exist gains α_{ϕ} and α_{Ω} such that the switching surfaces satisfy the following inequalities

$$\dot{S}_{\hat{\phi}} S_{\hat{\phi}} \leq -\eta_{\hat{\phi}} |S_{\hat{\phi}}|, \quad \dot{S}_{\hat{\Omega}} S_{\hat{\Omega}} \leq -\eta_{\hat{\Omega}} |S_{\hat{\Omega}}|.$$

Hence, the estimation and the tracking errors of the closed-loop system asymptotically converge to zero in finite-time.

Remark 7.3 When the control inputs are not persistent, the IM tracks indistinguishable trajectories, and by using the same methodology given in [85], the strong uniform practical stability is proved.

7.3.2 Experimental Results

Experimental results obtained using the observer-control scheme are displayed to show the performance of the proposed approach under different operation conditions.
   The observer parameters, satisfying the convergence conditions, are chosen as

Summary 7.3.2 Tuning parameters
   Observer
   $\alpha = 50$, $\varpi = 10$, $k = 0.16$, $k_{c1} = 250$, $k_{c2} = 0.5$, $k_{\omega_s} = 60$
   $\theta_1 = 5000$, $\theta_2 = 7000$ and $\theta_3 = 10^{-12}$.

To optimize the behavior and the performance of the controlled induction motor, and owing to technical reasons, two groups of tuning parameters have been chosen: the first has been chosen to induce the reaching of the motor flux, the second to reject the disturbance, (i.e., the load torque) and to ensure high level accuracy for the trajectory tracking.
   Then, the sliding mode controller parameters are chosen such that the time of convergence is set at $t_f = 0.3$ s and

Summary 7.3.2 bis Tuning parameters
   Controller the convergence time t_f is fixed to 0.3 s
      For $t \leq 0.3$ s, $\zeta_\Phi = 0.32$ $\zeta_\Omega = 0.32$, $\omega_{n\Omega} = 250$ rad/s,
                  $\omega_{ni_d} = 32$ rad/s, $\alpha = 5.10^4$
      For $t > 0.3$ s. $\zeta_\phi = 0.35$, $\omega_{n\phi} = 447$ rad/s, $\alpha_\phi = 15 \times 10^4$,
                  $\zeta_\Omega = 0.7$, $\omega_b = 200$ rad/s, $\alpha_\Omega = 8.10^6$.
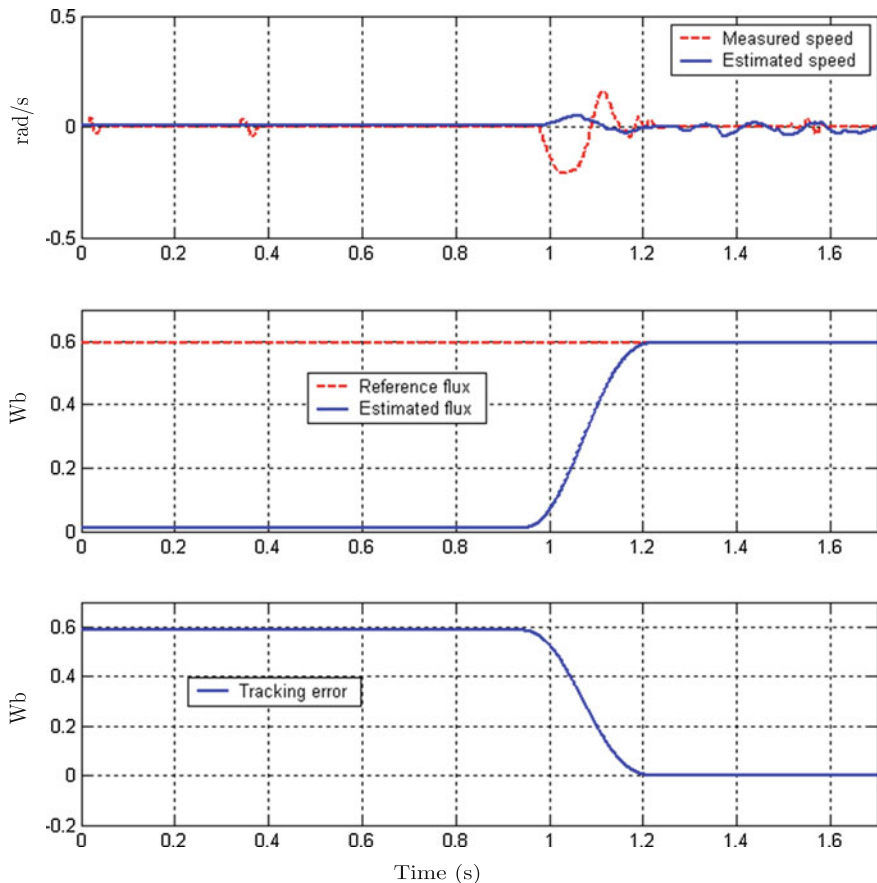
For experimental implementation of the observer-control scheme, we assume that only the stator currents are measured. Rotor speed and flux amplitude are provided by observer (3.110), whereas the flux angle is provided by estimator (7.15). The stator resistance observer is initialized as $R_{s0} = 1.9$ ohm. The initial value of ϕ_{rd} in the observer is $\phi_{rd0} = 0.1$ Wb. The experimental sampling time T equals 200 μs.
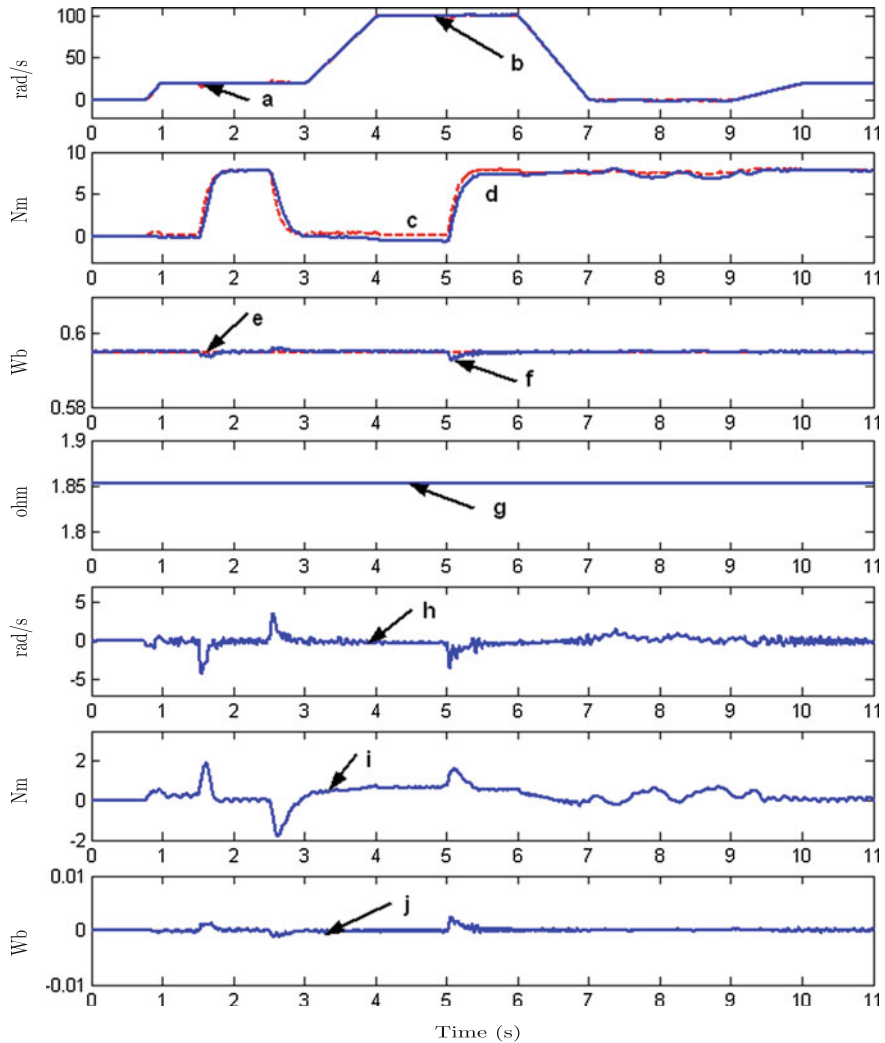
The aim of Fig. 7.15 is to show the control laws actions to drive the flux. The measured and estimated speeds are displayed in Fig. 7.15-Top. It can be viewed in this figure that the estimated speed reaches the measured speed at the convergence time t_f. Figure 7.15-Middle displays the desired and the estimated flux. It can be viewed in Fig. 7.15-Bottom that the flux tracking error converges to 0 in the a priori defined time of convergence t_f. This result confirms the good performance of the control law in the sense of tracking quality.

The experimental results[1] for the nominal case using the identified parameters (except stator resistance) are shown in Fig. 7.16. These figures show the good per-

Fig. 7.15 *Top* Measured speed Ω and its estimated versus time; *Middle* Reference flux and its estimated versus time; *Bottom* Flux tracking error versus time
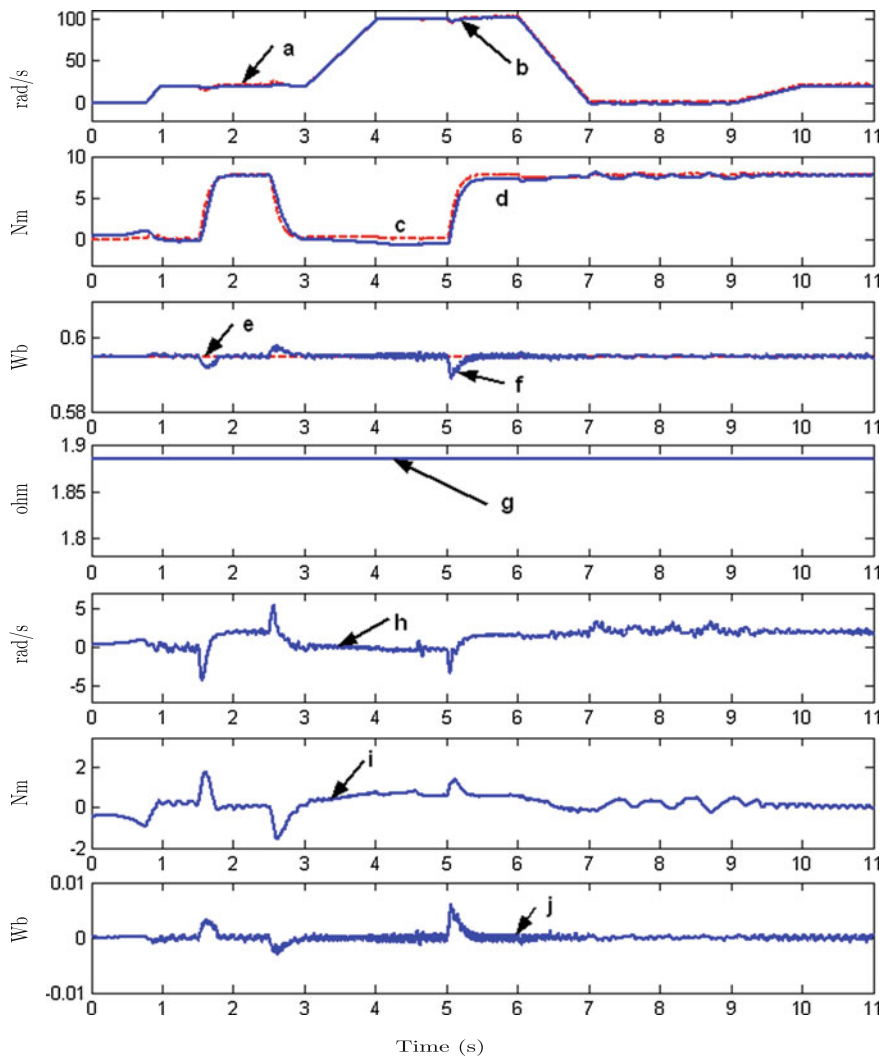
[1] For each figure, each line is refereed to a, c: measured speed and load torque, e: reference flux, b, d, f, g: estimated speed, load torque, flux, and stator resistance, h, i, j: speed, load torque, and flux estimation error.

Fig. 7.16 Experimental result in nominal case

formance of the complete system observer-controller for the trajectory tracking and
the disturbance rejection. In terms of trajectory tracking, we note that the estimated
motor speed (Fig. 7.16b) converges to the measured speed (Fig. 7.16a) near and under
conditions of unobservability. The same conclusion is obtained for the estimated flux
(Fig. 7.16f) with respect to the reference flux (Fig. 7.16e). The estimated load torque
(Fig. 7.16d) converges to the measured load torque (Fig. 7.16c), under conditions of
observability and at very low frequency (conditions of unobservability) from 7 to
9 s. Nevertheless, a small static error appears when the motor speed increases (from
4 to 6 s). In terms of disturbance rejection, we have noted that the load torque is well

rejected except at the time interval (1.5 and 5 s) when it is applied (see Fig. 7.16h
and j); and when it is removed at time 2.5 s (see Fig. 7.16h and j). In Fig. 7.16g, it can
be viewed that the stator resistance estimation remains almost constant despite the
noise and transient dynamics of speed and load torque. This test shows the capability
of the proposed controller to guarantee flux and speed tracking for slowly varying
speed reference with excitation frequency close to zero (in the time interval from 7
to 9 s).

Fig. 7.17 Experimental result with rotor resistance variation: $+50\%$

The robustness of the observer-controller scheme is confirmed from the result obtained under rotor resistance variations: $+50$ and -50% around the nominal value (see Figs. 7.17 and 7.18). These figures display similar experimental results as for the rotor resistance nominal case under conditions of observability. In conclusion, we can say that the variation in the rotor resistance value does not affect the performance of the speed trajectory tracking, when the observability conditions of the IM are satisfied. When the motor is under unobservable condition (from 7 to 9 s), a static error appears: see Figs. 7.17a, b and 7.18a, b. The static error transient increases when the load torque is applied at time 1.5 and 5 s: Figs. 7.17h, j and 7.18h, j.

Last robustness tests are made by taking into account variations of $+10\%$ of the nominal value of the rotor/stator self-inductance. The results of these tests are shown in Figs. 7.19 and 7.20. By analyzing these figures, we can see that the rotor and stator self-inductance variation does not significantly affect the performances of the observer+controller scheme. Nevertheless, a small oscillation appears when the load torque is applied at time 5 s (see Figs. 7.19a, b and 7.20a, b).

7.3.3 Conclusions

In this section is presented a study investigating the performance of an HOSM control of the IM without mechanical sensors: position, speed, and load torque sensors. The major contributions of this study are summarized as follows:

(1) The design of an adaptive interconnected observer that well estimates the rotor speed, rotor fluxes, and load torque even when an external load disturbance is applied.

(2) The successful development of a field-oriented control using an HOSM controller to achieve a robust speed and flux tracking for the IM under observable and unobservable conditions. The proposed HOSM controller ensures a finite time convergence, high accuracy (higher than "standard" SM), and robustness.

(3) The strong uniform practical stability based on the Lyapunov theory has been considered for the observer convergence. Stability of the observer-controller scheme has been also proved where sufficient conditions have been obtained ensuring that the tracking and the estimation errors tend to a ball of radius expressed in terms of the controller-observer parameters and system uncertainties.

(4) The successful application of the observer-controller scheme on an experimental setup with a significant sensorless control benchmark. The robustness of the observer and the controller is confirmed by significant parameter variations tests.
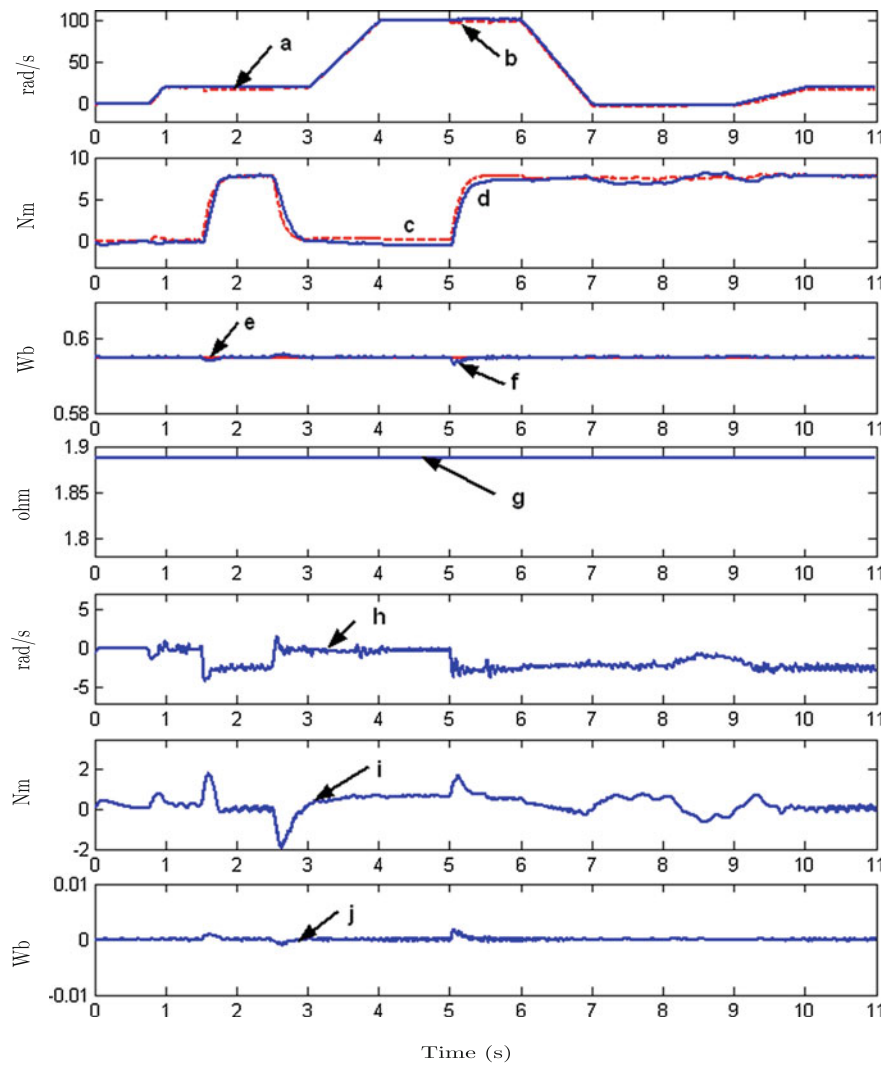
Fig. 7.18 Experimental result with rotor resistance variation: $-50\,\%$
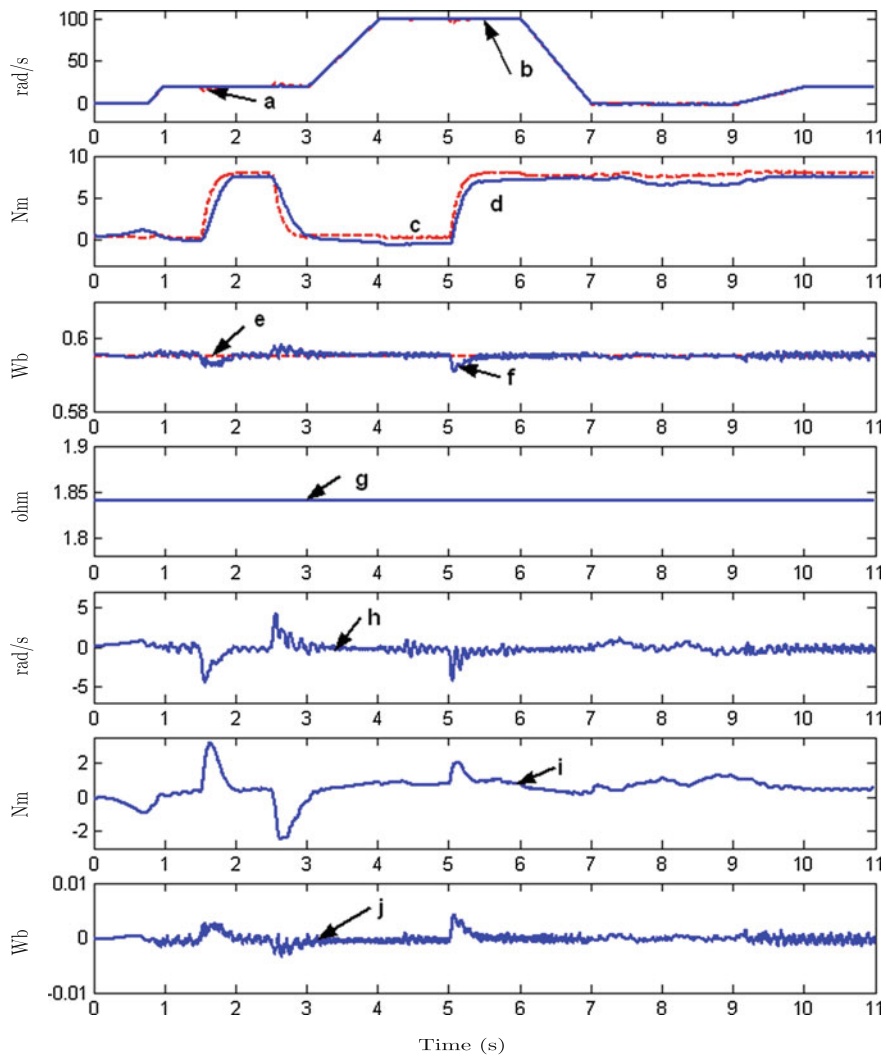
Fig. 7.19 Experimental result with rotor self-inductance variation: $+10\%$
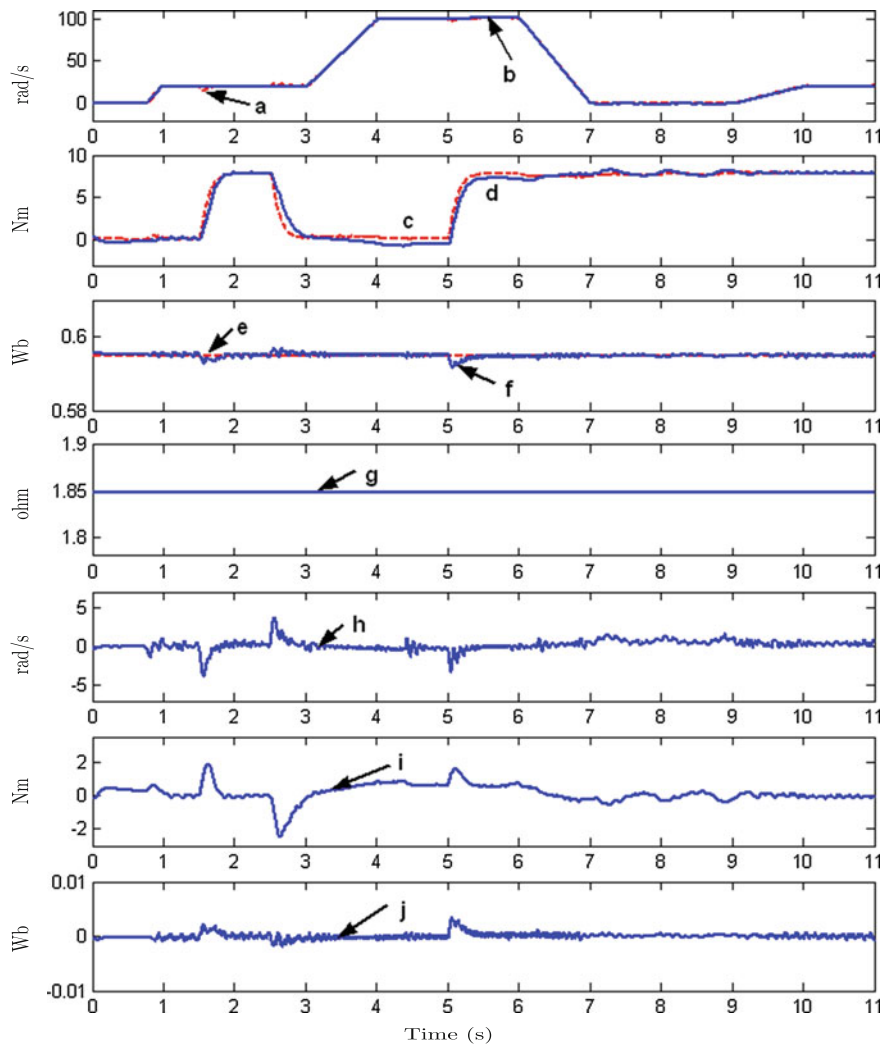
Fig. 7.20 Experimental result with stator self-inductance variation: $+10\,\%$

7.4 Conclusions

In this chapter, two observer-controller schemes have been presented to solve the tracking problem of the sensorless induction motor. One of these schemes is based on a backstepping control technique using the estimates given by an adaptive interconnected observer. A stability analysis of the closed-loop system has been developed, and sufficient conditions have been given to guarantee the strong uniform practical stability of the tracking error. The advantage of applying this observer-controller scheme is the simplicity to tune the control and observer gains. No important computational effort is necessary to implement such a control scheme.

On the other hand, a high order sliding mode controller combined with an adaptive interconnected observer has been studied. Thanks to the finite time convergence of the controller, which can be fixed in advance, and its attractive robustness properties, the proposed scheme becomes an interesting alternative to control induction machines.

Several experimental tests have been realized to show the real performance of both of the induction motor sensorless controllers. From the experimental results, we can conclude that the scheme constituted by the backstepping controller combined with the adaptive interconnected observer has shown better performance compared to the high order sliding mode control plus the adaptive interconnected observer. Simplicity to tune, less computational effort, and high quality of the responses have been the remarkable advantages of this scheme. Nevertheless, the HOSM controller is slightly more robust under parametric uncertainties than the integral backstepping controller.

7.5 Bibliographical Notes

As introduced in Chap. 5, for the sensorless control of the induction motor, the knowledge of the rotor speed is crucial for control applications, and generally a sensor is used. However, the minimization of the number of sensors contributes to simplify the installation and decreases the cost of both control and maintenance.

Consequently, there is considerable interest in IM control without mechanical sensors. A major difficulty is the estimation of the state variable at low frequencies. In [44], the authors have demonstrated that the main conditions to lose the observability of the IM are: the excitation voltages frequency is zero and the rotor speed is constant. A more complete analysis of the IM observability is given in Chap. 2 of this book. Another difficulty is to ensure the robustness against parameter variations. In the literature, several approaches have been proposed to estimate the rotor velocity, and/or the load torque, and/or some sensitive parameters from the measurements: the stator currents and voltages, and then to design sensorless controls, see for example: [26, 27, 29, 32, 35, 36, 49, 64, 67, 70, 71, 82]. Almost all the IM sensorless control papers do not validate the sensorless controls on significant trajectories and with robustness tests. It is essential to check the sensorless control when the observability property is lost to validate if the algorithms are robust with respect to this singularity.

Of course, this test has to be done with nominal torque and completed with robustness test with respect to parameters variation as the stator resistance variation [43] and the inductance variation. Regarding the observer developed in [85], it has been shown that the observer is sensitive with respect to a variation in the stator resistance. For example, in [84] an industrial sensorless drive was tested and did not succeed to track the significant test trajectories (see [34]) introduced in Chap. 1. This sensitivity problem clearly appears for the observation of flux and more particularly at low speed. This is an important point when a sensorless field- is implemented. By using the adaptive observer, the robustness with respect to the variation of the stator resistance is more confident.

The classical sensorless field-oriented control has been tested for the trajectory tracking control on significant references in [85][2]. A best result is obtained using a robust adaptive observer-backstepping sensorless control in [88][3] and [89][4]. In [89] an observer-controller stability analysis is given, with sufficient conditions to ensure that the tracking dynamics are strongly uniformly practically stable (see [59]). More precisely, the tracking errors converge to a ball whose radius can be reduced by tuning the gains of the observer-controller scheme. Furthermore, experimental results using this scheme are given.

Another approach is proposed in [86][5] where a robust adaptive high order sliding mode control combined with an adaptive interconnected observer is implemented in the IM. One of the most interesting characteristics of this approach is that the convergence time of the controller can be a priori fixed. Experimental results are also given where the robustness and the performance are shown.

Appendix: Stability of the Observer-Controller Scheme

Recall that the main goal of this chapter is to synthesize a robust sensorless control of induction motor, assuming that the speed and the flux are not available by measurement, and the load torque is considered as an unknown input. In order to implement the above control law it is necessary to replace speed and flux, the stator resistance,

---

[2] This chapter includes excerpts from "Traore D, De Leon J, Glumineau A, Loron L (2007) Speed sensorless field-oriented control of induction motor with interconnected observers: experimental tests at low frequencies benchmark. IET Control Theory Applications, 1–6(10):16811692, DOI 10.1049/iet-cta.2009.0648" with permission from IET.

[3] This chapter includes excerpts of "Traore D, De Leon J, Glumineau A (2010) Sensorless induction motor adaptive observer-backstepping controller: experimental robustness tests on low frequencies benchmark. IET Control Theory Applications 4(10):19892002, DOI 10.1049/iet-cta.2009.0648" with permission from IET.

[4] This chapter, includes excerpts of [89], originally published in the IFAC journal: Automatica, 48:682687, IFAC-PapersOnLine IFAC 2012.

[5] This chapter includes excerpts of [86], (2008) IEEE. Reprinted, with permission, from "Traore D, Plestan F, Glumineau A, de Leon J (2008) Sensorless induction motor: High-order sliding-mode controller and adaptive interconnected observer. IEEE Transactions on Industrial Electronics, 55(11):38183827".

and the stator frequency by their estimated values provided by the observer. To achieve this goal, one rewrites the speed and flux controllers (5.19), and the control inputs (5.28) as functions of the estimate variables as follows:

$$
\begin{cases}
i_{sq}^* = \frac{1}{m\hat{\phi}_{rd}}[\dot{\Omega}^* + c\hat{\Omega} + \frac{\hat{T}_l}{J} + (K_\Omega + K_\Omega')(\Omega^* - \hat{\Omega}) + K_\Omega K_\Omega' \int_0^t (\Omega^* - \hat{\Omega})dt] \\
i_{sd}^* = \frac{1}{aM_{sr}}[\dot{\phi}^* + a\hat{\phi}_{rd} + (K_\phi + K_\phi')(\phi^* - \hat{\phi}_{rd}) + K_\phi K_\phi' \int_0^t (\phi^* - \hat{\phi}_{rd})dt]
\end{cases}
$$
$$(7.21)$$

$$
\begin{cases}
u_{sq} = \frac{1}{m_1}[K_{iq}(i_{sq}^* - i_{sq}) + K_{iq}''(K_{iq} - K_{iq}')\int_0^t (i_{sq}^* - i_{sq})dt + 2m\hat{\phi}_{rd}(\Omega^* - \hat{\Omega}) \\
\qquad + K_\Omega' \int_0^t (\Omega^* - \hat{\Omega})dt + bp\hat{\Omega}\hat{\phi}_{rd} + (\gamma_1 + m_1\hat{R}_s)i_{sq} + \tilde{\omega}_s i_{sd} + i_{sq}^*] \\
u_{sd} = \frac{1}{m_1}[K_{id}(i_{sd}^* - i_{sd}) + K_{id}''(K_{id} - K_{id}')\int_0^t (i_{sd}^* - i_{sd})dt + 2aM_{sr}(\phi^* - \hat{\phi}_{rd}) \\
\qquad + K_\phi' \int_0^t (\phi^* - \hat{\phi}_{rd})dt - ba\hat{\phi}_{rd} + (\gamma_1 + m_1\hat{R}_s)i_{sd} - \tilde{\omega}_s i_{sq} + i_{sd}^*]
\end{cases}
$$
$$(7.22)$$

with $\tilde{\omega}_s$ is the estimation of the stator pulsation defined in (7.15). The reduced model of the induction motor (5.4) in closed-loop with the controls (7.22) is given by

$$
\begin{bmatrix} \dot{\Omega} \\ \dot{\phi}_{rd} \end{bmatrix} = \begin{bmatrix} m\phi_{rd}i_{sq}^*(\hat{\Omega}, \hat{\phi}_{rd}) - c\Omega - \frac{T_l}{J} \\ -a\phi_{rd} + aM_{sr}i_{sd}^*(\hat{\phi}_{rd}) \end{bmatrix}. \tag{7.23}
$$

Remark 7.4 In order to avoid a singularity problem in (7.21), the observer is initialized using a flux initial condition different from zero, such that controller (7.21) is well-defined. This condition is actually a physical condition of IM: no flux implies no torque (see [66] for more details). Moreover, the flux controller (7.21) allows to guarantee that ϕ_{rd} quickly reaches its reference ϕ^*. Before the motor is fluxed, (i.e., $\phi_{rd} = \phi^*$) the speed reference is kept to zero.

Here, it will be demonstrated that the singularities of controller (7.21) are avoided for all $t \geq 0$.

The speed and flux tracking error dynamics (5.18) can be rewritten in the following form:

$$
\begin{cases}
\dot{z}_\Omega = -K_\Omega z_\Omega - (K_\Omega + K_\Omega' - c)B_{\Omega_1}\epsilon_1 + \epsilon_2^T B_{\Omega_2}^T \Gamma(z_\Omega) + \frac{\epsilon_3}{J} - \Gamma(\epsilon_\Omega) \\
\dot{z}_\phi = -K_\phi z_\phi - (K_\phi + K_\phi' - a)B_\phi \epsilon_2 - \Gamma(\epsilon_\phi.)
\end{cases} \tag{7.24}
$$

where the estimation errors are

$$
\epsilon_\Omega = \Omega - \hat{\Omega}, \quad \epsilon_\phi = \phi_{rd} - \hat{\phi}_{rd},
$$

and the nonlinear terms:

$$\Gamma(z_\Omega) = \frac{1}{\hat{\phi}_{rd}} \left[\dot{\Omega}^* + c\hat{\Omega} + \frac{\hat{T}_l}{J} + (K_\Omega + K'_\Omega)(\Omega^* - \hat{\Omega}) + K_\Omega K'_\Omega \int_0^t (\Omega^* - \hat{\Omega})dt \right],$$

$$\Gamma(\epsilon_\Omega) = -K_\Omega K'_\Omega \int_0^t \epsilon_\Omega dt, \ \Gamma(\epsilon_\phi) = -K_\phi K'_\phi \int_0^t \epsilon_\phi dt,$$

$$B_{\Omega_1} = B_\phi = \begin{bmatrix} 0 & 1 & 0 \end{bmatrix}, \qquad B_{\Omega_2} = \begin{bmatrix} 0 & -1 & 0 \end{bmatrix}$$

Then, one can establish the following lemma.

Lemma 7.2 *Consider system* (1.108)*, and assuming that the reference signals i_{sq}^*, i_{sd}^*, Ω^* and ϕ^* are differentiable and bounded, and conditions given in Remark* 3.17 *hold. Then, system* (1.108) *in closed-loop with the speed, flux, and current tracking laws* (7.21) *and* (7.22)*, using the estimates provided by an adaptive interconnected observer* (3.110)*, is strongly uniformly practically stable.*

The proof follows the same procedure as the control analysis given in Chap. 5.

Chapter 8
Conclusions

Thanks to the considerable progress in technological developments, the applicability of recent control techniques for AC machines is now possible according to the requirements of manufacturers. This book has aimed to introduce some recent results in control and observation theories applied to the control of AC machines for a wide range of operations. Special attention has been paid to the sensorless AC machines case, in particular, by the application of nonlinear observers and robust control strategies.

It is clear that intensive research activity in AC machines control has been carried out recently. In this book, has been treated specific topics on control and observation theories. They have significant qualities thanks to their robustness in the presence of uncertainties and disturbances and thanks to their convergence property.

As an initial step, the observation problem for nonlinear systems was presented as well as the analysis of AC machines observability property. This topic attracts more attention in the sensorless case because the AC machines observability property fails at low speed. Taking into account that the observability for some classes of nonlinear system can depend on the input, some definitions have been introduced and used to determine whether the system is observable. This property is important for these systems because for the observer design, the convergence requires that the inputs satisfy the persistent condition: the inputs sufficiently excite the system to keep the observability property. Once the observability of the AC machines is verified, the study of an observer design can start. When a solution exists and if the observability depends on the system inputs, its convergence is ensured provided the input is persistent. Several structures for which an observer can be designed have been presented for the AC machines. In this way, Chap. 3 is devoted to the introduction of the different structures for which the mathematical models of the AC machines can be transformed into a form that allows the design of an observer.

The estimation of the non-measurable components of the state and the identification of some important unknown parameters or disturbances can be simultaneously done online by using the proposed adaptive interconnected observers. Mainly three kinds of observers have been studied: Luenberger like type, Kalman like type, and Sliding Mode Observer. Furthermore, the observers can be classified in terms of

their convergence: those with asymptotic convergence (interconnected observer and adaptive interconnected observer) and those with a finite-time convergence (sliding mode and super-twisting observers). Both classes of observers have interesting robust properties and advantages in their implementation. However, some considerations were taken into account in their selection. For instance: the tuning simplicity, computational effort, performance, and robustness under perturbations are aspects that play an important role to select the appropriate strategy.

For the industrial motion applications, the control of AC machines is one of the main goals for researchers and engineers due to the advantages of these machines: low cost, ruggedness, and versatility. However, they are complex to control, and some parameters are not well known.

Thanks to recent results in control design and to technological developments, it is possible to improve AC machines control and their performances. Recent results in control design are given in Chap. 4 for the PMSM and in Chap. 5 for the induction motor. Robust nonlinear techniques are introduced to design controllers that achieve the desired control objectives. One of the proposed techniques is the backstepping control (with or without additional integral terms). Its simplicity to tune and to implement allows to easily apply such controllers in this framework. The other presented control approach is the high order sliding mode control with finite-time convergence property and robust performance in presence of uncertainties.

Then, the design of the observer-controller schemes were described based on the main characteristics of each controller and each observer. The focus was to illustrate the performance of the proposed observer-controller schemes based on nonlinear observers and robust controllers applied to the AC machines control. In the framework of significant benchmarks and thus for a wide range of operation, according to the simulation and the experimental results, it was shown satisfactory performances for the speed tracking control algorithms associated with nonlinear observers. The experimental results obtained for the induction motor under parametric uncertainties and external disturbances have shown that the rotor speed control robustly tracks the desired reference under variation of the load torque and variation of the machine parameters.

Given the wide field of research in electrical machines, a lot of developments exist from a theoretical or practical point of view. Novel technologies must be integrated and more powerful control strategies must be implemented to answer to the new challenging problems for industrial applications. One of the most interesting prospects of research for AC machine control development could be to increase the applicability of these machines even if faults appear. Fault diagnosis methods can be used. These algorithms can be seen as natural extensions of the observation scheme developed in this book. Next, a prospect could be to adapt the control to the detected fault in order to carry on the machine control with limited but safe objectives. A direct application can be the electric traction system in automotive or aeronautic areas.

References

1. Aurora C, Ferrari A (2004) Speed regulation of induction motors: an adaptive sensorless sliding mode control scheme. IEEE American control conference ACC0'04
2. Barambones O, Garrido AJ (2004) A sensorless variable structure control for induction motor drives. Electr Power Syst Res 72:21–24
3. Besancon G (2007) Nonlinear observers and applications. Springer, Berlin
4. Besancon G, Hammouri H (1996) Observer synthesis for class of nonlinear control systems. Eur J Control 2:176–192
5. Besancon G, Hammouri H (1998) On observer design for interconnected systems. J Math Syst Estim Control 8(3):377
6. Besancon G, DeLeon J, Huerta O (2006) On adaptive observers for state affine systems. Int J Control 79:581–591
7. Blaschke F (1972) The principle of field orientation applied to the new trans-vector closed-loop control system for rotating field machine. Siemens Rev 93:217–220
8. Bodson M, Chiasson J, Novotnak R (1994) High-performance induction motor control via input-output linearization. IEEE Control Syst 14(4):25–33. doi:10.1109/37.295967
9. Bose B (2002) Modern power electronics and ac drives. Prentice Hall PTR, Upper Saddle River
10. Boussak M (2005) Implementation and experimental investigation of sensorless speed control with initial rotor position estimation for interior permanent magnet synchronous motor drive. IEEE Trans Power Electron 20(6):1413–1422. doi:10.1109/TPEL.2005.854014
11. Canudas C, Youssef A, Barbot J, Martin P, Malrait F (2000) Observability conditions of induction motors at low frequencies. In: IEEE conference on decision and control, Sydney, Australia
12. Cascella G, Salavatore N, Salvatore L (2003) Adaptive sliding-mode observer for field oriented sensorless control of spmsm. IEEE international symposium on industrial electronics, Rio de Janeiro, Brasil, pp 1137–1143
13. Castro-Linares R, Laghrouche S, Glumineau A, Plestan F (2004) Higher order sliding mode observer-based control, In: 2nd IFAC symposium on system, structure and control, Oaxaca, Mexico
14. Chen Z, Tomita M, Doki S, Okuma S (2003) An extended electromotive force model for sensorless control of interior permanent-magnet synchronous motor. IEEE Trans Ind Electron 50(2):288–295
15. Chiasson J (1995) Non linear controllers for induction motors. IFAC conference system structure and control
16. Chiasson J (1998) A new approach to dynamic feedback linearization control of an induction motor. IEEE Trans Autom Control 43(3):391–397. doi:10.1109/9.661597
17. Chiasson J (2005) Modeling and high-performance control of electrical machines. Wiley, New York

18. Ciabattoni L, Corradini M, Grisostomi M, Ippoliti G, Longhi S, Orlando G (2010) Robust speed estimation and control of pm synchronous motors via quasi-sliding modes. In: 49th IEEE CDC 2010, Atlanta, USA, pp 15–17

19. Davila J, Fridman L, Levant A (2005) Second-order sliding-mode observer for mechanical systems. IEEE Trans Autom Control 50:1785–1789

20. Ezzat M, De Leon J, Gonzalez N, Glumineau A (2010) Observer-controller scheme using high order sliding mode techniques for sensorless speed control of permanent magnet synchronous motor. In: Decision and control (CDC), 49th IEEE conference on decision control, Atlanta, USA, pp 4012–4017. doi:10.1109/CDC.2010.5717365

21. Ezzat M, De Leon J, Glumineau A (2011) Adaptive interconnected observer-based backstepping control design for sensorless pmsm. IFAC world congress, IFAC, Milano, Italy, vol 18. pp 6148–6153

22. Ezzat M, De Leon J, Glumineau A (2011) Sensorless speed control of pmsm via adaptive interconnected observer. Int J Control 84(11):1926–1943

23. Filippov AF (1988) Differential equations with discontinuous right-hand sides. Kluwer, Dortrecht

24. Floquet T, Barbot J (2007) Super twisting algorithm based step-by-step sliding mode observers nonlinear systems with unknown inputs. Int J Syst Sci 38(10):803–815

25. Furuhashi T, Sangwongwanich S, Okuma S (1992) Sensorless sliding-mode mtpa control of an ipm synchronous motor drive using a sliding-mode observer and hf signal injection. IEEE Trans Ind Electron 39(2):89–95

26. Gadoue S, Giaouris D, Finch J (2009) Sensorless control of induction motor drives at very low and zero speeds using neural network flux observers. IEEE Trans Ind Electron 56(8):3029–3039. doi:10.1109/TIE.2009.2024665

27. Gastaldini C, Azzolin R, Grundling H (2009) A comparison of speed-sensorless induction motor control with torque compensation. In: Electric machines and drives conference, 2009. IEMDC '09. IEEE International, pp 1480–1485. doi:10.1109/IEMDC.2009.5075398

28. Gauthier JP, Hammouri H, Othman S (1992) A simple observer for nonlinear systems applications to bioreactors. IEEE Trans Autom Control 37(6):875–880. doi:10.1109/9.256352

29. Ghanes M, Zheng G (2009) On sensorless induction motor drives: Sliding mode observer and output feedback controller. IEEE Trans Ind Electron 56(9):3404–3413

30. Ghanes M, DeLeon J, Glumineau A (2005) Validation of an interconnected high gain observer for sensorless induction motor on low frequencies benchmark: Application to an experimental set-up. IEE Proc Control Theory Appl 152:371–378

31. Ghanes M, DeLeon J, Glumineau A (2006) Observability study and observer-based interconnected form for sensorless induction motor. In: Proceedings of the 45th IEEE CDC, Manchester Grand Hyatt Hotel San Diego USA, December 13–15, pp 1240–1245

32. Ghanes M, Leon J, Glumineau A (2006) Novel controller for induction motor without mechanical sensor and experimental validation. In: Proceedings of the 45th IEEE CDC, Manchester Grand Hyatt Hotel San Diego USA, December 13–15, pp 4008–4013

33. Giri F (ed) (2013) AC electric motors control: advanced design techniques and applications. Wiley, Oxford. doi:10.1002/9781118574263

34. Glumineau A, Boisliveau R, Loron L (2005) iRCCyN, Ecole Centrale de Nantes. http://www2.irccyn.ec-nantes.fr/bancessai/

35. Guidi G, Umida H (2000) A novel stator resistance estimation method for speed-sensorless induction motor drives. IEEE Trans Ind Appl 36(6):1619–1627. doi:10.1109/28.887214

36. Hajian M, Soltani J, Markadeh G, Hosseinnia S (2010) Adaptive nonlinear direct torque control of sensorless im drives with efficiency optimization. IEEE Trans Ind Electron 57(3):975–985. doi:10.1109/TIE.2009.2029592

37. Hamida M, Glumineau A, De Leon J (2012) Optimum torque sensorless hosm controller for ipmsm via adaptive interconnected observer. In: IFAC PPPSC 2012, Toulouse, France, 2–5 September

38. Hamida M, Glumineau A, De Leon J (2012) Robust integral backstepping control for sensorless ipm synchronous motor controller. J Franklin Inst 349(5):1734–1757

39. Hamida M, De Leon J, Glumineau A (2013) High order sliding-mode observers and integral backstepping sensorless control of ipms motor. Int J Control. 87(10):2176–2193 doi:10.1080/00207179.2014.904523

40. Hamida M, De Leon J, Glumineau A, Boisliveau R (2013) An adaptive interconnected observer for sensorless control of pm synchronous motors with online parameter identification. IEEE Trans Ind Electron 60(2):739–748. doi:10.1109/TIE.2012.2206355

41. Hammouri H, de Leon Morales J (1990) Observer synthesis for state-affine systems. In: Proceedings of the 29th IEEE conference on decision and control, vol 2. pp 784–785. doi:10.1109/CDC.1990.203695

42. Hermann R, Krener A (1977) Nonlinear controllability and observability. IEEE Trans Autom Control 22(5):728–740. doi:10.1109/TAC.1977.1101601

43. Holtz J (2002) Sensorless control induction motor drive. Proc IEEE 90:1359–1394

44. Ibarra RS, Moreno J, Espinosa G (2004) Global observability analysis of sensorless induction motor. Automatica 40:1079–1085

45. Isidori A (1989) Nonlinear control systems, 2nd edn. Springer, Berlin

46. Isidori A (1995) Nonlinear control systems, 3rd edn. Communications and control. Engineering series. Springer, Berlin. ISBN 9783540199168

47. Kalman RE, Bucy RS (1961) New results in linear filtering and prediction theory. J Basic Eng 83(3):95–108

48. Ke S, Lin J (2005) Sensorless speed tracking control with backstepping design scheme for permanent magnet synchronous motors. In: Proceedings of 2005 IEEE conference on control applications, CCA, pp 487–492. doi:10.1109/CCA.2005.1507173

49. Khalil H, Strangas E (2004) Sensorless speed control of induction motors. In: Proceedings of the American control conference, vol 2. pp 1127–1132

50. Khlaief A, Bendjedia M, Boussak M, Gossa M (2012) A nonlinear observer for high-performance sensorless speed control of ipmsm drive. IEEE Trans Power Electron 27(6):3028–3040. doi:10.1109/TPEL.2011.2175251

51. Kim H, Huh KK, Lorenz R, Jahns T (2004) A novel method for initial rotor position estimation for ipm synchronous machine drives. IEEE Trans Ind Appl 40(5):1369–1378. doi:10.1109/TIA.2004.834091

52. Kim Y, Kim S, Kwon Y (2003) Mras based sensorless control of permanent magnet synchronous motor. In: SICE 2003 annual conference, vol 2. pp 1632–1637

53. Kokotovic P (1992) The joy of feedback: nonlinear and adaptive. IEEE Control Syst Mag 12(3):7–17

54. Krause PC (1986) Analysis of electric machinery. McGraw-Hill Book Company, New York

55. Krener A, Isidori A (1983) Linearization by output injection and non linear observers. Syst Control Lett 3:47–52

56. Kwan CM, Lewis F, Yeung K (1995) Robust adaptive control of induction motors without flux measurements. In: Proceedings of the 1995 American control conference, vol 5. pp 3515–3520. doi:10.1109/ACC.1995.533790

57. Lascu C, Boldea I, Blaabbjerg F (2003) Very low-speed sensorless variable structure control of induction machine drives without signal injection. IEEE Trans Ind Appl 41(2):591–598

58. Lascu C, Boldea I, Blaabjerg F (2004) Direct torque control of sensorless induction motor drives: a sliding-mode approach. IEEE Trans Ind Appl 40(2):582–590. doi:10.1109/TIA.2004.824441

59. Laskhmikanthan V, Leela S, Martynyuk AA (eds) (1990) Practical stability of nonlinear systems. Word Scientific, Singapore

60. Leonhard W (2001) Control of electrical drives. Engineering online library. Springer, Berlin

61. Levant A (2005) Homogeneity approach to high-order sliding mode design. Automatica 41(5):823–830

62. Levant A (2005) Quasi-continuous high-order sliding-mode controllers. IEEE Trans Autom Control 50(11):1812–1816. doi:10.1109/TAC.2005.858646

63. Lin FJ, Lee CC (2000) Adaptive backstepping control for linear induction motor drive to track periodic references. IEE Proc Electr Power Appl 147(6):449–458. doi:10.1049/ip-epa:20000647

64. Lin FJ, Wai RJ, Lin PC (1999) Robust speed sensorless induction motor drive. IEEE Trans Aerosp Electron Syst 35(2):566–578. doi:10.1109/7.766938
65. Marino R, Tomei P (1995) Nonlinear control design: geometric, adaptive and robust. Prentice Hall International (UK) Ltd., Hertfordshire
66. Marino R, Peresada S, Tomei P (1999) Global adaptive output feedback control of induction motors with uncertain rotor resistance. IEEE Trans Autom Control 44(5):967–983. doi:10.1109/9.763212
67. Marino R, Tomei P, Verrelli C (2004) A global tracking control for speed-sensorless induction motors. Automatica 40(6):1071–1077. http://dx.doi.org/10.1016/j.automatica.2004.01.022, http://www.sciencedirect.com/science/article/pii/S0005109804000494
68. Marino R, Tomei P, Verrelli CM (2005) Adaptive control for speed-sensorless induction motors with uncertain load torque and rotor resistance. Int J Adapt Control Signal Process 19(9):661–685. doi:10.1002/acs.874, http://dx.doi.org/10.1002/acs.874
69. Mobarakeh N, Meibody-Tabar F, Sargos M (2004) Mechanical sensorless control of pmsm with online estimation of stator resistance. IEEE Trans Ind Appl 40(2):457–471
70. Montanari M, Tilli A (2006) Sensorless control of induction motors based on high-gain speed estimation and on-line stator resistance adaptation. In: Annual conference of the IEEE industrial electronics society
71. Orlowska-Kowalska T, Dybkowski M (2010) Robust speed-sensorless induction motor drive for traction applications. In: IECON 2010 36th Annual conference on IEEE industrial electronics society, pp 2358–2363. doi:10.1109/IECON.2010.5675338
72. Ouassaid M, Cherkaoui M, Zidani Y (2004) A nonlinear speed control for a pm synchronous motor using an adaptive backstepping control approach. In: IEEE international conference on industrial technology (ICIT), Hammamet, Tunisia
73. Paponpen K, Konghirun M (2006) An improved sliding mode observer for speed sensorless vector control drive of pmsm. In: IPEMC 2006. CES/IEEE 5th International power electronics and motion control conference, vol 2. pp 1–5. doi:10.1109/IPEMC.2006.4778137
74. Plestan F (2008) Contributions methodologiques et appliquees pour la commande et l observation robustes des systemes non lineaires. Ecole Centrale De Nantes/Nantes University, Habilitation a Diriger des Recherches
75. Plestan F, Glumineau A (1997) Linearization by generalized input-output injection. Syst Control Lett 31:115–128
76. Plestan F, Glumineau A, Bazani G (2007) New robust position control of a synchronous motor by high order sliding mode. IEEE conference on decision and control, New Orleans, Louisiana, USA
77. Plestan F, Glumineau A, Laghrouche S (2008) A new algorithm for high-order sliding mode control. Int J Robust Nonlinear Control 18(4–5):441–453. doi:10.1002/rnc.1234
78. Rashed M, MacConnell P, Stronach F, Acarnley P (2007) Sensorless indirect-rotor-field-orientation speed control of a permanent-magnet synchronous motor with stator-resistance estimation. IEEE Trans Ind Electron 54(3):1664–1675
79. Rasmussen H, Vadstrup P, Borsting H (2001) Full adaptive backstepping design of a speed sensorless field oriented controller for an induction motor. In: Industry applications conference. Thirty-Sixth IAS annual meeting. Conference record of the 2001 IEEE, vol 4. pp 2601–2606. doi:10.1109/IAS.2001.955986
80. Sanchis R, Nijmeijer H (1998) Sliding controller-sliding observer design for non-linear systems. Eur J Control 4:208–234
81. Soltani J, Markadeh G (2003) A current -based output feedback sliding mode control for speed sensorless induction machine drive using an adaptive sliding mode flux observer. 5th IEEE conference on power electronics and drive systems, PEDS 2003, Singapore

82. Soltani J, Markadeh G, Hosseiny SH (2004) A new adaptive direct torque control (dtc) scheme based-on svm for adjustable speed sensorless induction motor drive. In: Industrial electronics society. IECON 2004. 30th annual conference of IEEE, vol 2. pp 1111–1116. doi:10.1109/IECON.2004.1431730

83. Souleiman I, Glumineau A (2007) Constructive transformation of nonlinear systems into a special state affine mimo forms and nonlinear observers. In: 7th IFAC symposium on nonlinear control systems NOLCOS 2007, Pretoria, South Africa

84. Traore D (2008) Commande non lineaire sans capteur de la machine asynchrone. Ph.D. thesis, Ecole centrale de Nantes

85. Traore D, De Leon J, Glumineau A, Loron L (2007) Speed sensorless field-oriented control of induction motor with interconnected observers: experimental tests on low frequencies benchmark. IET Control Theory Appl 1–6(10):1681–1692. doi:10.1049/iet-cta.2009.0648

86. Traore D, Plestan F, Glumineau A, de Leon J (2008) Sensorless induction motor: high-order sliding-mode controller and adaptive interconnected observer. IEEE Trans Ind Electron 55(11):3818–3827. doi:10.1109/TIE.2008.2003368

87. Traore D, De Leon J, Glumineau A, Loron L (2009) Adaptive interconnected observer for sensorless induction motor. Int J Control 82(9):1627–1640

88. Traore D, De Leon J, Glumineau A (2010) Sensorless induction motor adaptive observer-backstepping controller: experimental robustness tests on low frequencies benchmark. IET Control Theory Appl 4(10):1989–2002. doi:10.1049/iet-cta.2009.0648

89. Traore D, De Leon J, Glumineau A (2012) Adaptive interconnected observer-based backstepping control design for sensorless induction motor. Automatica 48:682–687

90. Uddin MN, Rahman MA (2007) High-speed control of ipmsm drives using improved fuzzy logic algorithms. IEEE Trans Ind Electron 54(1):190–199. doi:10.1109/TIE.2006.888781

91. Underwood SJ (2006) On-line parameter estimation and adaptive control of permanent magnet synchronous machines. Ph.D. thesis, University of Akron

92. Vaclavek P, Blaha P, Herman I (2012) Ac drives observability analysis. IEEE Trans Ind Electron PP(99):1. doi:10.1109/TIE.2012.2203775

93. Zaltni D, Ghanes M, Barbot JP, Naceur A (2010) Synchronous motor observability study and an improved zero-speed position estimation design. In: 2010 49th IEEE conference on decision and control (CDC), pp 4012–4017

94. Zhang Q (2002) Adaptive observers for mimo linear time-varying systems. IEEE Trans Autom Control 47:525–529

95. Zhang Y, Changxi J, Utkin V (2000) Sensorless sliding-mode control of induction motors. IEEE Trans Ind Electron 47(6):1286–1297

96. Zheng Z, Fadel M, Li Y (2007) High performance pmsm sensorless control with load torque observation. International conference on computer as a tool, EUROCON, Warsaw, pp 9–12

Index